

REPORT NO. *FRA-80-9* FRA/ORD-80/21

REFERENCE USE ONLY

OPERATIONAL PARAMETERS IN ACOUSTIC SIGNATURE INSPECTION OF RAILROAD WHEELS

D. Dousis
R.D. Finch

UNIVERSITY OF HOUSTON
Department of Mechanical Engineering
Houston TX 77004



APRIL 1980
FINAL REPORT

DOCUMENT IS AVAILABLE TO THE PUBLIC
THROUGH THE NATIONAL TECHNICAL
INFORMATION SERVICE, SPRINGFIELD,
VIRGINIA 22161

Prepared for

U.S. DEPARTMENT OF TRANSPORTATION
FEDERAL RAILROAD ADMINISTRATION
Office of Research and Development
Washington DC 20590

NOTICE

This document is disseminated under the sponsorship of the Department of Transportation in the interest of information exchange. The United States Government assumes no liability for its contents or use thereof.

NOTICE

The United States Government does not endorse products or manufacturers. Trade or manufacturers' names appear herein solely because they are considered essential to the object of this report.

1. Report No. FRA/ORD-80/21	2. Government Accession No.	3. Recipient's Catalog No. PB81 1 16768	
4. Title and Subtitle OPERATIONAL PARAMETERS IN ACOUSTIC SIGNATURE INSPECTION OF RAILROAD WHEELS		5. Report Date April 1980	
		6. Performing Organization Code	
7. Author(s) D. Dousis, R. D. Finch		8. Performing Organization Report No. DOT-TSC-FRA-80-9	
9. Performing Organization Name and Address University of Houston* Department of Mechanical Engineering Houston TX 77004		10. Work Unit No. (TRAIS) RR031/RO312	
		11. Contract or Grant No. DOT-TSC-1187	
12. Sponsoring Agency Name and Address U.S. Department of Transportation Federal Railroad Administration Office of Research and Development Washington DC 20590		13. Type of Report and Period Covered Final Report March 1976-Oct. 1978	
		14. Sponsoring Agency Code	
15. Supplementary Notes *under contract to:	U.S. Department of Transportation Research and Special Programs Administration Transportation Systems Center Cambridge MA 02142		
16. Abstract A brief summary is given of some prior studies which established the feasibility of using acoustic signatures for inspection of railroad wheels. The purpose of the present work was to elucidate operational parameters which would be of importance for the development of a prototype system. Experimental and theoretical investigations were conducted to obtain more information on the effects on wheel vibrations of geometrical variations, wear, internal stress etc. Hardware improvements and interfacing were carried out for a wayside installation, in addition to software development for real time data acquisition and processing. Field tests were made to evaluate system performance, to permit follow-up on certain wheels and to obtain tape recordings from a sample of axle sets in service. These tape recordings were used to optimize the data processing software and to attempt to correlate identifiable wheel conditions with characteristics of the acoustic signature. The greatest signature differences were obtained when one of a pair of wheels was cracked. Differential wear was found to be a major cause of differences in the signatures of good wheel pairs. It is claimed that the knowledge gained from this study is sufficient to warrant the installation of a prototype system with a reasonable likelihood of success. Another important finding is that the frequencies of certain resonant modes shift slightly with changes in residual stress.			
17. Key Words Railroad Wheels Acoustic Signature Inspection Systems Residual Stress		18. Distribution Statement DOCUMENT IS AVAILABLE TO THE PUBLIC THROUGH THE NATIONAL TECHNICAL INFORMATION SERVICE, SPRINGFIELD, VIRGINIA 22161	
19. Security Classif. (of this report) Unclassified	20. Security Classif. (of this page) Unclassified	21. No. of Pages	22. Price

METRIC CONVERSION FACTORS

Approximate Conversions to Metric Measures

Symbol When You Know Multiply by To Find Symbol

LENGTH

in	inches	2.5	cm	centimeters
ft	feet	30	cm	centimeters
yd	yards	0.9	m	meters
mi	miles	1.6	km	kilometers

AREA

in ²	square inches	6.5	cm ²	square centimeters
ft ²	square feet	0.09	m ²	square meters
yd ²	square yards	0.8	km ²	square kilometers
mi ²	square miles	2.6	ha	hectares
	acres	0.4		

MASS (weight)

oz	ounces	28	g	grams
lb	pounds	0.45	kg	kilograms
	short tons	0.9	t	tonnes
	(2000 lb)			

VOLUME

teaspoon	teaspoons	5	ml	milliliters
fl oz	fluid ounces	30	ml	milliliters
c	cups	0.24	l	liters
pt	pints	0.47	l	liters
qt	quarts	0.95	l	liters
gal	gallons	3.8	l	liters
ft ³	cubic feet	0.03	m ³	cubic meters
yd ³	cubic yards	0.76	m ³	cubic meters

TEMPERATURE (exact)

°F	Fahrenheit temperature	5/9 (after subtracting 32)	°C	Celsius temperature
----	------------------------	----------------------------	----	---------------------



Approximate Conversions from Metric Measures

Symbol When You Know Multiply by To Find Symbol

LENGTH

mm	millimeters	0.04	in	inches
cm	centimeters	0.4	in	inches
m	meters	3.3	ft	feet
km	kilometers	1.1	yd	yards
		0.6	mi	miles

AREA

cm ²	square centimeters	0.16	in ²	square inches
m ²	square meters	1.2	yd ²	square yards
km ²	square kilometers	0.4	mi ²	square miles
ha	hectares (10,000 m ²)	2.5		acres

MASS (weight)

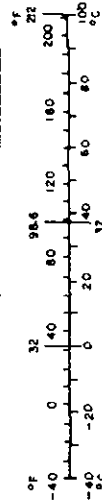
g	grams	0.035	oz	ounces
kg	kilograms	2.2	lb	pounds
t	tonnes (1000 kg)	1.1		short tons

VOLUME

ml	milliliters	0.03	fl oz	fluid ounces
l	liters	2.1	pt	pints
l	liters	1.06	qt	quarts
m ³	cubic meters	0.26	gal	gallons
m ³	cubic meters	35	ft ³	cubic feet
		1.3	yd ³	cubic yards

TEMPERATURE (exact)

°C	Celsius temperature	9/5 (then add 32)	°F	Fahrenheit temperature
----	---------------------	-------------------	----	------------------------



PREFACE

The authors would like to express their sincere appreciation and thanks to the following:

Mr. P. Higgins for the management of the project until February 1977, the study of different types of excitation mechanisms and the modification of the mechanical hammer type exciter, and for his assistance and efforts during the Pueblo and Bessemer tests.

Mr. A. Chaudhari for the frequency analysis of the railroad wheel vibrations using finite element analysis.

Mr. J. Herbster for the data transfer between the computer and diskette written software.

Mr. K. Gates for his assistance with the electronic experiment equipment.

Mr. W. Kucera, and the superintendent and personnel of the Griffin Wheel Manufacturing Plant at Bessemer, Alabama for their assistance during the residual stress measurements at the Bessemer Plant.

Mr. W. McCutchon and the personnel at TTC in Pueblo, Colorado for their assistance during the field tests at Pueblo.

Messrs R. Gill, B. Shewmake, J. Balusek and the personnel of the Southern Pacific Transportation Company for their assistance during the six weeks field tests at the Englewood classification yard in Houston.

Messrs R. Ehrenbeck, E. Sarkisian, J. Ferguson, P. Rhine, W. Kucera and B. Shewmake, members of the Project Advisory Committee, for their advice and valuable comments.

The Union Pacific Railroad Company for the loan of a Real Time Analyzer, and for their invitation to participate in their dynamometer tests. Thanks are due in particular to Mr. F. D. Acord, Mr. F. D. Bruner and Dr. P. E. Rhine.

Dr. O. Crenwelge and Shell Oil Company for the use of a Real Time Analyzer.

Dr. B. N. Nagarkar for his assistance during the Englewood field test.

The Association of American Railroads for assuming part of the funding and last but not least the Department of Transportation for providing the majority of the project funds.

TABLE OF CONTENTS

<u>Section</u>	<u>Page</u>
1. INTRODUCTION	1
1.1 Background	1
1.2 Types of Defects	3
1.3 Elements of Acoustic Signature Analysis	6
1.4 Theory	8
1.5 Experiments on Excitation and Detection Methods	12
1.6 Variables in the Acoustic Signature	13
1.7 Laboratory Demonstration System for Finding Cracks	16
1.8 Preliminary Field Tests	19
1.9 Objectives of the Present Study	21
2. THEORY OF RAILROAD WHEEL VIBRATIONS	25
2.1 Introduction	25
2.2 Stappenbeck's Ring Model of Wheel Vibrations	27
2.3 The Effect of Uneven Wear on Wheels Across the Axle	32
2.4 The Effect of Residual Stress	34
3. EXPERIMENTS ON WHEEL GEOMETRY AND MINIMUM DETECTABLE CRACK SIZE	37
3.1 Introduction	37
3.2 Data Bank of Wheel Types	37

CONTENTS (Cont'd)

<u>Section</u>	<u>Page</u>
3.3 Results from Data Bank Tests	38
3.4 Investigation of Minimum Detectable Crack Size	45
4. RESIDUAL STRESS EVALUATION IN RAILROAD WHEELS USING ACOUSTIC SIGNATURE ANALYSIS	54
4.1 Introduction	54
4.2 Test on Wheels with Different Heat Treatment in the Griffin Wheel Manufacturing Plant at Bessemer, Alabama	57
4.3 Dynamometer Tests at Wilmerding, Pennsylvania	73
4.3.1 Description of Tests	73
4.3.2 Data Processing	77
4.3.3 Results	77
5. SYSTEM COMPONENT DESIGN	90
5.1 Wheel Exciter	90
5.1.1 Mechanically Powered Excitation	91
5.1.2 Electrically Powered Excitation	94
5.1.3 Pneumatic Powered Excitation	96
5.1.4 Comparison of Exciter Types	99
5.2 Wheel Sensor	99
5.3 Microphones	102
5.4 Spectrum Analyzer, Computer and Diskette Interfacing	105
5.5 System Description and Software Development	109
6. WAYSIDE TESTS	127
6.1 Tests at TTC Pueblo, Colorado	127
6.2 First Pueblo Test	127
6.3 Second Pueblo Test	133

CONTENTS (Cont'd)

<u>Section</u>	<u>Page</u>
6.4 Tests at the Southern Pacific Englewood Yard, Houston	139
6.5 Englewood Test Site and Equipment	140
6.6 Performance of the Hardware during the Englewood Test	148
6.7 Performance of Software during the Englewood Test	155
7. SENSITIVITY ANALYSIS	160
7.1 Introduction	160
7.2 Identification and Correction of System Problems	161
7.3 Optimizing the DI Equation	166
7.4 The Effect of Wheel Conditions	173
7.4.1 Introduction	173
7.4.2 Data Reduction	175
7.4.3 Laboratory Measurement of Wear	183
8. CONCLUSIONS AND SUGGESTIONS FOR FURTHER WORK	189
8.1 Conclusions	189
8.1.1 Advances in Scientific Understanding	189
8.1.2 System Improvements	190
8.1.3 Software and Signature Recognition Improvements	192
8.2 Suggestions for Further Work	194
8.2.1 Installation of a Prototype ASI System	195
8.2.2 System Interaction Studies	198
8.2.3 Further Research on Residual Stress, Crack Growth and Wheel Removal Criteria	199

CONTENTS (Cont'd)

<u>Section</u>	<u>Page</u>
REFERENCES-	204
APPENDIX A - List of Wheels on Inventory at University of Houston	209
APPENDIX B - Equipment List Used in the Englewood Yard Tests	210
APPENDIX C - Software for Computer Interfacing and Data Processing	211
C.1 Pin Assignment	211
C.2 List of the Assembler Software Used for Digital Control of the Real Time Analyzer and Data Transfer to Computer/Diskette	214
C.3 List of the BASIC Software Used in the Englewood Yard Field Tests	247
APPENDIX D - Resonances of the Wheels Tested at the Griffin Wheel Plant in Bessemer, Alabama	253
APPENDIX E - Dynamics of a Hammer Exciter	256
APPENDIX F - Finite Element Analysis	260
F.1 Finite Element Analysis of the Railway Wheel	260
F.2 Mode Frequency Analysis	261
APPENDIX G - Relationship Among Operating Parameters	274
APPENDIX H - Report of New Technology	277

LIST OF ILLUSTRATIONS

<u>Figure</u>	<u>Page</u>
1.2.1 Wheel Showing Typical Cracks	4
1.3.1 Schematic of Acoustic Signature Inspection System Components	7
1.4.1 Mode Shapes Obtained with Finite Element Program for 33" Good Wheel. Note: The Hub Is Fixed for All Mode Shapes	10
1.4.2 Line Spectra of Resonances Obtained from the ANSYS Program, Compared with Experimental Spectra for 33" Good Wheels Obtained by Using a Rail-mounted Accelerometer	10
1.4.3 Mode Shapes Obtained with ANSYS Program for 33" Wheel with Plate Crack	11
1.4.4 Line Spectra of Resonances Obtained from the ANSYS Program for 33" Good and Flawed Wheels	11
1.6.1 Drawing of Impacter Used in First Test	14
1.6.2 Fixed Band Spectra of Impact on Good 33" Wheels on Either End of the Same Axle	15
1.6.3 Fixed Band Spectra of Impact on Two Good 33" Wheels, One a Griffin 9 Riser, One an ARMCO Wrought	15
1.6.4 Fixed Band Spectra of Impact on 33" Southern wheels, One with a Large Thermal Crack	17
1.6.5 Fixed Band Spectra of Impact on Two 33" Southern Wheels, One with a Thick Layer of Grease	17
1.6.6 Variation of Wheel Signature with Load for Wheel 3G (Accelerometer Pickup)	18
1.8.1 Train Consist for Second Test	22
1.8.2 Computer Output for an Eastbound Run at 6 MPH. Reliability Was 100%. Engine Is Car 5. Decision Limit Is 11.	22

ILLUSTRATIONS (Cont'd)

<u>Figure</u>		<u>Page</u>
2.1.1	Assumed and Actual Wheel Cross Sections	26
2.2.1	Cross Sections for Ring Model	31
3.2.1a	Wheel Information and Test Description Form	39
3.2.1b	Acoustic Signature Plot Form	39
3.2.2	Rolling Ball Apparatus	40
3.3.1	Signatures of Impact on Two Wheels on the Same Axle with Unevenly Worn Flanges	44
3.4.1	View of Wheel 15A	49
3.4.2a	View of Wheel 15C (Front Side)	50
3.4.2b	View of Wheel 15C (Back Side)	50
3.4.3	Signatures of Wheels, 15C with a Partial Plate Crack and 15A with a Full Plate Crack	52
3.4.4	Spectral Line Comparison Tests Among a Wheel with a Partial Plate Crack (15C), a Wheel with a Full Plate Crack (15A) and Two Good Wheels of the Same Type (1G and 4G)	53
4.2.1	Strain Test on a 33" One Wear 70 Ton Griffin Wheel	58
4.2.2	View of the Hammer with a PZT Disk Between Hammer and Cylinder to Provide the Triggering Pulse on Impact with the Test Object	60
4.2.3	Schematic Diagram of Cast Wheel Manufacturing	62
4.2.4	Spectra Plots for CJ36 Wheels with Different Internal Stress Distribution, Between 2400 and 2500 Hz	67
4.2.5	Differences in Resonant Frequency for CJ36 Wheels	68
4.2.6	Differences in Resonant Frequency for CJ33 Wheels	69
4.3.1	Setup for Acoustic Signature Recording	75
4.3.2	Strain Gauge Arrangement	76
4.3.3	Acoustic Signature of a CJ33 Wheel from 0-6.4kHz	82

ILLUSTRATIONS (Cont'd)

<u>Figure</u>	<u>Page</u>
4.3.4 Wheel UP 28, Acoustic Signature at 3 kHz before the Drag Braking Test	83
4.3.5 Wheel UP 28, Acoustic Signature at 3 kHz after the First Drag Braking Stop	83
4.3.6 Wheel UP 28, Acoustic Signature at 3 kHz after the Second Drag Braking Stop	84
4.3.7 Wheel UP 28, Acoustic Signature at 3 kHz after the Third Drag Braking Stop	84
4.3.8 Wheel UP 28, Acoustic Signature at 3 kHz after the Fourth Drag Braking Stop	85
4.3.9 Wheel UP 28, Acoustic Signature at 3 kHz after the Fifth Drag Braking Stop	85
4.3.10 Frequency shift, Δf , Versus Strain Change, $\Delta \epsilon$, at 3 kHz for Wheel UP 27 (Five Drag Braking Stops)	87
4.3.11 Frequency Shift, Δf , Versus Strain Change, $\Delta \epsilon$, at 3 kHz for Wheel UP 28 (Five Drag Braking Stops)	88
5.1.1 Drawing of the Modified Mechanical Wheel Exciter	93
5.1.2 Motor Exciter, Rotary	95
5.1.3 Pneumatic Leaf Spring Exciter	98
5.2.1 Output Voltage Circuit of the Wheel Sensor	103
5.3.1a Assembly of Weatherproof Microphone	104
5.3.1b Directional Response Patterns for the GR 1/2" Electret-Condenser Microphone	104
5.5.1 Schematic of Data Collection and Processing Hardware	110
5.5.2 Flow Diagram for the Series of Computer Programs used in the SP Englewood Yard, Houston Tests	116
5.5.3 Flow Diagram of the Read Acoustic Signatures Part of the Main Program	120

ILLUSTRATIONS (Cont'd)

<u>Figure</u>		<u>Page</u>
5.5.4	Flow Diagram of the Data Processing Section of the Main Program	121
5.5.5	Sample Output of the Main Program	123
5.5.6	Distribution of Difference Index for Run #21 and Run #23 from the Field Tests at Englewood Yard, 18 June 1975	125
5.5.7	Distribution of Difference Index for Run #10, Three Different Sampling Time Intervals, from the Field Tests at Englewood Yard, 18 June 1975	126
6.2.1	Modified Mechanical Hammer Exciter used at TTC, Pueblo	129
6.2.2a	View of the Exciter-Wheel Sensor	131
6.2.2b	View of the Microphones, Exciter and Wheel Sensor on the Bypass Section of the FAST track at TTC, Pueblo	131
6.2.3a	View of the Setup and Equipment used at TTC, Pueblo, Colorado	132
6.2.3b	Schematic of the System used at TTC, Pueblo, Colorado	132
6.3.1	Distribution of Difference Index for the Tests 5/6, 6/9, 14/18 at TTC, Pueblo, Colorado	135
6.3.2	Distribution of Difference Index for the Tests 14/18, 6/3, 13/13 at TTC, Pueblo, Colorado	136
6.3.3	Distribution of Difference Index for the Tests 13/17, 17/18, 13/14 at TTC, Pueblo, Colorado	137
6.5.1	Outline of the Southern Pacific's Classification Yard in Houston	141
6.5.2a	View of the Inspection System	145
6.5.2b	Schematic of the System Layout	145
6.5.3	View of the Microphones, Exciters and Wheel Sensors Through the Window of the Trailer	146
6.5.4a	View of the East Side of the Hump. Inspection Pits are Indicated by Arrow	147
6.5.4b	View of the Microphones, Exciters and Wheel Sensors	147

ILLUSTRATIONS (Cont'd)

<u>Figure</u>	<u>Page</u>
6.6.1a Typical Performance of the Exciters during the Late Tests	151
6.6.1b Typical Performance of the Exciters during the Early Tests Sweep Speed 500 ms/div	151
6.6.2a Exciter Performance, Double Impact	152
6.6.2b Exciter Performance, New Wheels, Low or No Impact; Sweep Speed 500 ms/div	152
6.6.3a Impacts on Wheels with High Flanges, Followed by Impacts on Wheels with Low Flanges	153
6.6.3b Uneven Impact on Wheels Across the Axle	153
6.6.4a Timing Relation, South Exciter, Impact about 40 ms after the Timing Pulse	154
6.6.4b Timing Relation, North Exciter, Impact about 110 ms after the Timing Pulse; Sweep Speed 50 ms/div	154
6.7.1 Distribution of Difference Index for the Last Ten Days of Field Tests at the Southern Pacific Yard (July 1977)	159
7.2.1 Distribution of Difference Index Values DI = C_1 SD, Sample Size: 137, Frequency Range: 0-10 kHz (No Correction for Timing Pulse Difference)	163
7.2.2 Distribution of Difference Index Values DI = C_1 SD, Sample Size: 168, Frequency Range: 0-10 kHz (With Correction for Timing Pulse Difference)	164
7.3.1 Distribution of Difference Index Values DI = C_1 SD, Sample Size: 372, Frequency Range: 0-10 kHz	168
7.3.2 Distribution of Difference Index Values DI = C_1 SD, Sample Size: 369, Frequency Range: 0-7200 Hz	169
7.3.3 Distribution of Number of Common Resonances, NC, Sample Size: 313, Frequency Range: 0-10 kHz	171
7.3.4 Distribution of Difference Index Values. DI = C_1 SD - C_2 (NC) ² , Sample Size: 371 Frequency Range: 0-7200 Hz	172

ILLUSTRATIONS (Cont'd)

<u>Figure</u>	<u>Page</u>
7.4.1 Signatures of Wheels with Uneven Impact	176
7.4.2 Timing Pulses and Sound Signals from Two Unevenly Impacted Wheels.	177
7.4.3 Signatures of Wheels on Axle 3, Car GTAX 13286, Progressive Frequency Shifts	178
7.4.4 Typical Timing Pulses and Sound Signals from a Pair of Wheels Tested at the Englewood Yard	179
7.4.5 Frequency shift Δf_n of a Pair of Unevenly Worn Wheels, versus Frequency f	180
7.4.6 Actual Cross Section of a Wheel Showing How the Tread and Flange Thickness Were Measured	184
7.4.7 Signature of Wheels IIA and IIC	186
7.4.8 Signature Differences at the Resonant Modes for Wheels IIA/C, due to Uneven Wear	188
C.1.2 SD 300A Digital Output Timing	213
F.2.1 View of a 33" Wheel with One Small Radial Flange Crack - ANSYS Geometry	265
F.2.2 View of a 33" Wheel with One Complete Flange and Tread Crack - ANSYS Geometry	265
F.2.3 View of a 33" Wheel with One Complete Radial Crack - ANSYS Geometry	266
F.2.4 View of a 33" Wheel with One Large Plate Crack - ANSYS Geometry	266
F.2.5 Comparison of Natural Modes for 33" Wheels	269
F.2.6a 33" Good Wheel Modal Analysis, Single Pulse on the Load Line	270
F.2.6b 33" Good Wheel Modal Analysis, Single Pulse 30° from the Load Line	270
F.2.7 Modal Analysis of a 33" Wheel with One Small Radial Flange Crack - Single Pulse Applied (Radial)	271
F.2.8 Modal Analysis of a 33" Wheel with One Small Flange Crack - Single Pulse Applied (Axial)	272

LIST OF TABLES

<u>Table</u>		<u>Page</u>
1.1.1	List of Wheel Failures for 1976	2
1.7.1	Sums of Differences of Wheel Spectra from Average Good Wheel Spectrum (Impact Excitation)	20
2.2.1	List of Resonances calculated with the Ring Model Compared with ANSYS Results and Experimental Data	30
3.2.1	Inventory of Wheels Tested at Southern Pacific Englewood Yard 18 June 1976	41
3.4.1	Range of Deviations from Good Wheel Spectral Averages in Experiments with Thermal Cracks	47
4.2.1	List of Wheels Tested at the Griffin Wheel Manufacturing Plant in Bessemer, Alabama for Residual Stress Evaluation	64
4.2.2	Preliminary Results - Residual Stress Tests, Bessemer, Alabama	65
4.2.3	Error Evaluation for Strong Resonances on CJ33 and CJ36 Wheels	72
4.3.1	Strain Gauge Indication Versus Acoustic Signature Changes from Drag Braking Tests on Wheel UP 28	78
4.3.2	Strain Gauge Indication Versus Acoustic Signature Changes from Drag Braking Tests on Wheel UP 27	79
4.3.3	Setup State on HP 5445 Real Time Analyzer	81
5.1.1	Rating of 3 Exciter Types against Ideal Specifications	100
5.5.1	Summary of the Line Spectra Analysis (Results Obtained Manually from Spectra Plots)	113
5.5.2	Summary of the Line Spectra Analysis (Tests were Computer Controlled)	114

TABLES (Cont'd)

<u>Table</u>		<u>Page</u>
6.5.1	Difference Index Values from Wheels Tested in the Laboratory, for Discrimination Level Selection	143
6.7.1	Summary of the Last Ten Days of Tests at the Southern Pacific Englewood Yard, Houston	156
7.4.1	Theoretical Estimate of Differential Wear on Wheels with High DI Values	182
7.4.2	Tread and Flange Thickness of Wheels at the University of Houston Laboratory	185
C.1.1	Computer-Analyzer Interfacing	212
D.1	Resonances of CJ33 Type Wheels with Different Internal Stresses	254
D.2	Resonances of CJ36 Type Wheels with Different Internal Stresses	255
F.2.1	Summary of Analysis	268

1. INTRODUCTION

1.1 Background

The impetus to the work covered in this report came from a feasibility study on the use of acoustic signatures for inspection of railroad wheels [1]. The basic idea was to see if it would be possible to automate the art of the carman, who by banging wheels with a hammer, can tell a defective one by its sound. There is a need for a fully automatic testing system to inspect freight car wheels. At present the standard way of finding cracked or overheated wheels depends on the visual acuity of inspectors stationed in pits at switching yards. These men have to watch for a variety of possible mechanical defects as the cars move past the pit. Although the inspectors are remarkably adept at finding problems there are still a number of mechanical defects which are not readily apparent and subsequently can result in derailments. Table 1.1.1 shows the AAR list of wheel failures for 1976 indicating the relative importance of different defects.

Having indicated the motivation for the research it is appropriate to proceed to summarize the findings of the earlier feasibility study [1]. The present work had the general objective of improving the laboratory demonstration system to the point that actual operating parameters could be

TABLE 1.1.1 LIST OF WHEEL FAILURES FOR 1976

From: Association of American Railroads
Mechanical Division Circular D.V. 1895

REPORT OF AAR WHEEL FAILURES FOR YEAR 1976	CAUSE - INTERCHANGE RULE 41 - SEC. F 6									
	Total Failures	Cracked or Broken Flange	Cracked or Broken Rim	Shattered Rim	Spread Rim	Thermal Cracks	Tread Shelled	Burst Hub	Cracked or Broken Plate	Subsurface Defect
		66	68	71	72	74	75	82	83	88
28 "										
1W - CS	21		18			1	2			
1W - WS	36		1	16		6			13	
2W & MW - CS										
2W & MW - WS	1		1							
TOTAL	58		20	16		7	2		13	
33 "										
1W - CS	273	3	30	17		176	25	1	20	1
1W - WS	255	5	63	75	1	25	22	1	63	
2W & MW - CS	16	1	3			9	2		1	
2W & MW - WS	87	2	12	30		26	7	1	9	
TOTAL	631	11	108	122	1	236	56	3	93	1
36 "										
1W - CS	69	8		2		17	37	1	4	
1W - WS	367	4	47	211		18	71		16	
2W & MW - CS	25		1	4		12	7		1	
2W & MW - WS	94	2	12	27	1	15	22		15	
TOTAL	555	14	60	244	1	62	137	1	36	
38 "										
1W - CS										
1W - WS	7			2		2	2		1	
2W & MW - CS										
2W & MW - WS	3		1			2				
TOTAL	10		1	2		4	2		1	
GRAND TOTAL	1254	25	189	384	2	309	197	4	143	1

1W = Single Wear

MW = Multiple Wear

CS = Cast Steel

WS = Wrought Steel

established and a secondary objective was to find if residual stresses could change the acoustic signature and in what manner. The specific objectives of the present program will be defined after the summary of the feasibility study.

1.2 Types of Defects

It is appropriate to summarize the principal in-service defects of wheels^{*}, and their causes. A good summary of this subject has been given by Carter and Caton [30]. At present one of the most frequently occurring classes of defect is the thermal crack, due to extended periods of brake shoe application and rapid cooling. The cracks may be found on only one or both wheels of an axle set. The cracks appear as hair lines on the tread or flange and there are frequently numerous cracks around the circumference of the wheel. Despite the barely visible exterior manifestation of this type of crack, below the surface it may occupy a sizeable fraction of the rim cross section. When a wheel with thermal cracks is withdrawn from service and subjected to metallurgical examination the cracks are typically found to extend over about a square inch in area perpendicular to the surface (see Fig. 1.2.1). This area is usually blackened, suggesting that the cracks may persist for long periods before progressing through the plate to cause a catastrophic failure. This final stage of the failure is surmised to be a result of changes in the internal state

^{*}The Association of American Railroads standard nomenclature for the parts of a wheel is illustrated in Fig. 1.2.1.

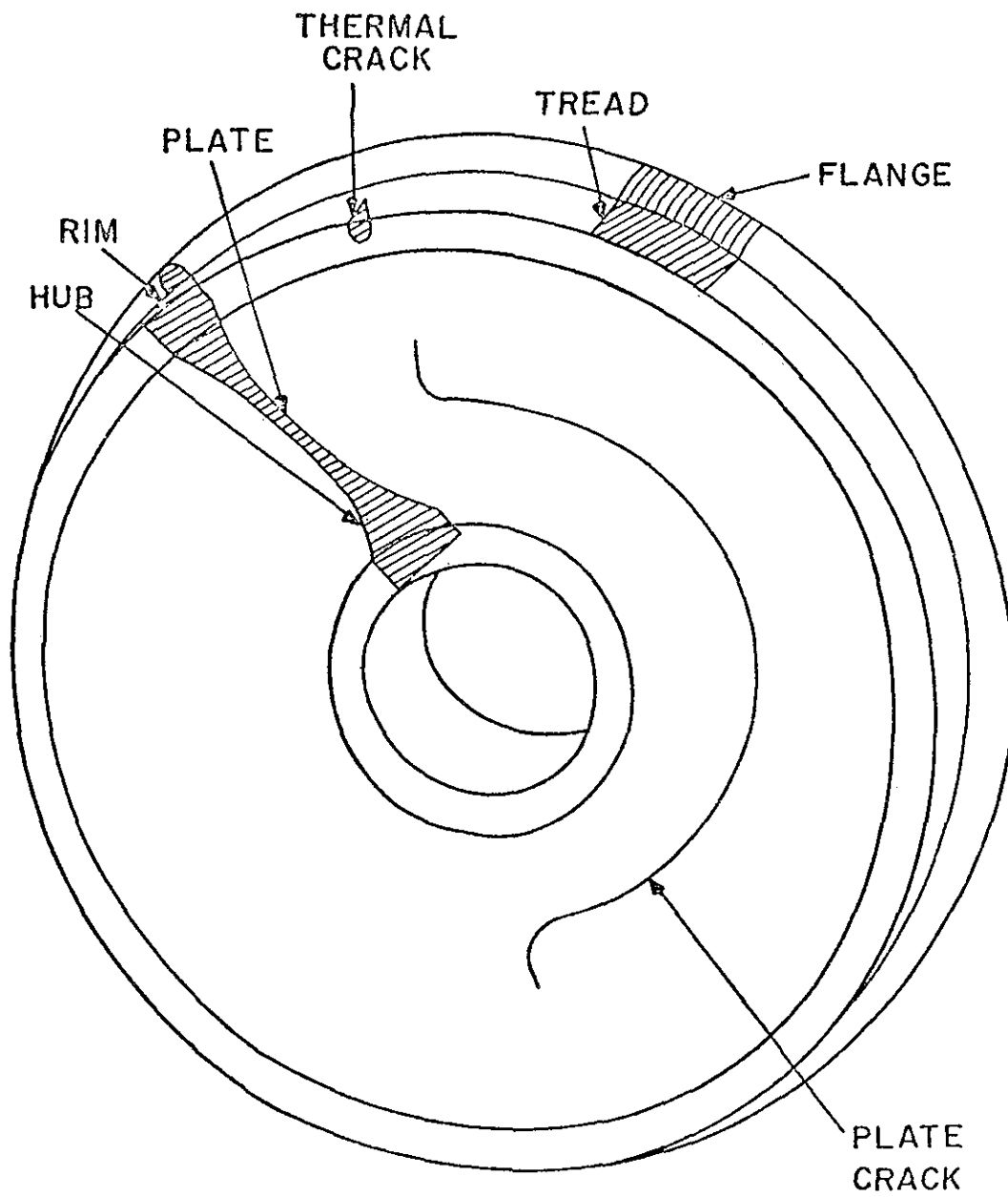


FIG. 1.2.1 WHEEL SHOWING TYPICAL CRACKS

of stress of the wheel. A method for detecting thermal cracks using ultrasonic surface waves has been described in an earlier publication by Bray et al. [3], but acoustic signature inspection is an alternative method.

Changes in internal stress are not readily measured, even under laboratory conditions, and so most railroads make it a practice to remove wheels showing a burnt or cindered road dirt and oil mixture or a typical discoloration associated with overheating. A means of determining internal stress on an automatic basis therefore would be a highly desirable feature of any wheel inspection system. Some evidence is presented in this report that changes in internal stress can be detected from acoustic signature inspection.

Plate cracks are usually found as extensive bow shape fractures running round the hub and extending into the plate. Cracks in the plate can develop due to lateral stresses in service or tension due to rim heating during drag braking. Some plate cracks have been ascribed to manufacturing defects. This type of defect is not found as frequently as thermal cracking or overheating but some of the most catastrophic wheel failures have been ascribed to plate cracks. The detection of plate cracks by acoustic signature inspection was investigated extensively as reported later.

Shattered rims, due to the growth of subsurface defects, are encountered quite often. Another common problem is the occurrence of flat spots on the tread, due to sliding along the rail when the brake locks the wheels. Large flat spots

cause repeated impacting which results in further damage to both the rail and the wheels. These tread surface defects can be detected using very simple acoustic signature inspection.

1.3 Elements of Acoustic Signature Analysis

The elements of an acoustic signature inspection system are illustrated schematically in Fig. 1.3.1. The excitation, in principle, could occur in normal railroad operations: impact at joints, friction of brakes and retarders; or simply the forces due to rolling. Flat spots provide their own source of excitation by periodic impact on the rail. Alternatively, it may be necessary to introduce an excitation, such as a hammer blow, which does not occur in normal operations. One of the objectives of the feasibility study was to decide which of these forms of excitation would be most suitable for a flaw detection system.

The vibratory mechanical energy of the excited wheel is partially degraded by sound radiated into the air and vibration of the track. It is these sounds and vibrations which are termed the acoustic signature. Sound can be picked up by a microphone, and vibration, by a rail mounted accelerometer. A second objective of the feasibility study was to decide whether sound or vibration is the better form of acoustic signature to monitor in the detection of various types of flaw.

The sound or vibration signal after transduction may be represented in various formats. The simplest of these is an overall, RMS sound level. Various weighting networks as

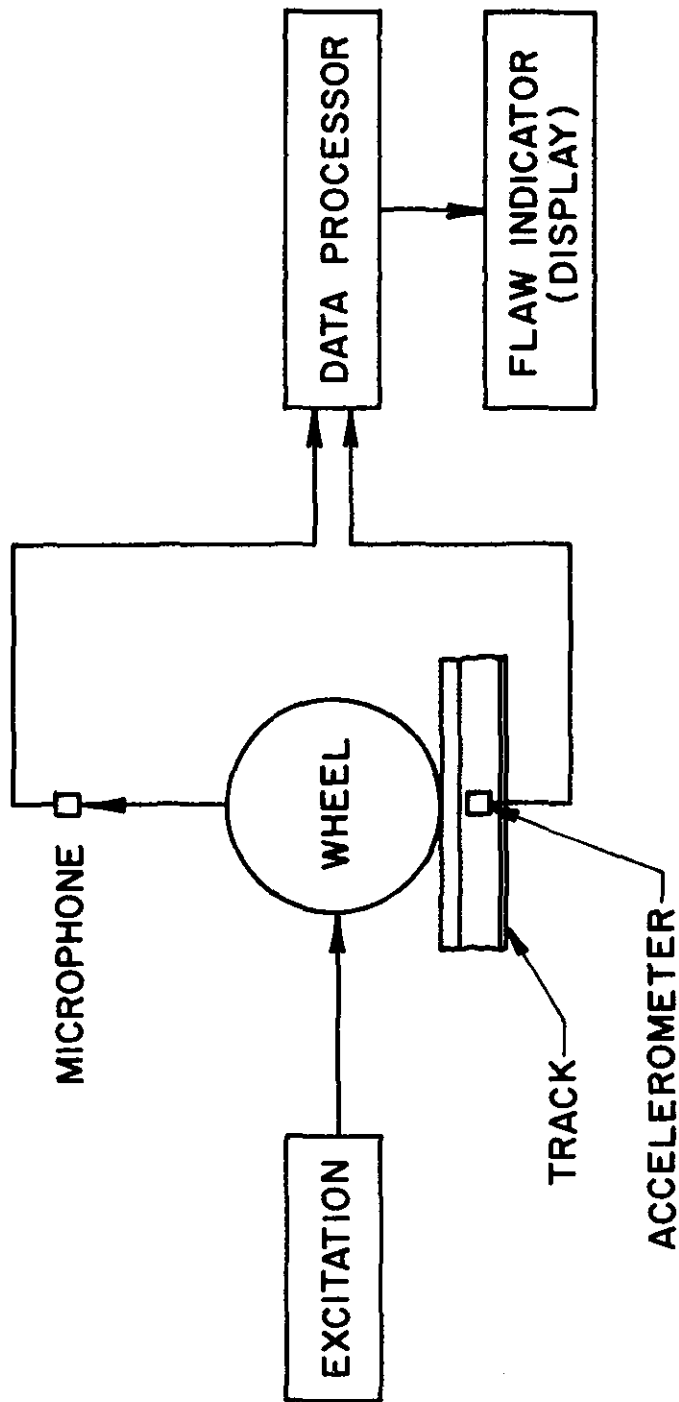


FIG. I.3.1 SCHEMATIC OF ACOUSTIC SIGNATURE INSPECTION SYSTEM COMPONENTS

well as band-pass filtering may be used to attenuate or exclude noise components in the signal. The frequency spectrum of the signal is a function of the filtering method employed. Both one-third octave band and constant bandwidth (250 channels per 10 kHz) analyzers were used in the feasibility study. Railroad wheel sound spectra were found to be dominated by high frequency components in the range of 1 to 5 kHz. One-third octave bands in this frequency range are wide, so that all the information from a wheel's acoustic signature is compressed into a few bands. Changes in the acoustic signature result in relatively small level changes in these 1/3 octave bands. However, when narrow constant bandwidth analyzers are used, the wheel signature is represented by more bands, thus perception of signature changes is considerably improved. The disadvantage is increased analysis time due to the increased amount of data.

The spectrum of a given signal can be processed with a minicomputer by comparison to reference spectra. Various possible comparison schemes were considered and are discussed later. Finally if the comparisons show that a wheel is defective, some form of flaw indicator is actuated. In the present research system this indication is made with a teletype.

1.4 Theory

A completely theoretical design procedure could be envisaged. The railroad wheel could be modelled using finite

element analysis so that various forcing functions, various wheel geometries and various defects could then be simulated. The wheel vibrations could then be related to sound radiated to obtain predictions of acoustic signatures. This information could then be used in selecting excitation, detection and data processing methods. Some progress on such a theoretical approach was made during the feasibility study. The free vibration frequencies of a wheel without damping were found. Figure 1.4.1 shows these theoretical results for the first 15 resonance frequencies and mode shapes of the wheel. Comparison with experimental results for 33" good wheels showed good agreement at the lower frequencies. The higher frequency resonances obtained using finite element analysis differed from experimental values (see Fig. 1.4.2), because at higher frequencies the wavelength becomes comparable to the size of the element.

Resonance changes were obtained with the finite element program for a 33" wheel having a simulated plate crack. The reason for studying the plate crack was that it appeared to present a particular challenge to other NDE methods such as inspection with ultrasonic surface waves on the tread. Figure 1.4.3 shows the first six resonances and mode shapes for the cracked wheel. In Fig. 1.4.4 comparison is made between the resonances of a good and a bad wheel from the finite element model. The outstanding feature of this comparison is the apparent increase in the model density of the flawed wheel.

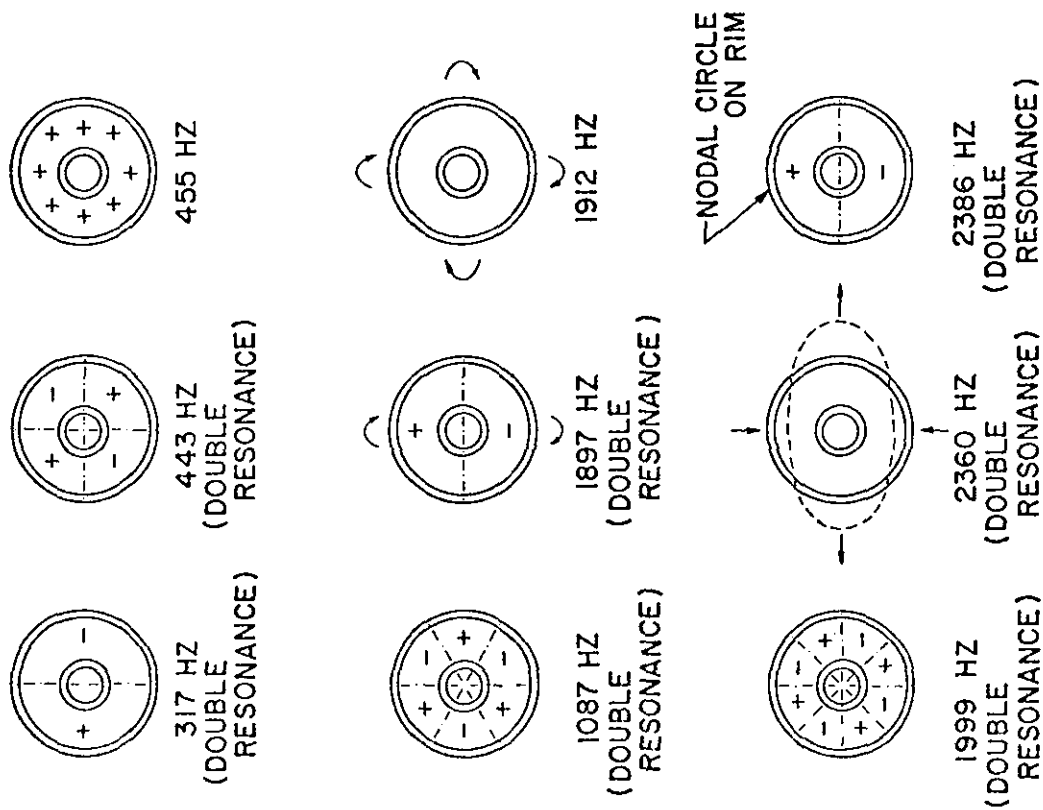


FIG. 1.4.1 MODE SHAPES OBTAINED WITH FINITE ELEMENT PROGRAM FOR 33" GOOD WHEEL. NOTE: THE HUB IS FIXED FOR ALL MODE SHAPES.

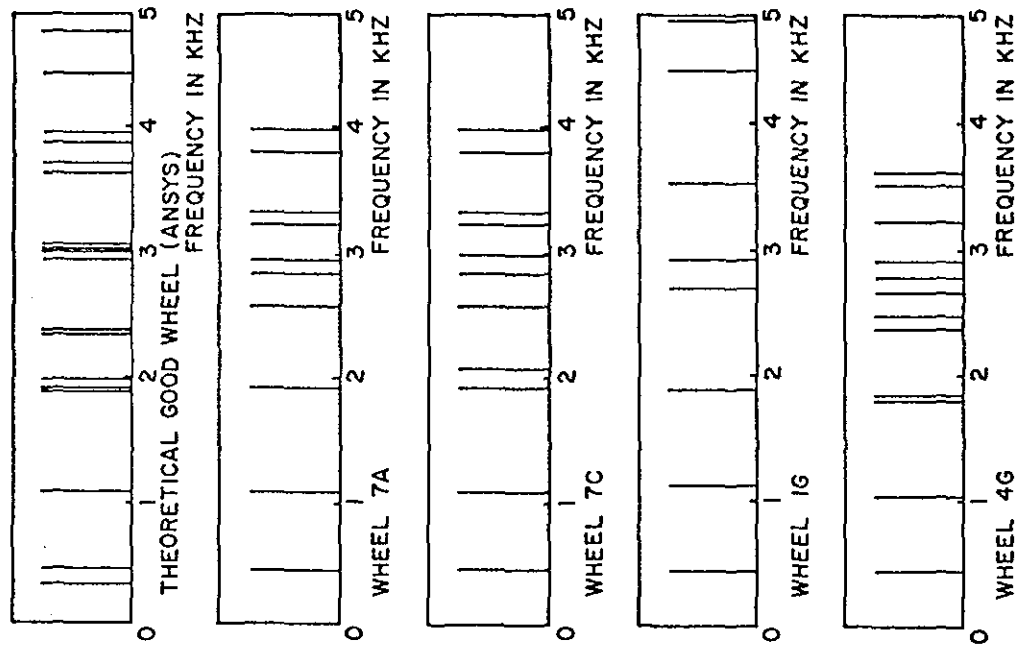


FIG. 1.4.2 LINE SPECTRA OF RESONANCES OBTAINED FROM THE ANSYS PROGRAM, COMPARED WITH EXPERIMENTAL SPECTRA FOR 33" GOOD WHEELS, OBTAINED BY USING A RAIL-MOUNTED ACCELEROMETER

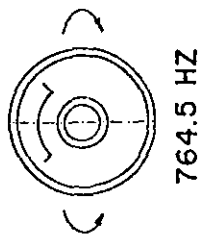
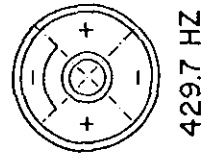
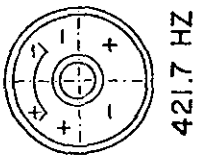
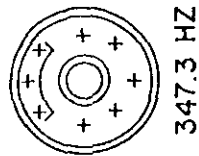
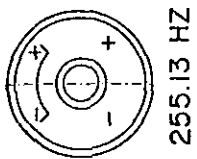
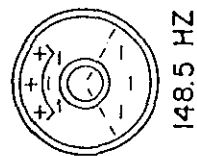


FIG.14.3 MODE SHAPES OBTAINED WITH ANSYS PROGRAM FOR 33" WHEEL WITH PLATE CRACK

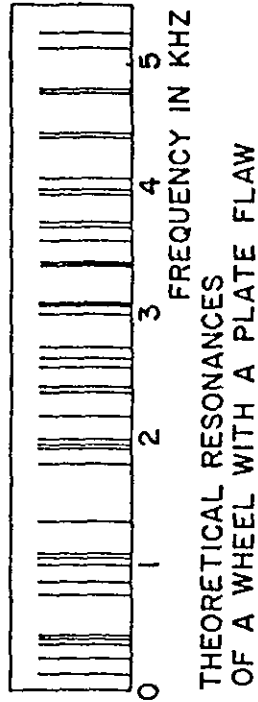
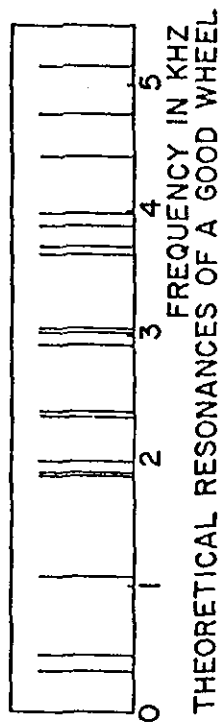


FIG.14.4 LINE SPECTRA OF RESONANCES OBTAINED FROM THE ANSYS PROGRAM FOR 33" GOOD AND FLAWED WHEELS

1.5 Experiments on Excitation and Detection Methods

In order to determine which of the various excitation methods would be most suitable a series of experiments were performed, during the feasibility study, both in the laboratory and in the field. Rolling noise was found to be predominantly low frequency sound from many sources and to mask the response of the wheel. Impact at a rail joint masks the wheel signature and even though some of the higher wheel resonances seem to be excited the response varies from wheel to wheel and with train speed. When passing through a retarder a wheel sometimes emits an intense screeching sound. It was found in this situation that only a few resonances of the wheel were excited, and different resonances were excited during successive passages of the wheel through the retarder. This lack of repeatability and the excitation of only one or two resonances ruled out the retarder as a choice of excitation.

When using active excitation methods, energy is imparted to the wheel from a device which is not part of normal railroad operations. In the feasibility study an electrodynamic shaker was used with random noise and sine wave inputs. This method of excitation does not appear to be feasible for field use. Tapping with a steel pendulum or a hammer excites a rich spectrum of wheel resonances (see Figs. 1.6.2 - 1.6.5). To obtain repeatability with this mode of excitation, it was found that there must be a good control of the momentum of the impacting hammer.

Various microphone and accelerometer configurations were experimented with. Except in the detection of flat spots [4], rail mounted accelerometers are not regarded as the best choice, the reason being that there are natural modes of vibration of the rail in the same frequency range as the wheel modes. These rail modes can be superimposed on the wheel signature thus compounding the difficulties of data processing. When a microphone is used only the sound from the wheel is detected because of the relatively small radiating area of the rail and its weak coupling to the wheel. Regulations permit installation of devices at ground level so that the microphone to receive airborne sound is best located close to the rails.

1.6 Variables in the Acoustic Signature

As part of the feasibility study wheel and axle sets were rolled over an automatic impacter (see Fig. 1.6.1) on the laboratory track. Unfortunately at the time this data was taken there was no provision in the system for a triggering pulse so that the timing of the scan made by the instrument could not be controlled relative to the duration of the impact sound. Even with this difficulty several interesting features were discovered.

Figure 1.6.2 shows the superposition of impact spectra from two good and equally worn Griffin 9 riser 33" wheels on either end of the same axle. The signal amplitudes differ somewhat but the values of the resonance frequencies are very closely reproduced. In contrast Fig. 1.6.3 shows the spectrum of one of these same wheels in comparison with the spectrum of a good Armco Wrought 33" wheel. There are some pronounced differences in the resonance frequencies. Even more differences in the resonance frequencies are

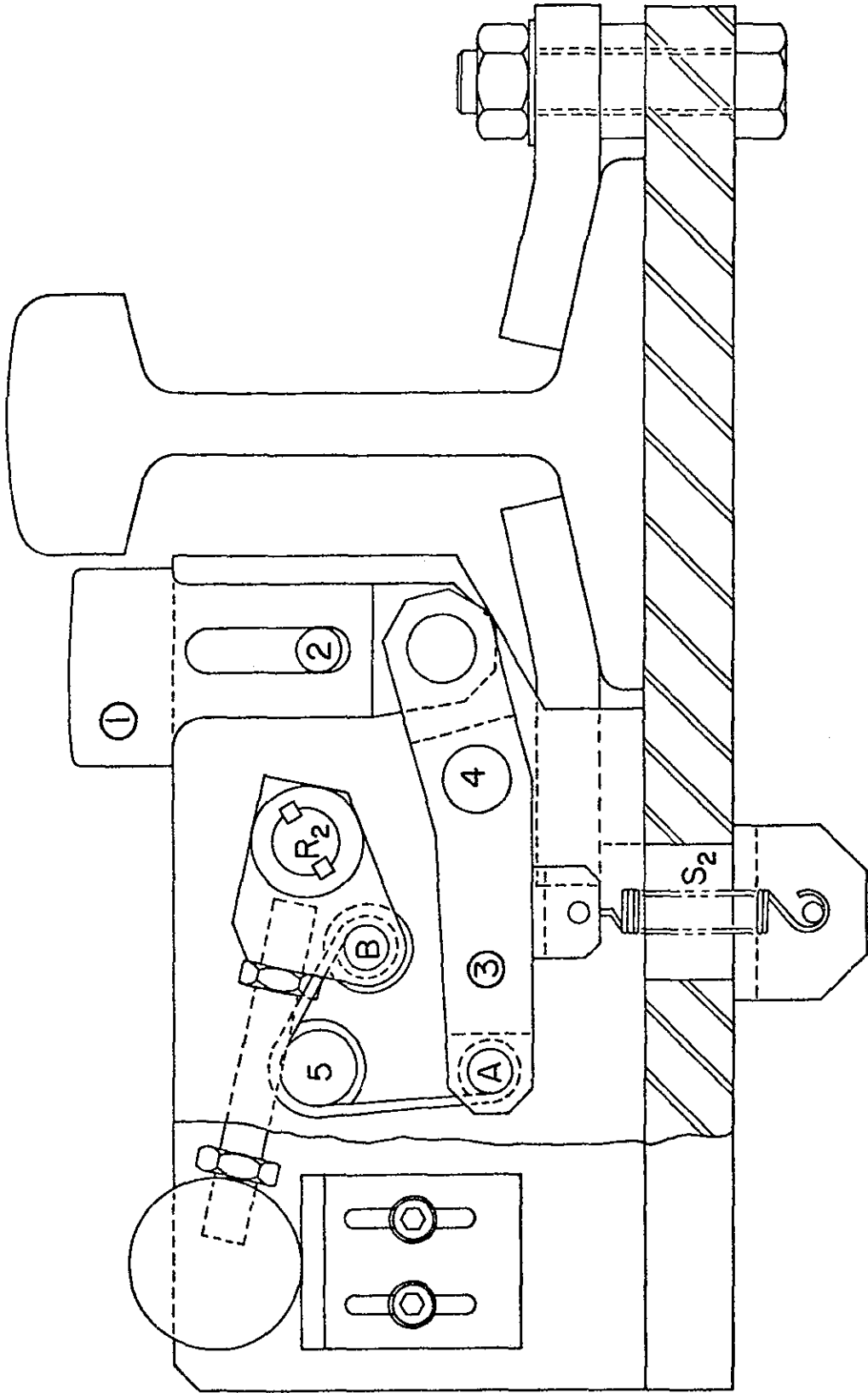


FIG. 1.6.1 DRAWING OF IMPACTER USED IN FIRST TEST

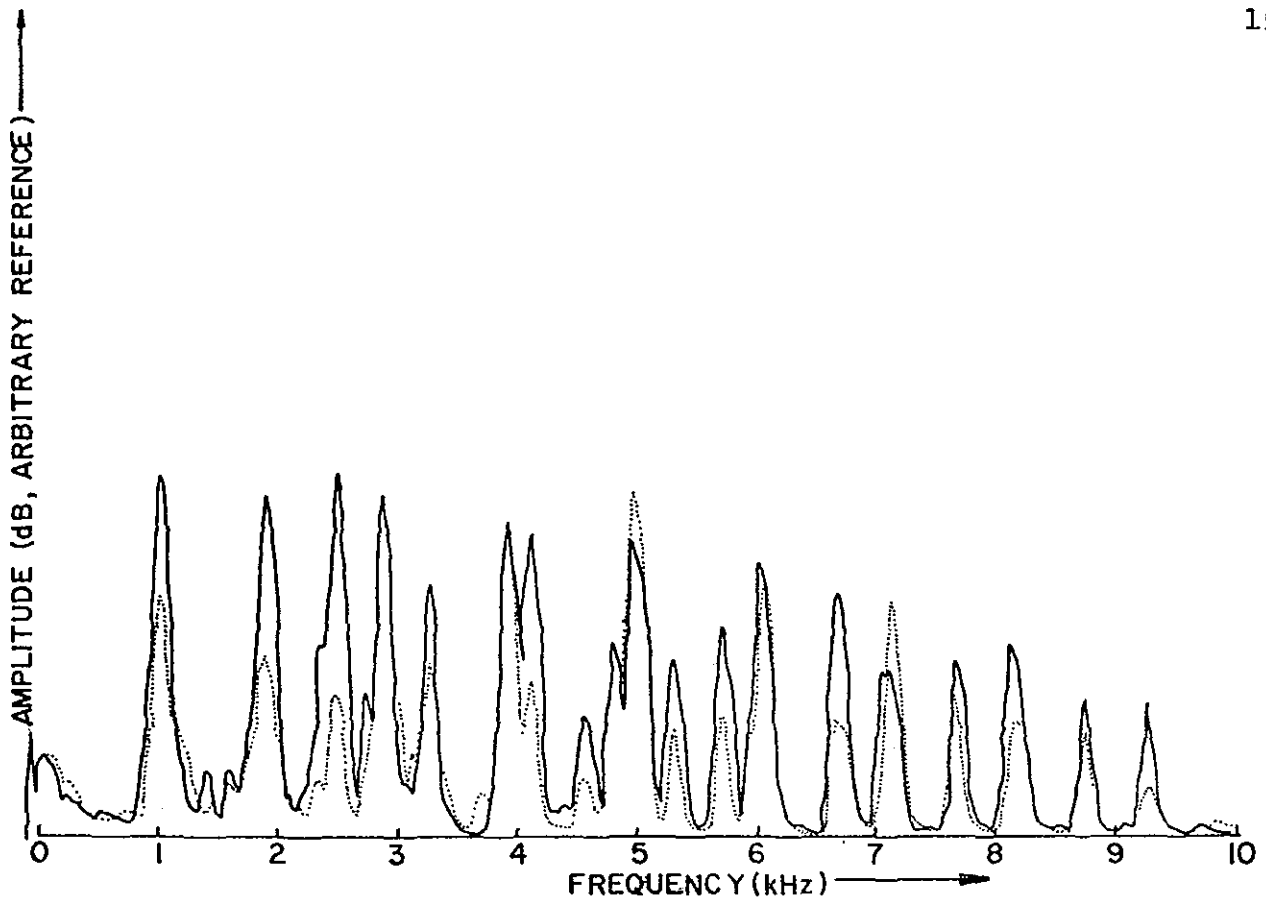


FIGURE 1.6.2 FIXED BAND SPECTRA OF IMPACT ON GOOD 33" WHEELS ON EITHER END OF THE SAME AXLE

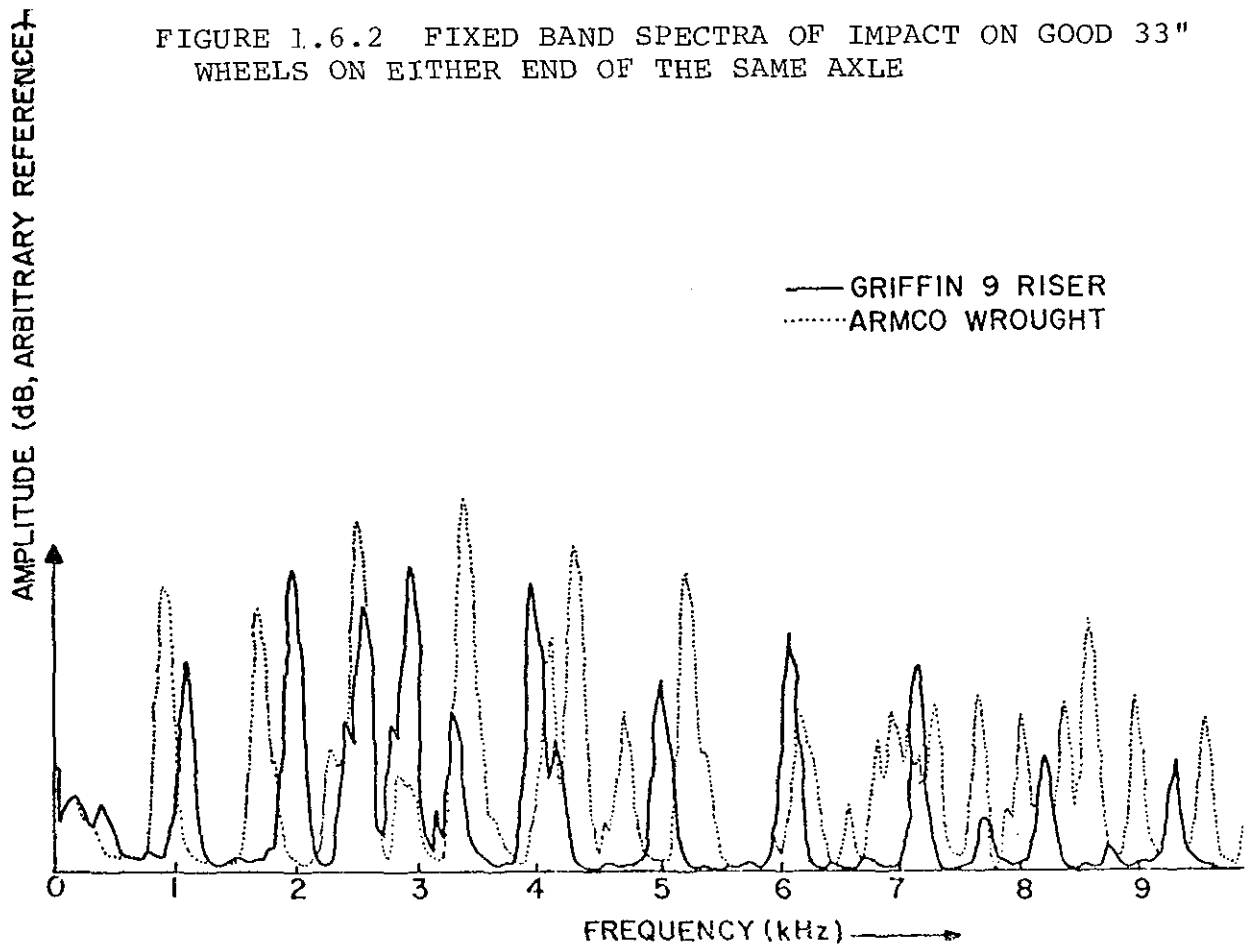


FIGURE 1.6.3 FIXED BAND SPECTRA OF IMPACT ON TWO GOOD 33" WHEELS ONE A GRIFFIN 9 RISER, ONE AN ARMCO WROUGHT

found between the spectra displayed in Fig. 1.6.4. These were obtained from two Southern 33" wheels on the same axle. One of them, however, has a thermal crack which has propagated clear through to the hub. Finally, Fig. 1.6.5 shows the comparison of the spectra of two identical good wheels (33" Southern), one of which has a heavy layer of grease. The most interesting aspect of the spectrum of the greasy wheel is the complete absence of sound above about 4 kHz. This was presumably due to damping of the plate vibrations. This feature, i.e., the damping of high frequency resonances, could be used as a means of identifying the spectra of greasy wheels, which might otherwise be mistaken for cracked wheels and give rise to a false alarm.

Also as a part of the feasibility study some laboratory experiments were performed with wheel pairs in a stationary load frame using a hydraulic jacking system to simulate loads up to 20 tons. Figure 1.6.6 shows a series of spectral analyses, each with increasing load. The traces are superimposed on one another but slightly offset to give a three dimensional perspective. Some resonances are enhanced by the load; some are diminished. Most shift slightly in frequency and some split into two separate resonance peaks. On the other hand, if one does not use too fine discrimination, it is clear that the changes do not produce complete disorder in the three-dimensional plot.

1.7 Laboratory Demonstration System for Finding Cracks

As the last part of the feasibility study a laboratory demonstration system was assembled to simulate field opera-

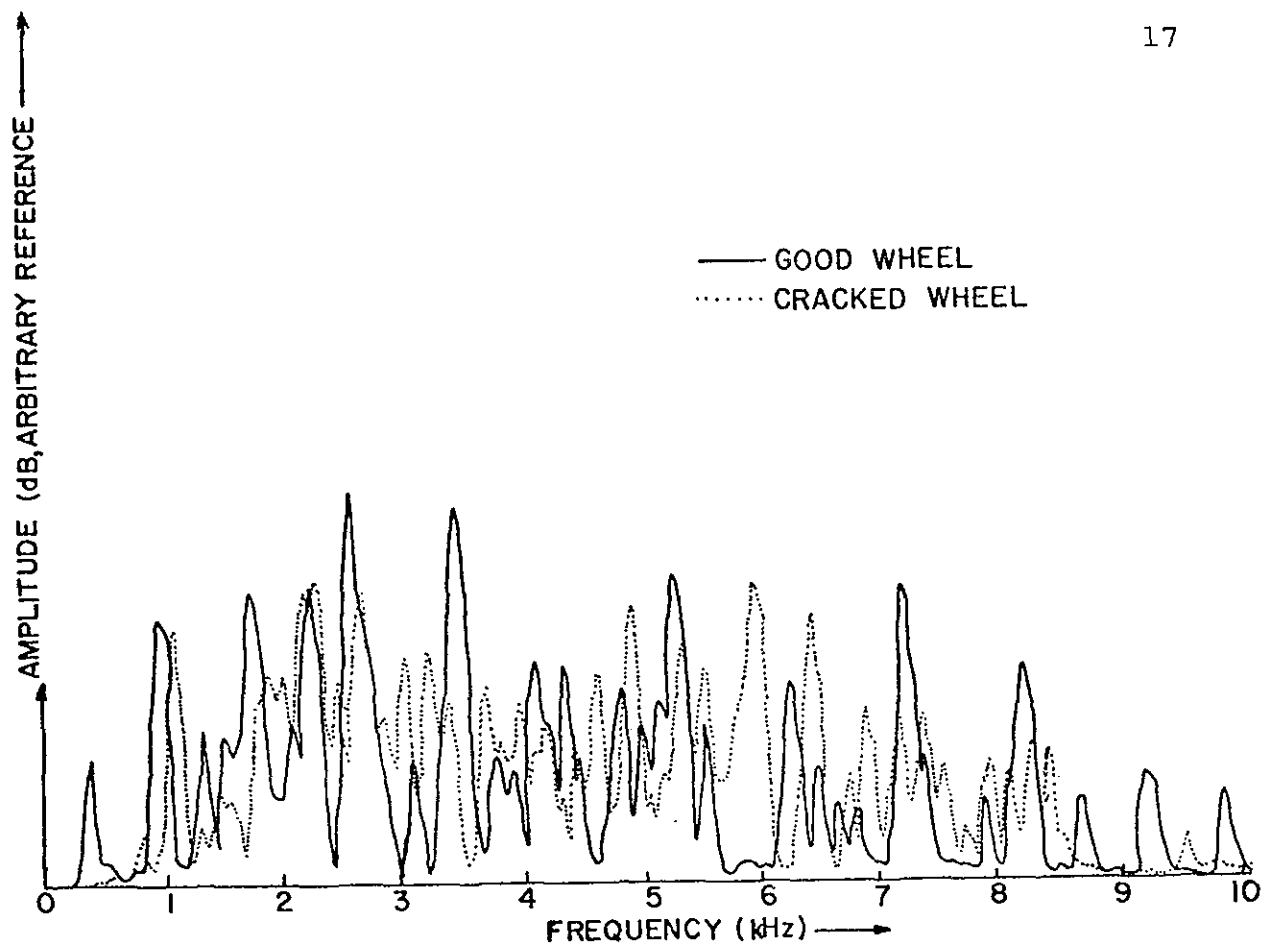


FIGURE 1.6.4 FIXED BAND SPECTRA OF IMPACT ON 33" SOUTHERN WHEELS, ONE WITH A LARGE THERMAL CRACK

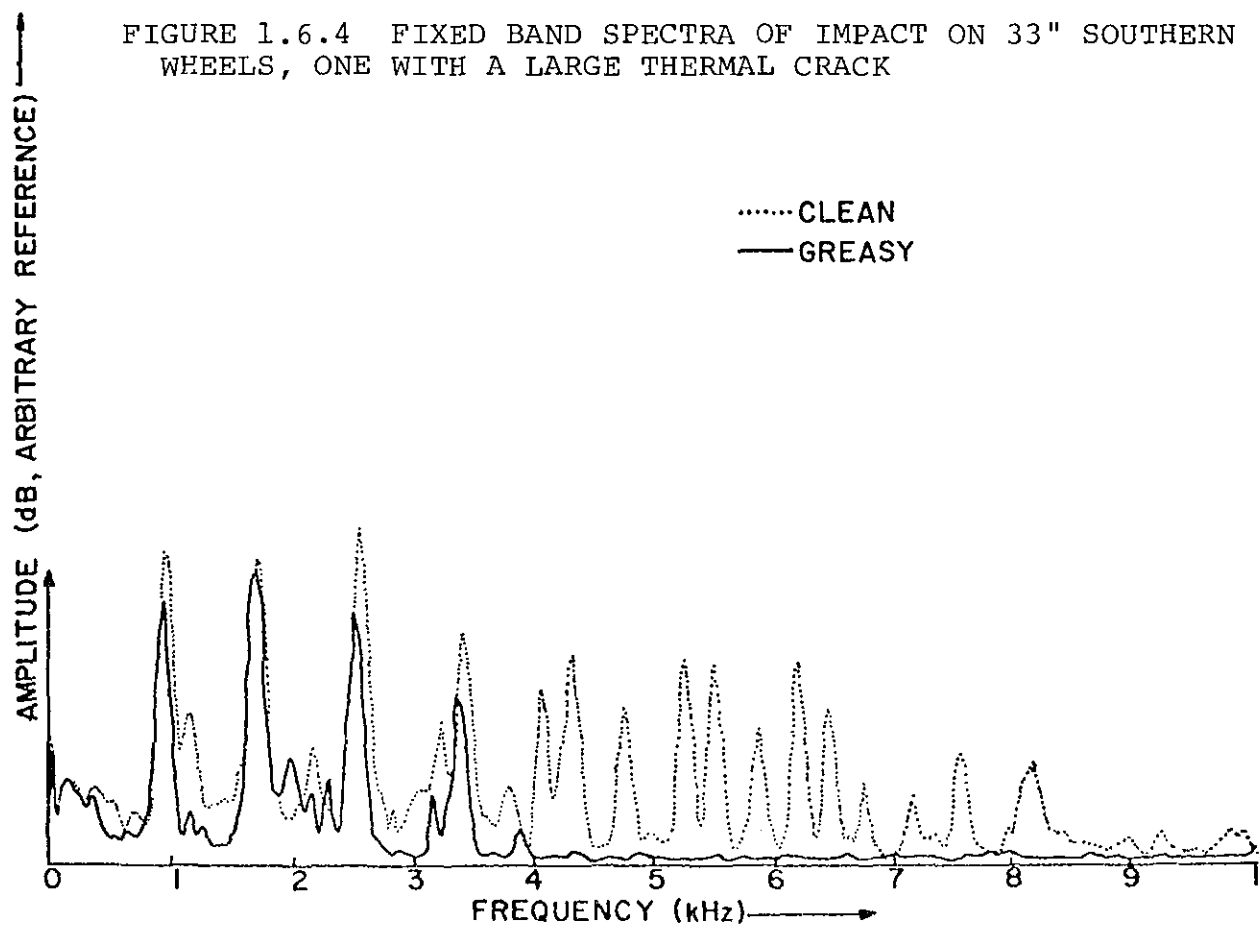


FIGURE 1.6.5 FIXED BAND SPECTRA OF IMPACT ON TWO 33" SOUTHERN WHEELS, ONE WITH A THICK LAYER OF GREASE

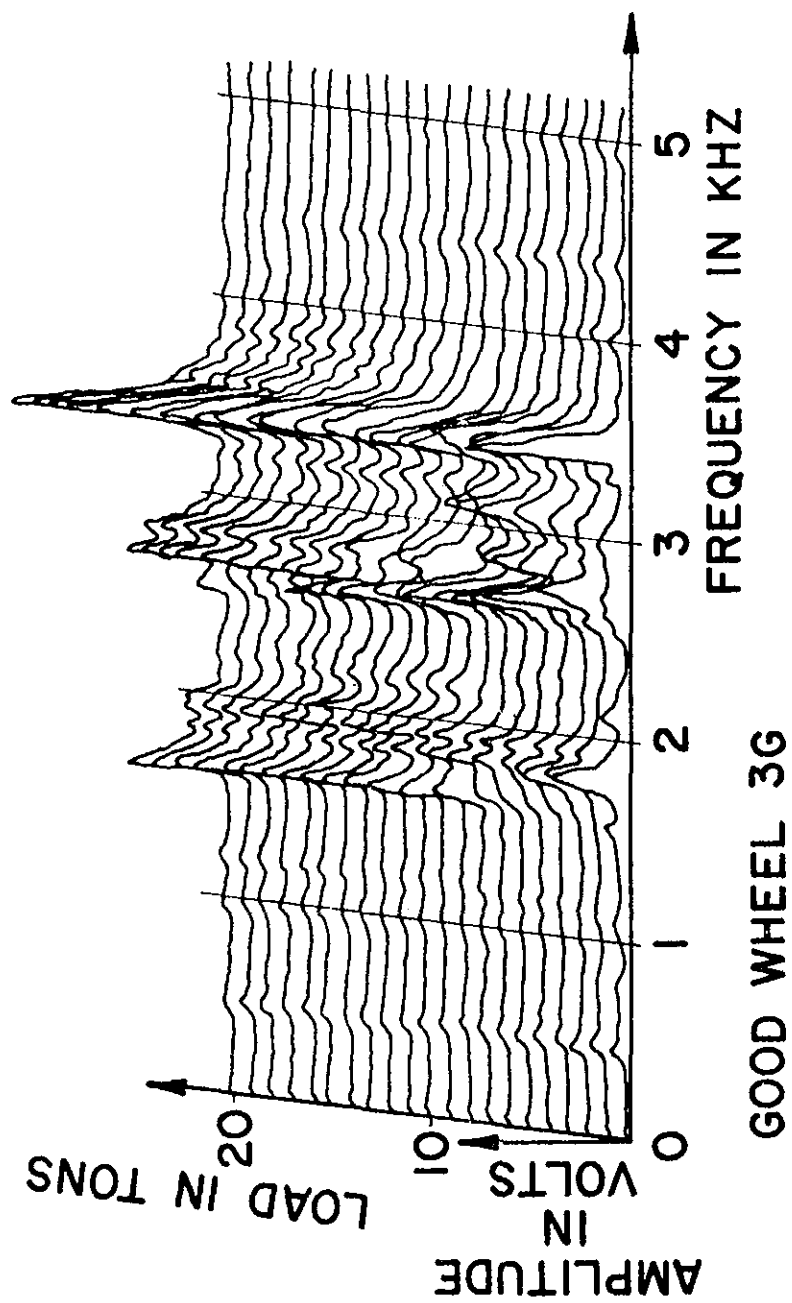


FIG.166 VARIATION OF WHEEL SIGNATURE WITH
LOAD FOR WHEEL 3G. (ACCELEROMETER PICKUP)

tions as far as possible. For this phase of the work only the third octave band analyzer was available. This was interfaced with the NOVA minicomputer. The minicomputer was programmed to read a given spectrum, generated by impact of a hammer or pendulum, and to compare this spectrum with either: 1) a standard spectrum, i.e., the average spectrum of good wheels, continuously averaged on a weighted basis, or 2) the spectrum of the mating wheel on the same axle. The output of the program was a number which is the sum of the squares of the differences in dB between the two spectra in the various third octave bands.

In Table 1.7.1 are tabulated values that were calculated in this way for a set of wheel signatures obtained from impact tests. Of all the wheels that were tested there was one wheel where the performance of the classifier was questionable. Wheel 8G did not have any apparent cracks, but it was worn beyond serviceable limits.

1.8 Preliminary Field Tests

Subsequent to the feasibility study, two preliminary field tests of the impacting system for crack detection were carried out. The first test was performed at the Omaha East Yard of the Union Pacific. Only one impacter was available so that across axle comparison was not possible. No timing pulse was provided for and the hammer arm broke at a train speed of about 17 mph. The second test, performed at the Southern Pacific's Englewood Yard in Houston, was more successful and will be briefly described. Because of the variations in signature due to wheel geometry,

TABLE 1.7.1 SUMS OF DIFFERENCES OF WHEEL SPECTRA FROM AVERAGE
GOOD WHEEL SPECTRUM (IMPACT EXCITATION)

- NOTE: a) Good wheel average based on all good wheels,
b) Summing of differences in dB for 1/3 octave bands
with center frequencies of 1.6 KHz to 8 KHz,
c) All spectra for this table were obtained by tapping
on the rim of the wheels with a steel bar.

WHEELS	ACTUAL CONDITION	CONDITION INDICATED BY CLASSIFIER WITH DISCRIMINA- TION LEVEL=70	DIFFERENCE FROM AVERAGE SIGNATURE	DIFFERENCE BETWEEN SIGNATURES OF WHEELS ON SAME AXLE
1G	Good	Good	27	157
1B	Flawed	Flawed	184	
3G	Good	Good	35	49
3B	Flawed	Flawed	84	
4G	Good	Good	41	82
4B	Flawed	Flawed	123	
8G	Good	Flawed	128	7
*Mispick	Badly Worn			
8B	Flawed	Flawed	121	
7A	Good	Good	42	4
7C	Good	Good	38	
9A	Good	Good	51	100
9C	Flawed	Flawed	151	
10A	Good	Good	63	4
10C	Good	Good	67	
11A	Good	Good	28	26
11C	Good	Good	54	

load, grease etc., the basis of this test was a comparison of spectra from wheels at either end of axle. Figure 1.8.1 shows the train consist in the test. Identical impacters were installed on the two rails, one train length apart. There were two defective wheels. Wheel N15 had a larger thermal crack and wheel S12, a shattered rim. The train was run forward and backward in successive runs and the sound tape recorded for laboratory processing.

Figure 1.8.2 shows typical printout using cross axle comparison with third octave band analysis. Car 5 is the engine. The numbers in the column labelled "Across Axle Comparison" are the sums of the algebraic differences in third octave band spectra of the two wheels. The decision that a wheel is bad is based upon this number exceeding 10.

1.9 Objectives of the Present Study

It was concluded from the feasibility study that it should be possible to use acoustic signature inspection for detection of thermal and plate cracks in railroad wheels. It appeared that the best form of excitation for detecting cracks is by impact and that the best sensor is a microphone. The cracks cause shifts in resonance frequencies and these shifts can be observed best in narrow band analysis but are also manifest in third octave band analysis. Grease layers cause damping of resonance lines above about 5 kHz. Recognition of defective wheels can be carried out by comparing sound spectra with a standard or by comparing the sound spectra of wheels on either end of an axle.

It was with this background that the present project was formulated. The overall objective was to obtain information on the parameters that might affect or limit the performance of an acoustic signature inspection in actual operation, as opposed to laboratory operation or operation in controlled field tests. To achieve this end the program was divided into three parts: first, to improve and expand scientific knowledge of the wheel's acoustic signatures; second, to improve the design of various system components; third, to test the improved system for an extended period under actual operating conditions.

Regarding the first part of the program, improvement of scientific knowledge, both experimental and theoretical studies were planned. The intention was to obtain a better grasp of the effect on signatures of wheel geometry, wheel wear, the wheel's internal state of stress, and various environmental conditions. Some of these studies were carried out at the DOT's Transportation Test Center at Pueblo, Colorado, some at the Griffin Wheel Company's plant at Bessemer, Alabama, and some at the Westinghouse plant at Wilmerding, Pennsylvania. It was decided to extend the theory of wheel vibrations to gain additional insight into the effects of a) variations in wheel geometry, b) variations in crack sizes and locations, c) various forcing functions and d) variation in internal stress.

Under the second part of the program, improvements in system component design, there were several major

developments. Firstly, the design of the excitation mechanism was subjected to some scrutiny, with a view to improving its reliability and operating speed range. The second major change was the acquisition of a narrow band RTA, its interfacing with the existing NOVA computer and the addition and interfacing of a diskette memory unit. Finally, reliable commercially made microphones and wheel sensors were acquired.

The final system test, the third part of the program, was carried out at the Southern Pacific's Englewood Yard in Houston. The objectives of this test were to elucidate remaining problems with the system and to ascertain, if possible, information on false alarm rates.

The study was concluded with a sensitivity analysis of the data recorded during the field tests. System problems were elucidated, an optimum form of the difference index (DI) equation was ascertained and the major cause of high DI values in uncracked wheels was determined.

2. THEORY OF RAILROAD WHEEL VIBRATIONS

2.1 Introduction

A brief summary of previous work on wheel vibrations was presented in Section 1. In these earlier studies a number of elementary models were considered and commercially available computer programs were used to simulate the vibrations of good and defective wheels. The cross section of a typical railroad wheel is shown in Figure 2.1.1. Ring or circular plate models are the simplest approximations that can be used. In the feasibility study of flaw detection in wheels using acoustic signatures, Nagy modeled the one-fourth scale model wheels and later full size wheels as flat annular plates. He also reviewed the literature on these subjects and concluded that the ring model gave a better fit to wheel data. The most accurate theoretical approach is to analyze the actual wheel geometry using finite element analysis. Nagy used the ANSYS program to study the vibrations of a good 33-inch wheel and compared those with the response of a defective wheel having a plate crack. His work was extended later by Chaudhari who studied the vibrations of wheels with different types and sizes of cracks, applying single or repetitive impulse excitation. Chaudhari's work improved on Nagy's by using more elements and more realistic boundary conditions. (The wheels were fixed at the hub and

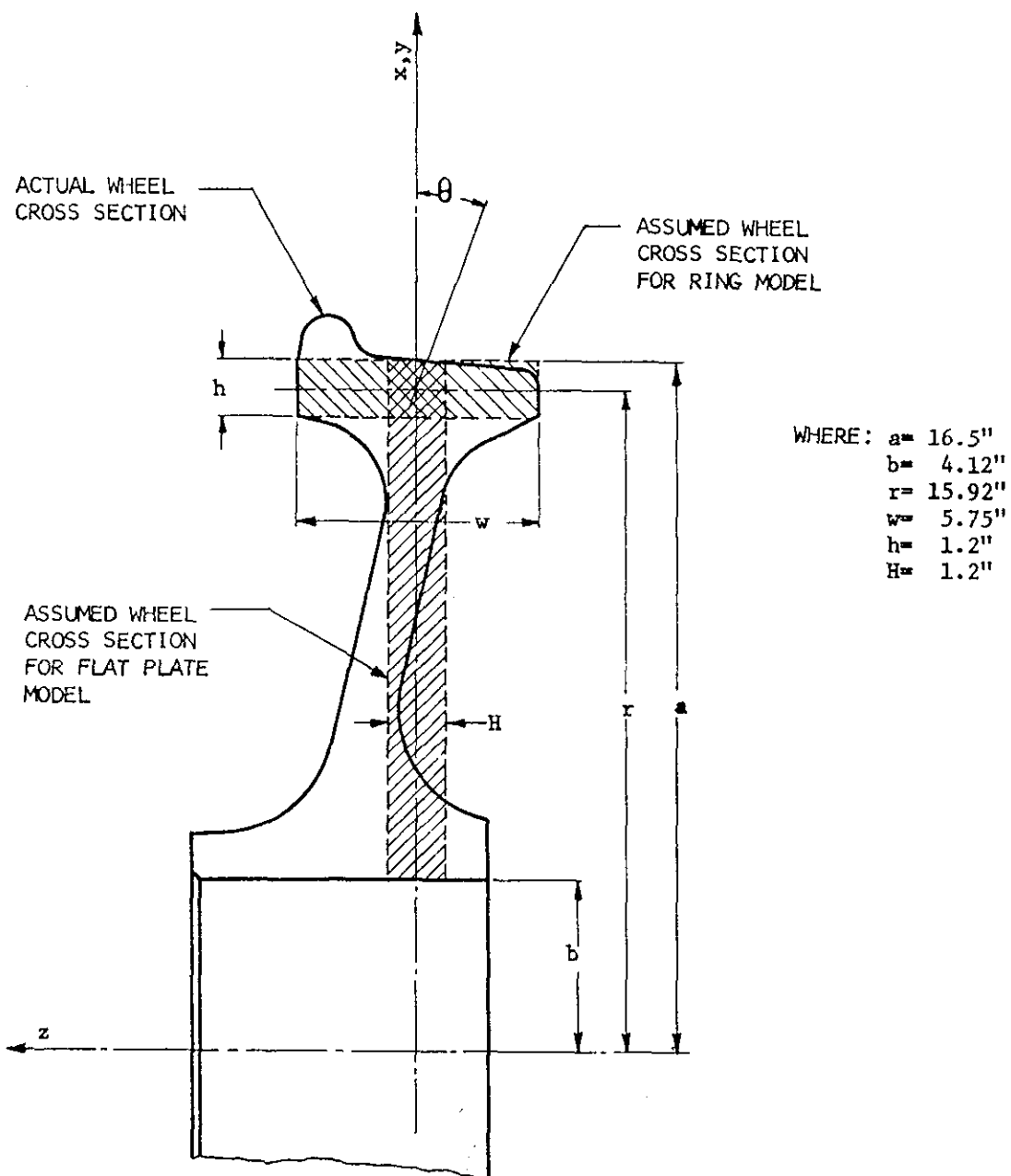


Fig. 2.1.1 Assumed and Actual Wheel Cross Sections

in addition at one node on the tread to simulate the contact of the wheel with the rail.) An abbreviated version of Chaudhari's work is presented in Appendix F.

Although the finite element approach is ultimately the most accurate it is expensive and time consuming. The more elementary models, especially Stappenbeck's [17] ring theory, can be used to gain an insight into certain effects, as explained in later sections, with comparative ease.

2.2 Stappenbeck's Ring Model of Wheel Vibrations

Stappenbeck [17] showed that the well known theory of the vibrations of rings could give a good explanation of the sounds emitted by a vibrating railroad wheel. To see why this is so it is appropriate to review his reasoning. The vibration of rings was first treated in 1890 by Mitchell [52], as an extension of the theory of bars, by regarding the ring as a curved bar whose two ends are joined together. Flexural modes of vibration, with displacements either in the plane of the ring or out of the plane, are the most readily excited.

For out-of-plane flexure the resonant frequencies are given by:

$$f_n = \frac{1}{2\pi} \left[\frac{EI_x}{\rho A r^4} \frac{n^2(n^2 - 1)^2}{(n^2 + 1 + \nu)} \right]^{1/2} \text{ for } n = 1, 2, 3, \dots \quad (2.2.1)$$

where

E = Young's modulus

A = the cross sectional area,

I_x = the moment of inertia of cross section with
respect to an axis in the plane of the ring,

r = the radius of the ring,

ν = Poisson's ratio,

n = the ratio of the number of wavelengths to the
circumference,

and ρ = the density of the ring.

It should be noted that the case for $n = 1$ yields a zero resonant frequency. This is not a vibrational mode and the motion consists of a free rotation about a diameter. The lowest vibrational mode occurs when $n = 2$, in which case there are four nodal points on the ring.

Now consider the addition of a thin circular plate within the ring. Again, in the case of a plate, the most readily excited modes are flexural. Thus when the coupling of ring and plate modes is considered, it may be seen that the out-of-plane flexure of the ring will readily couple with plate modes having an integral number of nodal diameters. Because the wheel rim is massive in comparison to the plate this was the model Stappenback proposed for the vibrations of the wheel and he demonstrated that the sound radiated from 765 mm diameter streetcar wheels contained a series of prominent resonances whose frequency ratios corresponded closely to values obtained from eqn (2.2.1). (Assuming the fundamental mode occurs when $n = 2$, the ratios of the frequencies of the higher order modes to the fundamental are 2.87, 5.53, 8.98,

13.2, for $n = 3, 4, 5, 6, \dots$ respectively). With this viewpoint in mind the massive rim forces the plate into vibration, and the plate is then the primary sound source because of its larger radiating surface. An alternative model, in which the plate forces the rim into vibration, was investigated by Nagy [1]. The ratios of the prominent resonance frequencies did not fit the experimental results.

The conclusion is then that the prominent resonances in the acoustic spectrum are due to wheel modes with two, three, four or more nodal diameters. This does not imply that other modes of vibration cannot be excited. Indeed the author has been able to excite the wheel in a vibratory mode with a single nodal diameter. (The hub of the wheel provides a stiffness for this mode which would not exist for an unconstrained plate.) Such a mode is also revealed by the finite element analysis. Numerical results for such experiments are shown in Table 2.2.1. The two columns showing the experimental results are for two different types of 33-inch wheel. The left-hand column corresponds to a wheel having the same cross-section as in Fig. 2.1.1, and the right-hand column corresponds to a 33-inch Griffin wheel having cross section as in Fig. 4.2.1. Three variations of calculations using the ring model are given. In column A the results are those given by Nagy. An attempt to improve these results was made by modeling the wheel as a ring with cross section identical to the

TABLE 2.2.1 LIST OF RESONANCES CALCULATED WITH
THE RING MODEL COMPARED WITH ANSYS
RESULTS AND EXPERIMENTAL DATA

Modes with Ring Model (Flex- ural Modes Perpendicular to Plane of Ring)					Experimental Resonances for 33" Wheel		ANSYS
n	approx. shape	frequency in Hz			freq. in Hz		freq. in Hz
		A	B	C			
1	↑	0	0	0	—	324	317
2	+	549	476	417	420	435	443
3	✱	1579	1365	1196	1093	1147	1087
4	✱	3049	2632	2308	1890	2018	1999
5	✱	4948	4271	3743	—	2990	—
6	✱	7272	6275	5501	—	4012	—

*

*

Note: Columns undermarked with an asterisk show results
obtained by Nagy.
A, B, C are three assumed ring cross-sections,
as shown in Fig. 2.2.1

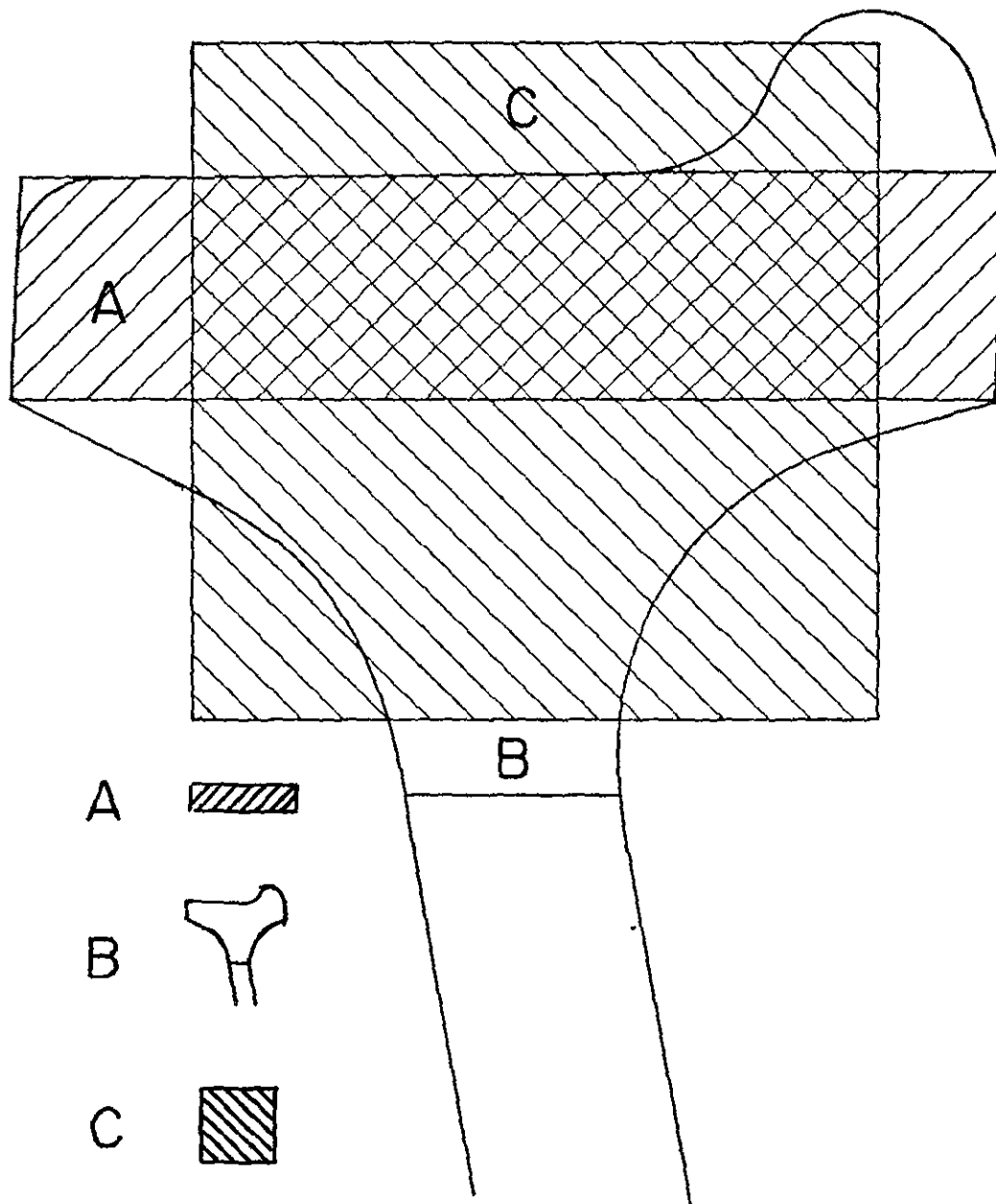


FIG. 2.2.1 CROSS SECTIONS FOR RING MODEL

rim. The radius of the ring was estimated after evaluating the centroid of the cross section by numerical-graphic integration. The area moment of inertia about the neutral axis was evaluated in a similar way. The results, shown in column B, are a much closer fit to experimental measurements than obtained from the rectangular cross section (see Fig. 2.2.1) model used by Nagy. Even better results are obtained using an "equivalent" square cross section. The optimum selection was a 4" x 4" cross section with corresponding radius of 15.1". The mode evaluation based on this model shows almost identical frequencies for the two nodal diameter mode and reasonable correspondence with experiment for the other nodal diameter modes. Comparison with the results from the ANSYS program also shows good agreement. The major point to be made is that Stappenbeck's ring model is a surprisingly good predictor of the prominent resonances of the acoustic spectrum of actual wheels.

2.3 The Effect of Uneven Wear on Wheels Across the Axle

A theoretical explanation of the effect of uneven wear can be given in terms of Stappenbeck's simple theory of wheel vibrations. The series of resonant frequencies is given by the expression (2.2.1). It is clear that uneven wear on a wheel pair will result in differences for I_x , A and r for the two wheels. Rewriting eqn. (2.2.1) to break out these factors, which are related to the wheel geometry, we have:

$$f_n = \frac{1}{2\pi} \left[\frac{E}{\rho} \right]^{1/2} \left[\frac{I_x}{Ar^4} \right]^{1/2} \left[\frac{n^2(n^2 - 1)^2}{n^2 + 1 + \nu} \right]^{1/2}$$

or

$$f_n = B \left[\frac{I_x}{Ar^4} \right]^{1/2} \left[\frac{n^2(n^2 - 1)^2}{n^2 + 1 + \nu} \right]^{1/2}$$

where B is a constant dependent on the material properties of the wheel. We shall assume that these properties are unaffected by wear. Assuming that the rim can be modelled as a ring of rectangular cross section (see Fig. 2.2.1), with width w and thickness h,

$$A = hw$$

and

$$I_x = \frac{hw^3}{12}$$

Hence,

$$f_n = \frac{B}{\sqrt{12}} \frac{w}{r^2} \left[\frac{n^2(n^2 - 1)^2}{n^2 + 1 + \nu} \right]^{1/2} \quad (2.3.1)$$

The effect of wear will be to reduce the effective radius r, but not the rim width w. Hence the change in frequency of the n^{th} mode will be:

$$\begin{aligned} |\Delta f_n| &= \frac{2B}{\sqrt{12}} \left[\frac{n^2(n^2 - 1)^2}{n^2 + 1 + \nu} \right]^{1/2} \frac{w \Delta r}{r^3} \\ &= \left(2 \frac{\Delta r}{r} \right) f_n \end{aligned}$$

Finally, since a change in the effective radius is approximately one half of a change in rim thickness, Δh , for small changes,

$$|\Delta f_n| = \left| \frac{\Delta h}{r} \right| f_n \quad (2.3.2)$$

Thus, for a given wheelset, a difference in wear on the two wheels, in the amount Δh , should result in frequency shifts proportional to the resonant frequencies. Experimental results which are in agreement with this finding, to a first approximation, are given in Section 7.

2.4 The Effect of Residual Stress*

The current interest in residual stress and its influence on the creation and propagation of cracks in wheels can be seen from the number of recent papers on this topic. Bray [18] cited 15 papers related to the subject at the 5th International Wheelset Conference in 1976. Wetenkamp and Kipp [19] and Yavelak and Scott [53] have also given papers on this subject recently.

The most general treatment of the dynamics of elastic media under initial stress was given by Biot [20, 21] who concluded that the presence of an initial stress tends to modify the effective rigidity of the medium. In general, tension tends to increase the rigidity, whereas compression tends to decrease it. The result is a corresponding increase or decrease in the frequency of the natural modes of a finite body. There are a number of well known examples of such effects, the vibrations of strings under tension and rods under load being among the best known.

*The definition of residual stress in this context refers to the system of stresses which can exist in a body when it is free from external forces, temperature gradients and rotational motion. In the case of a wheel these stresses are located in manufacture and may be modified in service.

There have also been a number of recent papers on the effect of in-plane forces on the vibration of plates [22-27]. For present purposes it is of considerable interest to realize that the well known effect of axial load on the natural modes of a bar can be applied to the problem of measuring wheel stresses. Following Stappenberg's model, a compressive or tensile stress in the wheel rim should have an effect similar to that found in a loaded bar.

For a simply supported vibrating beam under compression the natural frequencies of flexural vibrations are given [50] by:

$$\omega_n^2 = \frac{EI n^4 \pi^4 - Fl^2 n^2 \pi^2}{\rho A l^4} \quad , \quad (2.4.1)$$

where

l = the length of the beam,

F = the compressive axial force,

A = the cross sectional area,

ρ = the density,

EI = the flexural rigidity,

but the frequency of the n^{th} mode of the beam without external stress is

$$\omega_{n0}^2 = \frac{EI n^4 \pi^4}{\rho A l^4} \quad . \quad (2.4.2)$$

Then

$$\omega_{n0}^2 - \omega_n^2 = \frac{Fn^2 \pi^2}{\rho A l^2} \quad ,$$

For small frequency changes

$$\omega_{n0} + \omega_n \approx 2 \omega_{n0} .$$

Thus

$$(\omega_{n0} - \omega_n) 2\omega_{n0} = \frac{Fn^2 \pi^2}{\rho A l^2} ,$$

or

$$\Delta \omega_n = \frac{F}{2\{EI\rho A\}} l^{1/2} . \quad (2.4.3)$$

This result implies that the frequency shifts are the same for all modes and are proportional to the applied force. Since the ring model simply assumes that the rim is a circular bar, flexural vibrations of wheels with uniform compressive or tensile residual stresses in the rim should show similar effects; i.e., if a uniform stress is induced in the rim, all modes should show the same numerical change in resonant frequency. Some experimental results which appear to be consistent with this concept are presented in Section 4.

3. EXPERIMENTS ON WHEEL GEOMETRY AND MINIMUM DETECTABLE CRACK SIZE

3.1 Introduction

There were certain questions which could not be readily answered from the theoretical study and it was decided to tackle these by obtaining experimental data. There were two main tasks in this work: firstly, the compilation of a data bank of signatures of wheels with different geometries and from various manufacturers, and secondly, a study of the minimum detectable crack size.

3.2 Data Bank of Wheel Types

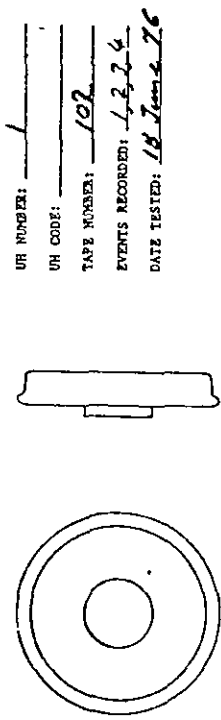
In brief, the idea behind this study was that the acoustic signatures of all types of good wheels and the signatures of all types of defective wheels might belong in two different clusters and there might be no overlapping in their characteristics. If this were the case a decision scheme for flaw detection could be based on the comparison of the signature of the wheel under test with a set of good wheel signatures. If the signature matched any of the good wheel signatures it would be declared a good wheel of a certain type, and if not, defective. A computer or other type of file that has the signatures of all geometrical variations of good wheels would house the data bank.

In order to develop the data bank, the Southern Pacific Transportation Company provided a number of new and used wheels for testing in their Houston repair shop facilities. A total of 34 wheels were tested and 136 wheel signatures were obtained. The sample included wheels of cast and wrought construction, having flat and dished plate configurations. Single wear and multiple wear rims were also encountered. The information acquired was kept in a data bank book, in the form of a series of description sheets as shown in Fig. 3.2.1a, accompanied by the signature plots, one of which is shown in Fig. 3.2.1b. For these tests an inclined guideway was constructed (see Fig. 3.2.2) and was used as a path guide for a 1.5 inch steel ball. Near the bottom end of the incline a photosensor unit was installed to detect the presence of the ball immediately before the impact. The photosensor's signal was recorded on the triggering pulse channel of a dual channel GR* recorder for later acoustic signature analysis in the laboratory. The design assured reproducible and constant force impact on the lower inner rim of the wheel. Acoustic signature tests were conducted on the wheels listed in Table 3.2.1.

3.3 Results from Data Bank Tests

About ten different types of wheels were tested in the SP shops. Another 14 axles having good/good and

*General Radio

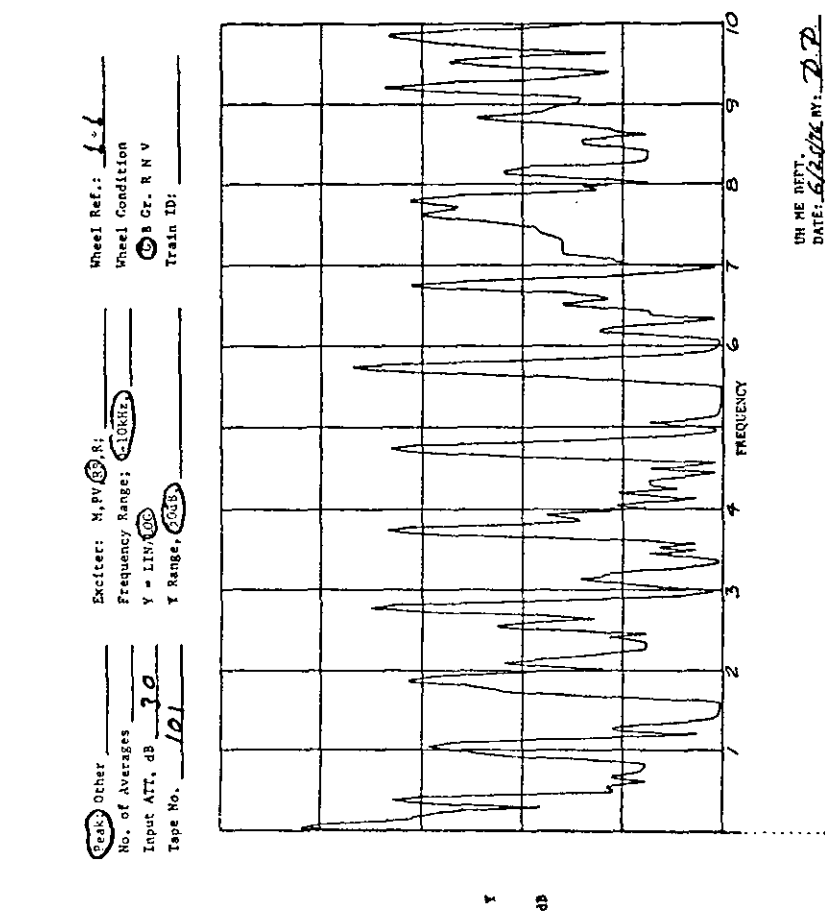


WHEEL DESCRIPTION
 WHEEL ID: 3-10-76 CJ52240 CJ33
 MANUFACTURER: SOUTHERN
 DIAMETER: 28 30 32 36 40
 CAST ☒ WROUGHT ☐ PLATE: DISHED ☐ FLAT ☒ HUB: 1W ☒
 CONDITION: GOOD ☐ BAD ☐ GREASY ☐ RUSTY ☐ NEW ☒ USED ☐
 DEFECTS: SLID FLAT ☐ THERMAL CRACK ☐ CRACKED FLAT ☐
 OVERHEATED ☐ OTHER ☐

TEST INFORMATION
 LOCATION: UN ☒ SPR ☐ OTHER ☐
 TRAIN ID:
 RECORDER TYPE: ☒ N ☐ S TAPE SPEED: ☒ 1 1/2 ☐ 3 3/4
 BACKGROUND LEVEL: 62 PEAK SPL: 96 ATTENUATION: 70 80 90 100
 IMPACTOR TYPE: MECHANICAL ☐ PNEUMATIC ☐ ROTARY ☐
 ROLLING BALL BEARING ☒ 1 1/2 ☐ FULL ☐ ANGLE 30
 LOCATION ON THE TRACK: N S ☒ W L R
 ROLLING WHEEL DIRECTION: N S E W STATIONARY ☒
 AXLE SPEED:
 NOTES & COMMENTS

UN ME DEPT.
 DATE: 18 June 76
 BY: W. J. Jimenez

FIG. 3.2.1a WHEEL INFORMATION AND TEST DESCRIPTION FORM



UN ME DEPT.
 DATE: 5/2/76 BY: D.P.

FIG. 3.2.1b ACOUSTIC SIGNATURE PLOT FORM

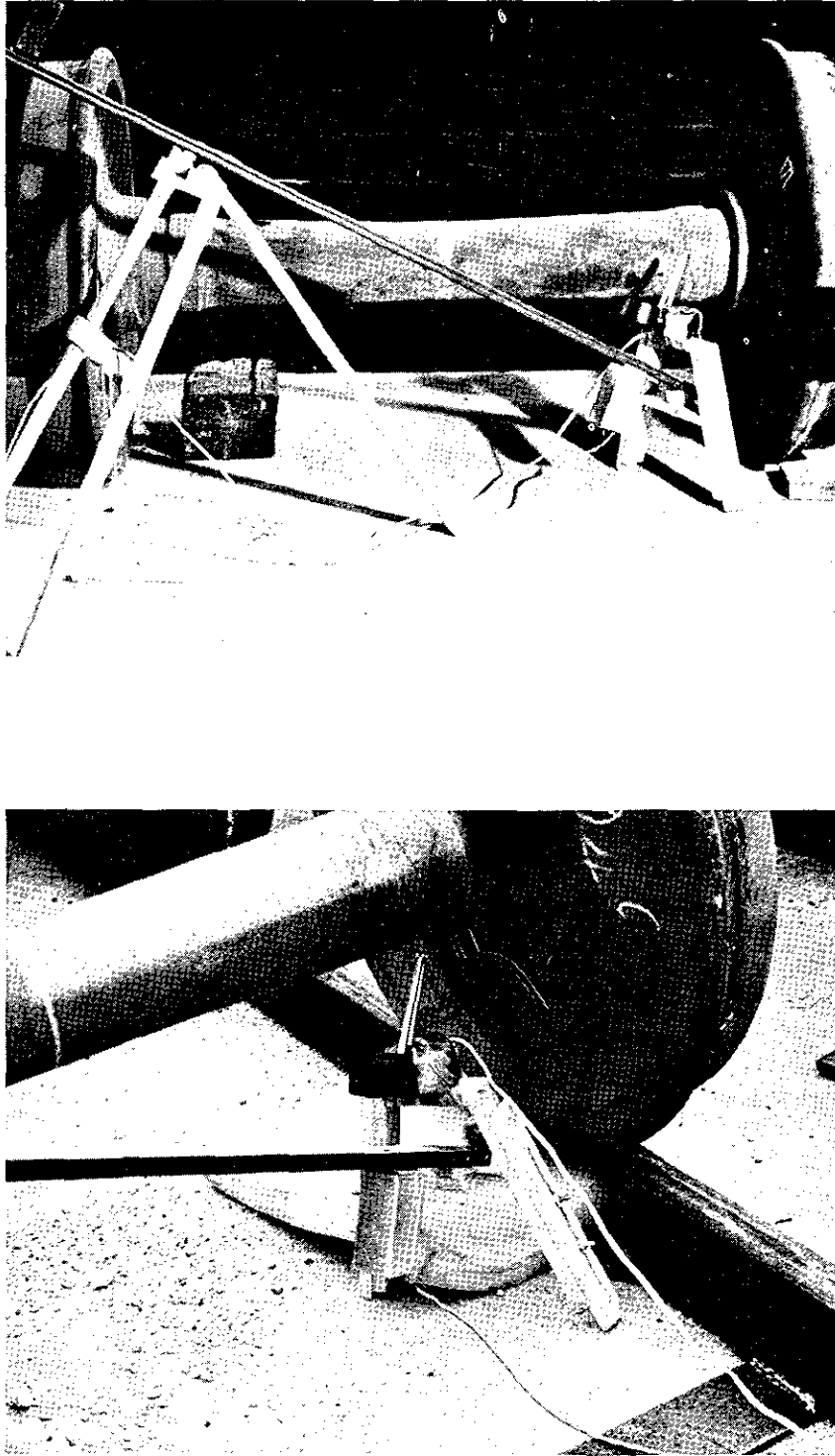


FIG. 3.2.2 ROLLING BALL APPARATUS

Table 3.2.1
INVENTORY OF WHEELS TESTED AT SOUTHERN PACIFIC ENGLEWOOD YARD
18 June 1976

AXLE NO.	EAST WHEEL IDENTIFICATION	WEST WHEEL IDENTIFICATION	DESIGN	TAPE NO. AND EVENTS RECORDED
1.	3/10/76 C532340 CJ33 SOUTHERN	3/10/76 C532311 CJ33 SOUTHERN	33" NEW, CAST FLAT, IW	102: 1, 2, 3, 4 (E) 5, 6, 7, 8 (W)
2.	3/76 GL 87022 CJ33 GRIFFIN	3/76 GL 87183 CJ33 GRIFFIN	33" NEW, CAST DISHED, IW	102: 9, 10, 11, 12 (W) 13, 14, 15, 16 (E)
3.	3/76 GL 67249 CJ33 GRIFFIN	3/76 GL 87204 CJ33 GRIFFIN	33" NEW, CAST DISHED, IW	102: 17, 18, 19, 20 (E) 21, 22, 23, 24 (W)
4.	5/66 GL 91686 CS-2 GRIFFIN	5/66 GL 91690 CS-2 GRIFFIN	33" USED, CAST, DISHED, MW	102: 25, 26, 27, 28 (W) 29, 30, 31, 32 (E)
5.	10/70 GL 17646 CM33 GRIFFIN	10/70 GL 17522 CM-33 GRIFFIN	33" USED, CAST, DISHED, MW	102: 33, 34, 35, 36 (W) 37, 38, 39, 40 (E)
6.	3/15/76 C995514 CH-36B, SOUTHERN	3/15/76, C995524 CH-36B, SOUTHERN	36" NEW, CAST, FLAT, IW	102: 41, 42, 43, 44 (E) 45, 46, 47, 48 (W)
7.	3/15/76, C995745 CH-36B, SOUTHERN	3/15/76, C995518 CH-36B, SOUTHERN	36" NEW, CAST FLAT, IW	102: 49, 50, 51, 52 (W) 53, 54, 55, 56 (E)
8.	10/68, GB02936 CCH-36, GRIFFIN	10/68, GB02939 CCH-36, GRIFFIN	36" USED, CAST DISHED, IW	102: 57, 58, 59, 60 (E) 61, 62, 63, 64 (W)
9.	10/74 \downarrow S \downarrow 15217 H36 STANDARD	9/74 \downarrow S \downarrow 7750 H36 STANDARD	36" USED, WROUGHT FLAT, IW	102: 65, 66, 67, 68 (W) 69, 70, 71, 72 (E)
10.	3/73 \downarrow S \downarrow 8952 H-36 STANDARD	3/73 \downarrow S \downarrow 9482 H-36 STANDARD	36" USED, WROUGHT FLAT, IW	102: 73, 74, 75, 76 (E) 103: 1, 2, 3, 4 (W)

General Radio Recorder set at 7 1/2 tape speed.
Attenuation on all recordings, 90 dB.
Impactor: Rolling Ball device set at 30°, first two events at full height; second two events at 1/2 height.

TABLE 3.2.1 (Cont'd)

AXLE NO.	EAST WHEEL IDENTIFICATION	WEST WHEEL IDENTIFICATION	DESIGN	TAPE NO. AND EVENTS RECORDED
11.	4/74 C24094 J-36, USS	4/74 C24224 J-36, USS	36" USED, WROUGHT, FLAT, MW	103: 5, 6, 7, 8 (W) 9, 10, 11, 12 (E)
12.	4/61 B8749647C027 BETHLEHEM	8/61 B10468650D003 BETHLEHEM	33" USED, WROUGHT FLAT, MW	103: 13, 14, 15, 16 (W) 17, 18, 19, 20 (E)
13.	NONE -	NONE -	36" USED, WROUGHT FLAT, MW, VERY HEAVY RIM	103: 21, 22, 23, 24 (W) 25, 26, 27, 28 (E)
14.	10/66 G75969 73M705, USS	10/66 G75758 GLM498, USS	36" USED, WROUGHT FLAT, IW	103: 29, 30, 31, 32 (E) 33, 34, 35, 36 (W)
15.	8/29/73 C607153 CH-36 SOUTHERN	8/27/73 C606076 CH-36 SOUTHERN	36" CAST, USED FLAT, IW	103: 37, 38, 39, 40 (W) 41, 42, 43, 44 (E)
16.	2/73 GY 45037 B CB28	2/73 GY 43344 B CB28	28" USED, CAST DISHED, IW	103: 45, 46, 47, 48 (E) 49, 50, 51, 52 (W)
17.	3/73 GY 44187 B CB28	2/73 GY 43019 B CB28	28" USED, CAST DISHED, IW	103: 53, 54, 55, 56 (E) 57, 58, 59, 60 (W)

good/defective wheels were tested in the University laboratory (hammer impact testing). The conclusions from these tests were as follows:

- a. The relative amplitude of the wheel resonances depends on the magnitude of the impact.
- b. The relative amplitude of the wheel resonances depends on the direction of the impact.
- c. Each type of wheel has a characteristic signature.
- d. Signature changes with wear. An axle with wheels whose flanges show different amounts of wear has spectral differences mostly above 4 kHz (see Fig. 3.3.1). The importance of this finding was not completely appreciated at the time of the earlier laboratory tests. After the field test it was realized that differential wear is a major cause of signature differences and further work on the subject was performed (see Section 7).
- e. The signature of a used worn wheel compared to the signatures of standard new wheels may show spectral differences of the same order as a cracked wheel.

It was already known that load on wheels has some effect on wheel signature, (see Fig. 1.6.6). Variations with wear and load are enough to exclude the use of the data bank as a classifier for the decision process in field tests. Another important reason is the extremely lengthy processing that would be necessary due to the

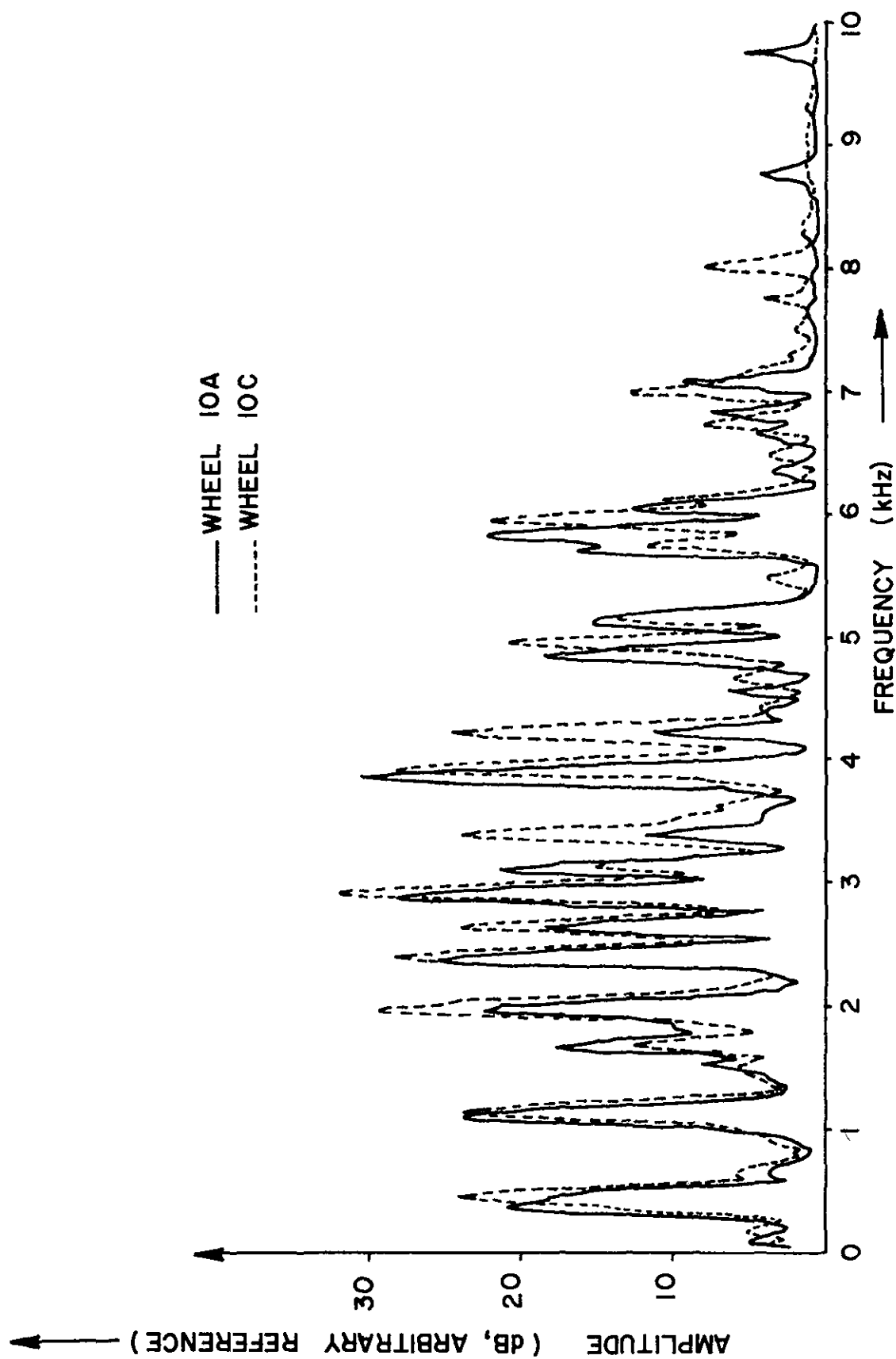


FIGURE 3.3.1 SIGNATURES OF IMPACT ON TWO WHEELS ON THE SAME AXLE WITH UNEVENLY WORN FLANGES

large number of comparisons between the signature of an unknown wheel type and the standard signatures. One single comparison takes about 30 seconds, and there are over 40 different types of wheel in use. It was concluded that across the axle comparison is therefore the only practical scheme.

3.4 Investigation of Minimum Detectable Crack Size

As mentioned earlier, one of the questions which arose from the feasibility study was the issue of the smallest crack that could be detected by signature analysis. In Appendix F it is shown on a theoretical basis that a single crack, not much larger than a dormant thermal crack, will change the signature slightly. The doubt remained however as to whether an experimental system would be capable of finding such a slight change. Consequently it was decided to perform some experiments to address this issue. As discussed in section 4 the critical crack length is at least one tenth of an inch. The key question is therefore whether or not the system can detect the presence of cracks of critical size. This leads to the difficulty that there is little agreement on what this size is. In practice cracked wheels are removed from service when they are found by visual inspection and thus it was decided to investigate wheel sets with the smallest cracks discovered in this way.

Firstly, it was decided to investigate the chances of finding thermal cracks. Some experiments were performed on a 36" wheel and axle set. One of these wheels had eight thermal cracks visible on the front face of the rim and extending onto the tread, i.e., at about the same location as that of the crack illustrated in Fig. 1.2.1. No cracks were visible on the other wheel. The experiments were performed using a 1.5" hard steel ball bearing on the end of a 3 ft. pendulum string. Analysis was performed in real time, using the third octave band RTA*. At a given site on the wheel, five impacts were made, the starting point of the pendulum's fall being accurate to about 1 mm and the maximum overall sound level of the impact being reproducible to about 1 dB. The RTA was set to read the maximum level in each spectral band and these values were transferred to the computer and stored after each impact. Two impact sites on the good wheel were chosen, one on the front face of the rim and one on the plate. The precisely equivalent locations on the bad wheel were then impacted. For each set of 5 impacts on the good wheel an average spectrum was computed. Each of the individual spectra for a given location on either wheel was then compared with the appropriate good wheel average. The algebraic sum of the deviations in dB in each spectral band was then calculated. The results are shown in Table 3.4.1.

*RTA (Real Time Analyzer)

TABLE 3.4.1

RANGE OF DEVIATIONS FROM GOOD WHEEL SPECTRAL
AVERAGES IN EXPERIMENTS WITH THERMAL CRACKS

Run Number	Good Wheel		Bad Wheel	
	Flange Impact	Plate Impact	Flange Impact	Plate Impact
1	200-500	300-800	1300-2800	700-1000
2	200-650	250-650	1100-2600	700-1400

The conclusion was reached that there was a definite difference between the good and bad wheel spectra. Some measurements were also made of decay times of impact sound levels, but no significant differences were found in that case.

These results indicate that the wheel with the thermal cracks should be readily distinguished from its mating wheel. The point should be made that the wheel under test had a large number of cracks, although each one is presumably not much greater than a square inch in area. However, the occurrence of dormant thermal cracks in such numbers on a wheel is probably the normal way for such cracks to appear, so it was concluded that there is a good chance of detecting them in the field.

It was also of some interest to know the smallest plate crack which could be detected. Railroad representatives were asked for help to find a small plate crack. The closest approximation that has come to our attention so far is a wheelset where one wheel (UH inventory number 15A) has a typical large plate crack as shown in Fig. 3.4.1 and wheel 15C, its mate, has a crack on the front plate near the hub (see Fig. 3.4.2a) which is not visible on the back side of the plate (see Fig. 3.4.2b). To be sure about the extent of the crack, a liquid penetrant test was performed on the

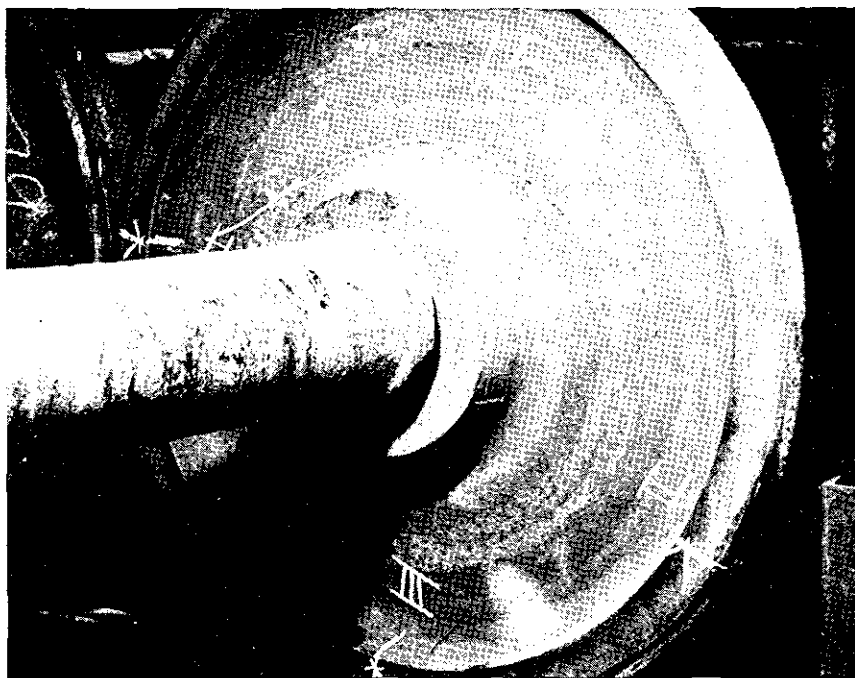


FIG. 3.4.1 VIEW OF WHEEL 15A

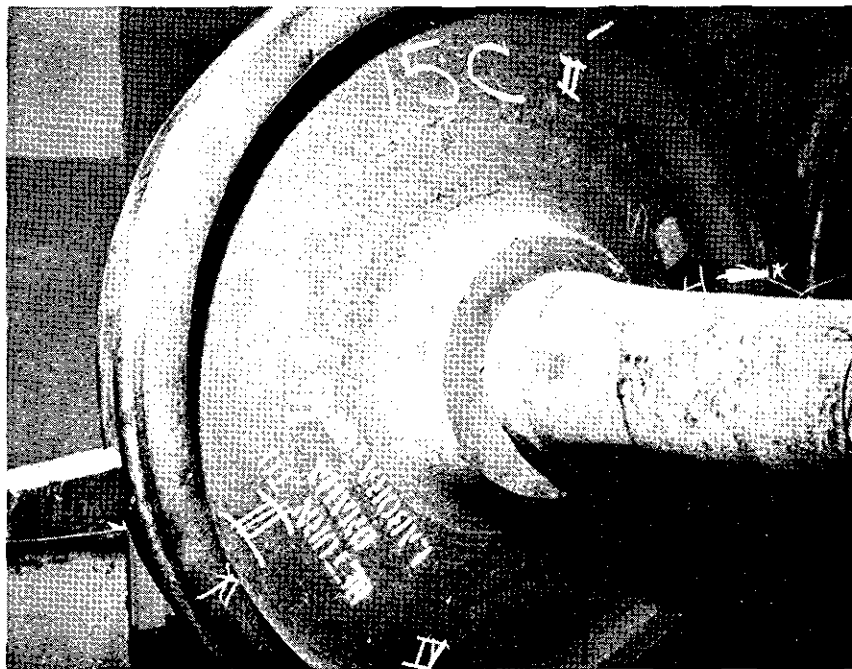
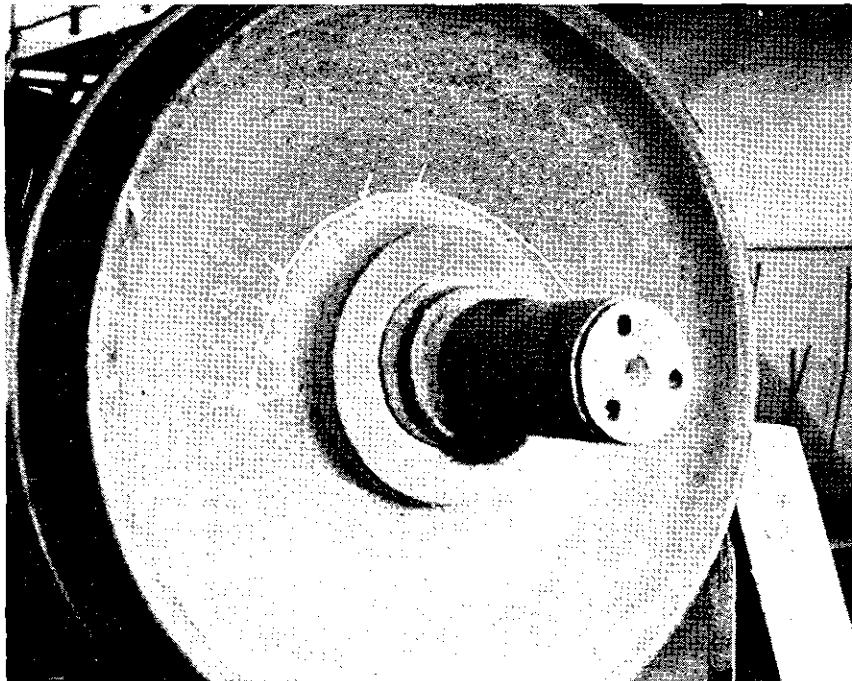


FIG. 3.4.2a VIEW OF WHEEL 15C (front side)
b VIEW OF WHEEL 15C (back side)

wheel. The suspected area was properly cleaned of dust and rust and then a liquid penetrant was applied as an aerosol spray. The penetrant was of the fluorescent type so inspection under ultraviolet light showed clearly the presence of a 20" crack around the hub on the front plate of wheel 15C, but nothing on the back plate. Acoustic signature comparison between the wheels showed only a 20% matching with line spectra comparison vs. 50-80% for most good wheels. The signatures of the two wheels are shown in Fig. 3.4.3.

A comparison was made of the signature of wheel 15C, the partially cracked wheel, with the signatures of wheels 4G and 1G which are good wheels of the same type. The results are shown in Fig. 3.4.4. The results showed 28% line spectra matching for wheel 4G compared to 15C, as also for wheel 1G compared to 15C. Comparison between 4G and 1G showed a better matching, 37%. These numbers indicate that it is possible to find small plate defects on wheels.

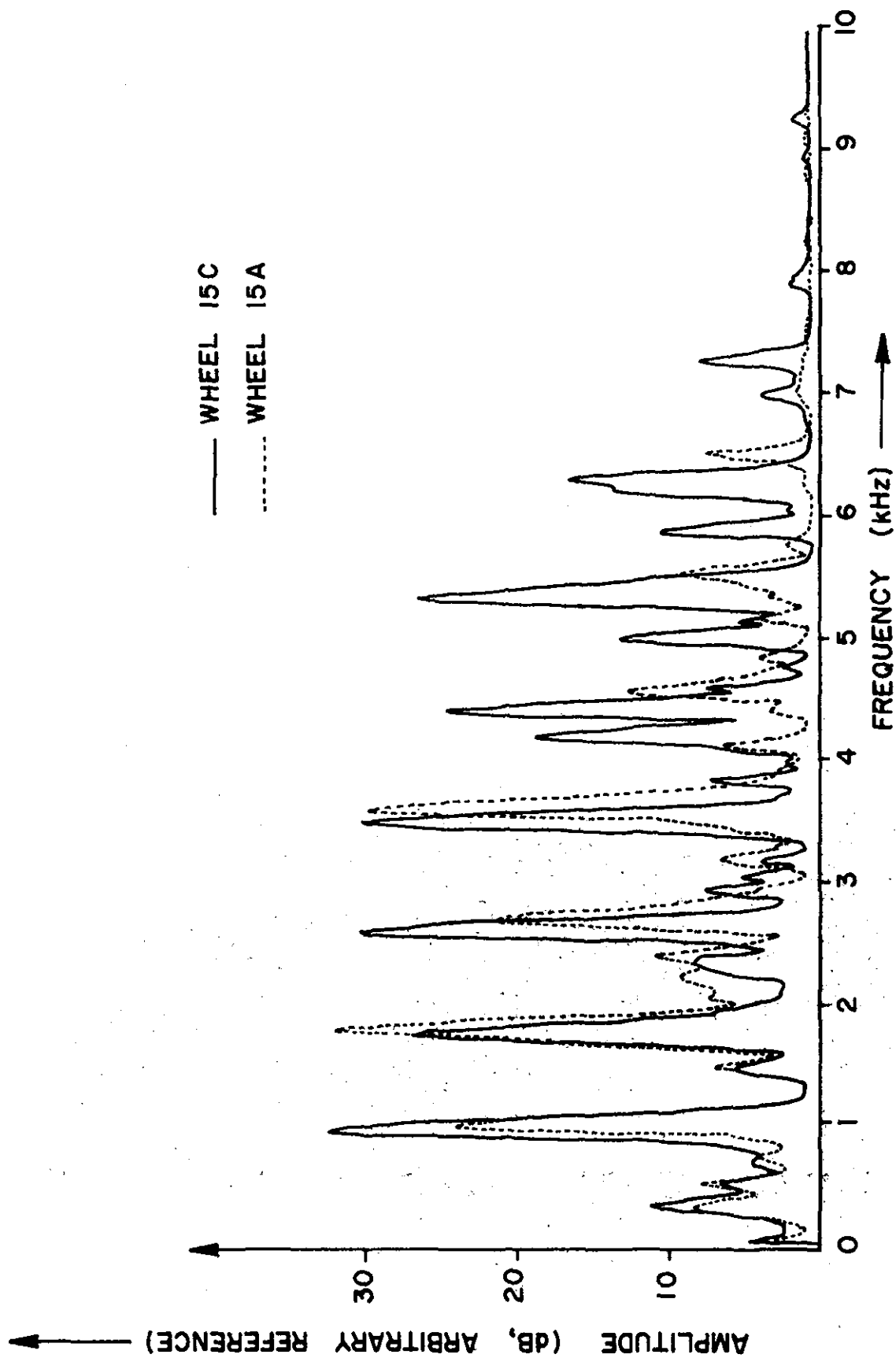


FIGURE 3.4.3 SIGNATURES OF WHEELS, 15C WITH A PARTIAL PLATE CRACK AND 15A WITH A FULL PLATE CRACK

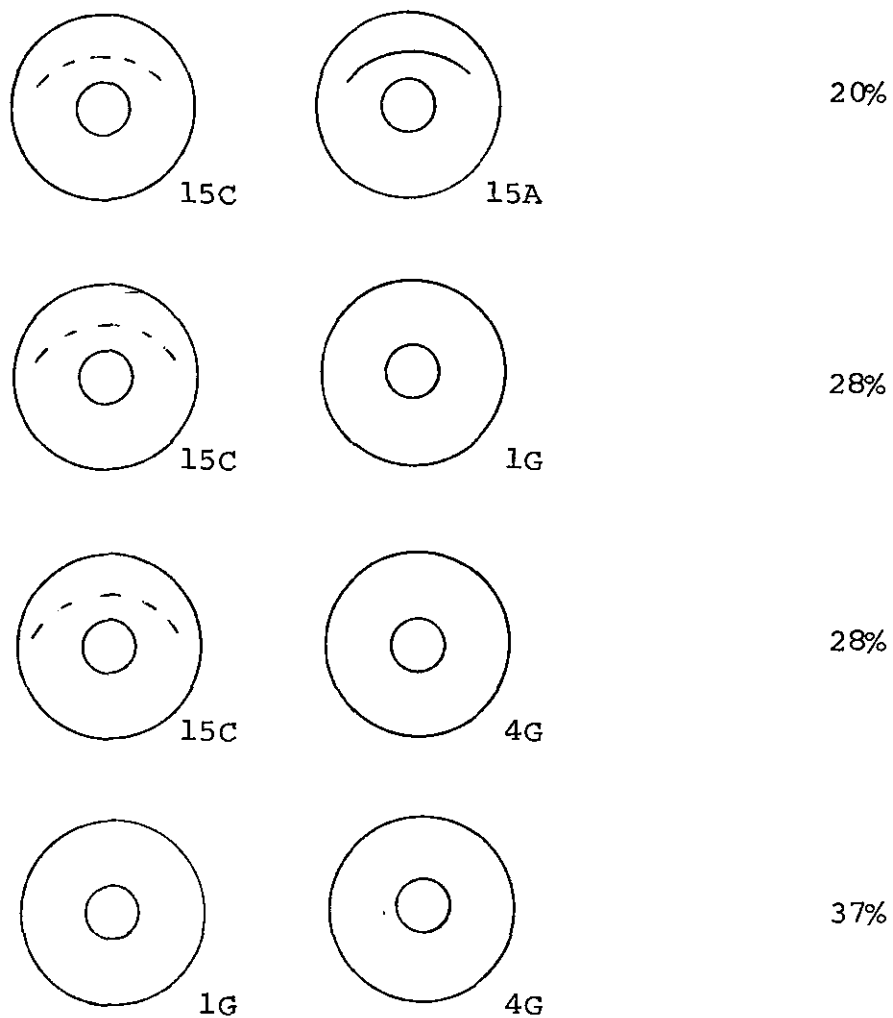
Percentage of Matching Lines

FIG. 3.4.4 SPECTRAL LINE COMPARISON TESTS BETWEEN A WHEEL WITH A PARTIAL PLATE CRACK (15C), A WHEEL WITH A FULL PLATE CRACK (15A) AND TWO GOOD WHEELS OF THE SAME TYPE (1G AND 4G)

4. RESIDUAL STRESS EVALUATION IN RAILROAD WHEELS USING ACOUSTIC SIGNATURE ANALYSIS

4.1 Introduction

The residual stress in a wheel may be as important in influencing wheel failure as the presence of an incipient crack. The reason for this, in terms of fracture mechanics, is apparent from the relationship

$$K_{IC} = A \sigma c^{1/2}$$

where K_{IC} is the fracture toughness parameter, a property of the material. Carter and Caton [30] give values of K_{IC} ranging from 25 to 40 Ksi in^{1/2}, depending on the wheel class. A is a constant which Carter and Caton found to vary from 0.9 to 1.98 for different crack locations.

σ is the applied tension needed to cause the crack to grow and c is the surface length of the crack. Carter and Caton quote 55 Ksi tensile stress as being representative of the peak of the stress generated during drag braking and hence conclude that critical crack lengths are a minimum of 0.1 inch for corner cracks in class U wheels to 0.65 inch for surface cracks in class A wheels.

However it does not follow that such cracks will cause a wheel to break. New wheels are manufactured with a residual compressive stress in the rim, which is usually in the range 20-25 Ksi according to Wandrisco and Dewez [31]. The plate of a new wheel is in tension. Extended periods of brake application can overheat the wheel and

eventually change the signs of the internal residual stresses. Clearly then the residual stress plays a major role in determining the growth of small cracks. Even if a crack grows through the rim it may be arrested in the plate for a long period before finally causing the wheel to disintegrate.

Some estimates of the number of wheels containing small rim cracks are quite high. However, on an annual basis there are less than 1000 derailments due to broken wheels. It might be concluded that many small cracks are not a problem. Hirooka et al. [33] have confirmed this impression as a result of drag brake tests and stated that such cracks are only dangerous if the rim has a high tensile stress. One concludes that a sensible inspection program would aim to find large cracks and wheels in which the compressive stresses in the rim have changed to a high tensile value. Large cracks are found quite effectively using ASI* but the measurement of residual stress is problematic.

None of the methods of residual stress measurement is readily applicable in this situation. The velocity of sound can be measured at ultrasonic frequencies and changes of the order of 1 part in 10^4 can be found per Ksi change in residual stress [43]. Obviously great accuracy and careful calibration is required, implying careful surface preparation. This method does have the advantage that the stress in the bulk of the material is measured.

*ASI (Acoustic Signature Inspection)

X-rays can be used in evaluation of lattice dimensions in homogeneous materials. Residual stresses can be deduced by evaluating strain from lattice dimensions. The method is restricted to surface stress-evaluation over a small area and careful surface preparation is necessary [32]. Barkhausen noise can also be used in residual stress evaluation [34]. Again in this case the most obvious limitation is surface preparation of the test material and only surface stress evaluation can be made. In the case of a wheel in service surface residual stresses on the tread, front and back rim are different from the "bulk" rim stresses due to braking action from retarders and the high local loading on the tread of a rolling wheel.

The objective of the work reported here was to investigate the possibility of using acoustic signature inspection to evaluate residual stress. The basic idea is that applied stress changes the natural frequencies of flexural vibrations in an object. The simplest example is the change of the natural modes of a string under different tension. For rigid bodies such as a beam, or column, there is a well known theoretical treatment and experimental evidence that the response changes with load, which has to be allowed for in the design of chimney stacks and the like. A similar effect occurs in the case of high speed turbine blades where the frequencies of the natural modes changes with speed. This question has been discussed in Section 2.

Nagy [1] showed that changes in resonant frequencies of wheels occurred under load. This gave rise to the idea that change in residual stress might be detectable from changes in resonant frequencies.

4.2 Test on Wheels with Different Heat Treatment in the Griffin Wheel Manufacturing Plant at Bessemer, Alabama

A first attempt to study this problem was made in the Griffin Wheel Manufacturing Plant at Bessemer, Alabama. A variety of manufacturing treatments had been applied to the wheels to generate a wide range of residual stresses. Acoustic signatures were recorded from 33- and 36-inch wheels that had normal treatment, and also from wheels that had high internal tension stresses. The standard procedure for measuring residual stresses is destructive testing by saw cut described in the manual of standards and recommended practices of the Association of American Railroads (AAR) [36]. In Fig. 4.2.1 are shown the results of strain test on a 33 inch one wear Griffin wheel. This figure was obtained from the Car and Locomotive Cyclopedia [37].

All wheels tested were sitting on their hubs on a concrete floor, so the plates and rims were free of contact. The following measurements were taken:

1. Hammer impacts on each wheel.

- a. Ten impacts were made on three different points on the circumference of the front rim of the wheel. The relative location of the impact points were approximately 120° apart.

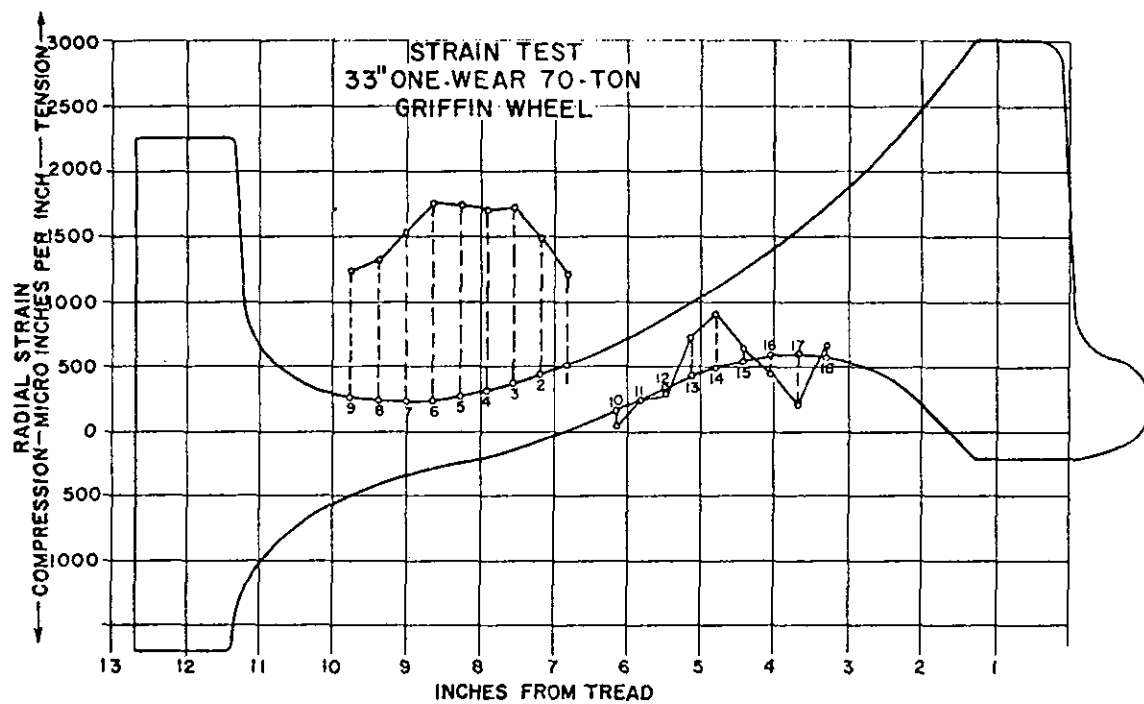


FIG. 4.2.1 STRAIN TEST ON A 33-INCH ONE WEAR 70 TON GRIFFIN WHEEL

- b. Five impacts on the plate, midway from the center to the rim of the wheel.
- c. Five impacts on the flange, along a radius.

For steps 1a, b, and c sound was detected by a microphone. The hammer is shown in Fig. 4.2.2. This design provides a triggering pulse simultaneously with the impact. Signals were recorded on a dual channel recorder.

2. Shaker excitation. In this series of tests a shaker was used as an exciter and the vibrations were picked up by a GR type 1560-P52 accelerometer. Input signals were:

- a. random noise,
- and b. slowly sweeping sine signal from a Wavetek Model 134 signal generator, in the range from 400 to 2000 Hz.

Most of the analyses were made from impact recordings.

The wheel manufacturing steps are as follows:

1. Pressure Pouring Pit: Steel wheels are formed as air pressure forces molten steel up from a sealed chamber into graphite molds. A mold is filled in 20 seconds.
2. Wheel Transfer: Depending upon the metal temperature at pouring, the wheel casting will solidify in five to seven minutes. The cope (top) of the mold is removed, and the wheel is lifted by the hub and conveyed to the final finishing and inspection stations.



FIG. 4.2.2 VIEW OF THE HAMMER WITH A PZT DISK BETWEEN HAMMER AND CYLINDER TO PROVIDE THE TRIGGERING PULSE ON IMPACT WITH THE TEST OBJECT

3. Cooling Kiln: Wheels are cooled from 2,000°F to 1,000°F to reduce stress formation.
4. Stopper Pipe Cut off and Shot Blast: Each wheel's stopper pipe is automatically cut off and the graphite stopper removed from the hub.
5. Torch Cutting: (a) Riser stubs are taken off with an electric arc torch. (b) An oxyacetylene torch automatically cuts out the wheel's hub bore.
6. Heat Treating: Wheels are moved by conveyor to a rotary hearth normalizing furnace, where they are heat treated.
7. Rim Quench: Following heat treatment, rims are quenched to harden the treads for more severe service.
8. Draw Furnace: The wheels are tempered again.
9. Hub Cooling: Final heat treatment for proper residual stress formation.
10. Shot Blasting: Each wheel is shot blasted to remove scale and permit surface inspection.
11. Magnaglo Test: Magnaglo testing detects surface and subsurface defects.
12. Ultrasonic Test: An additional test is made, using pulse echoes. This is to further insure that there are no subsurface flaws.

The manufacturing steps are shown in a schematic diagram in Fig. 4.2.3. If the wheel has been taken off line before the normalizing furnace, steps 3 to 6, it has a high stress. After step 6 it has normal stress.

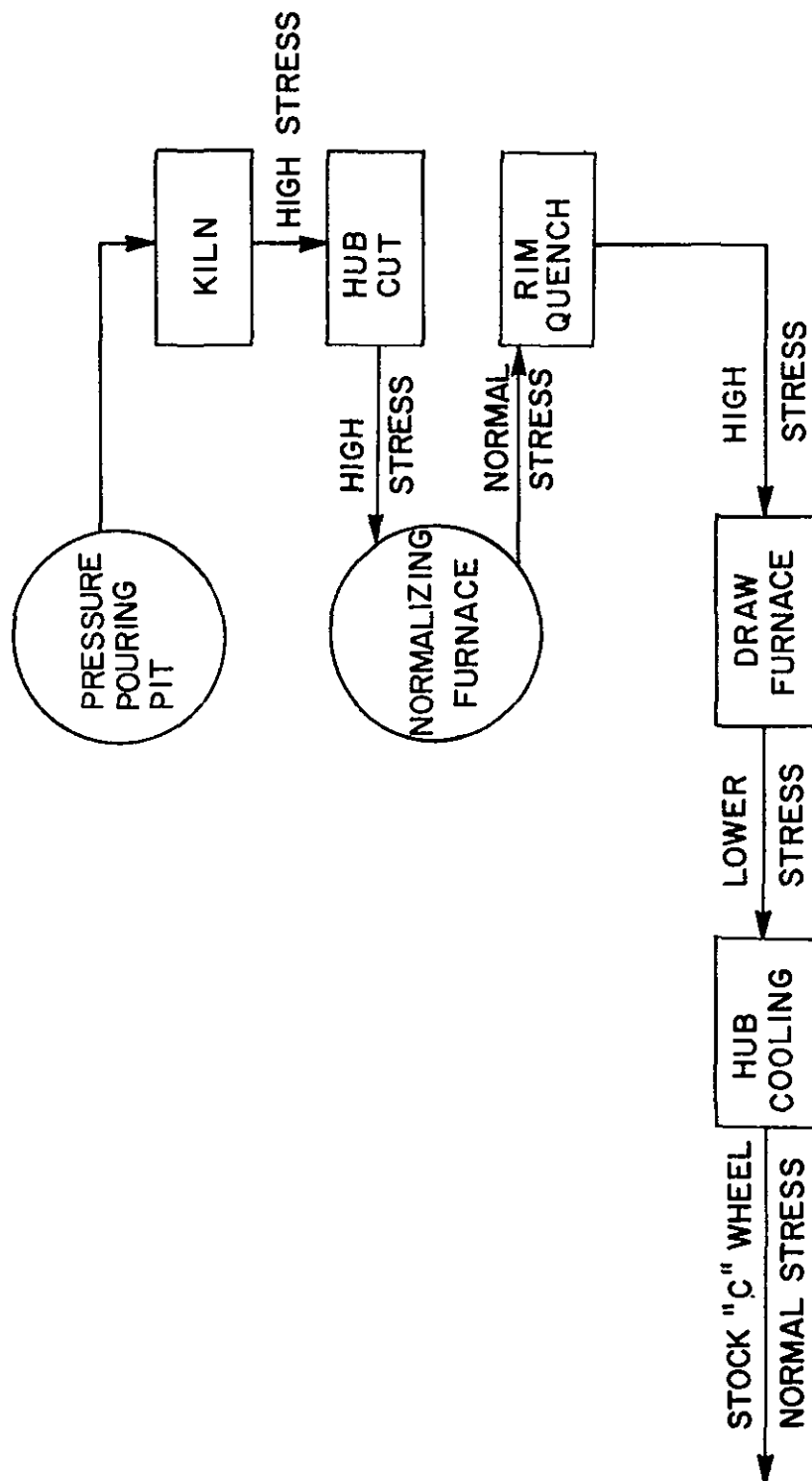


FIG. 4.2.3 SCHEMATIC DIAGRAM OF CAST WHEEL MANUFACTURING

Between steps 7 and 8 it has high stress. After step 8 it has lower stress and after step 9 it has the normal stress configuration. A list of wheels tested at the Griffin Wheel Plant in Bessemer, Alabama is presented in Table 4.2.1. The first column has the wheel identification, type and number. The second column has the tape numbers of tests as recorded. The third column has the description of the manufacturing treatment and the last column the estimated stress according to the treatment.

Preliminary results from comparisons between the acoustic signatures of the wheels are listed in Table 4.2.2. The difference index is based on a decision scheme which is a combination of line spectra and sum of the differences comparison between two spectra. There were only two conflicting results out of 25 tests. In run No. 5, the Difference Index for high/normal stressed wheels is small. In run No. 9, although wheels CJ36 26 425 and CJ 36 26 171 had the same heat treatment, history, and structure, they have a Difference Index of 10. One possible explanation is the existence of small geometric differences indicated by the rough surface appearance (the wheels were removed from the line before step 4).

A detailed study of the acoustic signatures was made using a spectrum translator to measure small shifts in resonance frequencies. This instrument was used in conjunction with the SD330 RTA. The spectrum translator can separate frequency bands from a spectrum and expand them,

TABLE 4.2.1

LIST OF WHEELS TESTED AT THE GRIFFIN WHEEL
MANUFACTURING PLANT IN BESSEMER, ALABAMA
FOR RESIDUAL STRESS EVALUATION

WHEEL NO. AND TYPE	TAPE NO.	DESCRIPTION	STRESS
CJ36-26425 "C"	141, 141A, 142, 155A	Hub Left In	High Stress
CJ36-26171 "C"	143A, 144	Hub Left In	High Stress
CH36-17180 "C"	147A, 149	Hubcut, Not Normalized	High Stress
CJ36-27910 "C"	145, 146A	Hubcut, Quenched Skipped Draw Furnace	High Stress
CJ36-27636 "C"		Hubcut, Quenched and Tempered but Not Hub Cooled	Lower Stress
CJ36-32784 "C"	145, 146A	Stock	Normal Stress
CJ36-23089 "U"	147A, 148	Stock	Normal Stress
CJ36-32769	153A, 154	Stock	Normal Stress
CJ33-30695	151A, 152	Hub Left In	High Stress
CJ33-31029	149, 150A	Hubcut, Quenched Skipped Draw Furnace	High Stress
CJ33-30695	149, 151A	Hubcut, Quenched Skipped Draw Furnace	High Stress
CJ33-97803 "C"	149, 150A	Stock	Normal Stress
CJ33-11092 "U"	151A, 152	Stock	Normal Stress
CJ33-21226 "U"	152, 153A	Stock	Normal Stress

TABLE 4.2.2

PRELIMINARY RESULTS - RESIDUAL STRESS TESTS, BESSEMER, ALABAMA
 (-H INDICATES HIGHLY STRESSED WHEEL, -N INDICATES NORMAL WHEEL)

RUN	TEST #	WHEEL #1	WHEEL #2	DIFFERENCE INDEX*	COMMENT
1	1	<u>CJ36 26425-H</u>	SAME	1	SAME WHEEL COMPARISON
2	18	CJ33 97803-N	SAME	3	SAME WHEEL COMPARISON
3	12	CJ36 32784-N	CJ36 23089-N	5	
4	27	CJ36 32769-N	CJ36 32784-N	5	
5	22	<u>CJ33 30695-H</u>	CJ33 11092-N	6	THIS IS ONLY CONFLICT- ING RESULT FROM 25 TEST
6	21	CJ33 97803-N	CJ33 11092-N	7	
7	19	CJ33 97803-N	<u>CJ33 31029-H</u>	9	
8	13	<u>CJ36 27910-H</u>	CJ36 23089-N	9	
9	5	<u>CJ36 26425-H</u>	<u>CJ36 26171-H</u>	10	**
10	10	<u>CJ36 26171-H</u>	CJ36 32784-N	10	
11	14	CJ36 23089-N	<u>CH36 17180-H</u>	27	DIFFERENT TREAD
12	25	CJ33 97803-N	CJ36 32769-N	29	33" COMPARED TO 36"
13	17	<u>CH36 17180-H</u>	CJ33 97803-N	33	33" COMPARED TO 36" DIFFERENT TREAD

* THE DIFFERENCE INDEX IS OBTAINED BY SUMMING THE DIFFERENCE BETWEEN SPECTRA TAKEN CHANNEL BY CHANNEL. BEFORE SUMMING, EACH SPECTRA IS NORMALIZED BY DIVIDING ALL ITS CHANNEL VALUES (IN dB) BY THE MAXIMUM VALUE. FURTHERMORE, WHEN RESONANCE LINES CO-INCIDE BETWEEN THE TWO SPECTRA, THEN THE CENTER CHANNEL AND ADJACENT CHANNELS FOR SUCH RESONANCES ARE DISREGARDED IN THE SUM.

** THIS MIGHT BE DUE TO SMALL GEOMETRIC DIFFERENCES (NO SURFACE TREATMENT)

thus improving the frequency resolution. In the range of 10 kHz the analyzer has a 40 Hz resolution. With the spectrum translator, translated bands had a 100 Hz range and 0.4 Hz resolution. In the range of 10 kHz the sampling period is 50 ms, for the 100 Hz range it is 2500 ms, hence only slowly decaying signals (resonances) can be analyzed. With the use of a spectrum translator significant differences in the resonant frequencies were revealed. Spectral plots were obtained for most of the strong wheel resonances. An example is shown in Fig. 4.2.4. The resonances of the normally stressed wheels were separated from those of the highly stressed wheels by more than 8 Hz. The estimated frequency shift for those resonances due to geometrical tolerance in manufacturing is 1 Hz.

A list of the measurements taken is presented in Table D.1 in Appendix D.1. The results are also shown in Fig. 4.2.5 for CJ36 type wheels and in Fig. 4.2.6 for CJ33 type wheels. These are rather unusual presentations and some explanation is needed. The points on the plot represent resonant frequencies. All the points lie on lines parallel to the Y axis. For example, the line AA' in Fig. 4.2.5 has the resonances of the CJ36 type wheels near 390 Hz. Dots represent resonances of normally stressed wheels and asterisks represent highly stressed wheels. At each wheel resonance, the value for the normally stressed wheel was set on the X-axis. The intersection of AA' and the X-axis represents the resonance of the wheel CJ 36 32784 at 390.8 Hz. The rest of the indications on AA' show the

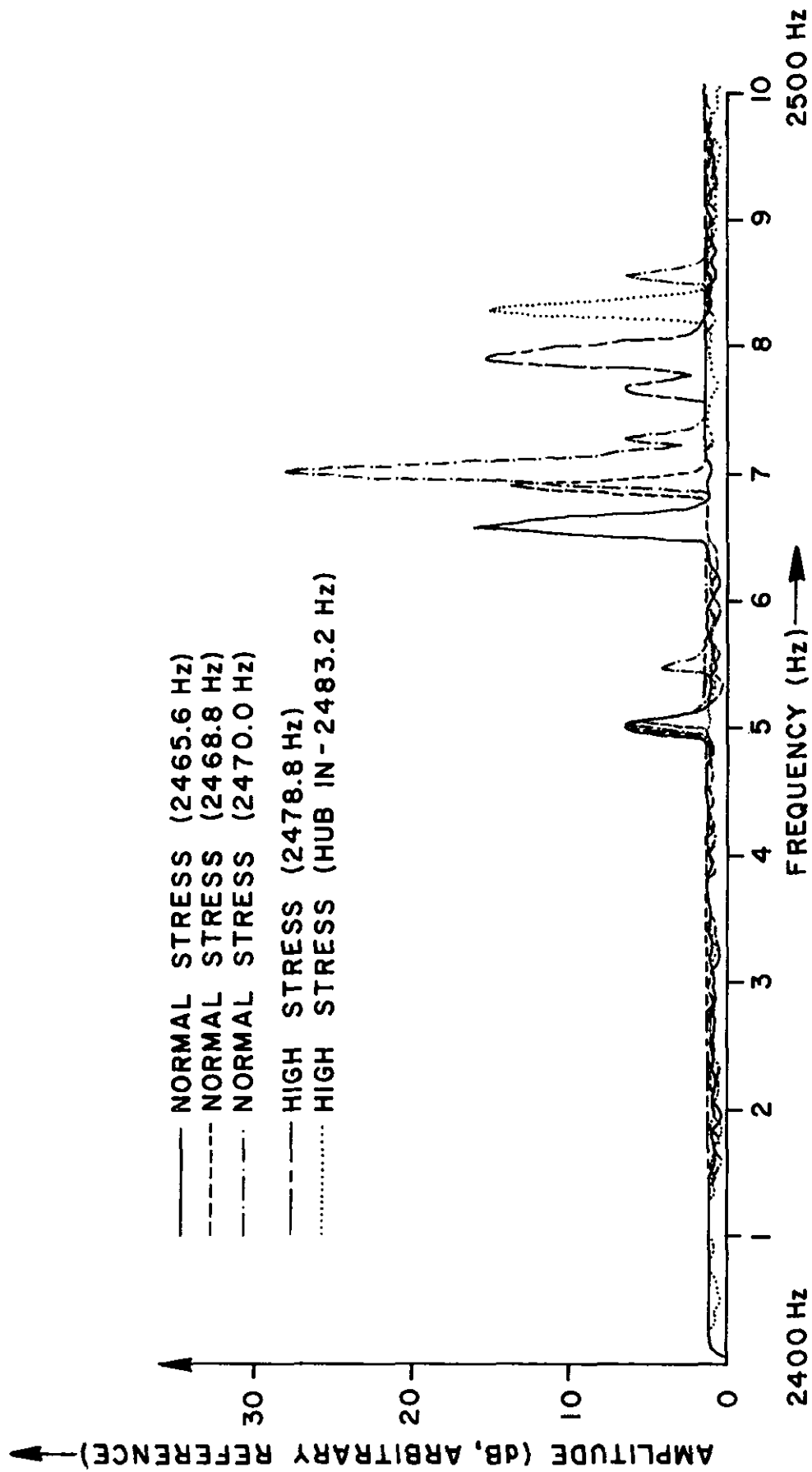


FIGURE 4.2.4 SPECTRA PLOTS FOR CJ36 WHEELS WITH DIFFERENT INTERNAL STRESS DISTRIBUTION, BETWEEN 2400 and 2500 Hz

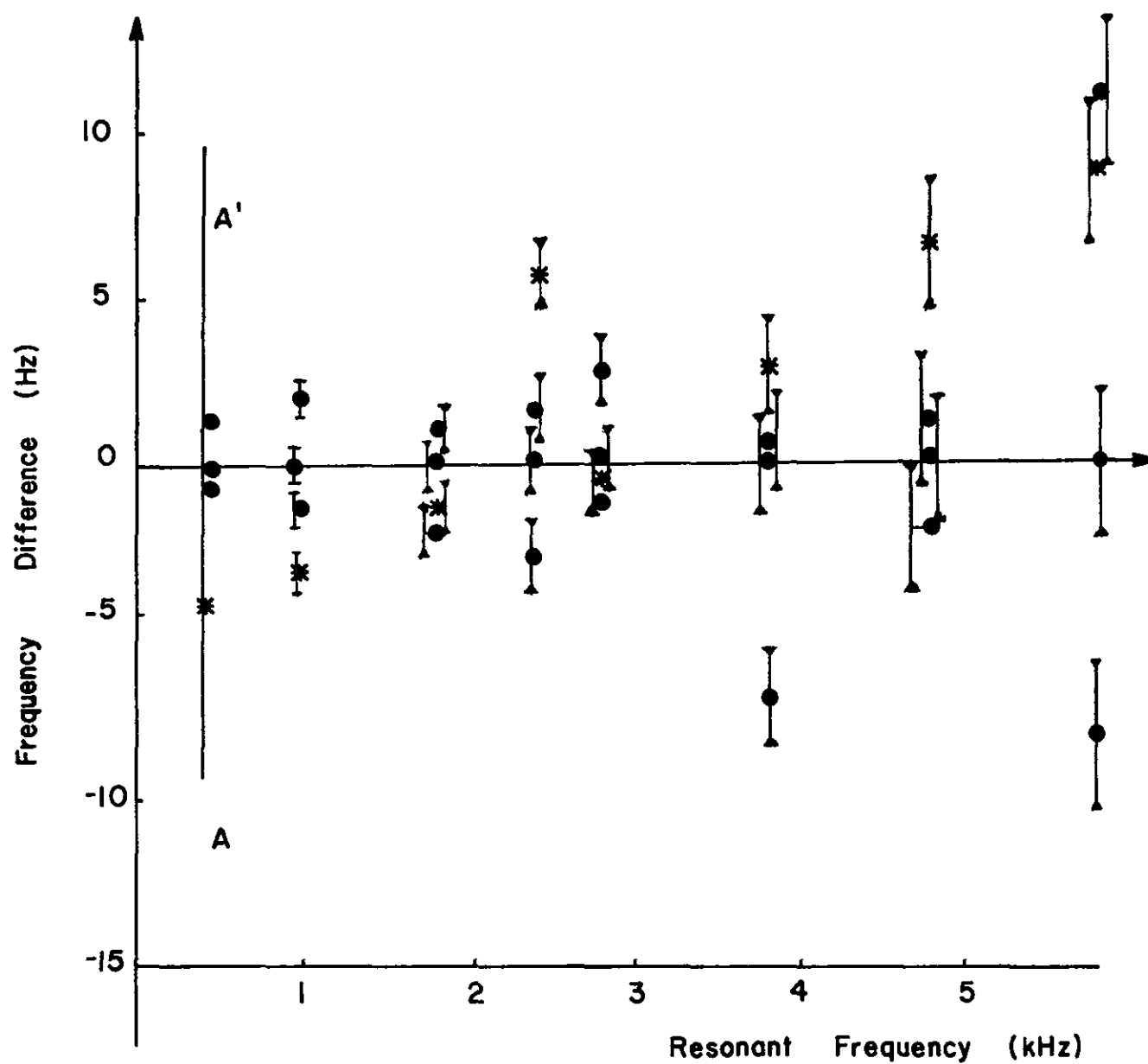


FIG. 4.2.5 DIFFERENCES IN RESONANT FREQUENCY FOR CJ36 WHEELS

● NORMALLY STRESSED WHEELS;
 * HIGHLY STRESSED WHEELS

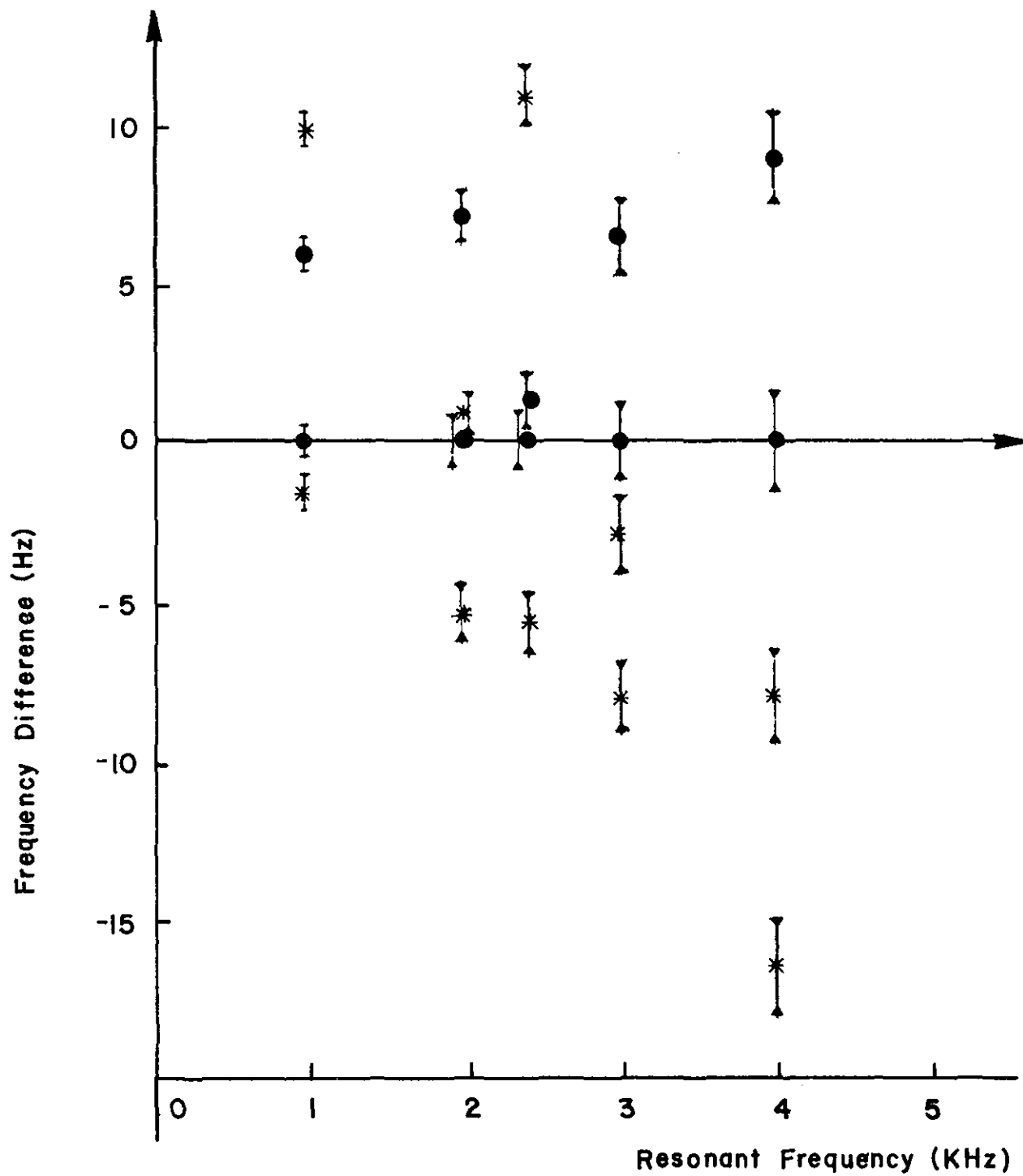


FIG. 4.2.6 DIFFERENCES IN RESONANT FREQUENCY FOR CJ33 WHEELS.
● NORMALLY STRESSED WHEELS; * HIGHLY STRESSED WHEELS

frequency deviation from that value of the corresponding resonance for other wheels in Hz. Positive deviations correspond to resonances above 390.8 Hz and negative deviations to lower values. In some cases the resonance of a highly stressed wheel lies among the resonances of the normally stressed wheels, but in other cases it is above or below. Thus, although the shift may be to higher or lower frequencies, in general there is a separation between the resonances of normally and highly stressed wheels. Hence a known type of wheel with unknown stress could be checked for stress distribution by comparing a few small portions of its signature with the same signature portions of normally stressed wheels. These frequency shifts could conceivably be due to variations in the geometry of the wheels because of dimensional tolerances. For this reason it was decided to estimate frequency shifts due to extreme variations in the dimensional tolerances.

The manufacturing error for a 36" wheel is about 5 lb or about 0.5% in weight; hence the volume error, ϵ_v , is also 0.5%

$$\text{i.e. } \epsilon_v = 0.5\%, \quad (4.2.1)$$

Approximating the wheel to a disk, the volume of the wheels is

$$v = \pi r^2 h. \quad (4.2.2)$$

Differentiating (4.2.2)

$$dv = 2\pi r h dr + \pi r^2 dh,$$

or,

$$\begin{aligned} \epsilon_v = \frac{dv}{v} &= \frac{2\pi r h}{\pi r^2 h} dr + \frac{\pi r^2}{\pi r^2 h} dh \\ &= \frac{2dr}{r} + \frac{dh}{h} = \epsilon_r + \epsilon_h \end{aligned} \quad (4.2.3)$$

where ϵ_r is the error due to the change in the radial direction and ϵ_h is the error due to the change in the thickness. Assuming $\epsilon_r = \epsilon_h$, for the sake of argument,

$$\epsilon_r = 2.5 \times 10^{-4} \text{ and } \Delta r = \frac{r}{2} \times 2.5 \times 10^{-4},$$

or

$$\frac{\Delta r}{r} = 1.25 \times 10^{-4}, \quad (4.2.4)$$

The resonance frequencies are given by

$$f_n = \frac{n(n-1)}{(n^2 + \nu)^{\frac{1}{2}}} \frac{1}{2\pi} (EI_x / \rho A r^4)^{1/2},$$

or

$$f_n = \frac{C}{r^2} \quad (4.2.5) \quad , \quad C = \text{constant.} \quad (4.2.5)$$

Thus

$$\Delta f_n = \frac{3C}{r^3} \Delta r, \quad (4.2.6)$$

and finally from (4.2.4), (4.2.5) and (4.2.6) the frequency error is

$$\epsilon_f = \frac{\Delta f_n}{f_n} \approx 4 \times 10^{-4}. \quad (4.2.7)$$

In Table 4.2.3 the estimated frequency error is given in Hz for the main resonances of the CJ33 and CJ36 type wheels. The estimated frequency shifts due to geometrical variations are much less than those measured.

TABLE 4.2.3

ERROR EVALUATION FOR STRONG
 RESONANCES ON CJ33 AND CJ36 WHEELS

WHEEL TYPE	RESONANT FREQUENCY	FREQUENCY ERROR Δf_1 Hz	MAX. FREQUENCY ERROR Δf_2 Hz
CJ33	440	0.2	0.4
	1130	0.5	1.0
	3010	1.2	2.4
	4040	1.6	3.2
CJ36	390	0.2	0.4
	1040	0.4	0.8
	1860	0.8	1.6
	2470	1.0	2.0
	2790	1.1	2.2
	3780	1.5	3.0
	4810	1.9	3.8
	5860	2.3	4.6

4.3 Dynamometer Tests at Wilmerding, Pennsylvania

An opportunity to correlate numerical stress indications with changes in the acoustic signature was offered by the Union Pacific Railroad Company (UPRR) who invited the University to participate in a series of dynamometer tests in the Westinghouse Plant at Wilmerding, Pennsylvania.

4.3.1 Description of Tests

The objective of the Union Pacific's test team was to study the thermal damage and premature wear to the tread and flange portion of the wheel. Preliminary internal study of the problem by the UPRR focused attention on three potential causes of the phenomena:

1. misalignment of the brake shoe with respect to the wheel center line,
2. misapplied brake shoe,
- and 3. high energy drag braking applications.

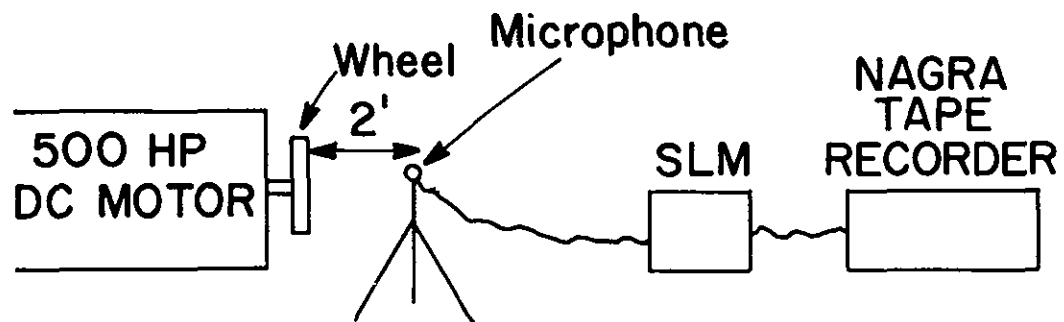
Subsequent discussion and correspondence between representatives of the Union Pacific Railroad and Westinghouse Air Brake Division (WABD) resulted in a proposal to conduct a dynamometer research test program to investigate the possible effect of these factors on usable wheel life. This program was conducted by WABD under contract to UPRR.

The dynamometer test program consisted of both stop tests and drag tests. The stop tests were emergency stops from 80 mph. Five stops were made on each wheel used. The drag test was run at a speed of 60 mph with a

shoe force simulating a 15 psi brake pipe reduction. Five drag tests were made on each wheel. Two different positions of the shoe on the wheel were tested: in the center of the tread, with the shoe overriding the outer edge of the tread, and with the shoe riding on the flange. Several types of brake shoes were used.

The acoustic signature of the wheel after each stop was obtained using the setup shown in Fig. 4.3.1. For excitation of the wheel a 16 oz, standard hammer was used and the wheel was impacted five times. In a few tests a 32 oz, hammer in addition to the 16 oz, one was used. The stress readings were obtained from three SR-4 foil strain gauges (BLH Electronics) welded on the wheel as shown in Fig. 4.3.2. The strain readings were obtained using two types of strain indicators. The first device was a multichannel indicator with an internal calibration to zero the initial reading, so that any subsequent reading indicated the change in strain directly. The second device gave indications whereby any strain change could be evaluated by subtracting the indication from the initial reading. In the following description the three gauges will be referred to as A, B, and C (see Fig. 4.3.2). The SR-4 gauge specifications indicate that the maximum advisable operational temperature without special coating is 705°F.

Acoustic signatures from a total of six wheels were obtained. All wheels tested were Griffin CJ33 and were



BACKGROUND NOISE : 88 dBA

IMPACT LEVEL : 113 dBA on fast at 2 feet

SLM : GR

TAPE RECORDER : NAGRA IV

FIG. 4.3.1 SETUP FOR ACOUSTIC SIGNATURE RECORDING

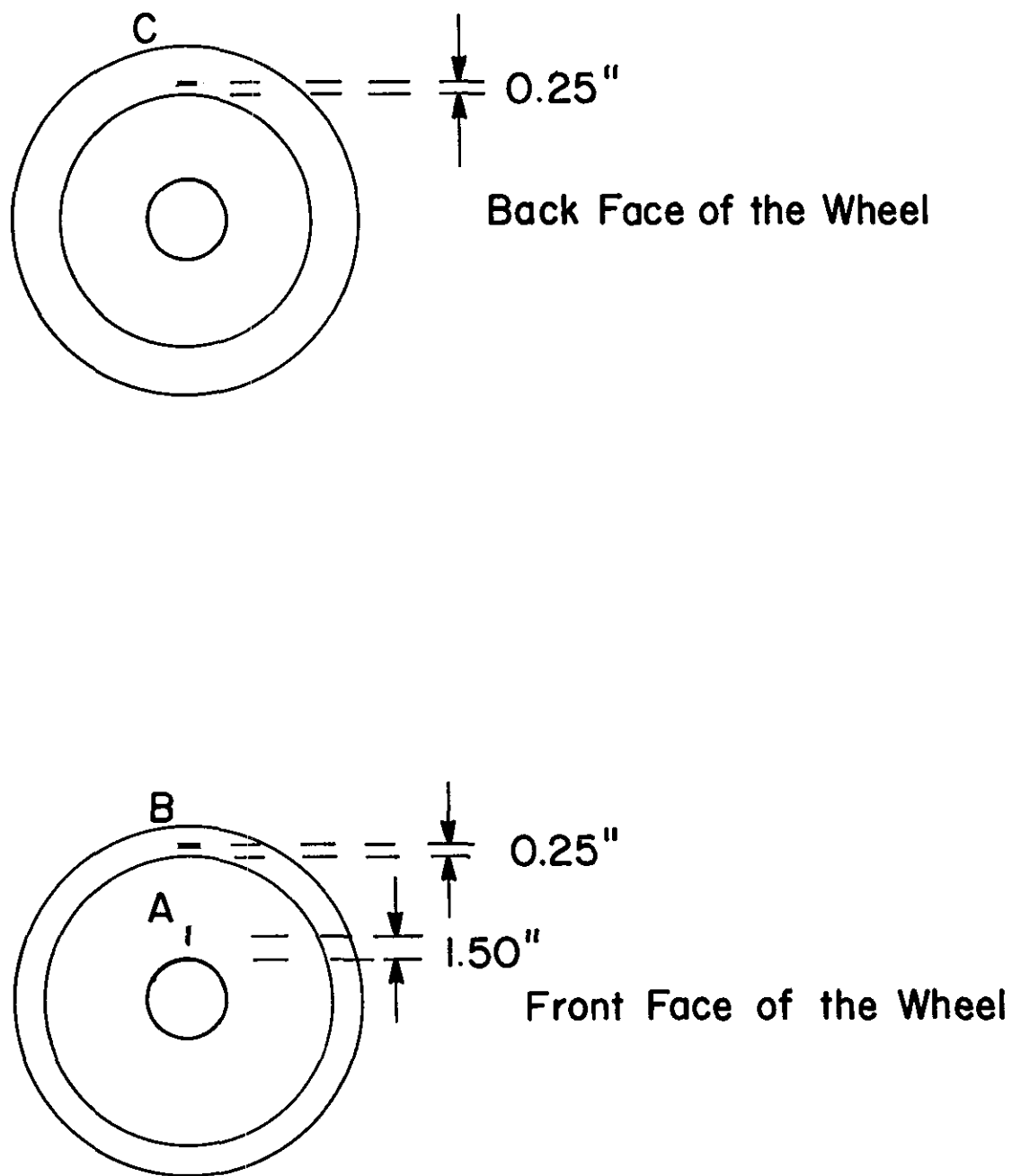


FIG. 4.3.2 STRAIN GAUGE ARRANGEMENT

identified as UP 12, 19, 20, 17, 27, and 28. In wheels UP 12, 19, 20 and 17 emergency braking tests were performed with different brake shoes and shoe positions. On wheels UP 27 and 28 drag braking tests were performed applying COBRA composition brake shoes. As was expected the highest stress changes occurred in the drag braking tests because of the high final wheel tread temperature of 600°F to 1100°F, as compared to emergency stops in which final temperatures are generally in the range of 150°F to 550°F.

4.3.2 Data Processing

The tape recordings were returned to the University for processing. An attempt to see changes in the signature using the SD 330 A RTA failed because of the low frequency resolution of 20-40 Hz while the range of interest is 0-10 Hz. By courtesy of the Shell Oil Co., a Hewlett Packard (HP 5445) real-time spectrum analyzer was made available. This instrument has a variety of features and options for optimum signal processing. Identification of the important resonances was achieved in a preliminary run shown in Fig. 4.3.3. Because of limited access time with the analyzer only signatures from wheels UP 27 and 28 (drag braking) could be obtained.

4.3.3 Results

The results are summarized in Table 4.3.1 and 4.3.2. These tables contain: in column 1, the test number; in

TABLE 4.3.1 STRAIN GAUGE INDICATION VERSUS ACOUSTIC SIGNATURE
CHANGES FROM DRAG BRAKING TESTS ON WHEEL UP 28

TEST No.	TAPE No.	STRAIN GAUGE INDICATIONS			ΔA	ΔB	ΔC	RESONANCE in Hz			
		A	B	C				420.70	3001.2	4034.3	5091.4
32	203	0 (-1248)	0 (+2227)	0 (+510)							
33	"	-392 (-1648)	(-980) (+1239)	+140 (+646)	-392 (-400)	-980 (-988)	140 (136)	.62	-1.2	-1.8	-2.7
34	"	-826 (-2104)	-1125 (+1074)	+279 (+788)	-826 (-856)	-1125 (-1153)	279 (278)	—	0.4	0.1	-1.5
35	"	-1342 (-2613)	GAUGE BURNED OFF	+809 (+1329)	-1342 (-1365)	NR	810 (819)	3.52	5.1	5.2	4.3
36	204	-1674 (-2960)	NR	(+825) (+1327)	-1674 (-1712)	NR	825 (817)	—	5.4	4.7	5.1
37	"	-1703 (-2985)	NR	+884 (1409)	-1703 (-1737)	NR	884 (899)	—	6.0	6.7	6.6

Note: The Strain Gauge Readings are in microinches per inch.
An Indication of 1000 Corresponds to about 30 Ksi.

TABLE 4.3.2 STRAIN GAUGE INDICATION VERSUS ACOUSTIC SIGNATURE
CHANGES FROM DRAG BRAKING TESTS ON WHEEL UP 27

TEST No.	TAPE No.	STRAIN GAUGE INDICATION			ΔA	ΔB	ΔC		RESONANCES in Hz				
		A	B	C					2012.1	2990.6	4019.5	5069.5	6129.4
25	203	0 (-340)	0 (+312)	0 (+1260)									
26	"	-330 (-674)	-800 (-500)	+120 (+1374)	-330 (-334)	-800 (-812)	+120 (+114)	0	0	0	-1.1	-1.2	-1.4
27	"	-764 (-1106)	-879 (537)	+286 (+1548)	-764 (-766)	-879 (-849)	+286 (+288)	2.2	2.6	2.6	2.4	2.1	3.0
28	"	-1412 (-1775)	NR	+51 (+1305)	-1412 (-1435)	NR	+51 (+45)	4.3	4.3	4.3	3.5	3.1	4.0
29	"	-1378 (-1732)	NR	+129 (+1403)	-1378 (-1392)	NR	+129 (+143)	—	—	3.7	1.1	0	-0.4
30	"	-1356 (-1725)	NR	+404 (+1675)	-1356 (-1385)	NR	+404 (+415)	—	—	4.7	3.9	3.0	3.0

column 2, the magnetic tape number; in columns 3, 4, 5, the strain gauge indications from A, B and C gauges; in columns 6, 7, 8, the changes in strain are evaluated from columns 3, 4 and 5, and the last five columns show the initial resonant frequency and the frequency shift that occurred in the subsequent braking stops. Table 4.3.3 is an example of the machine setup data for narrow band analysis which includes information about the type of measurement, the number of averages, the type of signal, the type of trigger, the center frequency, the bandwidth, and the sampling time length, from which the frequency error ΔF is given, about 0.4 Hz. The frequency shift shown in the last columns of Tables 4.3.1 and 4.3.2 was obtained from 54 graphs, such as those shown in Figs. 4.3.4 through 4.3.9. These figures correspond to the signature of wheel UP 28 at about 3000 Hz, taken before the drag braking test started (Fig. 4.3.4) and after each successive drag test (Fig. 4.3.5 through 4.3.9).

The limited results shown in Tables 4.3.1 and 4.3.2 show the interesting feature of a frequency shift almost independent of the resonant mode. This behavior is consistent with the theory discussed in Section 2. It is interesting to compare this frequency shift with the theoretical result given by eqn 2.4.3. Rearranging this equation one obtains

$$\frac{F}{A} = \sigma = 2\pi\Delta f_n \left[\frac{EI\rho}{A} \right]^{1/2}$$

TABLE 4.3.3

SETUP STATE ON HP 5445 REAL TIME ANALYZER

MEASUREMENT :	LINEAR SPECTRUM			
AVERAGE :	5	, STABLE		
SIGNAL :	TRANSIENT			
TRIGGER :	INTERNAL	, CHNL 1		
CENT FREQ :	6.12500 KHZ			
BANDWIDTH :	100.000 HZ			
TIME LENGTH :	2.56000 S			
ΔF :	390.625 mHZ	ΔT :	5.00000 mS	
ADC CHNL	RANGE	AC/DC	DELAY	CAL (C1/C2)
* 1	1 V	AC	50.0000 mS	1.00000
2	10 V	DC	0.0 S	1.00000

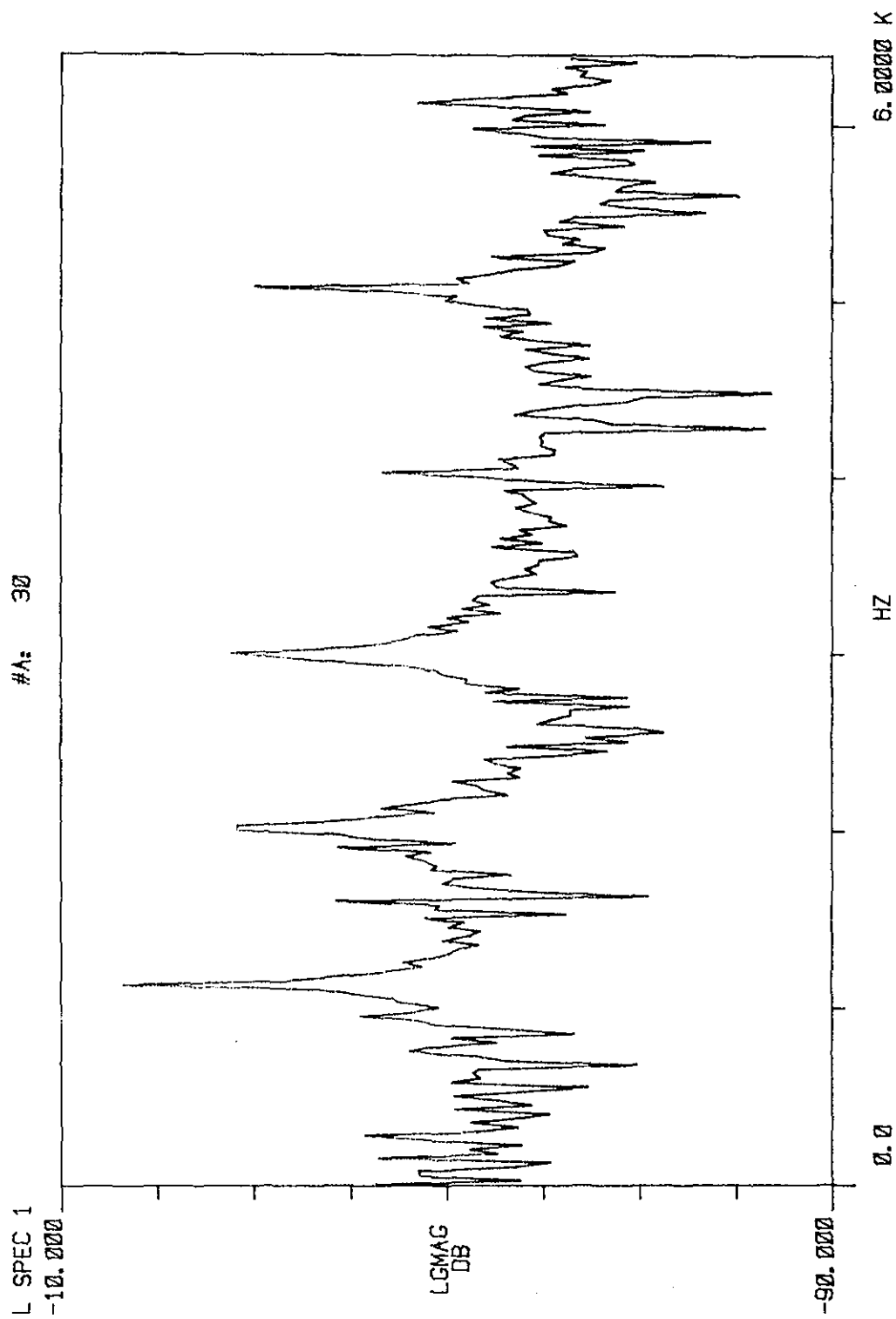


FIGURE 4.3.3. ACOUSTIC SIGNATURE OF A CJ33 WHEEL FROM 0-6.4 kHz

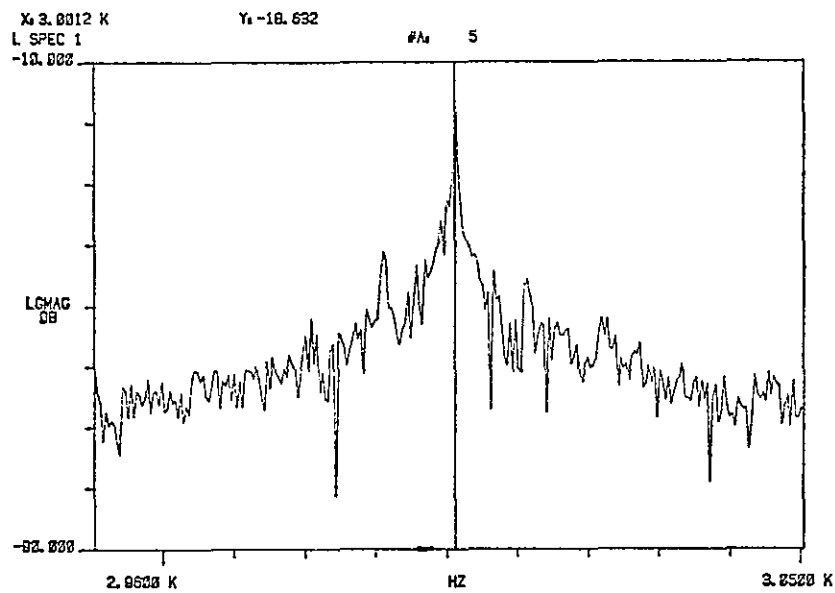


Fig. 4.3.4 Wheel UP 28 A.S. at 3 kHz before the Drag Braking Test

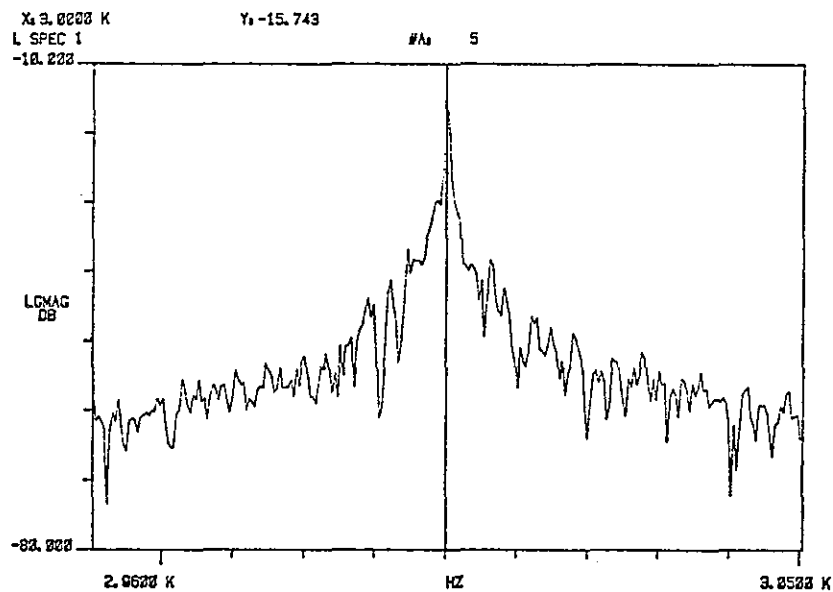


Fig. 4.3.5 Wheel UP 28, A.S. at 3 kHz after the first Drag Braking Stop

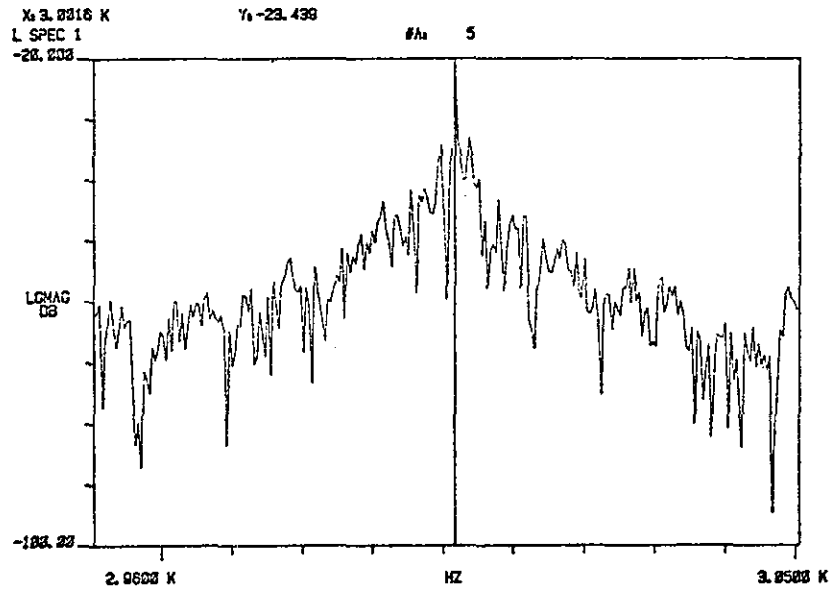


Fig. 4.3.6 Wheel UP 28, A.S. at 3 kHz after the Second Drag Braking Stop

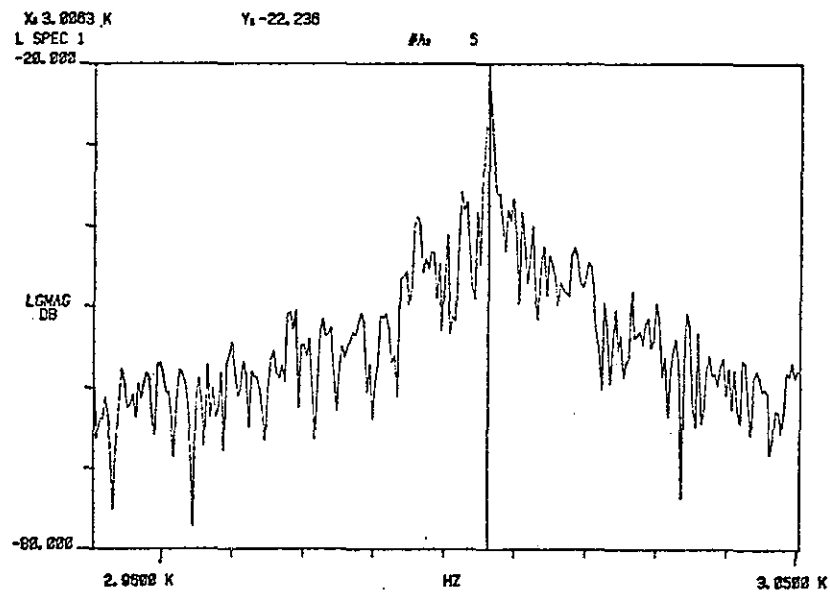


Fig. 4.3.7 Wheel UP 28, A.S. at 3 kHz after the Third Drag Braking Stop

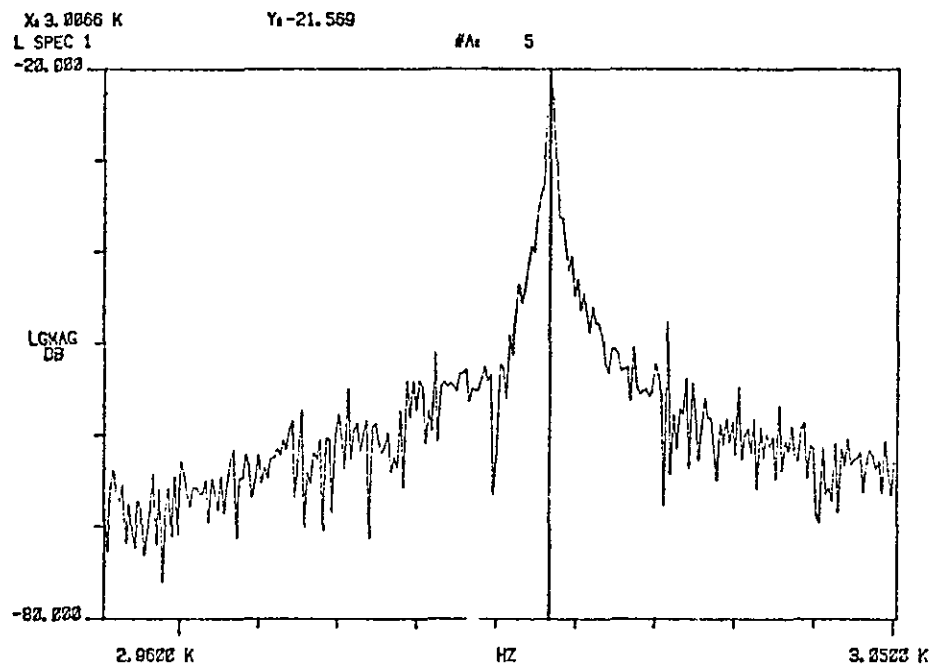


Fig. 4.3.8 Wheel UP 28, A.S. at 3kHz after the fourth Drag Braking Stop

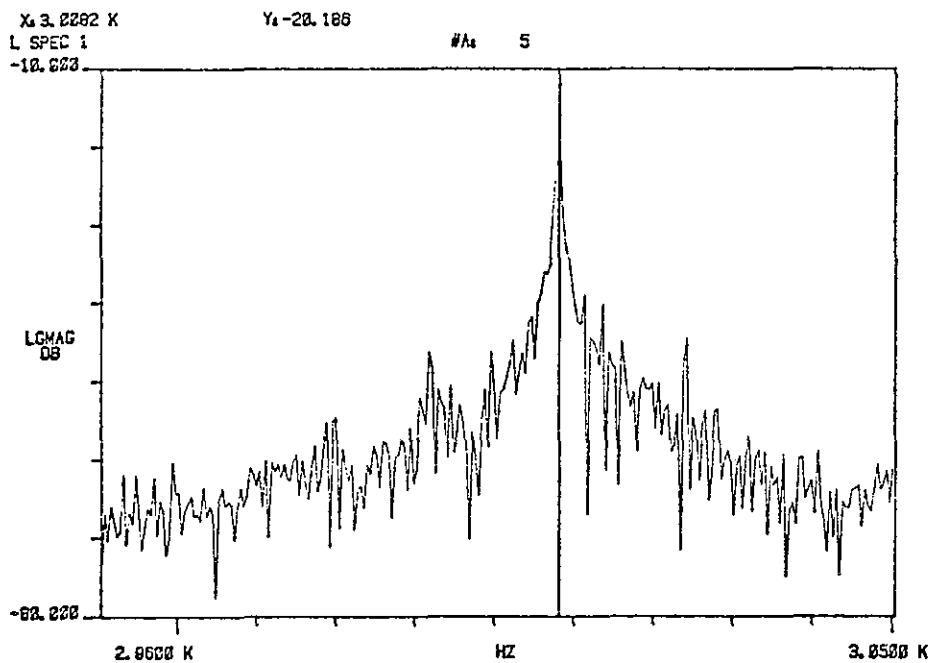


Fig. 4.3.9 Wheel UP 28, A.S. at 3kHz after the fifth Drag Braking Stop

Hence a shift of 6 Hz corresponds to a stress change of 15 Ksi. It should be noted that this value must correspond to an average stress change in the rim. Strain gauge readings at the front and back of the rim were often of different sign and varied from about 50 Ksi tension to about 25 Ksi compression with a 6 Hz frequency shift. It is therefore felt that the theory seems to give a reasonable indication of average stress.

The correspondence between strain indications and frequency shift is shown in Fig. 4.3.10 and 4.3.11. These figures show that stress conditions and frequency shift were best correlated for the readings from strain gauge A welded on the plate. This seems quite reasonable because the changes in the stress at gauge A on the plate are due to the overall condition of the rim. But there may be considerable local variations in the rim itself. The least correlated indications were from strain gauge C on the back rim. Comparison of the readings from gauge C from wheels UP 27 and 28 under similar drag braking conditions show large differences. Data from gauge B on the front rim were limited to two values for each wheel before extreme heat conditions burned them off. As has been indicated, acoustic signature differences are functions of the bulk stress, and thus might not be expressed directly by indications from a single strain gauge. It is hoped that completing the analyses on wheels UP 27 and

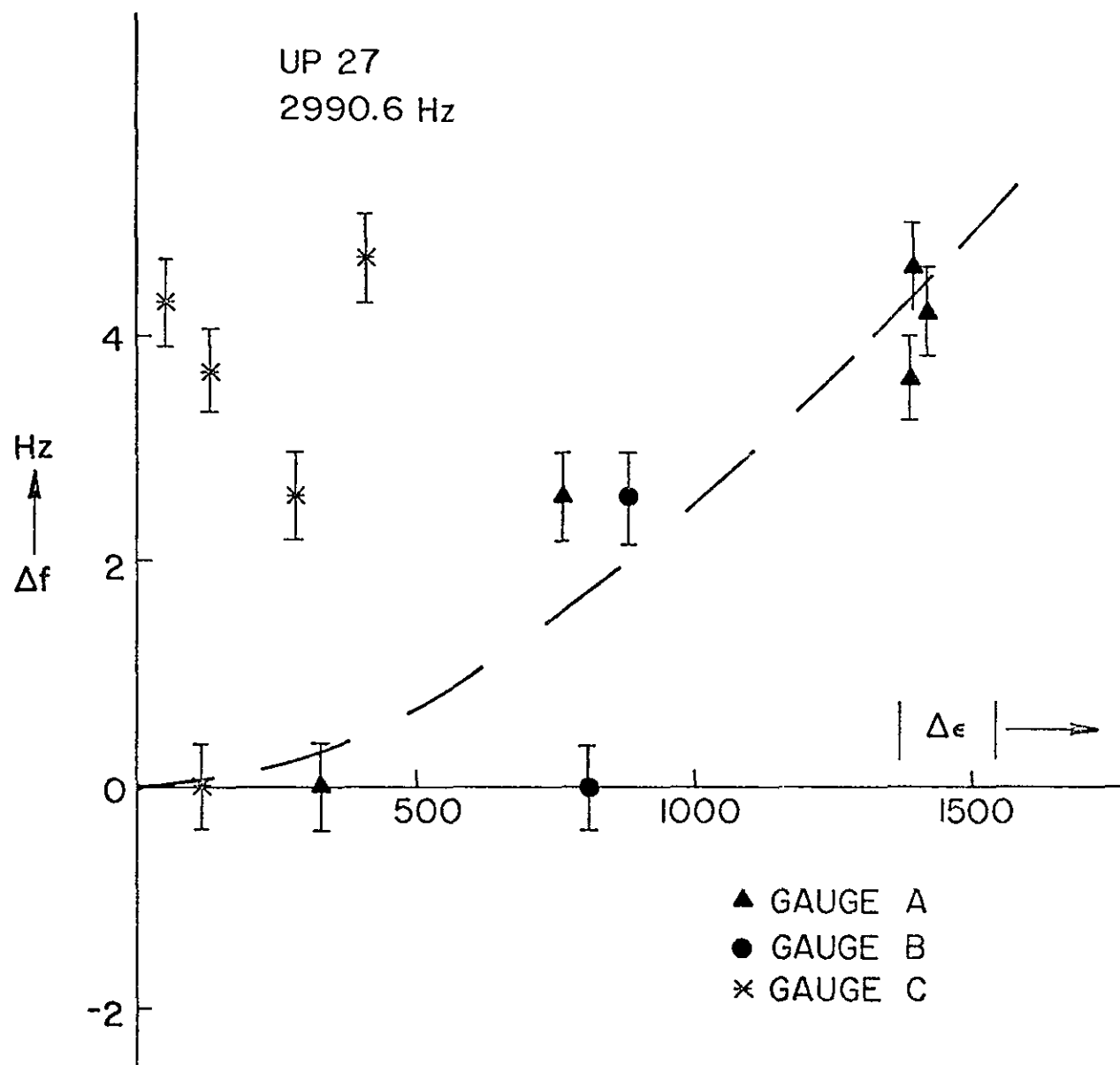


FIG. 4.3.10 FREQUENCY SHIFT Δf VERSUS STRAIN CHANGE $\Delta \epsilon$ AT 3 kHz FOR WHEELS UP 27 (FIVE DRAG BRAKING STOPS.)

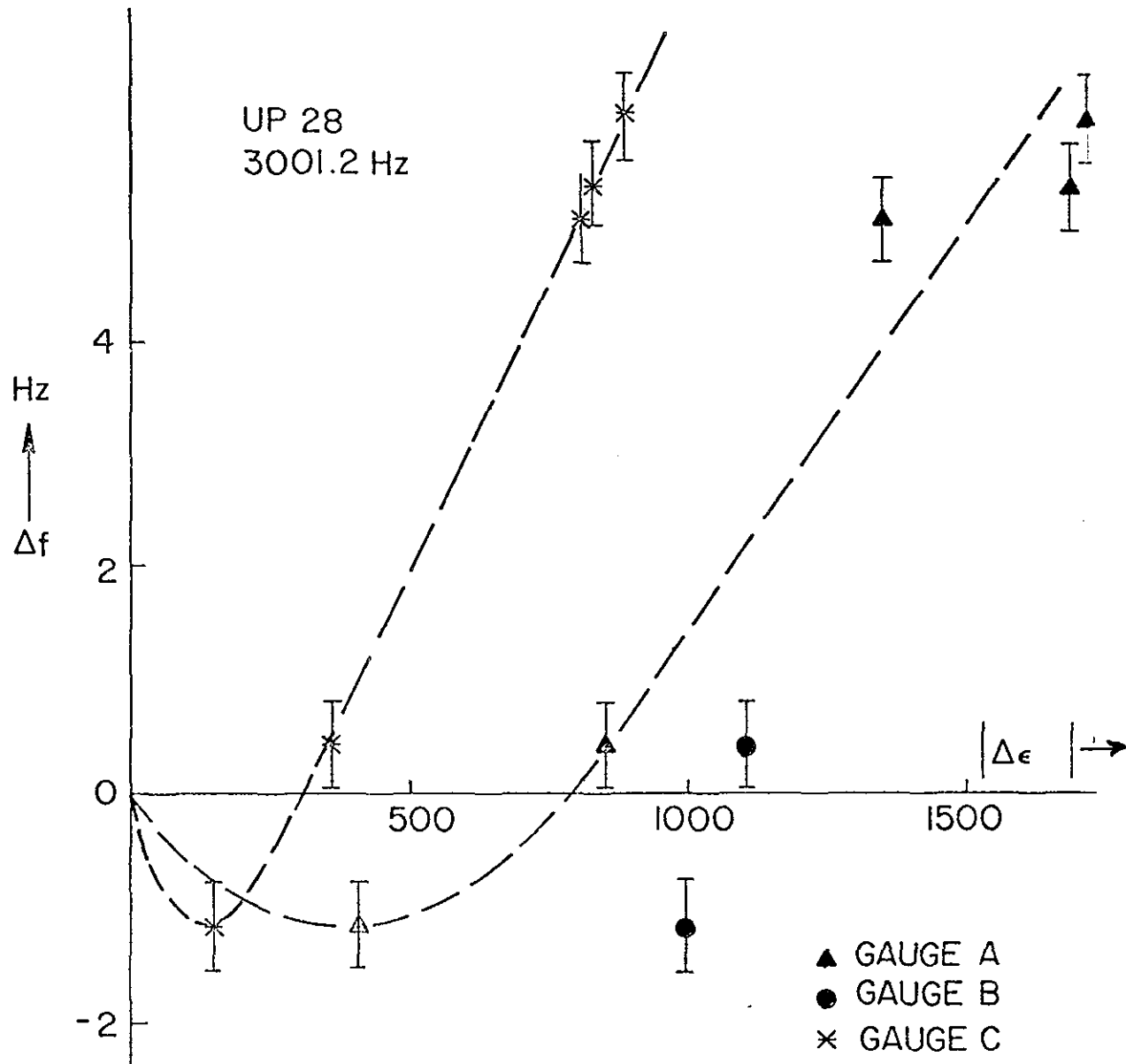


Fig. 4.3.11 Frequency shift Δf versus Strain change $\Delta \epsilon$ at 3 kHz for wheel UP 28 (Five Drag Braking Stops)

28 and also on wheels UP 12, 17, 18 and 20 will give a better understanding of the acoustic signature as a function of the wheel stress conditions.

The changes in frequency are small, of the order of a few Hz; hence a rather careful error analysis must be made. Errors in the data collection and data processing can be divided into error due to the tape transportation mechanism of the recorder and errors in the signal processing. The latter error depends on the sampling rate and time duration of the signal, which for these analyses was 0.4 Hz. Equally or even more important is the error due to the tape transport speed and fluctuation. Manufacturer's data for the NAGRA IV at 15 in/sec indicate a maximum $\pm 0.05\%$ tape speed error which could give an error of 2.5 Hz at 5 KHz. If tape speed changes occurred during the recording, the resonances ought to show frequency shifts proportional to frequency. There are indications, from comparisons of repeated impacts on the same wheel in the same condition, that if such an error occurred it was much smaller than 0.1 Hz at 1000 Hz or less than 0.01%.

A significant experimental error might be included in some of the Bessemer results. It is believed now that the results for CJ36 wheels shown in Fig. 4.2.5 are more accurate than those for CJ33 wheels shown in Fig. 4.2.6. The maximum frequency difference should be about 10 Hz instead of 25 Hz. There is no indication at this point of any important error in the dynamometer test results.

5. SYSTEM COMPONENT DESIGN

5.1 Wheel Exciter

An ideal wheel exciter should:

1. Produce vibrational excitation in the range 0-10 kHz in all types of railroad wheels. The C-weighted intensity at 3 feet must equal or exceed 100 dB. Acoustic signatures resulting from the use of the exciter must be reproducible independent of train speed and not contain resonances other than those of wheels.
2. Induce vibrations in the wheel from a point of contact low on the wheel's rim or flange. This point of contact shall be independent of the train velocity.
3. Have an auxiliary power source (electrical or pneumatic) or be mechanically powered by the train. In the latter case, the exciter must not cause a vertical displacement of the wheel.
4. Excite wheels on both rails with train speeds of up to 45 MPH (for yard operations 10 MPH should be sufficient).
5. Not present a hazard to the train or to itself for train speeds up to 80 MPH (30 MPH for yard operations).
6. Be suitable for use at any railroad track location outdoors within the continental United States.

7. Be designed to comply with requirements for track-side apparatus now imposed by the railroads. This includes OSHA safety requirements for personnel.
8. Have a Mean Time to Failure such as to allow operation for 6 months under normal conditions without probable failure.

These specifications represent an ideal to be aimed at. The designer is confronted with a large variety of conceivable devices and many choices. In the feasibility study [1] a mechanism driven by the wheel itself was used. In the present work it was decided to explore the feasibility of some alternative approaches and these are categorized according to the power source. Since some field experience had been obtained with the original hammer mechanism it was decided to pursue this design concept in parallel with the other studies to ensure that at least one form of operating exciter would be available for the field tests.

5.1.1 Mechanically Powered Excitation

The original version of the hammer exciter is shown in Fig. 1.6.1. The device operates as follows: the flange of the wheel depresses the plunger, 1, whose travel is guided by the pin, 2. Thus the link, 3, starts to rotate around the pivot point, 4. Due to this rotation point A moves towards point B compressing the hammer spring, 5. At low speeds this spring acts as an energy

storage device. When the torque about B due to the hammer spring exceeds the torque due to the weight of the hammer the spring starts to expand and drives the hammer up to impact the wheel flange. At higher speeds (above 2.5 MPH) the link, 3, actually impacts the roller 6 thus setting the hammer into essentially free rotation until it impacts the wheel. The hammer spring then does not contribute much to the forward motion of the hammer but acts only to reset the hammer following wheel impact. The forces of acceleration and deceleration on the hammer mechanism can be very large (see Appendix E). The associated stresses in this mechanism probably were excessive in the device tested in Omaha in 1974, and led to its failure when activated by a fast train passing over it. A tentative solution to this problem was to make the entire hammer, and hammer mounting, a one-piece unit cut from steel plate. In addition, the impacting face of the hammer was heat treated to harden it against wear. A view of the modified exciter is shown in Fig. 5.1.1. This is the version of the hammer exciter used in the field tests to be described in Section 6. It should be noted that a full dynamic analysis of the hammer mechanism remains to be completed. However, a simplified model is discussed in Appendix E. Some snapbuckling mechanisms have been proposed by Fazekas [41] and these devices were given some consideration as means of achieving the requirements of a wheel activated hammer. Although the conceptions are

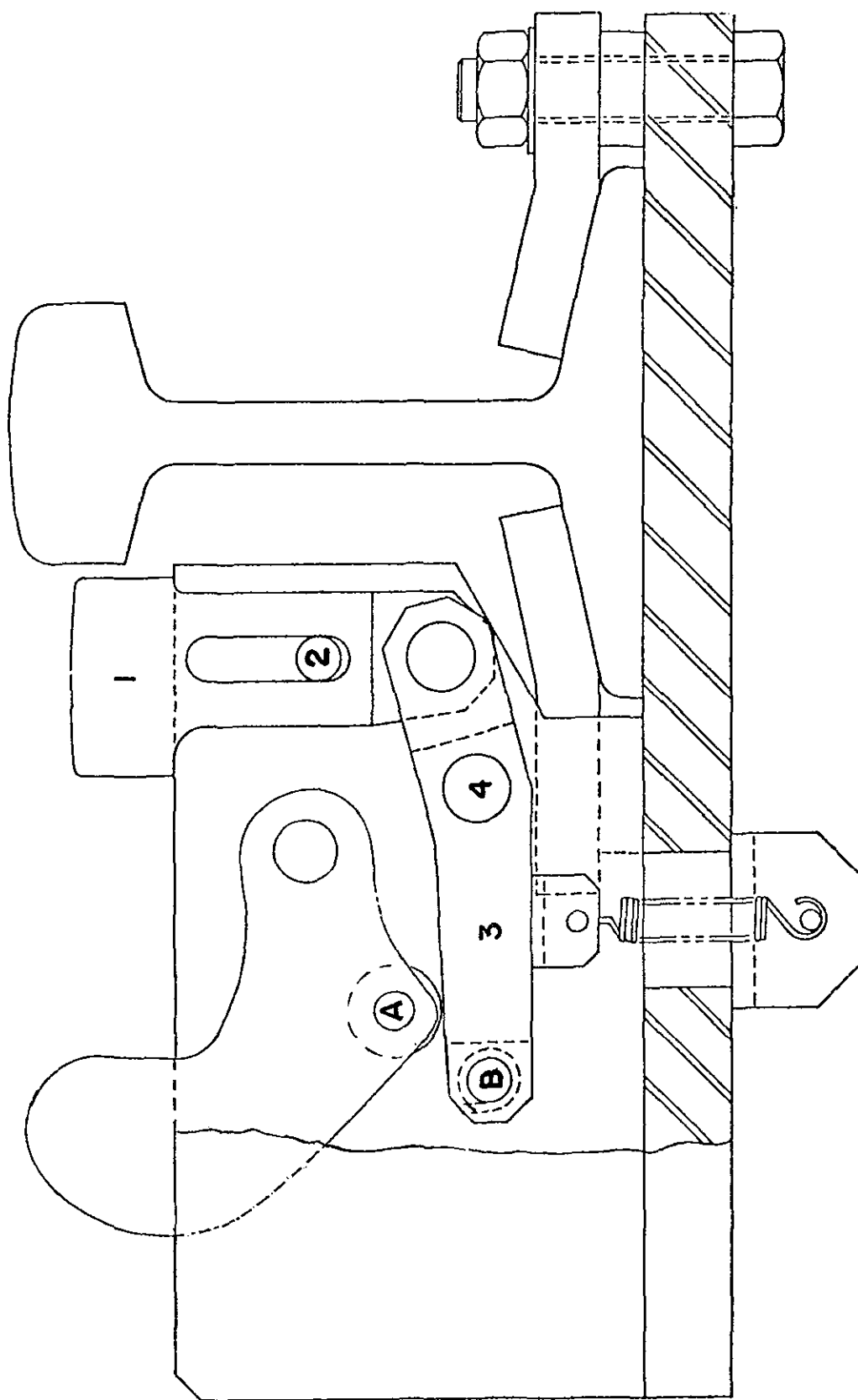


FIG. 5.1.1.1 DRAWING OF THE MODIFIED MECHANICAL WHEEL EXCITER

elegant, time and resources simply did not permit the design and construction of a working device.

5.1.2 Electrically Powered Excitation

An electric motor to spin two or more impacters, preferably 4, 8, etc., for balance reasons, against the rim of the wheel was also examined (see Fig. 5.1.2). The first tests were performed using a 1/4 HP 1725 rpm motor; in later tests a 1/2 HP universal-type AC-DC motor was used with speed controlled by a VARIAC. The motor exciter represents two significant departures from the hammer type exciter concept. It is electrically powered and therefore the impact is independent of the train speed. However, it may produce multiple impacts on the same wheel. The attraction of this design is its ability to produce impacts at train speeds up to 40-45 MPH and to survive at any train speed. It is a simple design but it must be well guarded for safety reasons. The electric motor and spinning impacter combination was tested on good, bad and greasy wheels. The preliminary conclusions on the feasibility of using this design were: a) the spectra obtained from the good, bad and greasy wheel are noticeably different, and b) spectra from the same wheel were reasonably reproducible.

An impacter to be actuated by a solenoid, such as an automobile starter, was also given some consideration. However, the concept was not pursued since a triggering pulse would be required and this would involve further

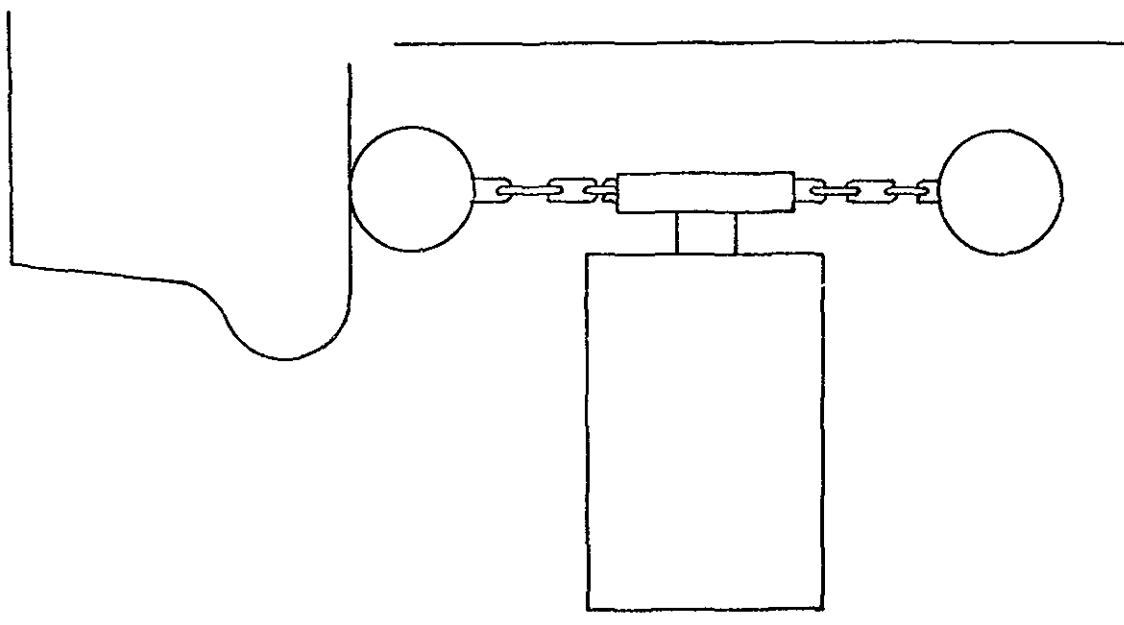
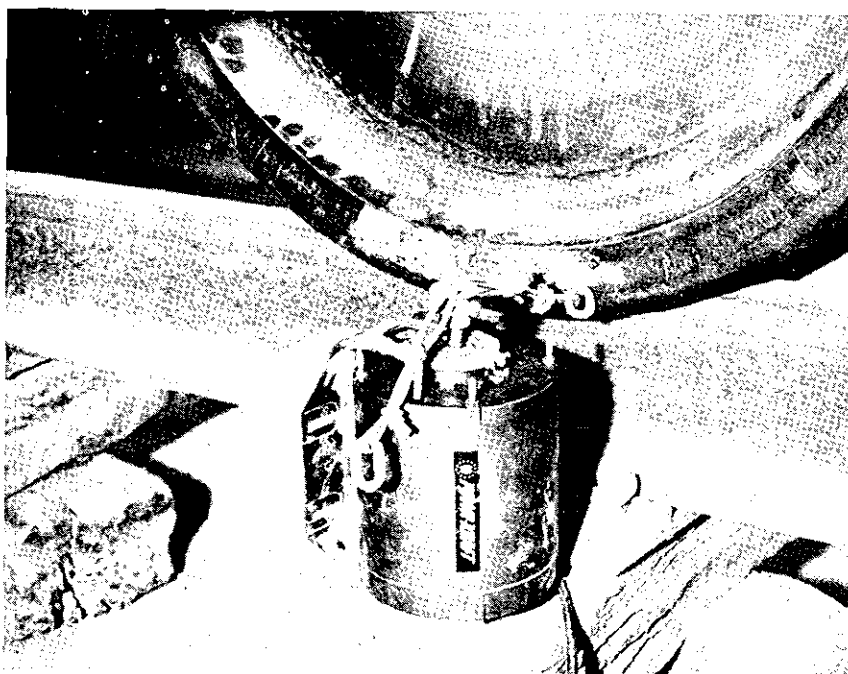


FIG. 5.1.2 MOTOR EXCITER, ROTARY

complication of the system. The motor exciter could be left running during the passage of a train.

5.1.3 Pneumatic Powered Excitation

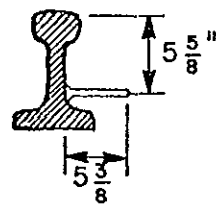
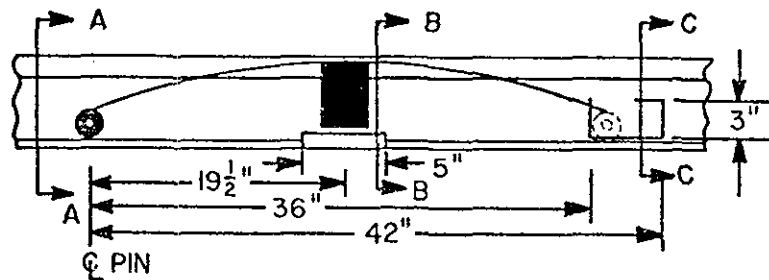
Another concept examined was that of a pneumatic vibrator impacting a ramp depressed by the wheel flange. The main attraction of such an exciter is the ruggedness and the safety. Pneumatic vibrators are also commercially available in a variety of types, sizes and are low priced. A problem is the background noise of the hammer itself.

Pneumatic vibrators were obtained for preliminary testing of the feasibility of this type of wheel excitation. Included were large and small reciprocating piston types, and five different sizes of rotary vibrators. Testing involved holding each vibrator in contact with the wheel, and obtaining taped wheel signatures associated with differing points of contact and differing air pressures. These tapes were then analyzed using both the 1/3 octave band B & K analyzer and the Spectral Dynamics narrow band analyzer. The results of this investigation were: a) the large piston type vibrator was difficult to keep in contact with the wheel, and therefore no conclusions could be drawn; b) the small piston type vibrator produced usable wheel signatures which were reproducible and comparable in quality to those obtained by rolling ball impact; and c) the rotary vibrators did not excite a broad spectrum of the natural modes of vibration in the wheels. An explanation

for the failure of the rotary vibrators to excite the wheels is evident in the fact that an off-center spinning mass produces a frequency of vibration which is the inverse of its orbital period. This is not comparable with the rich spectrum of frequencies associated with the delta function of an impacting mass. Consequently, the rotary vibrators will only excite the few natural wheel frequencies which are close to that of the vibrator's frequency. The piston vibrator, on the other hand, induces frequencies of vibration almost uniformly throughout the 0-10 kHz band of interest.

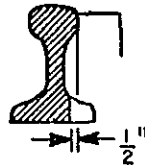
To test the performance of a pneumatic vibrator and mounting, a NAVCO model BH 1-1/4 impact type was installed on a custom made leaf spring ($K = 150 \text{ lbs/in}$) which was mounted on the test track. The leaf spring parallels the inside of one of the rails, with the vibrator directly attached to the underside center of the leaf spring. In use, the vibrator operates continuously. The wheel flange depresses the leaf spring in passing over it and the impact vibrations are then transmitted into the wheel. This design is attractive for its simplicity and suitability for outdoor use. As it was mentioned earlier the background noise level produced by the pneumatic vibrator was high but a 6-8 dB reduction was achieved through the use of an exhaust muffler and damping compound applied to the vibrator and leaf spring. Figure 5.1.3 shows the details of this design.

MODIFICATIONS REQUIRED TO MOUNT LEAF SPRING VIBRATOR WHEEL EXCITER TO TEST TRACK. THIS DEVICE USES 80 PSI-REGULATED AIR SUPPLY. SECTION AA SHOWS A 5 AND 3/8 INCH STEEL BOLT WELDED TO INSIDE OF TRACK PARALLEL TO TOP OF TRACK. SECTION BB SHOWS THE INSIDE BOTTOM OF THE RAIL CUT AWAY 1/2 INCH BEYOND THE INSIDE EDGE OF THE TOP OF THE RAIL. THE CUT AWAY IS 5 INCHES LONG. SECTION CC SHOWS 1/4 INCH STEEL PLATE WELDED TO THE INSIDE BOTTOM OF THE TRACK. THIS ALLOWS THE FREE END OF THE LEAF SPRING TO FLEX WHEN THE SPRING IS DEPRESSED BY THE WHEEL. THE LEAF SPRING IS 3 AND 1/16 INCHES WIDE. THE INSIDE EDGE OF THE LEAF SPRING JUST TOUCHES THE INSIDE EDGE OF THE TOP OF THE RAIL.

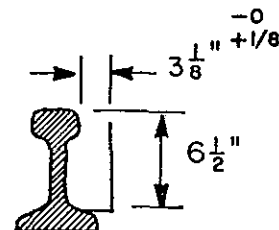


INSIDE OF TRACK
(BOLT IS 5/8 INCH DIAMETER)

SECTION AA



SECTION BB



SECTION CC

FIG. 5.1.3. PNEUMATIC LEAF SPRING EXCITER

The problem with this type of design is that the amplitude of the sound from a wheel rolling over the leaf spring is much less than from the directly impacting devices, such as mechanically and electrically actuated hammers.

5.1.4 Comparison of Exciter Types

Table 5.1.1 is a summary of ratings of these various types of exciters assessed according to the specifications of an ideal exciter. The characteristics of the acoustic signature are given a higher weighting than the other specifications since if the device does not give a reproducible signature, it is useless for the present purpose. Overall the mechanical hammer appeared to be the best device to use despite its dependence on wheel speed in its present form. The pneumatic exciter was downgraded because of the weakness of the signature intensity. The electric motor driven impactor was downgraded slightly as regards signature because of the problem of multiple impacts and because of possible safety problems. It would also present a profile above the top of the rail. As a result of these considerations it was decided to use the modified hammer exciter in the field test.

5.2 Wheel Sensor

The search for a device to be used to generate a trigger pulse was restricted to three possible types:

TABLE 5.1.1 RATING OF 3 EXCITER TYPES AGAINST IDEAL SPECIFICATIONS

SPECIFICATION	MECHANICAL HAMMER	PNEUMATIC VIBRATOR	ELECTRIC MOTOR
Signature	5 x 2	1 x 2	4 x 2
Contact Point	4	4	4
Operational to 45 mph	3	4*	4*
No Hazard at 80 mph	3	3*	4*
Weather Resistant	4	4*	3*
Safety	4	4*	2*
Mean Time to Failure	3	4*	4*
TOTAL	32	25	29

Note the quality of the signature is rated twice as important as other considerations.

5 = Excellent
 4 = Very Good
 3 = Good
 2 = Fair
 1 = Poor

*Rating based on surmise, rather than experience.

a) microswitches, b) photosensors, and c) commercially available metal sensors. Microswitches had already been used in an earlier test. Their performance could be rated as moderate because they are susceptible to rough operational conditions. Stable mounting of the microswitch on the track or exciter was also a problem due to vibrations induced by the train rolling over it. Electric contact noise was another problem, although it could be eliminated with proper electronic filtering. Photosensors would be an ideal solution if they could survive the dirt of the yard and severe weather conditions. In the third class the best available wheel sensor system appeared to be the DUAL DIRECTIONAL WHEEL SENSOR by ACI, since many engineering problems had been solved in its development. It has solid state circuitry, which is shock mounted and temperature independent from -40° to $+140^{\circ}\text{F}$. It has a waterproof casing and is easily installed and adjusted. The wheel speed can range from 0 to 80 MPH. The operation of the wheel sensor is based on the principle of magnetic flux change in a coil to detect the presence of a wheel. The device has two sensing units to determine wheel direction. During the present tests only one unit was used because the direction of wheel travel was not needed. The basic elements of each sensor unit are a permanent magnet as the source of the magnetic flux and a coil whose inductance

changes when a wheel is present due to the change in the magnetic flux in the core of the coil. The unit is also equipped with a light-emitting-diode (LED) which stays on when the sensor indicates a wheel presence and which can be used to check if the sensor is functioning. The output voltage circuit is shown in Fig. 5.2.1. In this figure, S1 is a solid state relay whose contacts close in the presence of a wheel and are rated for a maximum current of 25 mA at 24 VDC. The triggering pulse was the voltage obtained across the resistor $R2 = 1200 \Omega$. For tape recording, the voltage E was about 3.0 Volts, for direct real-time sensing it was about 4.5 Volts.

5.3 Microphone

General Radio had recently introduced a weatherproof microphone system for outdoor noise monitoring. This microphone system is shown in Fig. 5.3.1a. The microphone element is an electret condenser random incidence microphone. It has flat response, wide dynamic range and high sensitivity. It also has a permanently charged diaphragm so it does not require a polarization voltage and it does not become noisy in a humid environment. The General Radio system includes a preamplifier after the microphone element to transform the impedance from high to low, so that long cable can be used. The first outdoor test of the microphone in Pueblo, Colorado under very dry and cold weather conditions was satisfactory

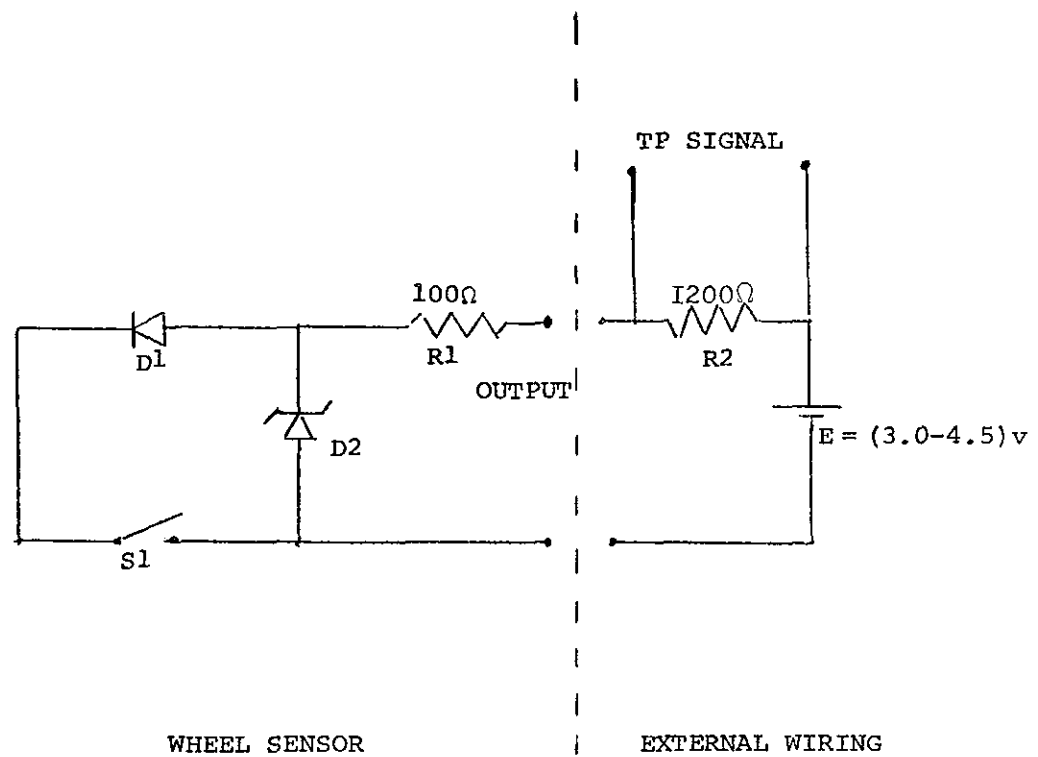


FIG. 5.2.1 OUTPUT VOLTAGE CIRCUIT OF THE WHEEL SENSOR

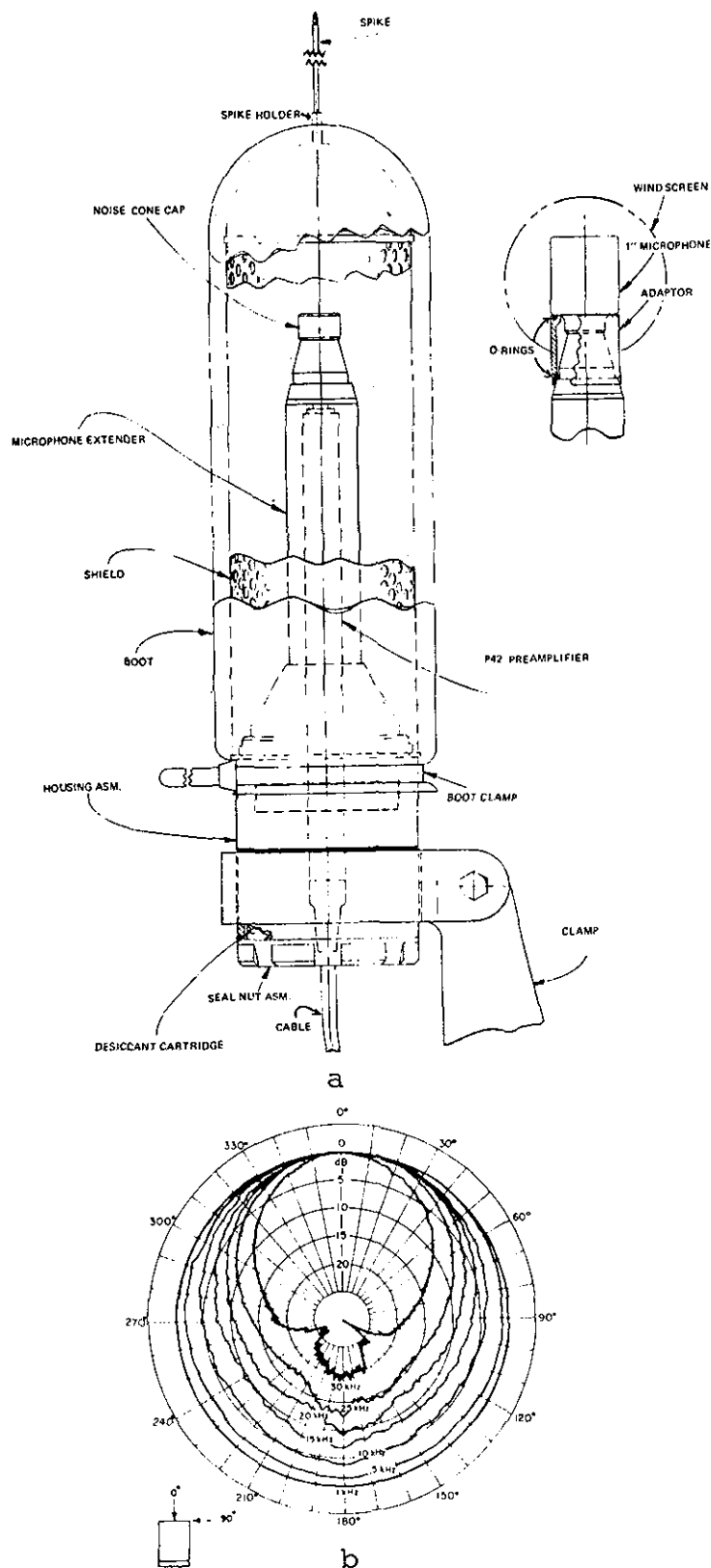


FIG. 5.3.1a ASSEMBLY OF WEATHERPROOF MICROPHONE
 b DIRECTIONAL RESPONSE PATTERNS FOR THE GR $\frac{1}{2}$ INCH
 ELECTRET-CONDENSER MICROPHONE

and encouraged the acceptance of this type of microphone for the final field test. The only negative aspect was the need for a power supply for the microphone's preamplifier. A directional microphone would have been a better choice than the random incidence type actually used. The directional response patterns of the present microphone are shown in Fig. 5.3.1b. The system used in the final field test included two microphones installed on either side of the track. The sound signals go into a microphone mixer whose output goes to a filter and then to the real-time analyzer.

5.4 Spectrum Analyzer, Computer and Diskette Interfacing

The most important parts of the system are the real-time analyzer (RTA) and the mini-computer. At the present time there are basically two ways to extract frequency information from a sound signal: a) using an analog to digital (A/D) converter and subsequently analyzing the digitized signal through the use of computer software or b) using a RTA. The selection of the proper device is based on the duration, frequency range, amplitude, type (transient or stationary) of the signal and the frequency resolution of the analyzed spectrum. Different commercial devices have similar specifications and it is hard to select the best. Rapid improvements and development of these products make the selection even more complicated.

A NOVA 1220 computer interfaced with a 39 channel, 1/3 octave band analyzer had already been used in previous wheel testing by Nagy [1] and Dousis [4]. Some spectral analysis had also been done using a Spectral Dynamics model 330A real-time analyzer on loan from the Company for a short period of time but without any digital interfacing. The cost of the SD330A, its fast signal analysis for the frequency range needed in the tests and the familiarity of the researchers with it led to the selection of this device as the spectrum analyzer for the system. However the use of an A/D converter should be given serious consideration as a part of a prototype system. Some advantages and disadvantages of the SD330A analyzer in respect of transient signal analysis will be presented in the appropriate chapter.

The computer for the system was a 16K NOVA 1220. Because of the medium memory size of the computer the bulk of the software was written in BASIC language. The digital output of the SD330A analyzer was interfaced with the NOVA's I/O board according to Table C.1 in Appendix C.

The next major task after the interfacing was the development of NOVA computer software needed to operate the analyzer and retrieve data from it. To accomplish this the following software was written:

1. Assembly subroutines for control of the SD330A analyzer, including the following commands: start, stop, peak, cursor/plotter, sweep or reset [35],
2. Assembly subroutines for use of the NOVA Real-Time Clock.
3. Assembly subroutines to read and operate on individual spectra (250 channels) from the SD330A using the slow speed plotter output mode.
4. Assembly subroutines to read, print, and operate on individual spectra in the high speed (53 ms) output mode, i.e., levels from the 250 channels are sequentially read in 53 ms directly into core memory.
5. Assembly subroutines to store complete spectra in NOVA core memory in sequential order.
6. BASIC language programs to call the above Assembly subroutines for processing spectra.

The core memory requirement for a single spectrum is 250, 16 bit, words. After the BASIC interpreter and the program was stored in the memory, 3K of core was available for data, which means only 10 spectra could be stored in the computer. Approximately 5 ms are required to retrieve one data word for processing. Retrieval of two complete spectra for an across-the-axle comparison takes about 2.5 seconds which does not include the analysis program execution time.

Considering this relatively long execution time for BASIC instructions, it was concluded that the analysis for wheel fault detection would not be done immediately following reading the spectra as the train cars pass over the exciters. (For a car speed of 10 MPH, wheels on the same side of a truck will pass over the exciter in approximately 0.4 seconds). Thus it appeared that the analysis ought to be done in near real-time, i.e., immediately after the last wheel spectra is read into the computer. Furthermore, since core memory was limited to approximately 1 car, and since additional core memory boards would not greatly increase this capacity to store wheel spectra, a peripheral memory device of several hundred thousand word capacity was needed if long trains were to be scanned with this apparatus. The speed of data transfer from the SD330A of 4717 words per sec is too fast for the NOVA Cassette which writes at 800 words per second. A Data General Diskette unit, model 6031 was the best technical choice having a transfer rate of approximately 16,000 words per second and a storage capacity of 157,696 words. The track to track head positioning time is 20 ms. Eight spectra may be stored per track. The assembly routines for data transfer from the computer to the Data General Diskettes and retrieval are presented together with the rest of the software in Appendix C.

5.5 System Description and Software Development

The general configuration of the system for railroad wheel inspection is as shown in the layout of Fig. 5.5.1. Airborne sound or vibrations of the test object were detected using a microphone or an accelerometer respectively. The signal was preamplified near the transducer, and then filtered for further signal processing. In the field tests it was recorded in channel No. 1 of a dual channel tape recorder. The triggering pulse was recorded in channel No. 2; this being very important because timing reference and information are essential for short duration transient signals, such as impact recordings. The tape recordings were later analyzed in the laboratory. In the Englewood Yard test the signal could be both recorded and processed in real time. The sound signal was fed into the analyzer for Fourier analysis. During the early stages of the project no digital interfacing and control were available, hence precise data sampling was impossible due to timing errors, and data collection was slow. The analyzer was then operated in the PEAK, STORE mode, because that was the only way to avoid the timing problems. In the peak mode the maximum response of the test object was obtained on the analyzer's screen and it could be traced on the X-Y plotter for permanent record and inspection. Numerical data were taken sweeping the spectrum, through the CURSOR, manually.

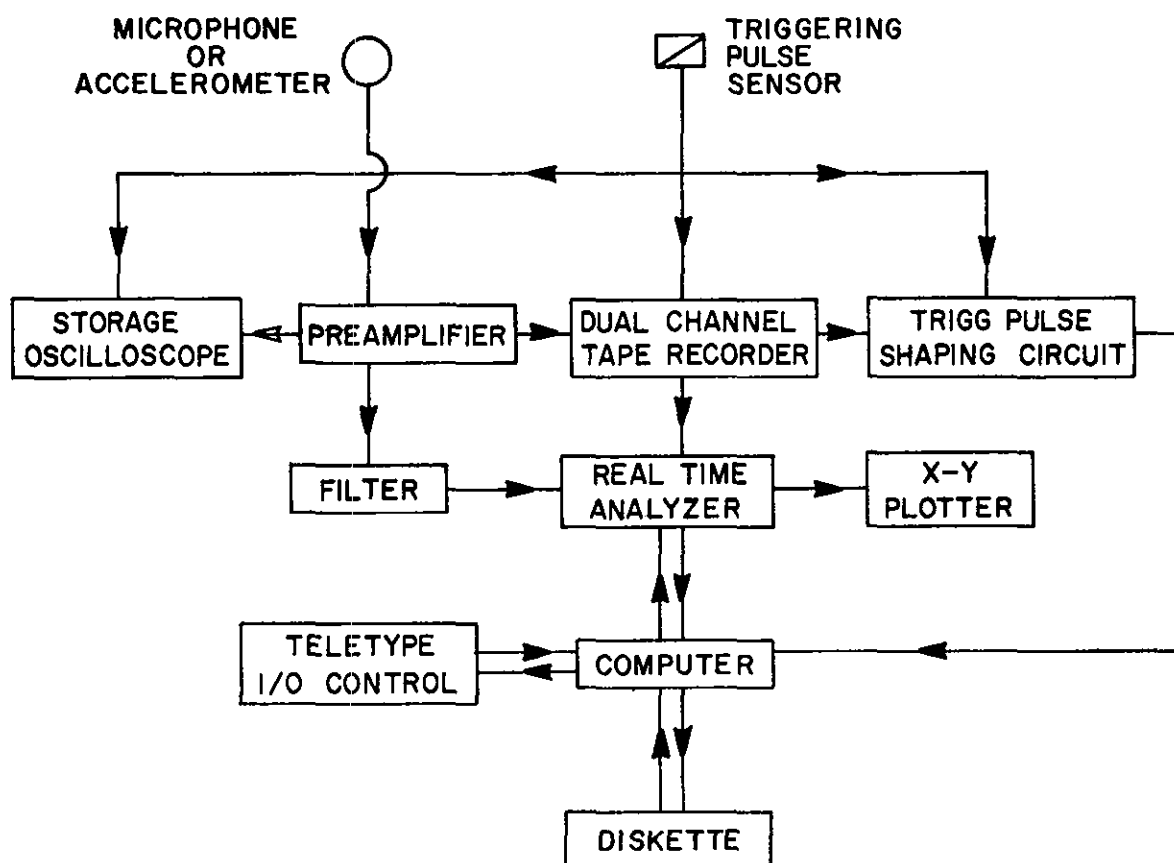


FIG. 5.5.1 SCHEMATIC OF DATA COLLECTION AND PROCESSING HARDWARE

One disadvantage in the case of impact analysis using the PEAK mode is the presence of the shock wave produced during the impact together with the response of the test object. This means that the spectrum obtained includes the Fourier components of the shock wave, which theoretically is a continuous spectrum. In practice though (narrow band analysis), it does not appear as continuous, but as a very dense low amplitude line spectrum. When another mode is used such as EXP. AVG. (exponential average) or START where the spectrum in the analyzer's memory is the sum of N successive analyzed spectra divided by N, the number of averages selected, these peaks disappear rapidly due to the short duration of the shock.

One of the recognition and decision schemes used early in the project was line spectra comparison. The line spectrum of a signal is a representation of its spectrum with lines at the resonances whose amplitude is above a certain level. An example of a line spectrum is shown in Fig. 1.4.2. From the finite element analysis studies it was known that a good wheel has fewer resonance lines compared to the same type of defective wheel. Another characteristic is the frequency shift in some of these resonances in defective wheels of the same structure and geometry. Therefore, comparison of good wheels of the same type should give identical or well matched line spectra, whereas a good to bad wheel comparison ought to show significant line mismatching.

During the first experiments line spectra acquisition was done manually using the X-Y plots of the acoustic signatures. An example of these results is shown in Table 5.5.1. The first column of the table has the wheel code; the second, the wheel description. The third column has the total average number of lines based on three or four signatures from impacts on the same or different points on the rim of the wheel. The fourth column has the number of common lines between these spectra and represents the "average" line spectrum of the wheel.

As an example, the first axle tested had good 33" cast, single wear wheels. Three different impacts (signatures) on the same point showed an average of 38 lines on both wheels. On the east side there were 28 common lines, on the west side, 32. Finally, there were 19 lines common to both sides (fifth column). In the case of a good 33" wheel compared to a 33" wheel with a partial crack, the number of matched lines was 11, and comparison between the partially cracked wheel and the one with the large crack indicated only 4-7 common lines, although for some lines it was difficult to see if they had identical frequencies or if there was a one channel shift. The line spectra comparison procedure was later automated using BASIC/ASSEMBLY language software. Analyzing taped acoustic signatures with the above software, results were obtained as shown in Table 5.5.2. Important conclusions were obtained from

TABLE 5.5.1

SUMMARY OF THE LINE SPECTRA ANALYSIS
(RESULTS OBTAINED MANUALLY FROM SPECTRA PLOTS)

WHEEL CODE	WHEEL DESCRIPTION	NUMBER OF SPECTRAL LINES (AVERAGE OF 3 OR 4 SPECTRA)	NUMBER OF COMMON SPECTRAL LINES	NUMBER OF COMMON LINES FROM WHEELS ON THE SAME AXLE	REMARKS
SP1E	GOOD 33" CAST 1W	38(3) Same Point	28	19	Same Axle
SP1W	GOOD 33" CAST 1W	38(3) Same Point	32		
15 A	LARGE PLATE CRACK	42(4) Diff. Point	24	6 - 7	Same Axle
15 C	PARTIAL PLATE CRACK	41(4) Diff. Point	30		
15 A	LARGE PLATE CRACK	45(3) Same Point	28	4 - 7	Same Axle
15 C	PARTIAL PLATE CRACK	44(3) Same Point	31		
15 C	PARTIAL PLATE CRACK	40(4) Diff. Point	28	11	Diff. Axle
SP1W	GOOD 33" CAST 1W	41(4) Same Point	32		

TABLE 5.5.2

SUMMARY OF THE LINE SPECTRA ANALYSIS
(TESTS WERE COMPUTER CONTROLLED)

Number of Wheels Tested	% Range of Lines Matched Between Two Signatures	Remarks
18	70-100	Same wheel-same point. All good wheels.
18	40-90	Wheels across the same axle. All good wheels.
14	10-50	Good/Bad wheel, across the same axle.

these tests:

- a. There is some overlapping in the percentage of matched lines in good/good and good/bad wheels.
- b. Large defects (plate cracks) showed a 10-20% line matching and therefore should be easily detected under this scheme.
- c. A comparison was made between the spectra of two good wheels on the same axle, one having a very worn flange. A low matching percentage of about 30% was found.
- d. A change in the input attenuation by a few dB caused a different percentage of matching. This was to be expected, because it changes the discrimination window.
- e. Small defects, such as thermal cracks, had 50% or higher of matching lines.
- f. The Line Spectra comparison scheme could not be used alone for detection of defective wheels. Thermal cracks would be difficult to detect and small changes in the wheel geometry, such as worn flanges, would appear as defects.

The BASIC software developed for the Englewood Yard tests is given in Appendix C. A simplified general flow diagram is shown in Fig. 5.5.2. The most important change from earlier versions was to base the decision on consideration of several factors: the number of coincident resonances, the amplitudes of signals in the same spectral

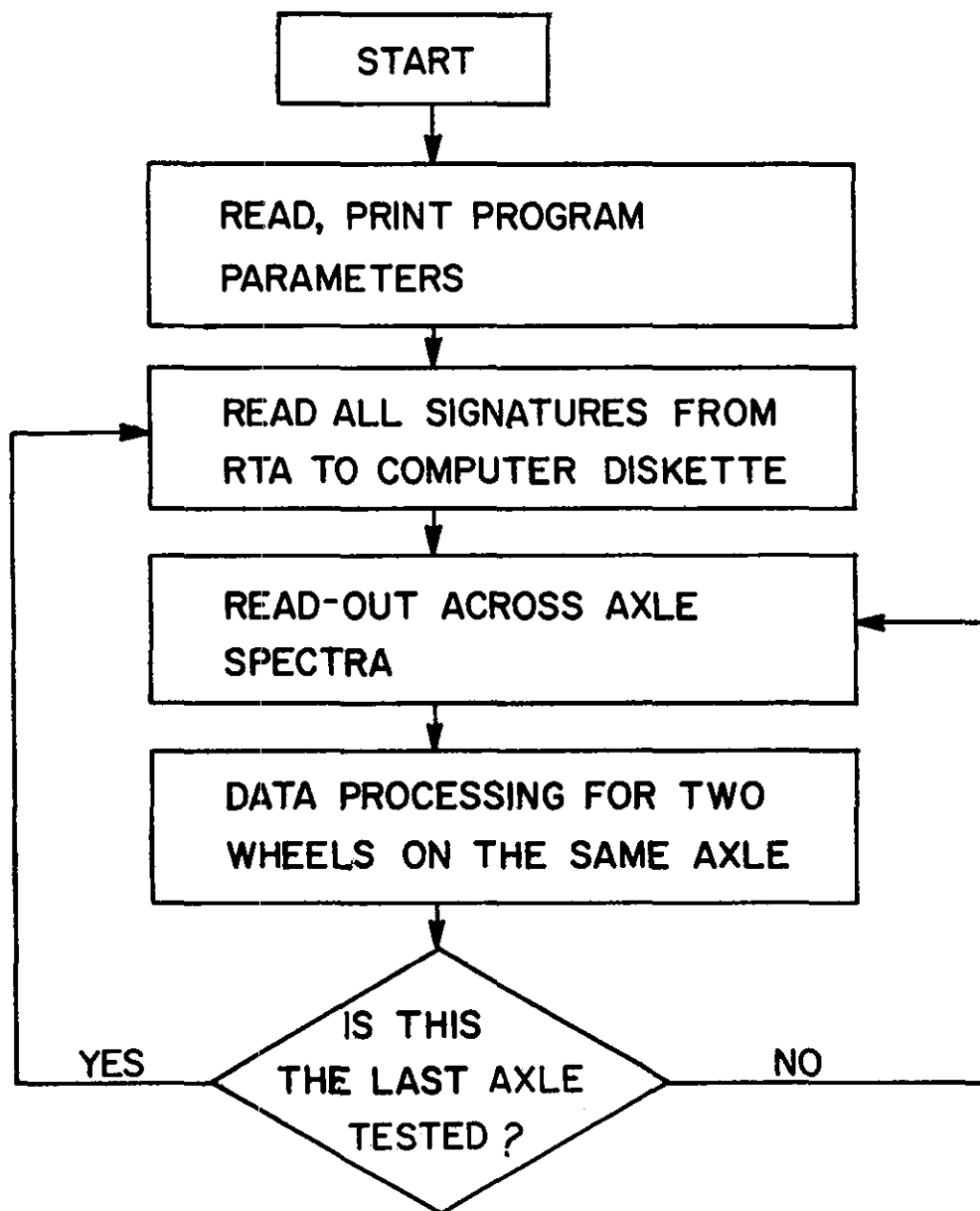


Fig.5.5.2 Flow diagram for the Series of Computer Programs used in the SP Englewood Yard, Houston Tests

range and the decay rates of sound from the two mating wheels. A number, called the difference index (DI) was computed as follows:

$$DI = C_1 SD + C_2 (1/SP_1 + 1/SP_2) + C_3 (DR_1 - DR_2) + C_4 (DR_1 + DR_2)$$

where C_1 , C_2 , C_3 and C_4 are weighting coefficients.

SD is the sum of the absolute value of the differences between corresponding channels ignoring 3 channels at common resonances. (Resonances are found using subroutines from the line spectra comparison program).

SP1 is the sum of all channels for the spectrum of wheel No. 1.

SP2 is the sum of all channels for the spectrum of wheel No. 2.

DR1 is the decay rate for wheel No. 1.

DR2 is the decay rate for wheel No. 2 (across the axle).

Some comments on the terms of this empirical formula are in order.

1. The first term SD. This is the most important term and the decision is based mainly on the value of SD. The amplitude of the resonances depends on the impact, and spectra from the same wheel under different impact forces, at the same impact point will give spectra of varying resonance amplitude. To reduce the error introduced because of the intensity of the

impact, the differences between the spectra are ignored at common resonances and the differences of the two channels adjacent to the peak are also ignored.

2. The second term, $1/SP1 + 1/SP2$. $SP1$ and $SP2$ are the sums of all channels for each wheel. Good wheels have low damping compared to defective and greasy wheels, and in that case $SP1$ and $SP2$ are large numbers and have small inverse values.
3. The third term, $DR1-DR2$. Good wheels have low decay rates and hence this term is then a small number. Greasy wheels have significant DR , but they are usually both greasy on the same axle and again this term is small. Only in the case of good/bad wheel pairs does this term contribute to the difference index.

The decay rate (DR) is defined as the number of channels, $K2$, which dropped more than $L2$ dB ($L2 = 8$ dB in these tests) between the first and second reading, divided by the number of channels, $K1$, which exceeded $P4$ dB ($P4 = 8$ dB in these tests).

4. The fourth term, $DR1 + DR2$. This term is small when wheels are good, and large in cases of greasy or defective wheels. To separate defective from greasy wheels a subroutine checks the pattern of the signature. If the high frequencies are damped more than the low, this is an indication that the wheel is greasy.

The flow diagram of the READ and acoustic signature sections of the main program is shown in Fig. 5.5.3. Details of the flow diagram of the data processing section of the program are shown in Fig. 5.5.4.

A sample of the computer printout is shown in Fig. 5.5.5. The operator types RUN on the teletype, the date and number of the test, then the computer starts printing information about identification of the program and values of the parameters. The program calls for the time and number of the tape where the test will be recorded. At this point, being ready to start collecting data, the execution goes to a subroutine which checks for a triggering pulse. After sensing the TP, the RTA starts sampling and processing the sound signal in the Exponential Average mode for 150 ms, the values on the 250 channels of the analyzer being transferred to the computer through the digital interfacing. A second spectrum is read into the computer 150 ms later (300 ms after the TP). Comparison of the two spectra gives the decay rate of the sound. Following that the two spectra are stored on the diskette, a process which can take from 40 to 200 ms. The computer then gets ready for a new reading, which will start with the next TP. Although the maximum time interval required for one signature is 500 ms, the average is about 385 ms.

When all the signatures initially asked for have been received, the computer calls for the car I.D. For

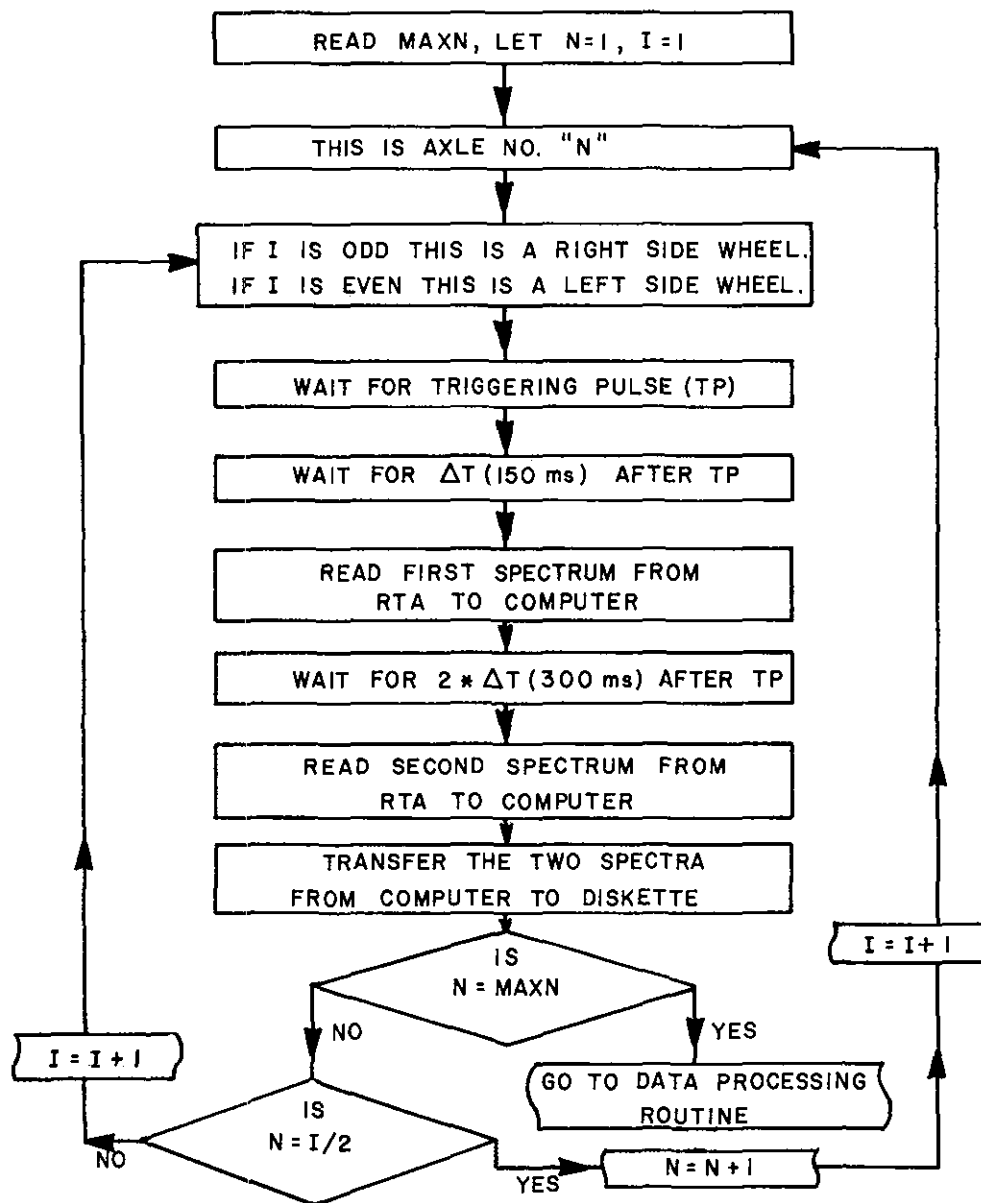


FIG. 5.5.3 FLOW DIAGRAM OF THE READ ACOUSTIC SIGNATURES PART OF THE MAIN PROGRAM.

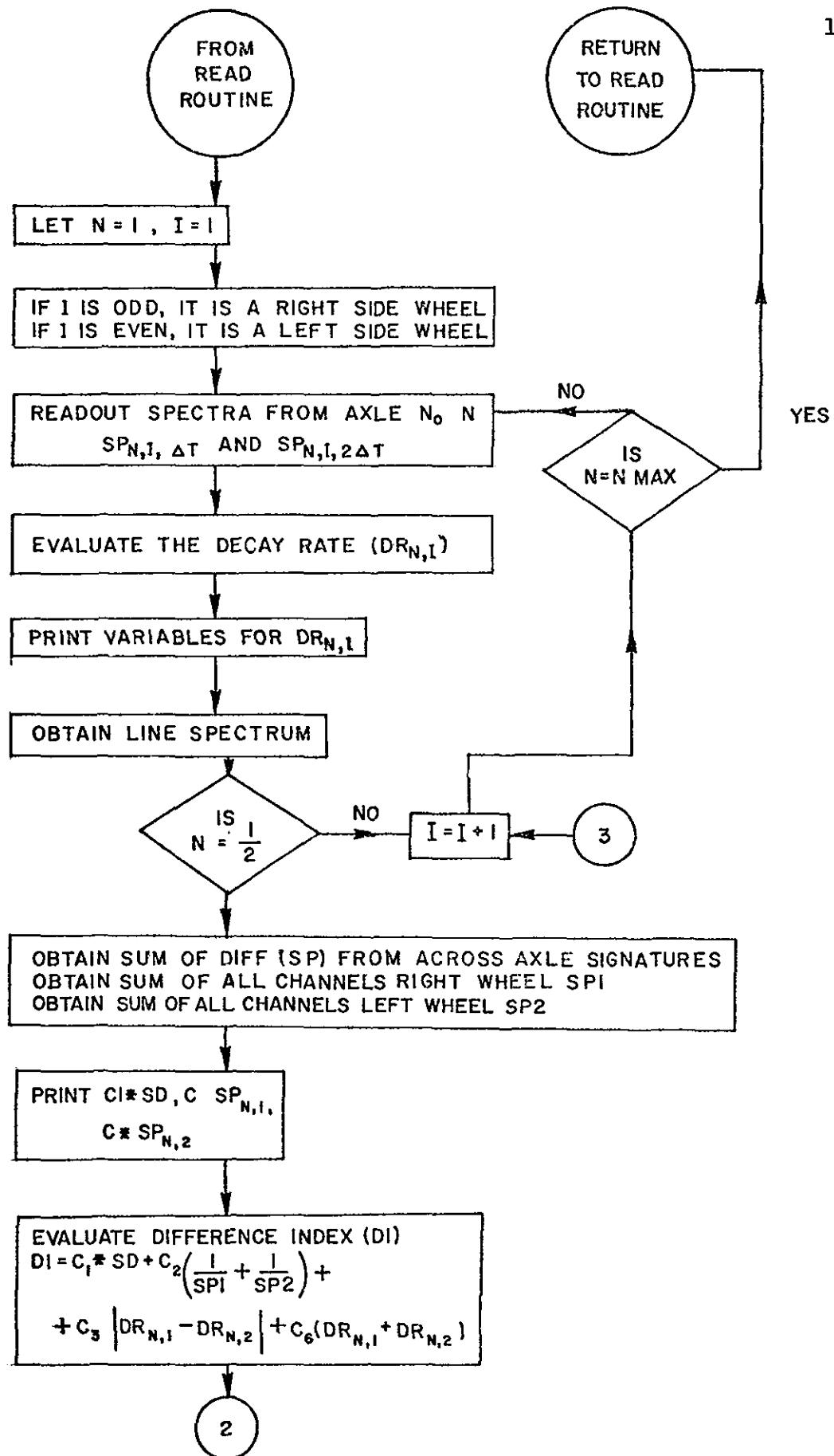
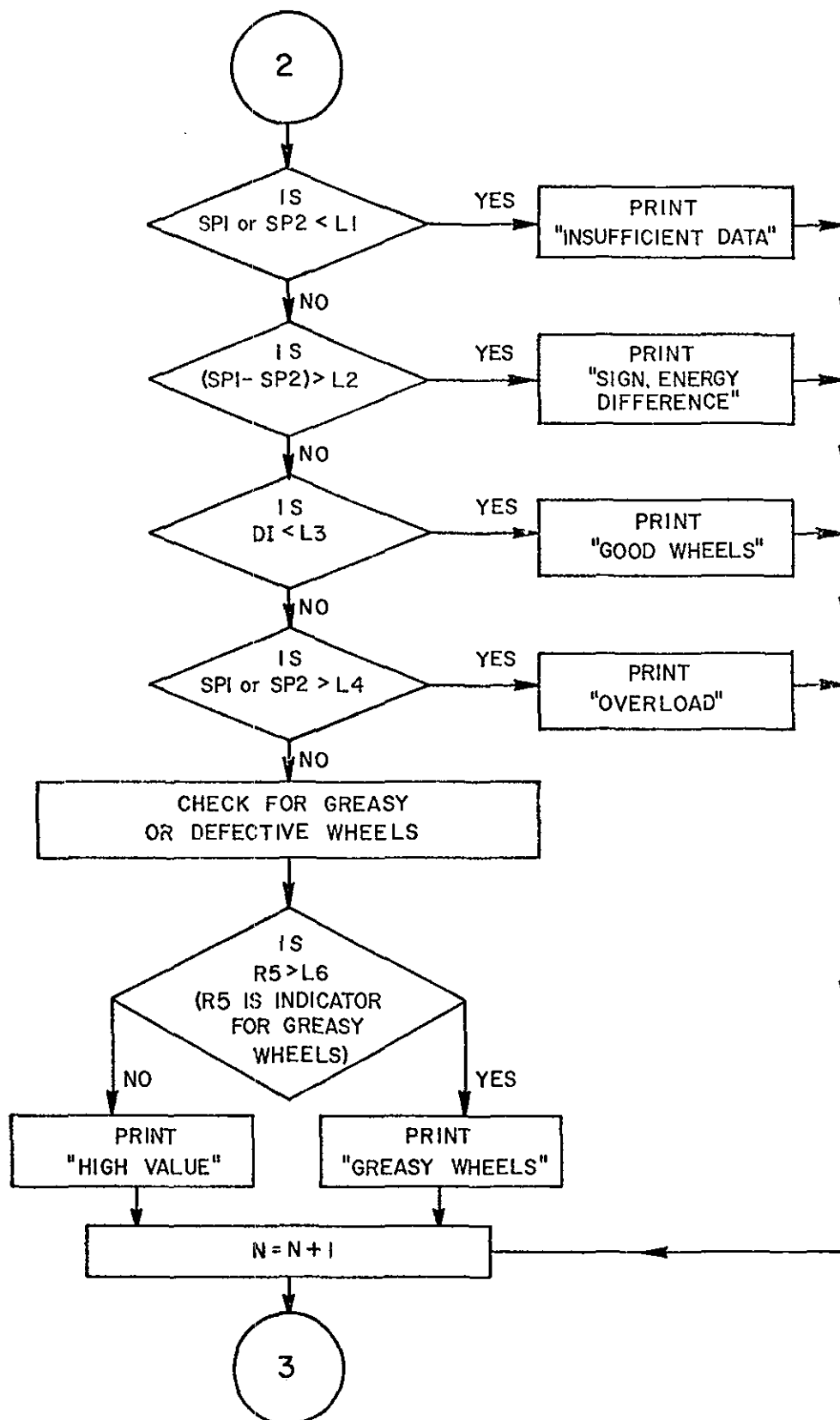


FIG. 5.5.4. FLOW DIAGRAM OF THE DATA PROCESSING SECTION OF THE MAIN PROGRAM



NOTE: L1, L2, L6 ARE INPUT PARAMETERS

FIG. 5.5.4 (continued)

RUN 770712-IV

 T-562-VIII
 EXP. AVG.
 SPECTRA PROCESSING ROUTINES
 ENGLEWOOD YARD TESTS-JUNE 77
 +ASSEMBLY A-140-IX
 12 JULY 1977

NUMBER OF CHANNELS; 250
 NUMBER OF SPECTRA ; 24
 FREQUENCY FACTOR DBAND HZ; 40
 DISCRIMINATION LEVEL; 8
 D.INDEX DECISION LEVEL; 85
 DATE-TIME? 12 JULY 77 15:10:00? 0
 TAPE#? 180
 CAR I.D.? TP 78217CL/SSW 79457 CL/ATSF 81338 CL? 1
 J1,K1,K2 0 162 34
 J1,K1,K2 1 157 48
 472 39 45 57

I	TEST	I	SP1	I	SP2	I	ID.INDEX	I	REMARKS	I
I	1	I	138	I	111	I	61	I	GOOD WHEELS	I
J1,K1,K2	0	140	12							
J1,K1,K2	1	180	64							
573	47	51	62							
I	2	I	239	I	182	I	75	I	GOOD WHEELS	I
J1,K1,K2	0	187	11							
J1,K1,K2	1	173	52							
956	79	83	91							
I	3	I	274	I	130	I	103	I	SIGNIFF. ENERGY DIFF.	I
J1,K1,K2	0	173	26							
J1,K1,K2	1	168	47							
638	53	58	63							
I	4	I	176	I	160	I	74	I	GOOD WHEELS	I
J1,K1,K2	0	157	23							
J1,K1,K2	1	145	19							
708	59	64	70							
I	5	I	234	I	137	I	70	I	GOOD WHEELS	I
J1,K1,K2	0	155	11							
J1,K1,K2	1	193	39							
816	63	72	78							
I	6	I	238	I	157	I	84	I	GOOD WHEELS	I

FIG. 5.5.5 SAMPLE OUTPUT OF THE MAIN PROGRAM

long train cuts the first and last car I.D.s were given, and thus intermediate cars could be identified by consulting the consist lists. For short tests, of two to four cars, all I.D.s were typed. Data processing then begins by retrieving from the diskette the spectra of wheels across the axle. The decay rate is evaluated from the two readings with a 150 ms interval.

In order to test the efficiency of the system and the software, recordings made during the 1975 field test described in Section 1.8 were analyzed. The distribution of difference index for 2 runs (Run #21, 23) is shown in Fig. 5.5.6. The circles indicate a defective wheel. The distribution of difference index for the same run (Run #10) for 3 different sampling time intervals is also shown in Fig. 5.5.7. The analyses indicated better discrimination and reproducibility compared to analyses made using the 1/3 octave band RTA.

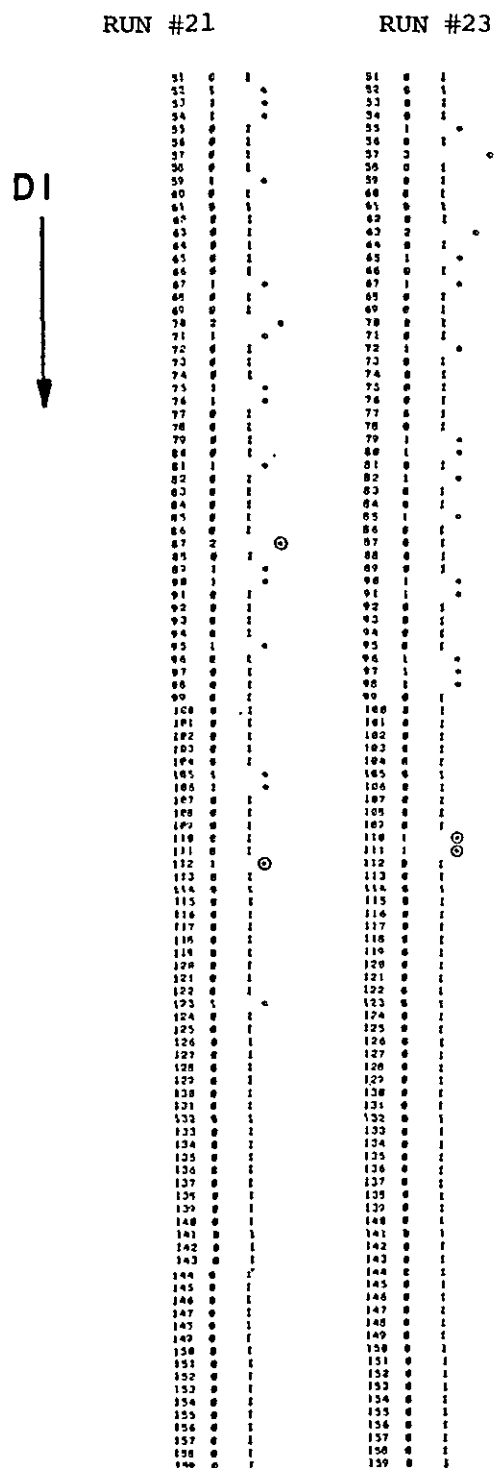


FIG. 5.5.6 DISTRIBUTION OF DIFFERENCE INDEX FOR RUN #21 AND RUN #23
FROM THE FIELD TESTS AT ENGLEWOOD YARD, 18 June 1975

⊙ Indicate D. I. for defective wheel.

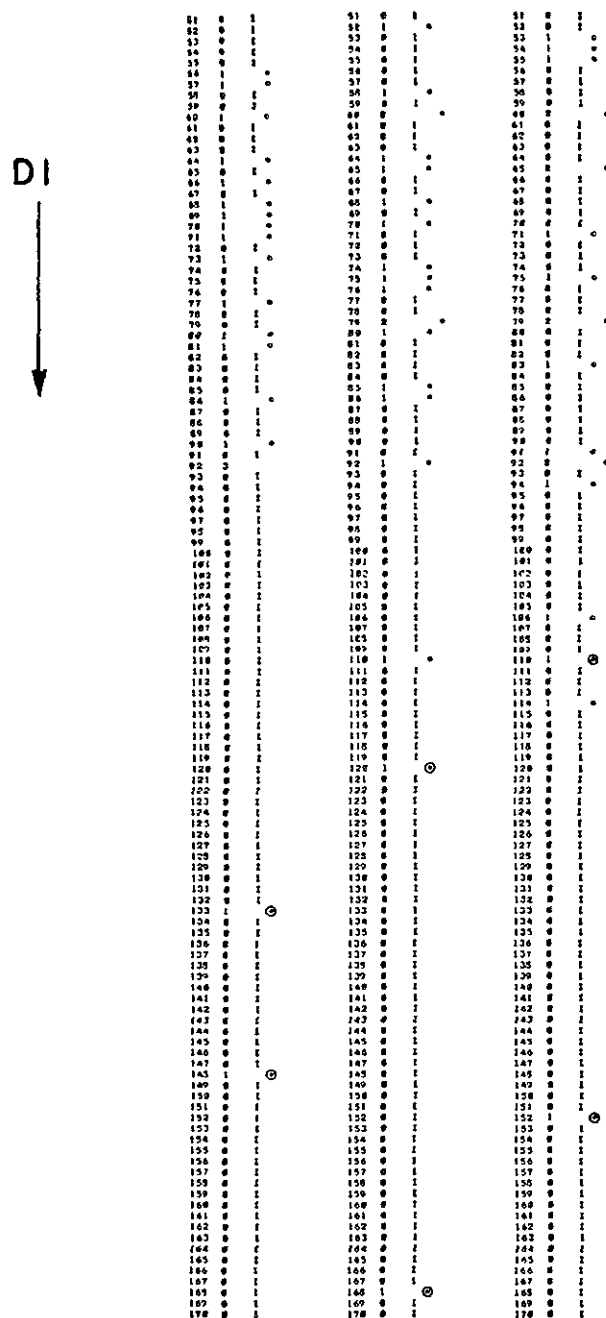


FIG. 5.5.7 DISTRIBUTION OF DIFFERENCE INDEX FOR RUN #10, THREE DIFFERENT SAMPLING TIME INTERVALS, FROM THE FIELD TESTS AT ENGLEWOOD YARD, 18 June 1975

⊙ Indicate D. I. defective wheel.

6. WAYSIDE TESTS

6.1 Tests at TTC Pueblo, Colorado

Two field tests were performed in the Transportation Test Center (TTC) in Pueblo, Colorado, at a three month interval. The objectives of these tests were:

1. To test certain parts of the system, such as the microphone, the modified exciter, and the wheel sensor, in the field.
2. To simulate the operating conditions for the Acoustic Signature Inspection system under development.
3. To determine the signature change, over a certain time period, due to wear of the wheels.

6.2 First Pueblo Test

In all 10 tests were done on the bypass of the FAST track. These are described as follows.

<u>Test</u>	<u>Date</u>	<u>Description</u> (train speed, direction)
1	11-16-78	5 MPH; counterclockwise
2	11-16-78	5 MPH; counterclockwise
3	11-16-78	8 MPH; counterclockwise
4	11-16-78	8 MPH; counterclockwise
5	11-17-78	5 MPH; clockwise
6	11-17-76	5 MPH; clockwise
7	11-17-76	8 MPH; clockwise
8	11-17-76	8 MPH; clockwise
9	11-17-76	5 MPH; brakes lightly applied
10	11-17-76	12-15 MPH; clockwise

Tape recordings of acoustic signatures were obtained from each of the project FAST train wheels. This was done for all wheels on one side of the train

on Tuesday evening, 16 November 1976 and for the wheels on the other side on Wednesday evening. A consist description was obtained for car identification. The first four cars in the 70-car consist were replaced in the Wednesday night test, otherwise the consist remained the same for both tests.

Wheel excitation in these tests was done with the improved model of the UH mechanical hammer exciter, as described in section 5.1.1. A photograph of the installed exciter is shown in Fig. 6.2.1. This hammer exciter performed without mishap during the tests, and showed only minor wear following the 3124 test impacts. At the time the first series of Pueblo tests were made, it was believed that the hammer could be activated by impact from the link, 3, (see Fig. 1.6.1), so the springs, 5, were disconnected from the hammer at point B and instead connected to the frame. Thus the hammer was allowed to swing free from the link, 3, on impact and the springs, 5, served to reset the link, 3, rather than the hammer. This change, although of interest from the design standpoint, gave rise to some problems, as indicated below.

The wheel impact response was judged to be best for the 5-8 MPH train speed. The hammer exciter would not operate effectively for train speeds above 12 MPH and did not impact at all below 3 MPH. About 1/3 of the wheels were not struck by the hammer during the 12-15 MPH test presumably because the hammer could not reset as

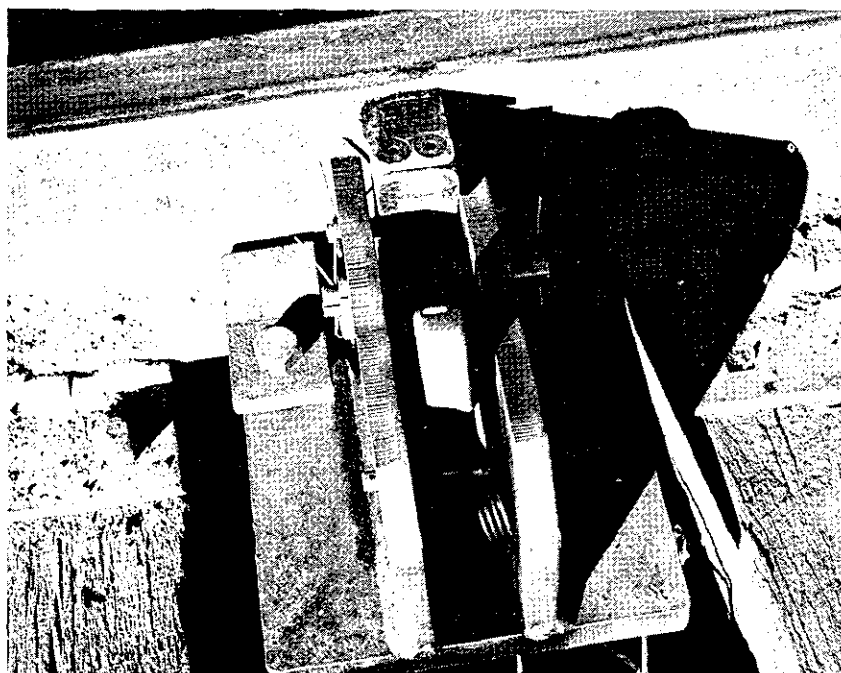


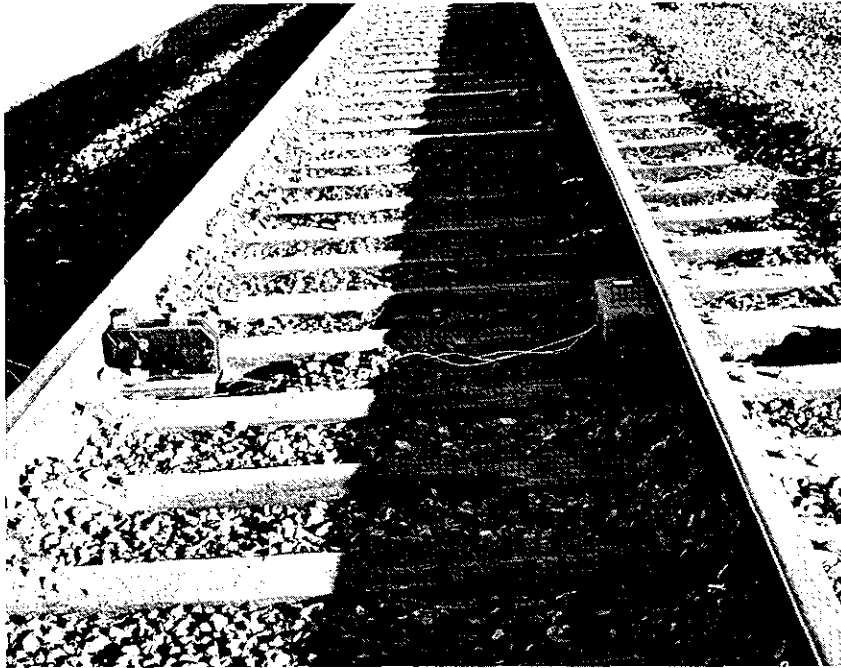
FIG. 6.2.1 MODIFIED MECHANICAL HAMMER EXCITER USED AT TTC,
PUEBLO

needed in the time between the passage of wheels on the same truck. However, the hammer mechanism was not damaged in this test nor did it appear to present a hazard to the train or personnel in attendance. The impact sound levels measured approximately 6 feet from the wheel usually exceeded 95 dB which was at least 10 dB above the background train noise.

The performance of the wheel sensor was good. It was installed and calibrated easily. For calibration a small vehicle provided by TTC was used. Views of the system used at TTC Pueblo are shown in Figs. 6.2.2 and 6.2.3.

The acoustic signature of the wheels was recorded on two different tape recorders simultaneously. One recorder was a General Radio dual channel. It was used for simultaneous recording of the sound in channel No. 1 and the triggering pulse in channel No. 2. This recorder operates with a 115 Volt AC, 60 Hz power supply. Unfortunately there was no such line available at the test location and a portable generator was used. That later proved to be a major obstacle in the analysis, because the speed of the tape transport mechanism is directly dependent on the frequency of the power supply. The other recorder was a NAGRA single channel, battery operated instrument. This is a very good recorder, but only the sound could be recorded on the single channel.

a



b

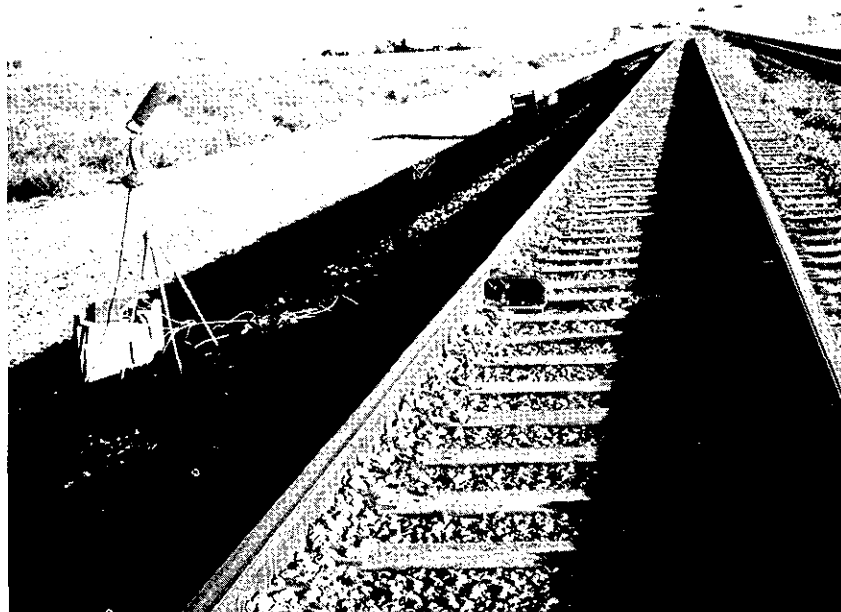


FIG. 6.2.2a VIEW OF THE EXCITER-WHEEL SENSOR
b VIEW OF THE MICROPHONES, EXCITER AND WHEEL SENSOR
ON THE BYPASS SECTION OF THE FAST TRACK AT TTC,
PUEBLO

a.



b.

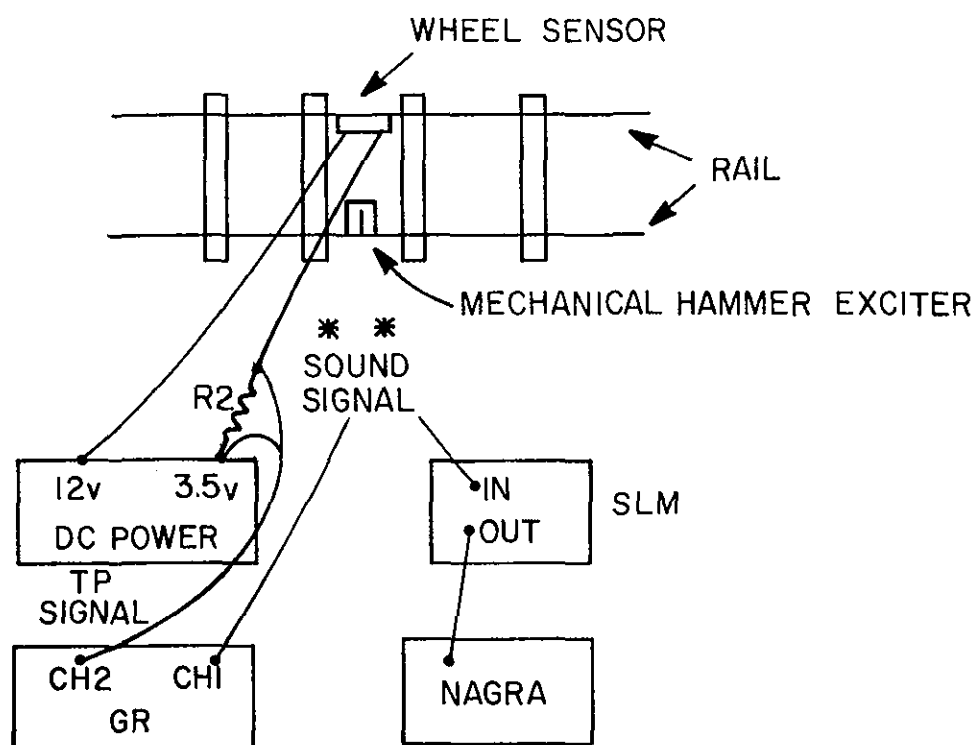


FIG. 6.2.3a. VIEW OF THE SETUP AND EQUIPMENT USED AT TTC,
PUEBLO CO

b. SCHEMATIC OF THE SYSTEM AT TTC, PUEBLO CO

Preliminary analyses of these tapes were made to test and refine the recognition logic. Comparisons were made between two impacts on the same wheel, impacts from two wheels on the same axle, and from two different wheels on the same side of the train. Some studies of this type are reported in the next section. Since the train speed of 8 MPH is close to the maximum speed for which the fourier analysis and data transfer into the computer could be effected, the tape playback speed was 7-1/2 inch/sec instead of the recording speed of 15 inch/sec. This gives double the time for sampling and data transferring, compared to direct real-time analysis.

6.3 Second Pueblo Test

A second series of tests similar to the first was conducted in the evening of 10 February 1977 on the main FAST track. These are described as follows:

<u>Test No.</u>	<u>Description</u>
11	5 MPH; Clockwise
12	5 MPH; Clockwise
13	8 MPH; Clockwise
14	8 MPH; Clockwise
15	5 MPH; Counterclockwise
16	5 MPH; Counterclockwise
17	8 MPH; Counterclockwise
18	8 MPH; Counterclockwise

For these tests the same devices and arrangements as in the first tests were used (see Fig. 6.2.3). The only additional precaution taken was continuous monitoring of the frequency of the AC power line by a frequency

counter. During the second tests a better and bigger generator was available. The frequency of the generator was reasonably stable, although it drifted slowly within the range of 59.0 - 60.2 Hz, during the 5 hour tests. This introduced a maximum frequency error of 2% in the acoustic signatures. Errors of this size can be important in the data analysis, because line spectra comparison will be impossible. Note that in the line spectra comparison the tolerable error is 0.4% (a spectrum from SD330A RTA has 250 channels). During a single test the frequency of the generator drifted in the range of 0.0 - 0.3 Hz with an average less than 0.2 Hz. Indications are that during the first test the phase frequency of the power supplied was between 52.8 and 54.2 Hz. As a final note on the error introduced by the change of tape speed, manufacturers data for the GR data recorder type 1525 indicates that 'flutter and wow' is below 0.2% rms. According to the Houston Lighting & Power Company, the maximum average frequency change of the power lines is 0.2% - 0.3%. In unusual cases this may go a little higher. Therefore there is no error introduced in the analysis due to the tape transport mechanism due to the frequency of the laboratory power supply.

Most of the recordings made were good. Comparisons between wheels on the same side, across the axle and at different speeds were made. The results are presented in Fig. 6.3.1, Fig. 6.3.2 and in Fig. 6.3.3. These

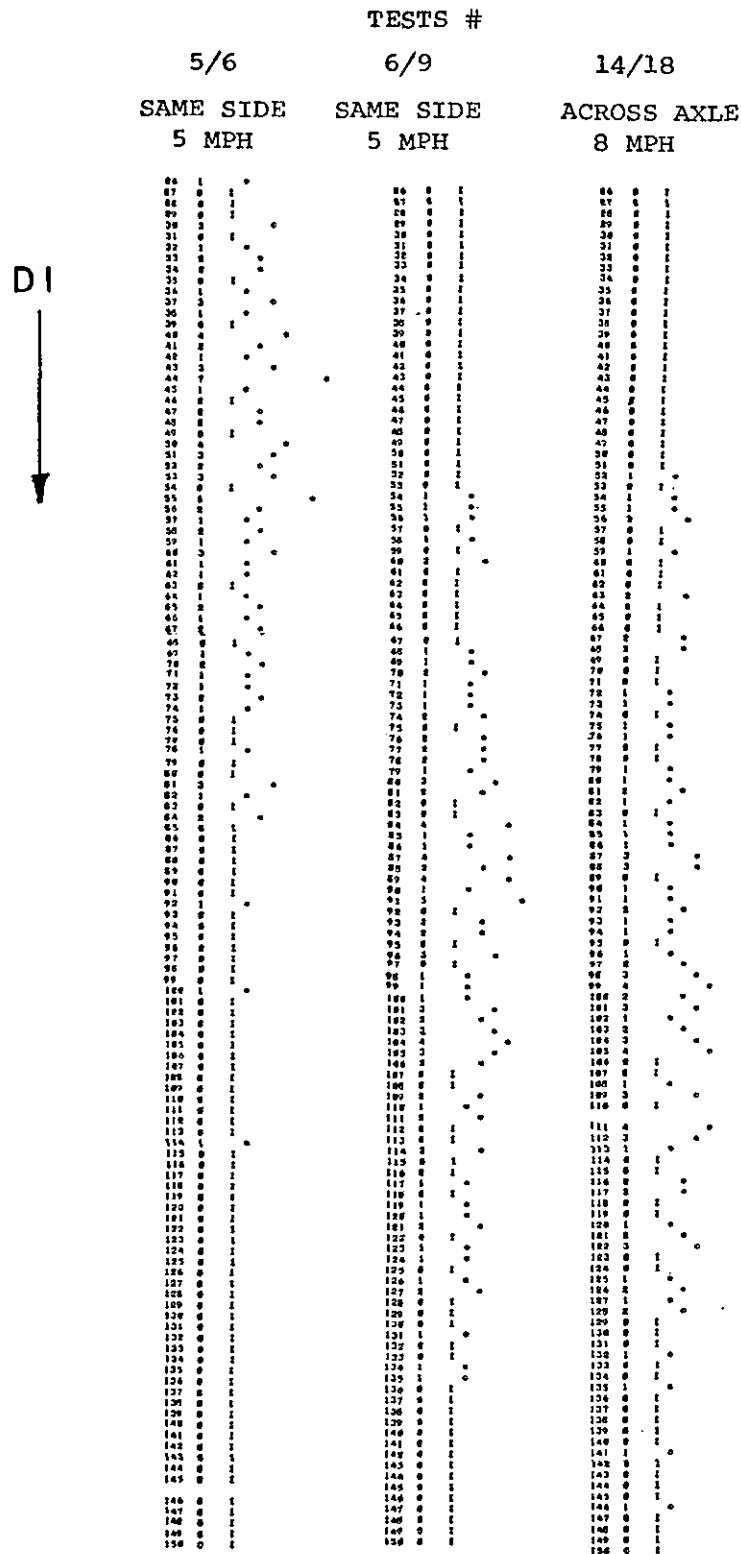


FIG. 6.3.1 DISTRIBUTION OF DIFFERENCE INDEX FOR THE TEST 5/6,
6/9, 14/18 AT TTC PUEBLO COLORADO

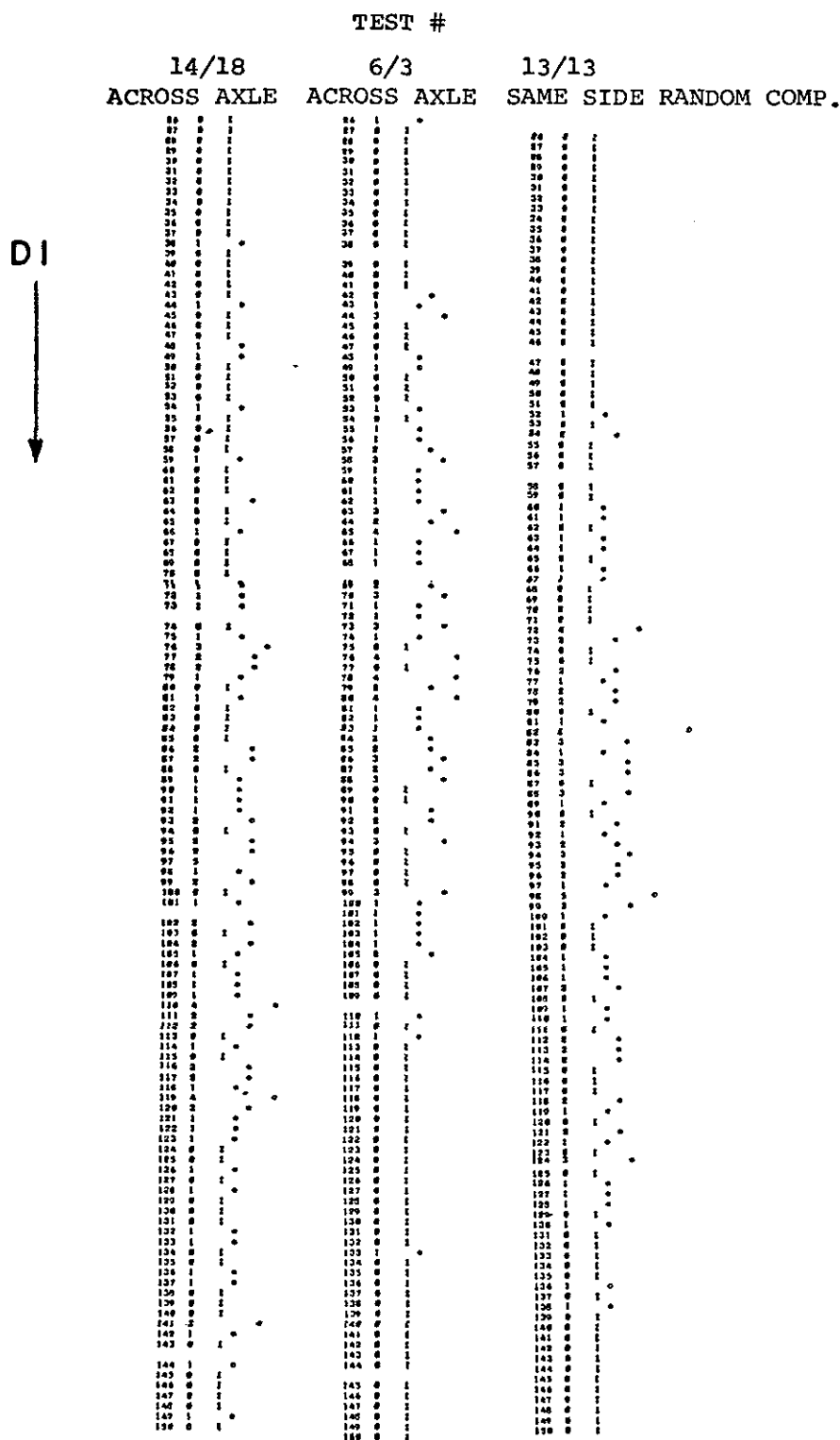


FIG. 6.3.2 DISTRIBUTION OF DIFFERENCE INDEX FOR TESTS 14/18, 6/3, 13/13 AT TTC PUEBLO COLORADO

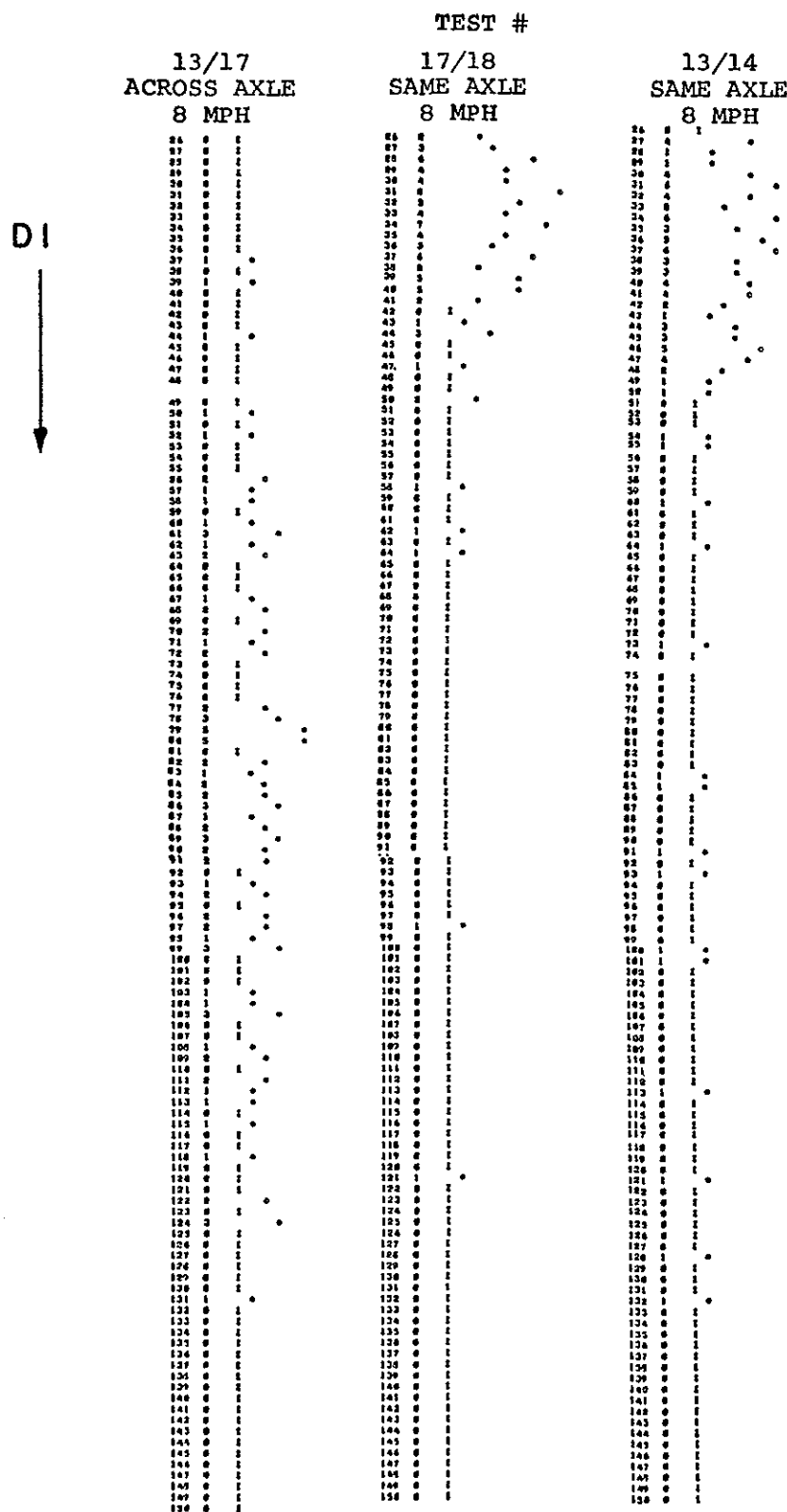


FIG. 6.3.3 DISTRIBUTION OF DIFFERENCE INDEX FOR THE TESTS
13/17, 17/18, 13/14

figures show the distribution of the difference index values for most of the tests. The best results were obtained comparing the same wheels recorded in successive tests where the train was moving at the same speed. Problems related to the tests and subsequent laboratory analyses are:

1. The train speed varied in most of the tests about ± 2 MPH from the nominal speed, the reason being the steep grade existing in the particular section of the FAST track used.
2. The power frequency was different in tests separated by long time intervals. This is probably the reason why across the axle comparison did not show results as good as expected.
3. Because of the large power frequency difference between the first and second Pueblo tests (53 and 60 Hz respectively) it was impossible to come to any reliable conclusions on the effect of wheel wear.

The following conclusions were arrived at from the Pueblo tests:

1. The spring assembly of the mechanical exciter was necessary.
2. Distant mounting of the exciters should be avoided. A 200 ft separation between exciters was used in the 1975 Englewood yard tests where the wheels on one side were inspected first and then those on the other.

But the Pueblo tests showed that the greater the exciter separation the greater is the effect of varying train speed.

3. The exciter was strong enough to operate and survive for a large number of impacts.

6.4 Tests at the Southern Pacific Englewood Yard, Houston

The final wayside testing of the Acoustic Signature wheel inspection system took place in July 1977, in the Southern Pacific Englewood yard in Houston. Traffic speed inbound to the yard is sometimes higher than 15 MPH, and hence too fast for the inspection system, but incoming to the hump the speed is 2-3 MPH. There are about 3000 cars/day humped in the yard on 3 tracks. The rail size is 136 lb. (mechanical hammer exciters were designed for this size of rail). In a previous 2 year period the inspection personnel had discovered 6 broken and 12 overheated wheels.

The objectives for the tests were:

1. To obtain data for a statistically significant sample of wheels in service. This data sample could then be used for further studies to find the optimum DI equation and to ascertain what wheel conditions, other than cracks, might give rise to high DI values.
2. To rate the performance of the hardware to identify weaknesses and problems.

3. Using the best software available at the time to permit immediate follow-up on some wheels with high DI values. It was hoped that a cracked wheel might be found but this was recognized as a somewhat unlikely occurrence in the time available.

6.5 Englewood Test Site and Equipment

The location for the tests was selected after a visit to the site and discussions with representatives of Southern Pacific. A simple chart of the hump is shown in Fig. 6.5.1. The figure shows the location of the trailer, where the electronic equipment of the system was stored, and the mechanical exciter on the north track. The location for the trailer had to comply with and fulfill the objectives and requirements set for the tests. For that reason it was placed at the bottom of the slope which is about 400 yards from the top of the hump. It would then take more than two minutes for a car moving at the regular humping speed to cover the distance from the trailer to the inspection pits. An observer sitting in the trailer had an unobstructed view of the inbound or outbound traffic as well as all train cuts moving over the hump. Electric power was easily accessible from an electric tower a few feet away.

Modifications in the hammer exciter and the software were needed under the new operational conditions and

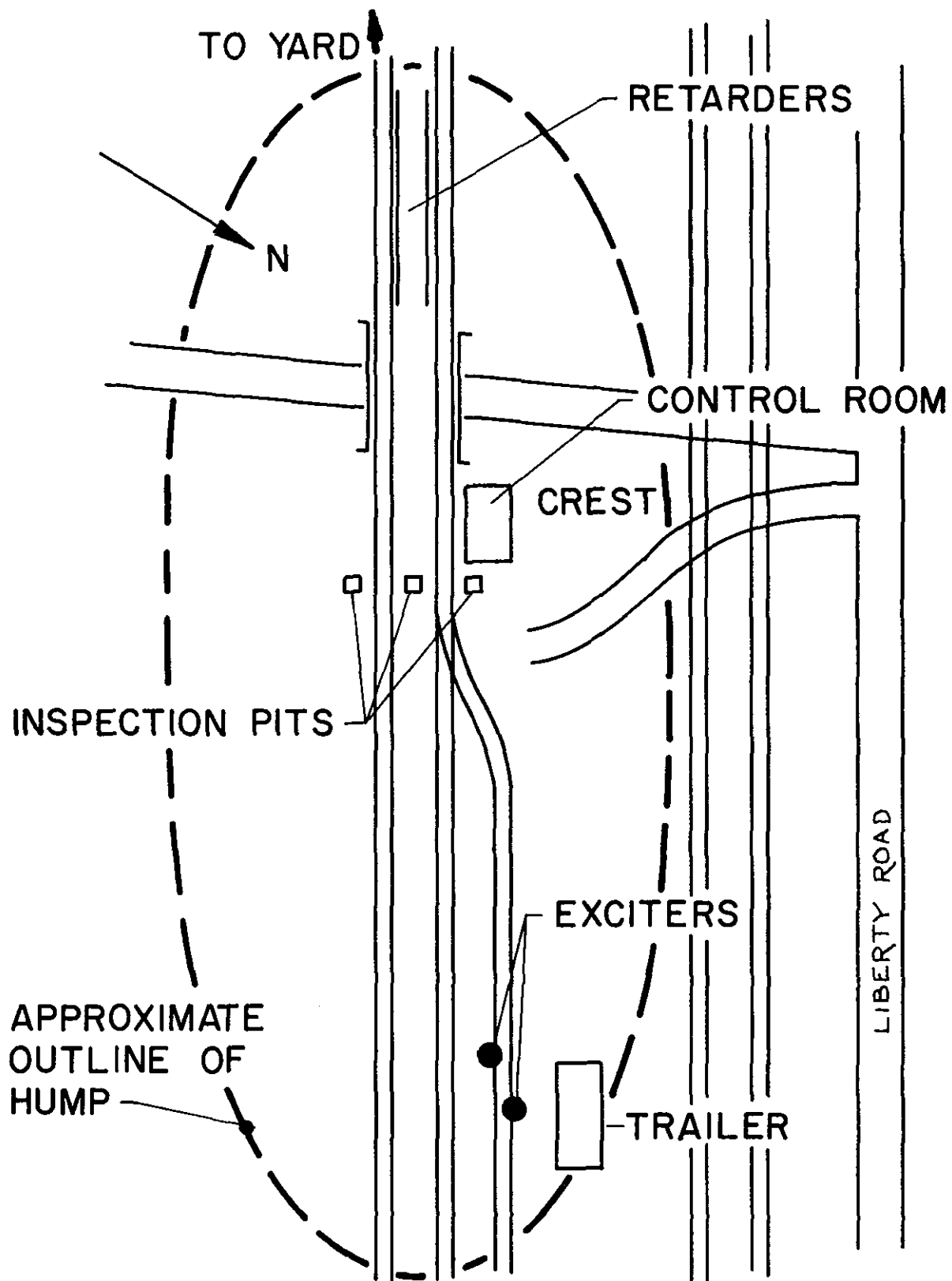


FIG.6.5.1 OUTLINE OF THE SOUTHERN PACIFIC'S CLASSIFICATION YARD IN HOUSTON.

requirements for these tests. The exciter used at Pueblo did not operate for train speeds below 3 MPH. Consequently, the spring configuration was returned to the original design as shown in Fig. 5.1.1. After these changes the exciter operated best in the range 1.5 to 3.0 MPH. It is obvious that with this design the performance of the exciter is speed and flange depth dependent.

The tests were scheduled daily between 9:00 a.m. and 5:00 p.m. An average of 400 cars/day was estimated to pass through the test location. Only a fraction of those cars were actually tested, hence the chances of finding a defective wheel were remote. To define the discrimination level for good/bad wheels a complete simulation test was performed in the laboratory. The discrimination level of 85 was chosen after testing a selection of wheels, as shown in Table 6.5.1.

An air-conditioned 8' x 21' trailer was installed in the yard on 15 June 1977. It took about a week to install, calibrate and make the first complete test of the system. Two problems arose due to the condition of the rail. i) Although the size of the rail was 136 lbs., parts of the exciters had to be machined and plates of variable thickness were attached to the top of the plunger because the rail was worn down about 3/8 inch. ii) Calibration of the wheel sensor was

TABLE 6.5.1 DIFFERENCE INDEX VALUES FROM WHEELS TESTED IN THE
LABORATORY, FOR DISCRIMINATION LEVEL SELECTION

RUN #,	PROGRAM	TAPE #	AXLE & WHEEL IDENTIFICATION				
			GOOD/BAD				GOOD/GOOD
			15C-15A	8B-8G	4G-4B		
770701-II	T-562-V	175	91	101	142	127	69
770615-IV	T-562-I	175	99	93	106	119	71

very difficult for the same reason. No such problem had been encountered during the test at TTC in Pueblo or the laboratory simulation. As a result of this difficulty multiple triggering or missing triggering pulses were observed. Consequently, the maximum number of wheel signatures per test had to be reduced to 80, because faulty triggering invalidates an entire run.

The trailer and the outdoor hardware are shown in Fig. 6.5.2. Through the window on the left the test controller could watch the cars moving uphill towards the crest. The schematic of the inspection system is shown in Fig. 6.5.2b, distances between different devices being marked on the drawing. The exciter and the wheel sensors were mounted between the ties. The clearance was very small, and therefore inevitably there was some difference in the time between the triggering pulse and the impact on the two sides of the track. During the TTC and simulation tests, the exciter-wheel sensor alignment was much better. In Fig. 6.5.3, the microphones, exciters and wheel sensors are shown from the same angle as seen by the test controller looking through the window of the trailer. In Fig. 6.5.4a,b the system and the east part of the hump are shown. The inspection pits are indicated by arrows (Fig. 6.5.4a).

All testing was performed in real time. During the last two weeks, when all necessary changes and corrections had been made the sound and triggering

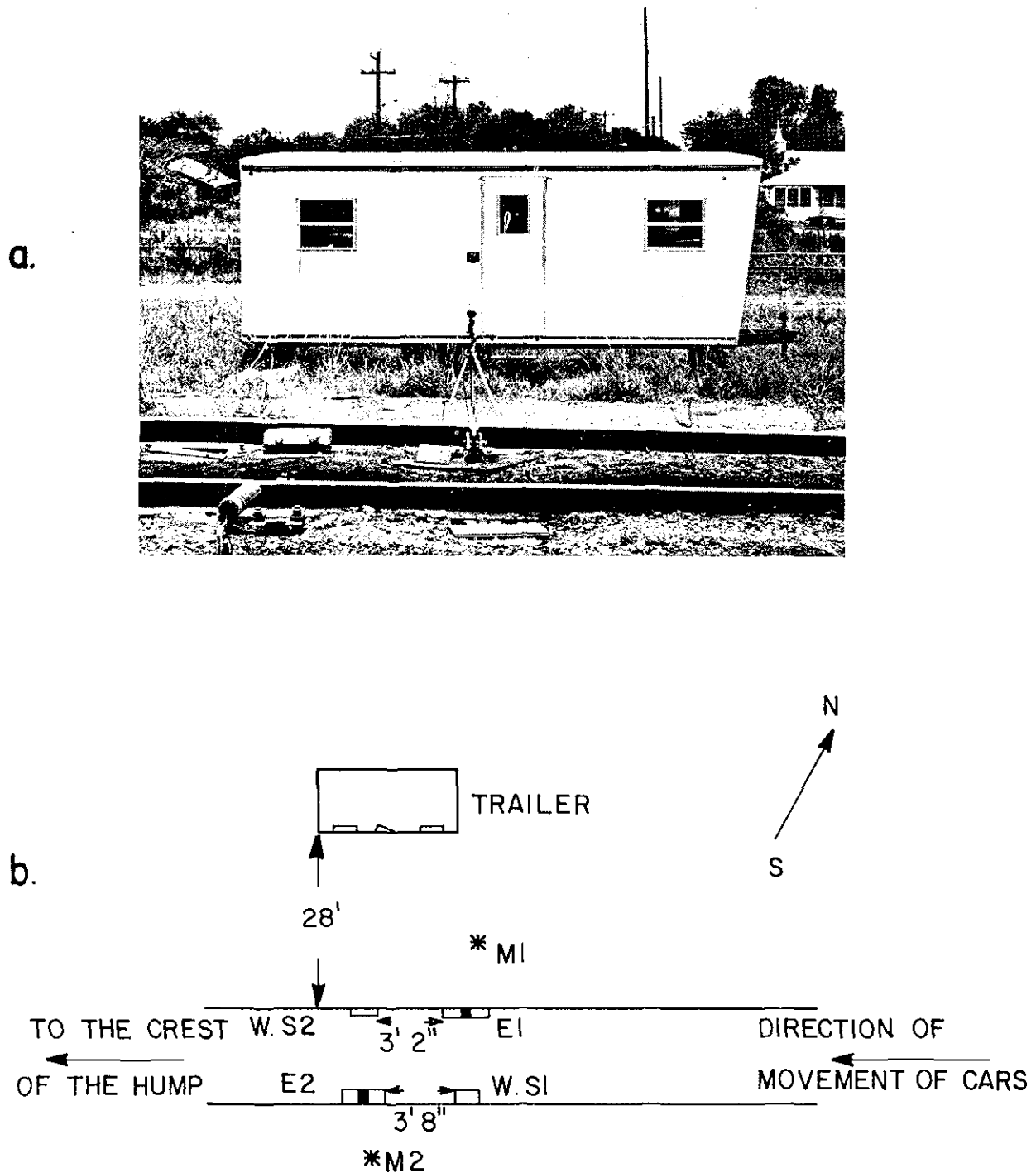


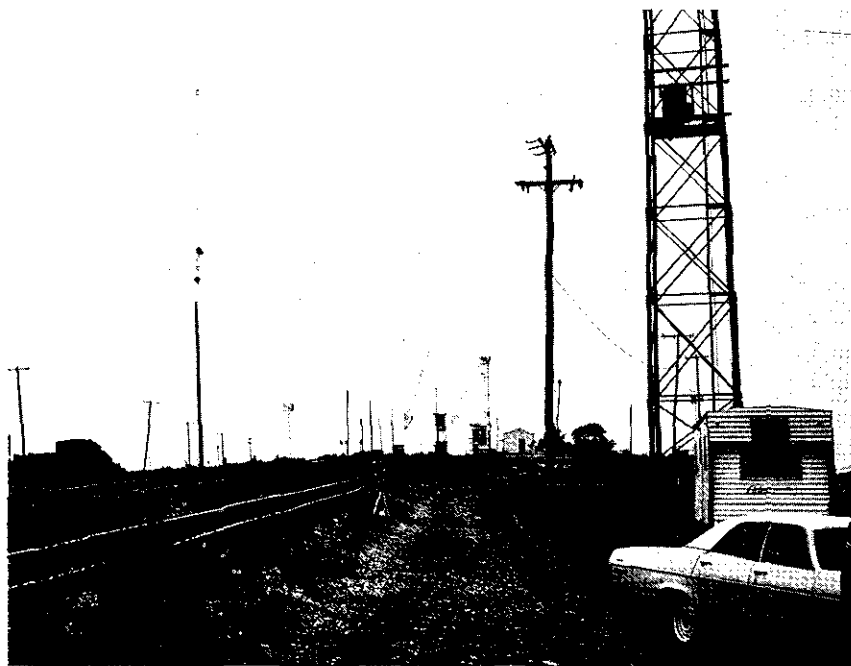
FIG. 6.5.2a VIEW OF THE INSPECTION SYSTEM

b SCHEMATIC OF THE SYSTEM LAYOUT



FIG. 6.5.3 VIEW OF THE MICROPHONES, EXCITERS AND WHEEL SENSORS
THROUGH THE WINDOW OF THE TRAILER

a



b



FIG. 6.5.4a VIEW OF THE EAST SIDE OF THE HUMP, INSPECTION PITS
ARE INDICATED BY ARROW

b VIEW OF THE MICROPHONES, EXCITERS AND WHEEL SENSORS

pulse signals were tape-recorded simultaneously with the real time testing.

6.6 Performance of Hardware during the Englewood Test

The duration of the tests was approximately five weeks instead of the scheduled four due to the initial one week delay in the installation of the system.

The components of the system performed as follows during the tests:

- a) Microphones: No problem or failure. Some indications of excessive attenuation or low gain in the pre-amplifier of one of the microphones during the second week of the tests were finally attributed to a bad cable. Rain did not have any adverse effect on the microphones which survived three heavy rainstorms during the test period.
- b) Wheel Sensors: One of the dual wheel sensing units failed a couple of days before the end of the tests. It was easily replaced by the other unit. Some triggering problems could be attributed to wheel sensors. In the late afternoon hours, under extreme heat, the temperature on the cover of the wheel sensors was estimated to be above 130°F.
- c) Mechanical Hammer Exciters: Most of the parts operated satisfactorily. Each exciter performed about 27,000 impacts. One hammer had to be replaced due to excessive wear, possibly because of improper

heat treatment. One pair of springs was also replaced with new and stiffer springs.

- d) SD330A Real Time Analyzer: Some problems developed when the temperature inside the trailer was above 85°F.
- e) NOVA 1220 Minicomputer: Some serious problems (computer failure) occurred when the temperature inside the trailer was above 85°F. The temperature related problems in the RTA and computer were corrected by improving the air circulation in the trailer.
- f) Diskette System: No problems. Further verification of proper data transferral from the computer to diskette and vice-versa was checked with a specially written test program.

The performance of the exciter is shown in the figures 6.6.1 through 6.6.4. In each figure the top trace is the triggering pulse signal, and the bottom trace is the sound signal. These pictures were taken during the tests using a TEKTRONIX 564 storage oscilloscope and a polaroid camera.

The events shown in the pictures from left to right are: The triggering pulse (TP) and the corresponding impact on the north wheel of the first axle is shown first, then the TP and the impact on the south wheel of the same axle, then the TP and impact on the north wheel of the second axle, etc.

Figures 6.6.1.a and b show the typical form of the signals. The top picture which shows normal impact during the last few days of the test after all possible improvements were made may be compared to the bottom picture which was taken in the early experiments. Figures 6.6.2a and b show some of the impact problems. In the top figure double impact of the hammer on the wheel is shown. This impact is more prominent on one side. In the bottom figure very weak impact or no impact occurred at low speed when new wheels with low flanges were passing over the exciter. These impacts usually appeared as "insufficient data" in the printout. Figure 6.6.3a shows, two impacts on old used wheels with high flanges, followed by two impacts on rather new wheels with low flanges. In Figures 6.6.3b are shown impacts of the type which sometimes gave rise to the indication Significant Energy Difference. In Figs. 6.6.1 through 6.6.3 the sweep speed of the oscilloscope was 500 ms/div., except in Fig. 6.2.3b where it was 200 ms/div. Figure 6.6.4a shows the signals from the south exciter, at a sweep speed of 50 ms/div. Figure 6.6.4b shows the corresponding signals from the north exciter. On the south side the impact occurred 45-50 ms after the TP, on the north side the impact occurred 100-105 ms after the TP, hence there was a difference of 50-60 ms in the data processing between

a



b

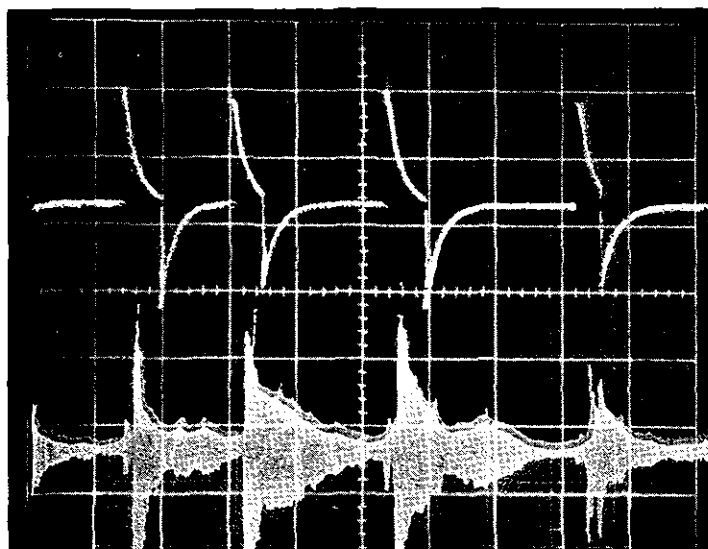
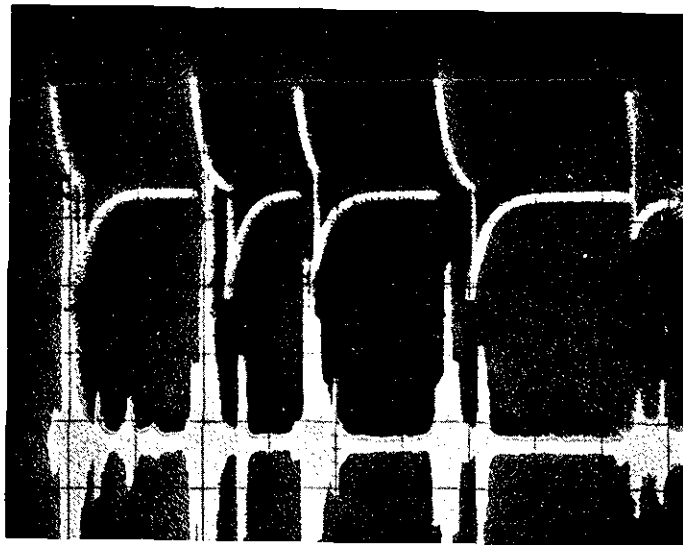


FIG. 6.6.1a TYPICAL PERFORMANCE OF THE EXCITERS DURING THE LATE TESTS

b TYPICAL PERFORMANCE OF THE EXCITERS DURING THE EARLY TESTS, SWEEP SPEED 500 ms/DIV

a



b

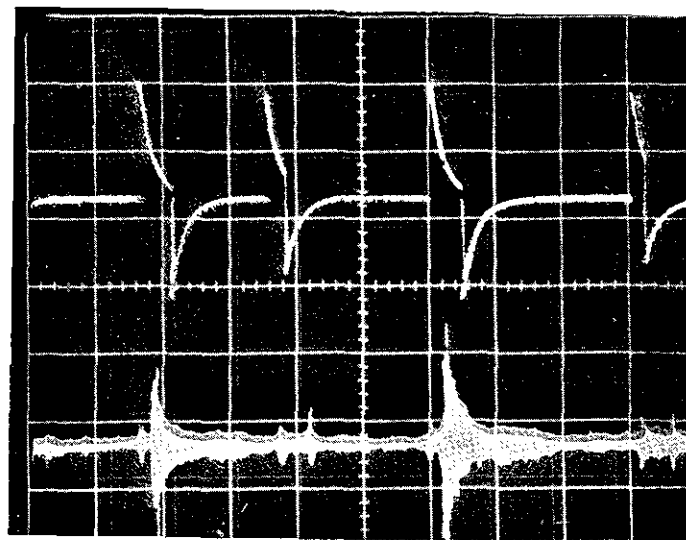
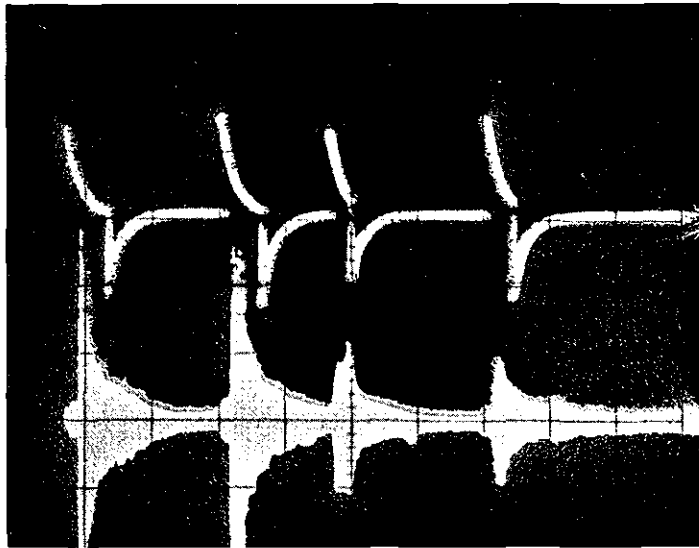


FIG. 6.6.2a EXCITER PERFORMANCE, DOUBLE IMPACT
b EXCITER PERFORMANCE, NEW WHEELS, LOW OR NO IMPACT;
SWEEP SPEED 500 ms/DIV

a



b

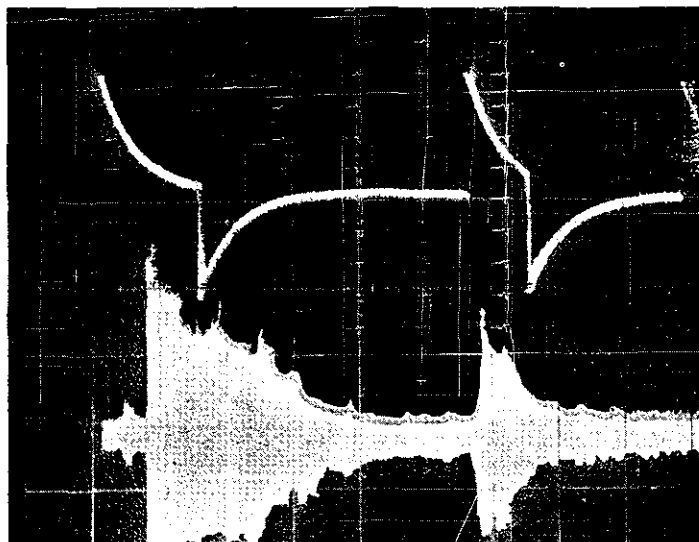
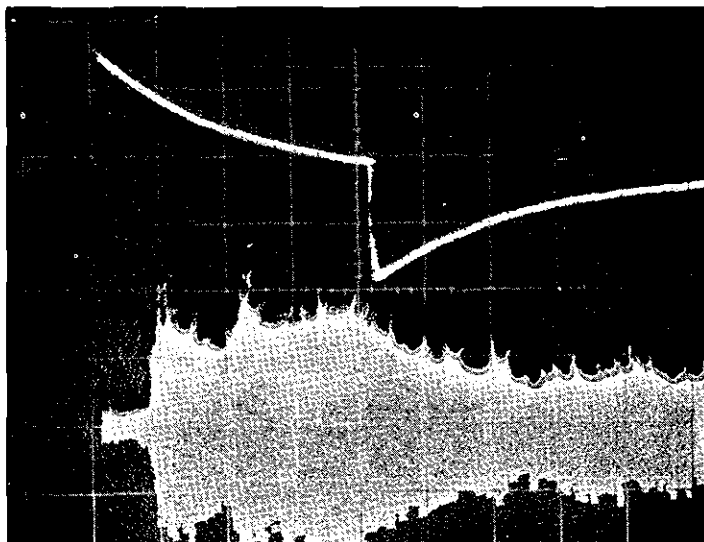


FIG. 6.6.3a IMPACTS ON WHEELS WITH HIGH FLANGES FOLLOWED BY
IMPACTS ON NEW WHEELS WITH LOW FLANGES
b UNEVEN IMPACT ON WHEELS ACROSS THE AXLE

a



b

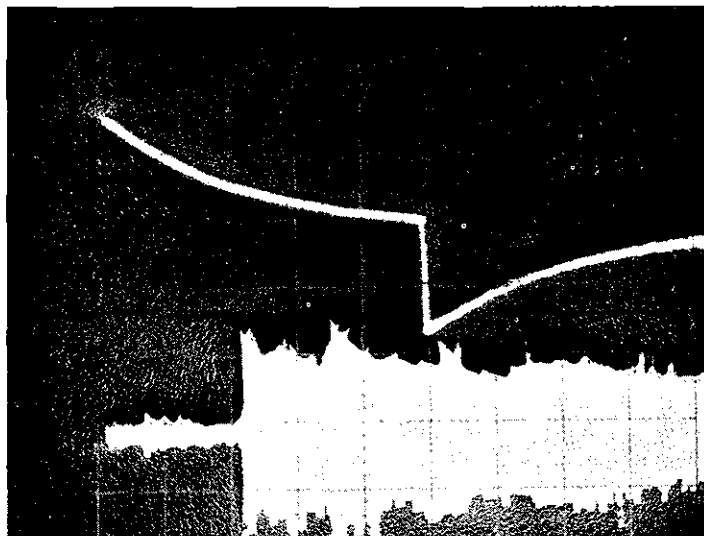


FIG. 6.6.4a TIMING RELATION, SOUTH EXCITER, IMPACT ABOUT 40 ms
AFTER THE TIMING PULSE
b TIMING RELATION, NORTH EXCITER, IMPACT ABOUT 110 ms
AFTER THE TIMING PULSE; SWEEP SPEED 50 ms/DIV

the two sides. This time interval corresponded to one sampling cycle of the analyzer and obviously introduced some error. This difference could have been corrected with alignment of the exciter-wheel sensor, but due to the tie spacing that was impossible. The alternative way to correct this error is through the software which was also difficult because of the lack of time for major software changes during the test.

6.7 Performance of Software during the Englewood Test

Table 6.7.1 has a summary of the printout obtained during the last ten days of the tests. The first column has the RUN identification number. The second column has the number of cars tested during the run. The third column has the number of the tape on which the run was recorded. The fourth column has the total number and condition of the wheels tested (clean, greasy, etc.). The next five columns have the results, which include "good," "insufficient data," "significant energy difference," "overload" and "high value." The next column contains the levels of the high values. Visual inspection on some of those wheels with difference index over 110 did not show any apparent defect. The axle with the highest difference index (164) had 9 year old iron wheels but without any cracks. Only one axle was in rather bad condition. It had extensive built-up tread, but was not condemnable according to the railroad inspectors. During the period

TABLE 6.7.1

SUMMARY OF THE LAST TEN DAYS OF TESTS AT THE
SOUTHERN PACIFIC ENGLEWOOD YARD, HOUSTON

RUN NUMBER	NUM- BER OF CARS	TAPE NUMBER	NUMBER OF WHEELS GR-GREASY CL-CLEAN	RESULTS				LEVELS OF H.V.	REMARKS
				GOOD	INSUFF. DATA	SIGNIFICANT ENERGY DIF.	OVER- LOAD	HIGH VALUE	
770721-I	3	184	16CL-8GR	6	6	-	-	-	New Wheels
770721-II	3	184	24CL	5	-	5	-	2	
770721-III	3	185	24CL	11	1	-	-	-	
770721-IV	3	185	24CL	7	-	2	-	3	
770719-Ib	10	183	80CL	19	21	-	-	-	
770719-II	10	183	64CL-16GR	21	12	3	-	4	
770719-IIb	10	183	72CL-8GR	26	12	1	-	1	
770718-I	9	183	72CL	21	10	3	-	2	
770718-II	6	183	48CL	12	3	4	-	5	
770718-IIb	6	183	48CL	15	8	-	-	1	
770716-I	3	-	24CL	10	1	-	-	1	Possible microphone mixing problem
770715-I	3	-	16CL-8GR	6	6	-	-	-	
770714-I	1	182	4CL	20	16	-	-	-	
770714-II	9	182	72CL	3	1	-	-	-	
770713-III	5	181	32CL-8GR	15	5	-	-	-	
770713-IV	6	181	48CL	14	-	1	-	9	
770712-IV	6	180	48CL	12	-	1	4	7	
770712-III	6	180	40CL-8GR	18	5	-	-	1	
770712-II	15	180	104CL- 16GR	39	6	3	-	12	
TOTAL	117		864CL- 72GR	280	113	23	4	48	

of the tests the READ assembly subroutine did not have an error flag for the case of improper reading of the digital output of the RTA by the computer. When this error flag was added later it showed on average that 2% of the indications contained a reading error. It is not known how much this error might have affected the results.

In some of the runs with a large number of high values, certain indications showed improper setting or calibration in parts of the system. For example in run 770713-IV improper microphone mixing was indicated from the fact that north side readings had a substantially higher overall sum compared to the south side. In the case of run 770712-IV the 4 overload indications showed low input attenuation in the RTA. Indications of Insufficient Data, Significant Energy Difference, and Overload are related to the performance of the exciter, as shown in Fig. 6.6.1 through 6.6.3.

Another point that should be mentioned is the large number of insufficient data indications. This is mostly due to greasy wheels. The majority of these wheels are on cars with plain journal bearings where oil has leaked from the journal box. For spectral comparisons, the second reading, 300 ms after the TP, was used. The signal from greasy wheels in that instance is very low or completely decayed. This problem could be corrected

by checking the first spectrum in cases of fast decay. Another point of some interest is that wheels with dragging brake shoes or even squealing under the application of brake shoe pressure did not appear to generate especially high Difference Index values.

The distribution of DI values for the last ten days of field test in SP Englewood yard (July 1977) is shown in Fig. 6.7.1. In the same figure indications from defective axles tested in the UH laboratory are marked with circles.

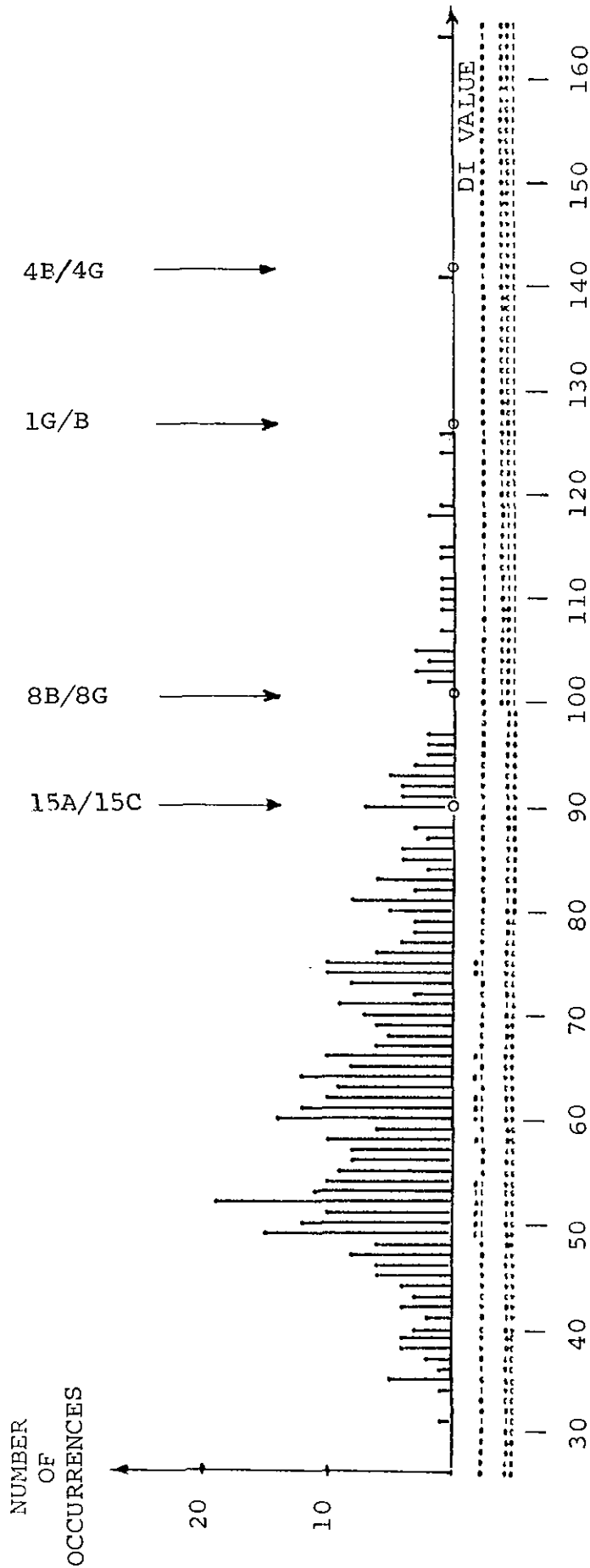


FIG. 6.7.1 DISTRIBUTION OF DIFFERENCE INDEX FOR THE LAST TEN DAYS OF FIELD TEST AT SOUTHERN PACIFIC YARD (July 1977)

⊙ Indicate DI for defective wheels

Sample size: 443 Frequency Range: 0-10,000 Hz
Real Time Data. No correction for timing difference
DI includes terms in SD, DR, LD

7. SENSITIVITY ANALYSIS

7.1 Introduction

Figure 6.7.1 is the histogram of DI values obtained in real time during the tests. It was pointed out in section 6.7 that a number of system problems occurred during the tests and that the DI equation used was based on prior experience with small samples. The idea at the time of the test was to follow up on a few wheels with high values. Further study of the analog tape recordings taken during the test was divided into three parts with the following objectives:

- 1) to identify recordings with system problems and to correct for deficiencies, where possible, in the data processing software,
- 2) to use the corrected data to find the optimum DI equation, and
- 3) to study the remaining high DI values from the Englewood data to ascertain what wheel conditions besides cracks could cause high values.

The maximum sample size (number of axles) used in this study was 370, a little smaller than the sample shown in Fig. 6.7.1. The reason for this difference is that analog tape recordings were not made for a few cars included in the real-time data. Each time a correction was introduced into the data processing or a change was

made in the DI equation, the procedure was to plot a histogram of the results. If, as a result of the change, the modal value of the histogram showed an increased separation from a reference sample of defective wheels, the change was regarded as an improvement. In some cases improvements were obvious with relatively small sample sizes (130 to 170 axle pairs) and the histogram plot was discontinued to save processing and analysis time.

The good/bad wheels used for reference are 15A/15C, 1G/1B and 4G/4B. They were tested on the UH laboratory track, where the wheel sensors and exciters were spaced as in the SP Englewood Yard. The setup prevented data collection from axle 8B/8G which appears in the reference sample of Fig. 6.7.1. The indications for the bad axles shown in this report are the average values of seven runs. Two good wheel pairs were also included in the laboratory measurements and these are also shown in comparison to each histogram.

7.2 Identification and Correction of System Problems

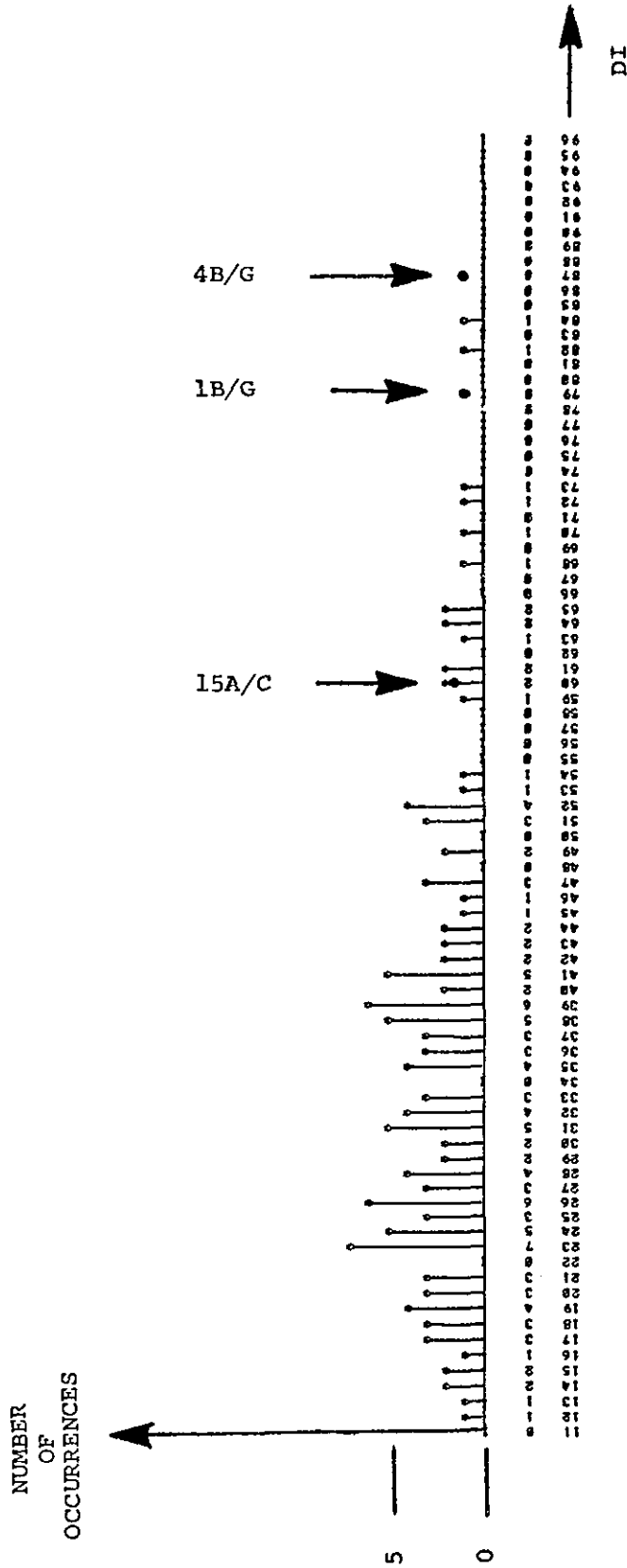
The hardware performance during the Englewood tests was described in Section 6.6. Some of the problems that are important for data processing are summarized and explained below.

1. Difference in timing of the triggering pulse: As mentioned in section 6.6 the tie spacing prevented the proper alignment between impacters and wheel sensors, thus introducing an average difference of $\Delta t = t_N - t_S = 60 \text{ ms}$,

where t_N is the time interval between triggering pulse (TP) and impact on the north side of the track and t_s is the time interval between TP and impact on the south side, as shown in Figs. 6.6.4a and b. This problem was partially overcome by introducing an additional 60 ms delay after the TP and before the first data reading for the north side exciter. The word "partially" is used because not every axle shows this 60 ms timing difference which is dependent on the train speed and the condition of the axle. There was a considerable improvement in data analysis shown by the corresponding DI histograms before and after the time delay correction (see Figs. 7.2.1 and 7.2.2). Obviously with an electronically activated exciter these timing problems could be eliminated completely.

2. Difference in impact force: This problem was also described in section 6.6. Examples are shown in Figs. 6.6.3a and b. To overcome this problem a redesign of the exciter in order to make the impact independent of the flange depth and train speed will be necessary. An important requirement of the new design must be electric or electronic disengagement of the hammer mechanism when trains are moving at speeds beyond the operational limit of the exciter. At this time no corrective action in the data processing is possible.

3. Failure to read the RTA or to read twice: This problem could introduce significant errors in the data processing. During the Englewood tests there was no error flag in the



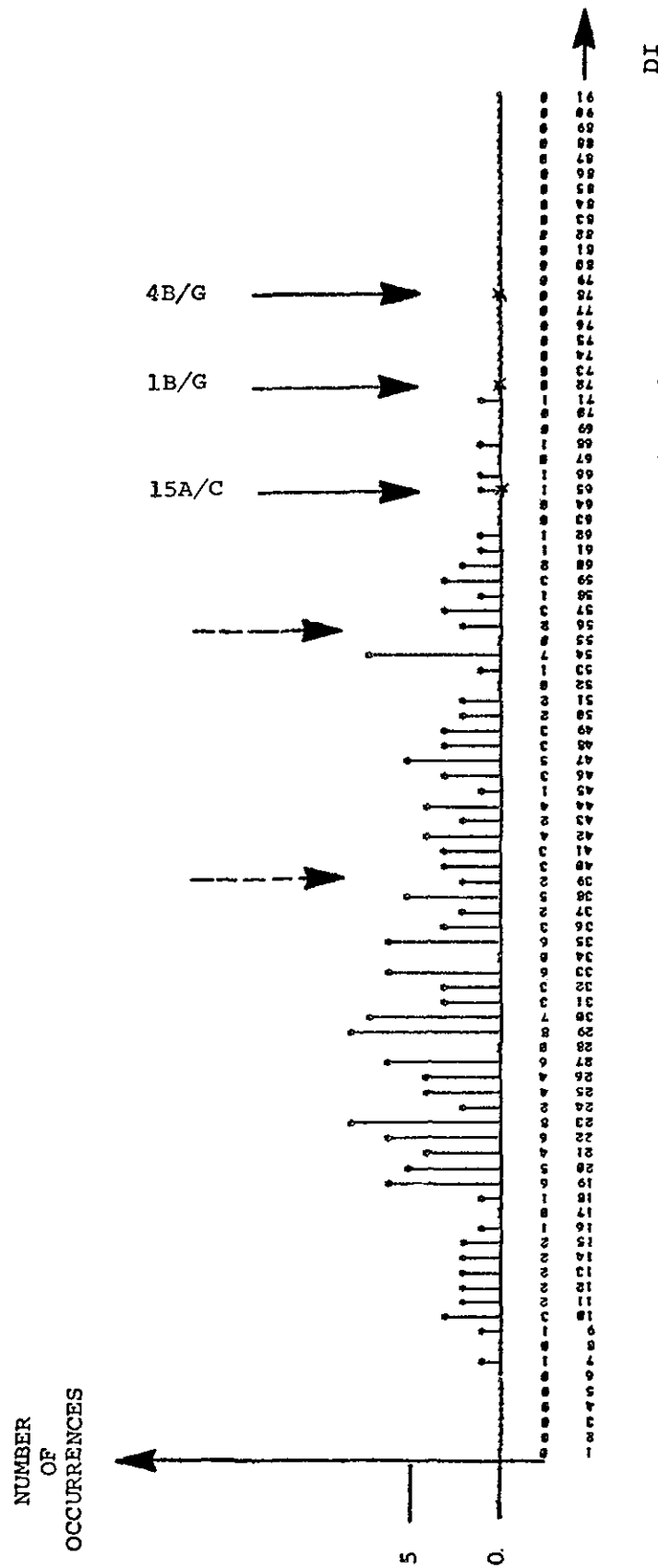


FIGURE 7.2.2. DISTRIBUTION OF DIFFERENCE INDEX VALUES

software to pinpoint this anomaly. The problem has been overcome now by making appropriate changes in the assembly software. The misreadings appear to be related to overload of the RTA.

4. Missing timing pulse: This is another serious problem, because the computer starts comparing signatures from wheels on different axles. The problem is probably due to the position of the wheel flange in respect to the sensing element of the proximity detector. The difficulty was recognized early during the field tests but despite continuous efforts to make an ideal adjustment of the sensors, it was not possible to store data from a long train without missing one or more TP's. This was the main reason that it was decided to test only a few cars at a time. Similar problems at other installations using this type of proximity detector have been reported. The highest DI indication (164) in Fig. 6.7.1 was due to a missing TP. For the present the few axles in the Englewood data with missing TP are not included in the analysis. The recommended solution is to avoid using this type of sensor, with preference for strain gauges, or photocells. An alternative solution is to incorporate circuitry and an error flag in the software when two successive TP's come from the same sensor.

5. Missing timing pulse at high train speed: This is due to the length of sampling time for data collection and storage. No action has been taken at present. The

recommended solution is a hardware-software change to give an error flag. No recordings at high speed are included in the present sample.

7.3 Optimizing the DI equation

There are several features of the acoustic signals from two wheels which could be used for comparison purposes:

- SD: the sum of the absolute values of the differences between the sound pressure levels of the two signals in the same frequency channels.
- NC: the number of common resonances, i.e., the number of resonances occurring in the same frequency channels in the two signals.
- DR: the difference in decay rates of the two signals.
- LD: the difference in the overall levels of the two signals.
- NR: the difference in the total numbers of resonances in each signal.

A variety of experiments were performed to obtain the optimum DI equation. In each case a histogram of the results was obtained in the same manner as for Figs. 7.2.1 and 7.2.2 which showed the effects of making a correction for the time delay.

It was decided to take one variable at a time and only add additional terms to the equation as proven to be efficacious. The first tests were made using the sum of the differences, SD. The principal issue here is the

most effective frequency range. In order to resolve this issue, 25 different histograms were plotted dividing the frequency range between 0 and 10 kHz into 400 Hz bands. It was clear from these histograms that the separation between the Englewood sample and the bad wheels was lost at frequencies above about 7200 Hz. Consequently, in all subsequent tests the frequency range was restricted to 0-7200 Hz. The improvement resulting from this restriction of the frequency range can be seen by comparing Figs. 7.3.1 and 7.3.2. Note that in Fig. 7.3.2 only one wheel from the Englewood sample appears in the range of the bad wheel reference set. This was the first histogram obtained in which one of the bad wheel sets showed a DI value higher than any in the Englewood sample.

This test was followed by several attempts to incorporate terms involving the differences in decay rates. Although earlier laboratory tests had shown that the sound from cracked wheels damps more rapidly than from good wheels the present set of tests did not lead to an improvement in separation. It is believed that this disappointing outcome was because of the uncertainties in the time reference, and the availability of only two data samples of the sound from each impact. It is possible that when the TP problems have been completely eliminated, then terms involving the difference in decay rate may still lead to improvement in the DI separation.

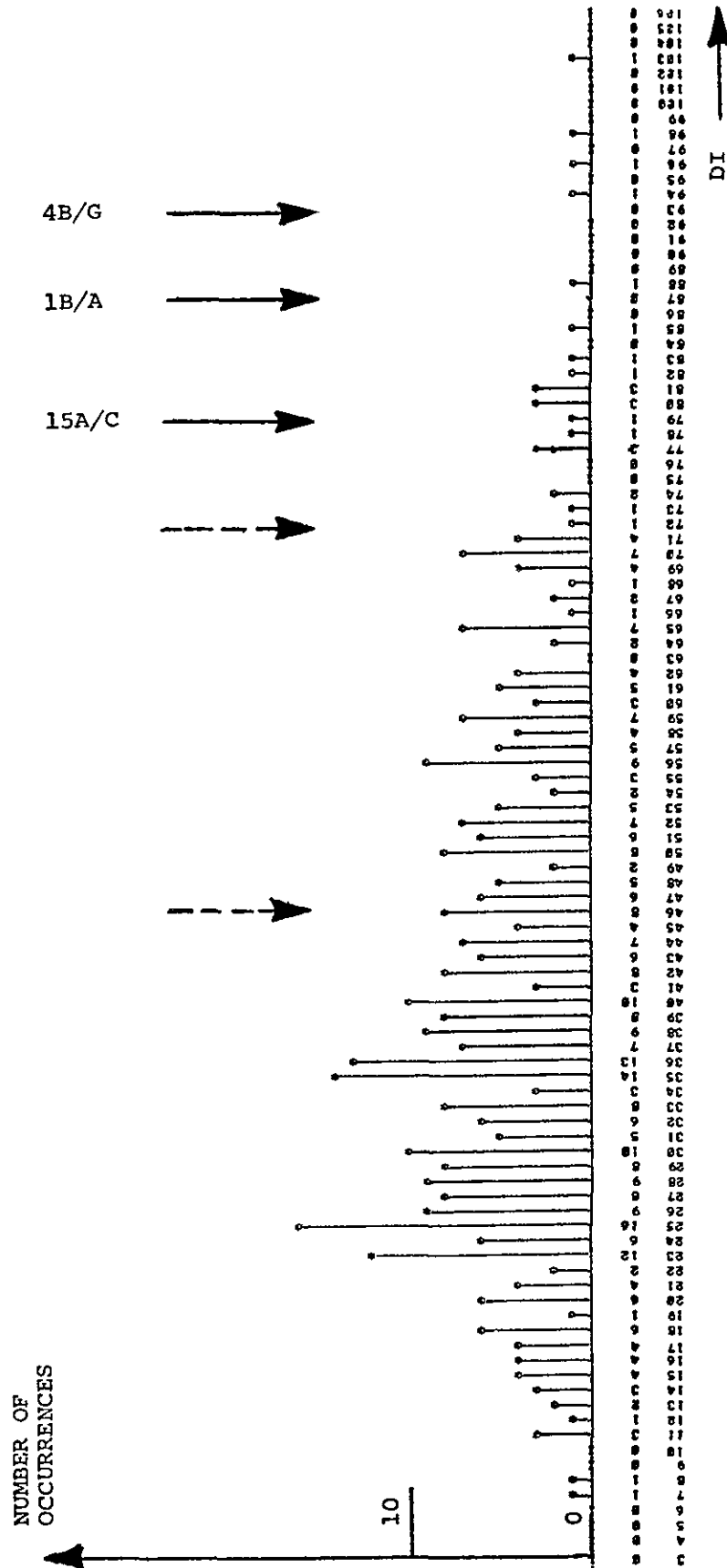


FIGURE 7.3.1. DISTRIBUTION OF DIFFERENCE INDEX VALUES

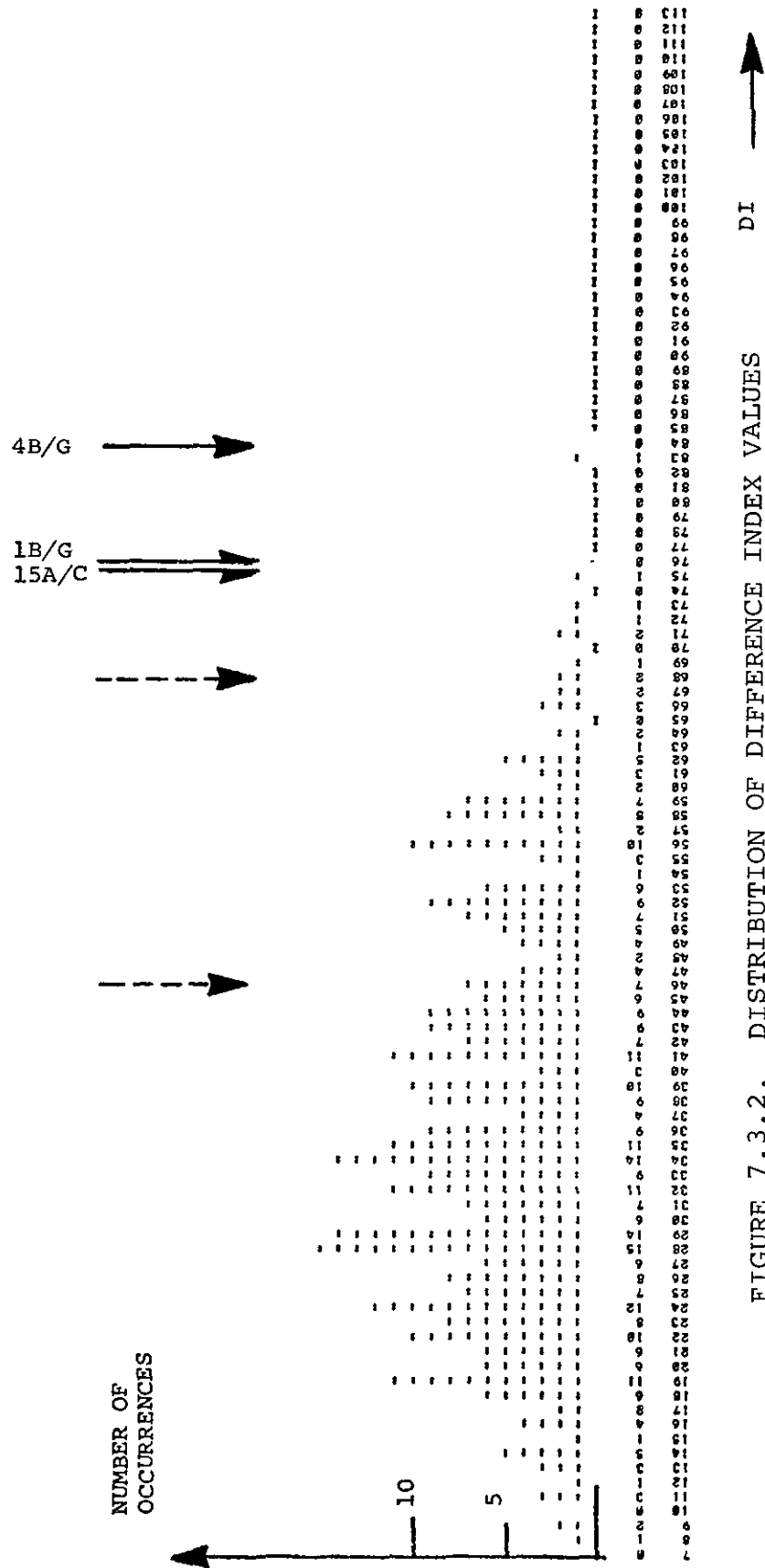


FIGURE 7.3.2. DISTRIBUTION OF DIFFERENCE INDEX VALUES

DI = C_1SD

— INDICATES DI FOR DEFECTIVE WHEELS

--- INDICATES DI FOR GOOD WHEELS IN LAB. TEST

SAMPLE SIZE: 369. WITH CORRECTION FOR TIMING PULSE DIFFERENCE
Frequency Range is 0-7.2 kHz. Compare with Fig. 7.3.1

The last set of experiments involved the inclusion of a term in NC, the number of common resonances. Figure 7.3.3 is a histogram of NC values from the Englewood sample with those from the reference bad wheel set. Note that the bad wheels show up to 5 common resonances, but the modal value is around 6 or 7. It was felt that this feature could be used by putting a heavy emphasis on the similarity of wheels with a high number of common resonances. Consequently, experiments were run using the following DI equations:

$$DI = c_1 SD - c_2 NC \quad (7.3.1)$$

and

$$DI = c_1 SD - c_2 (NC)^2 \quad (7.3.2)$$

The best results were obtained from equation (7.3.2) with the ratio

$$\frac{c_2}{c_1} = 5.$$

These results are shown in Fig. 7.3.4. In comparison with Fig. 7.3.2 it may be argued that there is an improvement in that there are now two bad wheels with DI values higher than any from the Englewood sample.

On the other hand, there are still three values from the Englewood sample falling in the range of the bad wheel reference group.

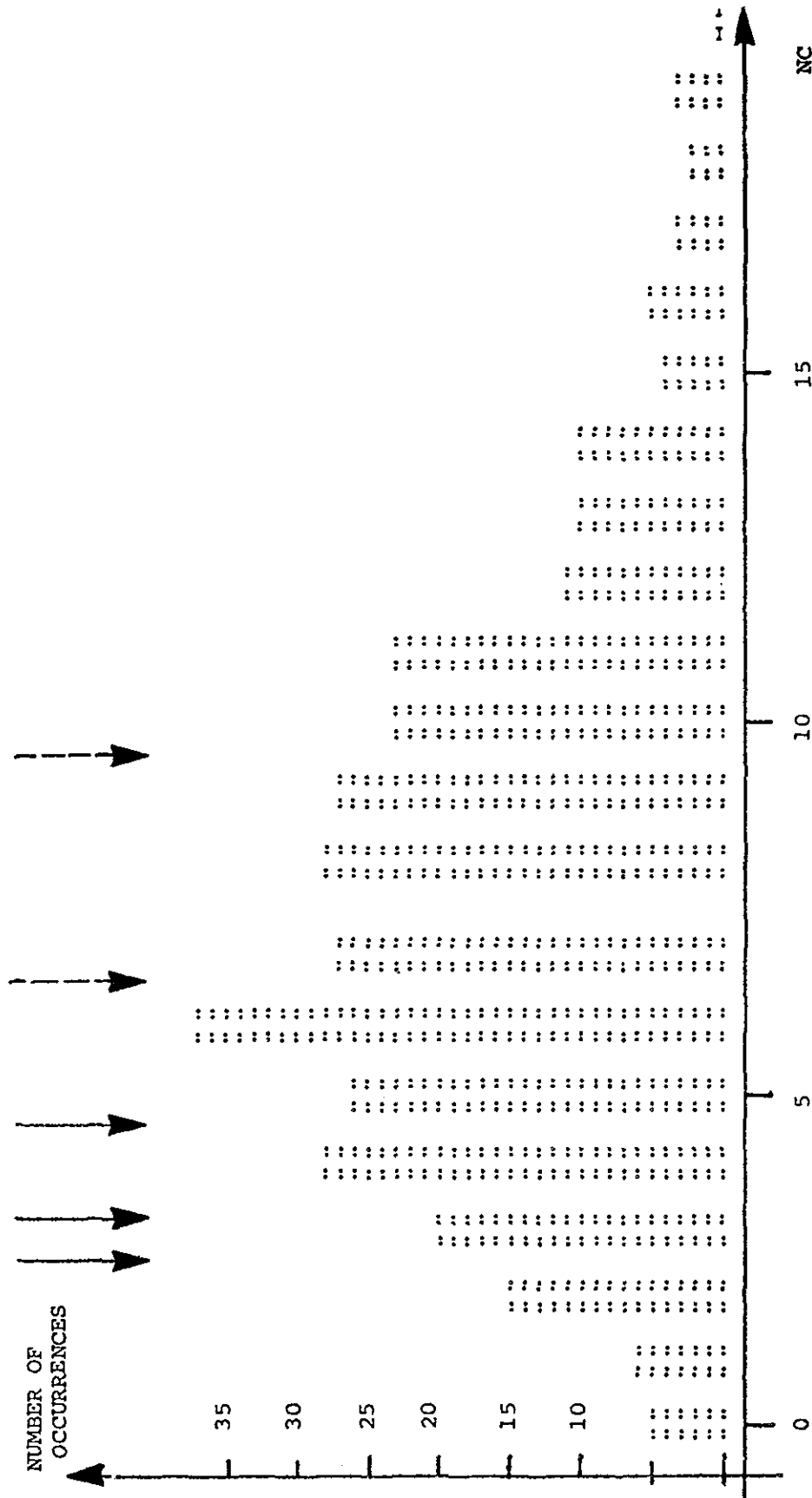


FIGURE 7.3.3. DISTRIBUTION OF NUMBER OF COMMON RESONANCES, NC
 — INDICATES AVERAGE VALUE OF NC FOR DEFECTIVE WHEELS
 - - - INDICATES AVERAGE VALUE OF NC FOR GOOD WHEELS IN LAB. TEST

Sample Size: 313. Frequency Range is 0-10 kHz

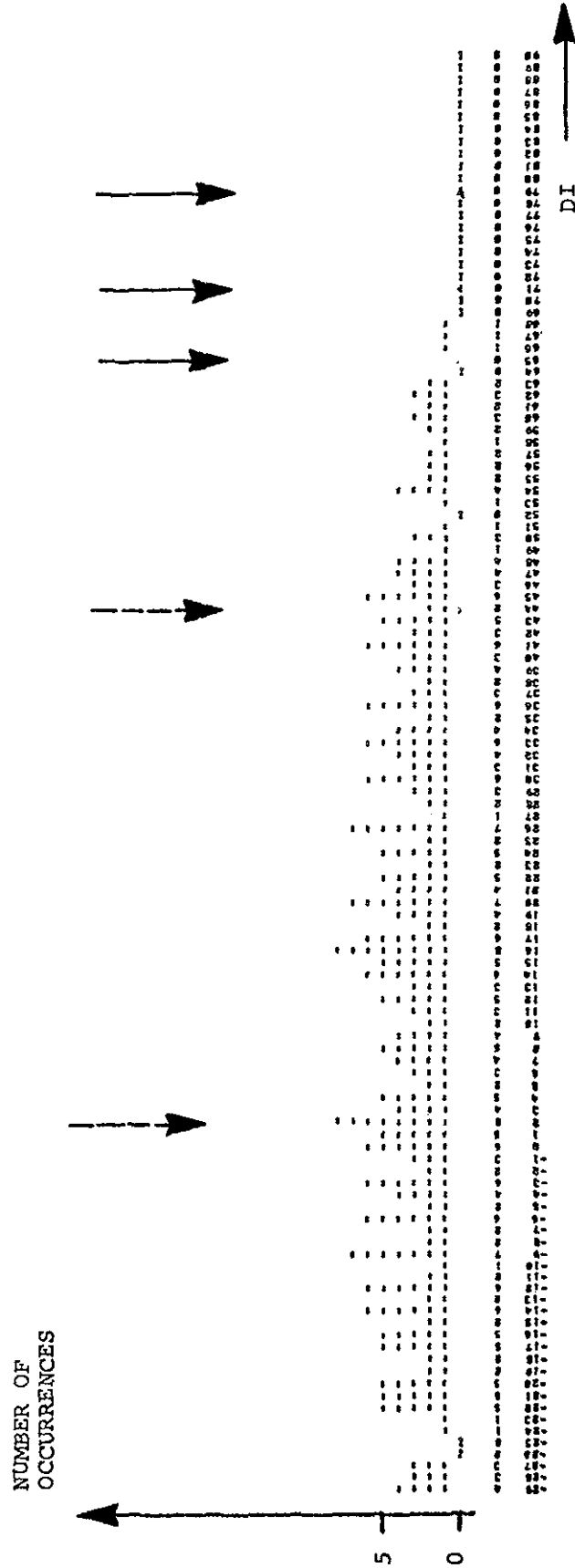


FIGURE 7.3.4. DISTRIBUTION OF DIFFERENCE INDEX VALUES

$$DI = C_1SD - C_2(NC)^2$$

← INDICATES DI FOR DEFECTIVE WHEELS

← INDICATES DI FOR GOOD WHEELS IN LAB. TEST

Sample Size: 371. With correction for Timing Pulse Difference
Frequency Range is 0-7.2 kHz. Compare with Fig. 7.3.2

Several other histograms were made for DI equations including terms in the difference of total levels LD and terms in the difference of total numbers of resonances in each spectrum NR. None of the variations tried led to any further improvement in the separation.

At this stage therefore there are two variations of the DI equation which appear to be promising as illustrated in Figs. 7.3.2 and 7.3.4. The question to be addressed in the next section is whether or not the high DI values shown in Figs. 7.3.2 and 7.3.4 are indicative of wheel/axle conditions, and, if so, what conditions.

7.4 The Effect of Wheel Conditions

7.4.1 Introduction

In the previous sections the identification and correction of system problems and the optimization of the DI equation was presented. As a result of these studies there was a considerable improvement in the histogram of DI values in the sense that the DI values for defective wheels showed the greatest separation yet from the modal value of the rest of the population. But there is clearly a wide spread in DI values among the sample. The purpose of the study reported now was to ascertain, if possible, what wheel conditions, besides cracks, could give rise to high DI values. Before starting this phase of the investigation it was anticipated that a variety of possible conditions might have caused such high values:

1. skewed axles
2. uneven load
3. uneven wear
4. greasy wheels
5. differences in internal stress
6. cracks.

There is evidence that some skewed axles were present in the Englewood sample, but these occurrences did not result in extremely high DI values. Greasy wheels are highly damped at high frequencies and usually resulted in an "insufficient data indication." None of the very high DI values in Fig. 7.3.5 showed very high damping, and consequently grease is not believed to be the cause of the high values. Although changes in internal stress do cause changes in resonant frequencies, such changes are very small. Even if there were substantial differences in internal stress between two wheels of a given axle set (which is hard to believe), the effect in the DI value should still be very small. The effects of uneven load should presumably be similarly small since the effect on the acoustic properties of the wheel does not depend on whether the stress field is residual or is applied externally.

Thus, by this process of elimination uneven wear and cracks were left as potential causes of the high DI values. However, in a sample of 400 wheel sets, it is very unlikely that there is a cracked wheel as mentioned previously.

One therefore suspects that uneven wear is the most likely cause of the large number of high DI values.

7.4.2 Data Reduction

In order to investigate this hypothesis it was decided to make a further study of the data on the ten wheel sets from the Englewood sample showing the highest DI values. For these wheel sets the following data was available:

- 1) plots of the acoustic spectra from the two wheels
- 2) oscillograms of the impact and timing pulse
- and 3) the car identification number.

In each case the first point of concern was to ascertain if uneven impact level was a problem. In only two of the ten cases investigated was there a substantial difference in impact levels. Figures 7.4.1 and 7.4.2 show the effect for one of these cases. The impact level was about the same in the other eight instances. However, all of these other eight instances showed a common feature in the spectral comparisons as seen in Figs. 7.4.3 and 7.4.4 for a typical case.

The feature of importance which distinguishes these cases is a frequency shift between resonance peaks. Such shifts are marked in Fig. 7.4.3. The interesting aspect of this phenomenon is that the amount of the shift appears to increase proportionally with frequency to a first approximation. This effect is illustrated in Fig. 7.4.5 where the frequency shifts are plotted as a function of

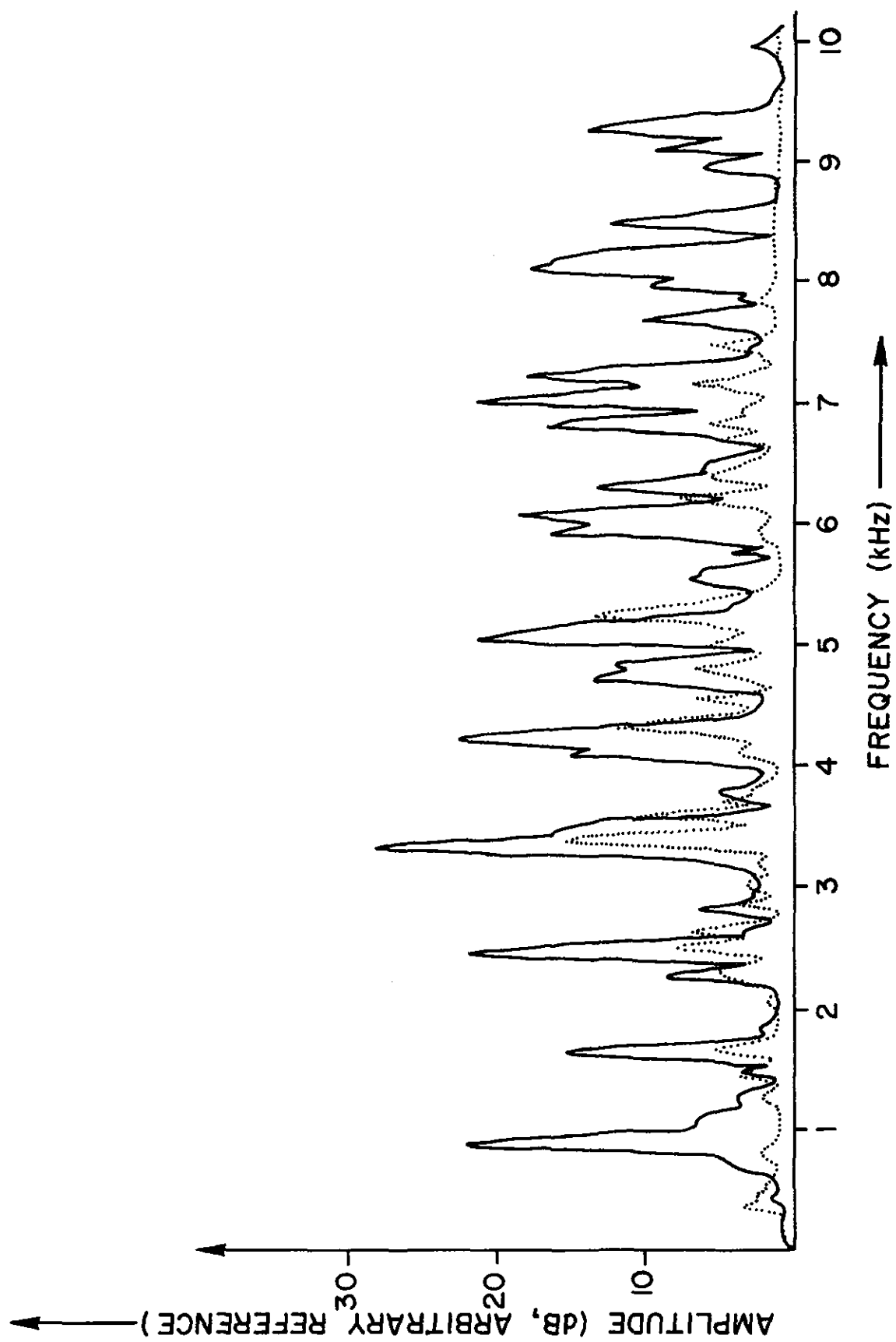


FIGURE 7.4.1.1 SIGNATURES OF WHEELS DUE TO UNEVEN IMPACT

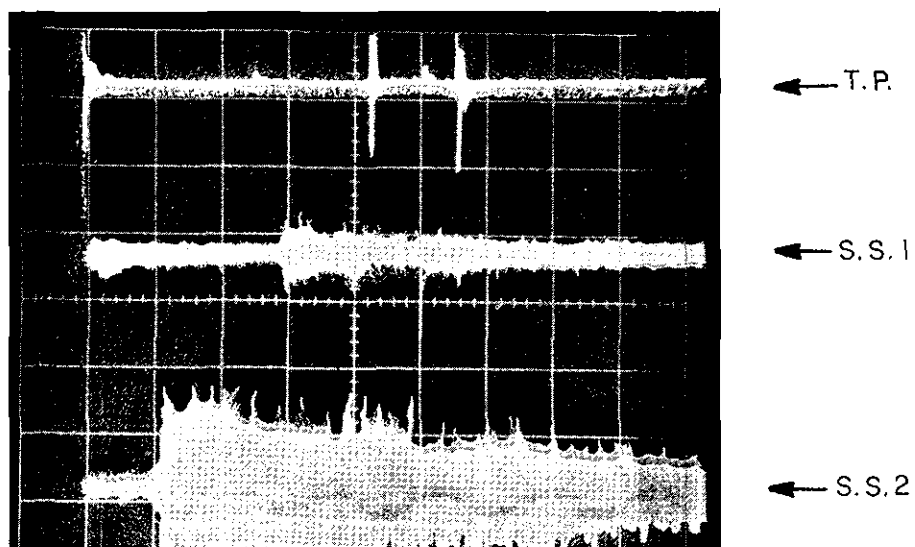


Fig. 7.4.2 Timing pulses (T.P.) and sound signals (S.S.) from two unevenly impacted wheels. Sweeping speed 50 ms/div. (The signatures in Fig. 7.4.1 correspond to the above signals.)

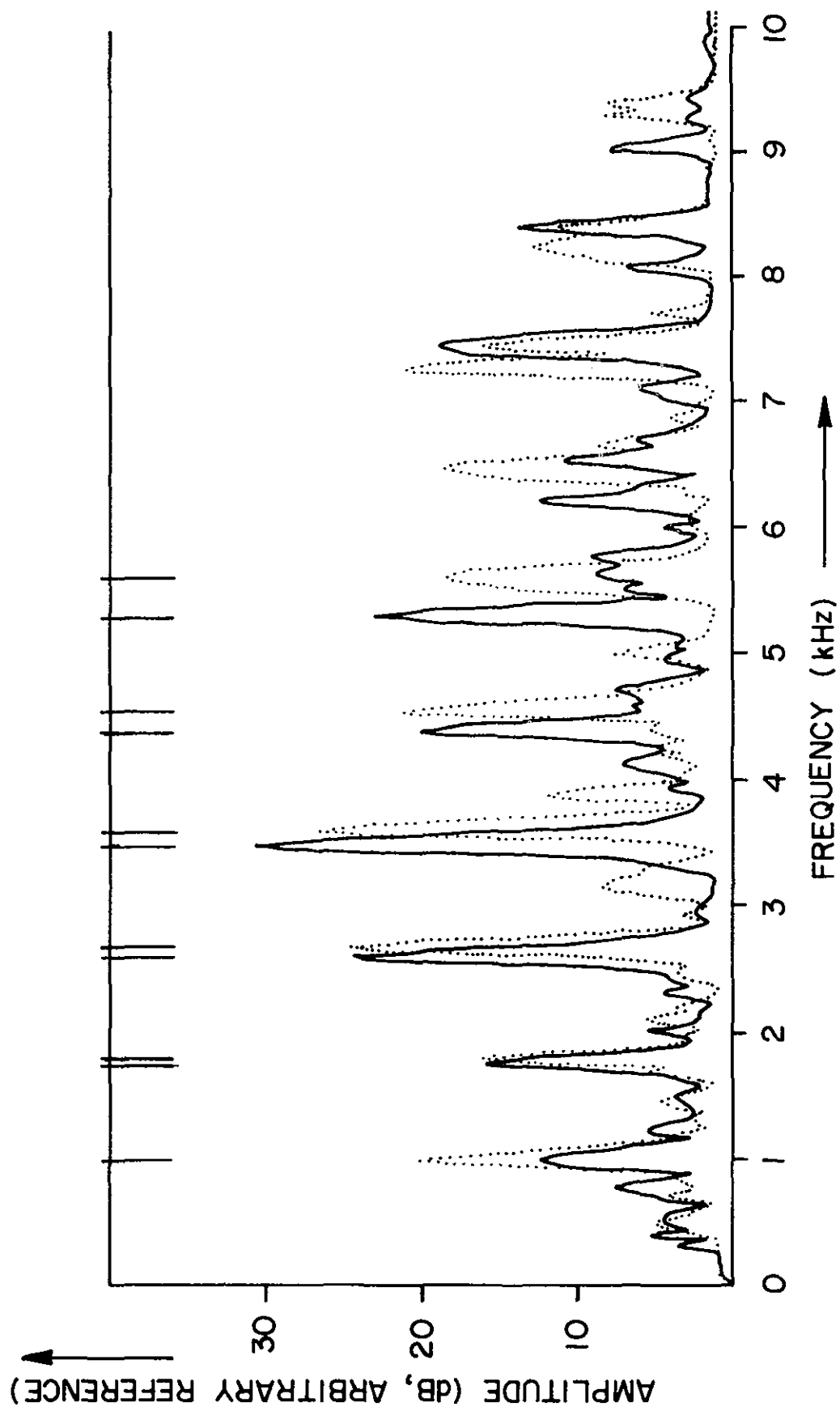


FIGURE 7.4.3 SIGNATURES OF WHEELS ON AXLE 3, CAR GTAX 13286

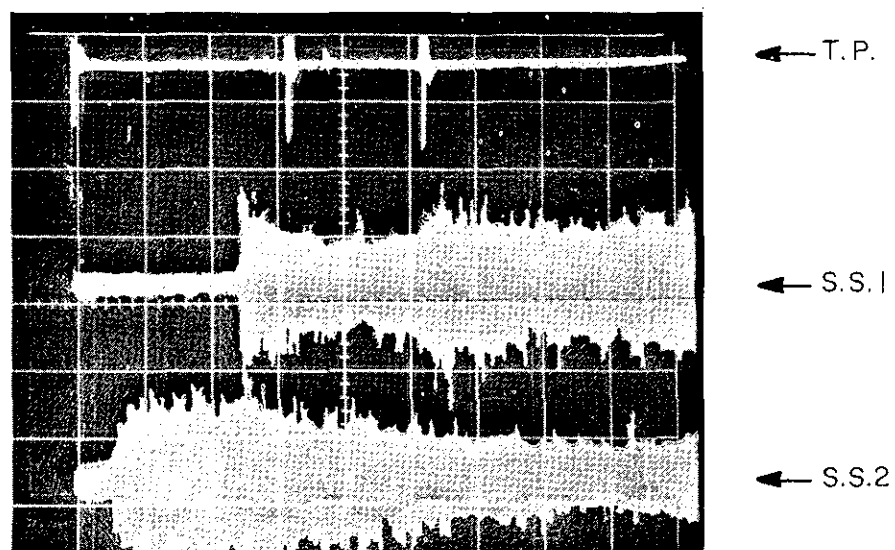
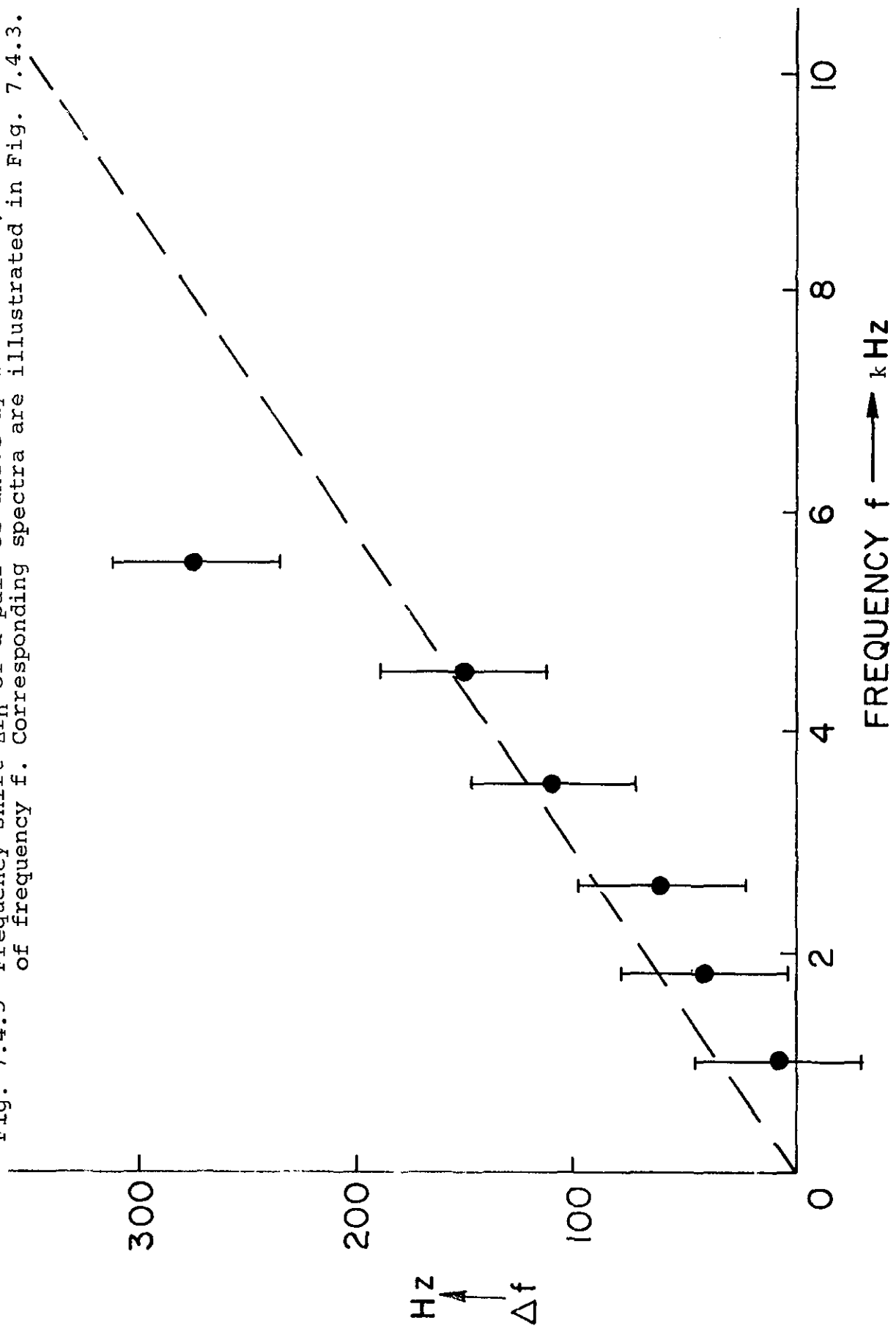


Fig. 7.4.4 Typical timing pulses and sound signals from a pair of wheels tested at the Englewood yard. Sweeping speed 50 ms/div. (The signatures in Fig. 7.4.3 correspond to the above signals.)

Fig. 7.4.5 Frequency shift Δf_n of a pair of unevenly worn wheels, as a function of frequency f . Corresponding spectra are illustrated in Fig. 7.4.3.



resonant frequency, as measured from the spectrum of one of the wheel pairs illustrated in Fig. 7.4.3. In most cases it was found that the frequency shifts at the higher resonances (above about 5 kHz) departed from the linear relation to even higher values, as seen in Fig. 7.4.5 for the resonance at 5.5 kHz. This made it increasingly difficult to recognize the corresponding modes at the higher frequencies.

A theoretical study on the effect of uneven wear on wheel vibrations was presented in Chapter II and the conclusion was that for small changes in rim thickness, Δh the frequency shift in the n^{th} mode, Δf_n is given by

$$|\Delta f_n| = \left| \frac{\Delta h}{r} \right| f_n \quad (7.4.1)$$

This simple theory offers a qualitative explanation of the results shown in Fig. 7.4.5. It is of interest to see if the theory and experiment have a reasonable quantitative relationship. From Fig. 7.4.5 the slope of the fitted line is about 250 Hz in 10 KHz, thus from eqn. (7.4.1)

$$\frac{\Delta h}{r} = \frac{250}{10 \times 10^3}$$

Assuming r to be about 16 in. we estimate $\Delta h = 0.40$ in. (10 mm). Table 7.4.1 shows the slopes and differential wear estimated for the eight wheel sets investigated. These values range from 9 to 18 mm. Obviously the theory given above has a number of simplifying approximations and the question arose as to whether such amounts of differ-

TABLE 7.4.1 THEORETICAL ESTIMATE OF DIFFERENTIAL WEAR
ON WHEELS WITH HIGH DI VALUES

Car Identification and Axle Number	DI Value	$\frac{\Delta f}{f}$	Estimated Δh in (mm)
GN 171932 axle 1	63	0.045	0.72 (18)
IC 75536 axle 4	39	0.040	0.64 (16)
ATSF 521735 axle 2	55	0.021	0.34 (9)
SSW 76704 axle 2	61	0.025	0.40 (10)
C & S 565500 axle 4	61	0.030	0.48 (12)
C & S 565500 axle 2	66	0.035	0.56 (14)
ATSF 81338 axle 4	68	0.045	0.72 (18)
GTAX 13286 axle 3	67	0.035	0.56 (14)

ential wear are encountered in practice. The expense of recalling the wheels in question was not felt to be justifiable, and in any case the wheels would have received almost a year of additional usage since the Englewood test. Instead it was decided to make some careful measurements on wheels in the laboratory collection at the University.

7.4.3 Laboratory Measurement of Wear

Measurements of the tread and flange thicknesses were made between the points indicated in Fig. 7.4.6 using a pair of calipers. Because of difficulty in positioning the calipers at precisely the same orientation it is estimated that the accuracy was ± 0.5 mm for tread measurements and ± 1.5 mm for flange measurements. The results are given in Table 7.4.2. Measurements made at different circumferential positions showed no more than ± 1 mm variation.

The first observation to be made is that the range of values of differential tread wear, from 0.0 to 6.9 mm, while not showing values as high as those hypothesized is, nevertheless, of the same order of magnitude. It was decided to study the spectra of the laboratory wheel sets to ascertain the magnitude of frequency shifts, if any. Wheels 6B/C, showing the highest differential tread wear, are 36 in. wheels with thermal cracks and the spectra are very complex. The next highest values of differential wear are for wheels 10A/C and 11A/C. Both of these sets also show considerable differential flange wear. Figures 3.3.1 and 7.4.7 show the spectra for these wheel

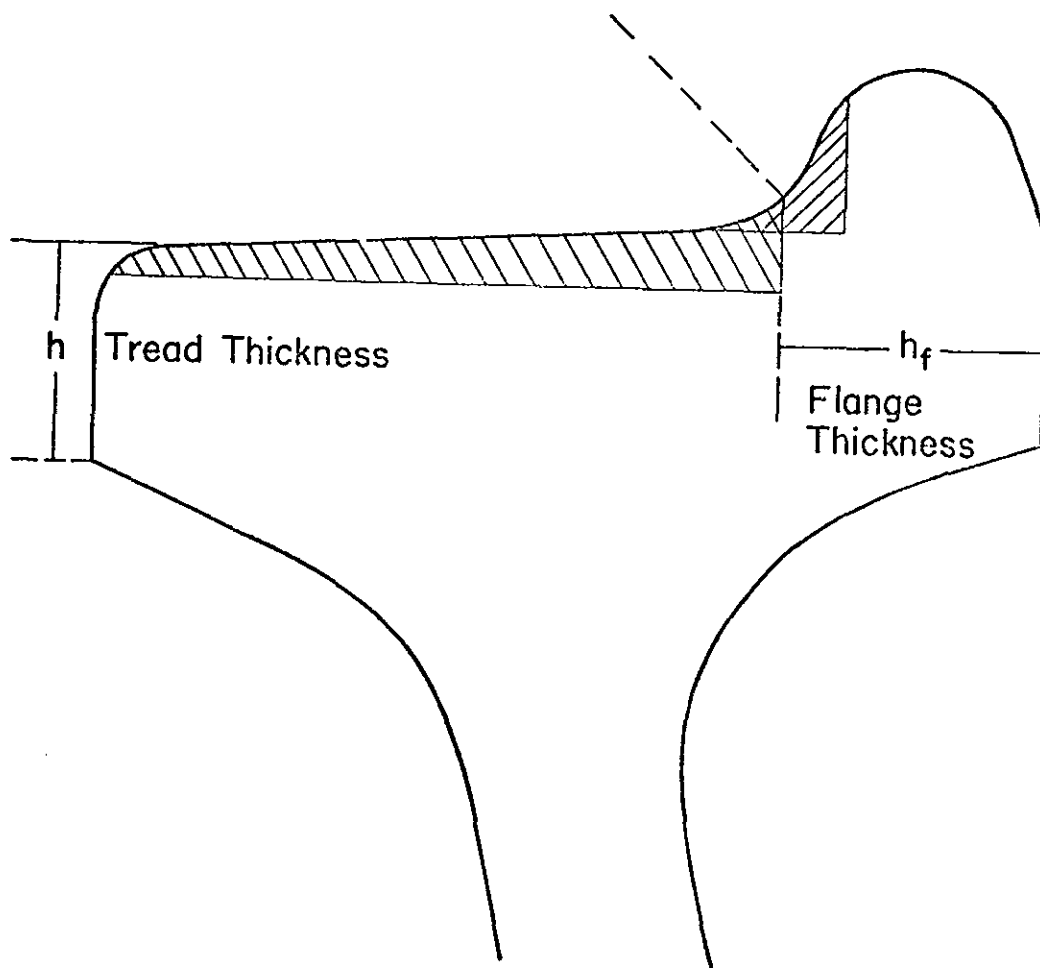


FIG. 7.4.6 Actual Cross Section of a Wheel Showing How the Tread and Flange Thickness Were Measured. Crosshatched Area Reveals the Relative Importance of the Tread and Flange Wear.

TABLE 7.4.2. TREAD AND FLANGE THICKNESS OF WHEELS
AT THE UNIVERSITY OF HOUSTON LABORATORY

UH Wheel Identification Number	Flange mm	Tread mm	Δh for Tread mm
9A	32.6	35.5	1.5
9C	26.2	34.0	
10A	29.5	29.5	3.7
10C	38.4	25.8	
11A	29.3	33.6	3.6
11C	39.0	30.0	
12A	31.4	28.2	0.9
12C	32.4	27.3	
13A	40.0	25.0	0.0
13C	41.0	25.0	
14A	41.0	31.2	0.0
14C	42.0	31.2	
15A	36.0	35.2	0.2
15C	34.4	35.0	
1B	33.0	34.0	1.8
1G	37.3	32.2	
2B	29.0	32.2	0.2
2G	36.2	32.0	
4B	41.0	32.5	0.5
4G	40.5	32.0	
5B	42.5	47.0	1.5
5G	30.2	48.5	
6B	38.3	42.1	6.9
6G	33.7	49.0	
8B	38.8	24.0	0.5
8G	33.5	24.5	

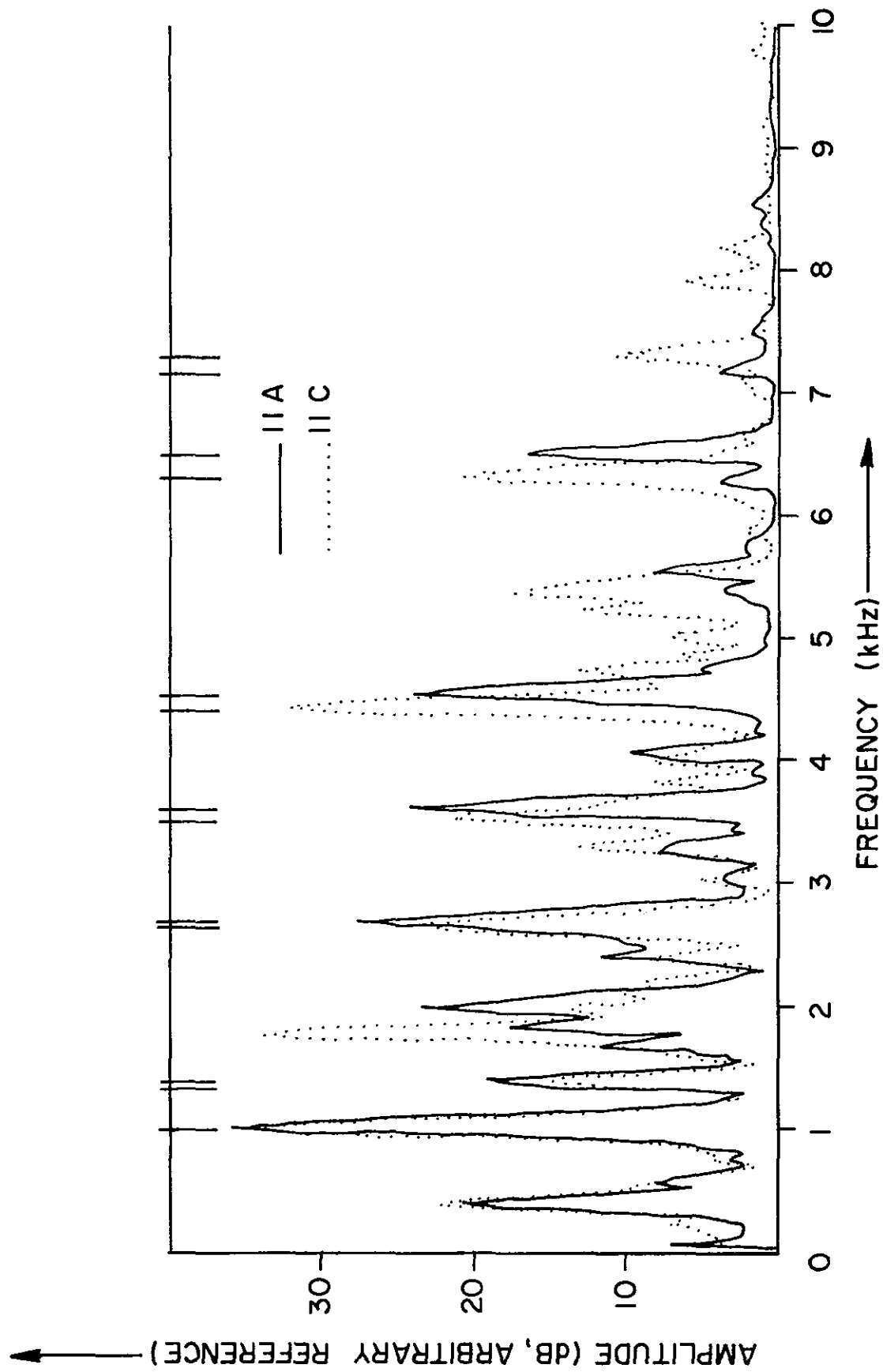


FIGURE 7.4.7 SIGNATURE OF WHEELS IIA AND IIC

sets. Proportional frequency shifts are more easily seen in the spectra of 11A/C. Plotting Δf_n versus f_n for 11A/C results in the plot shown in Fig. 7.4.8. From the slope of the best straight line fit, using eqn (7.4.1) Δh is estimated to be 8 mm, about twice the measured value. A possible explanation for this apparent discrepancy could be that wear on the inside of the tread is greater than on the edge, where the measurement was made.

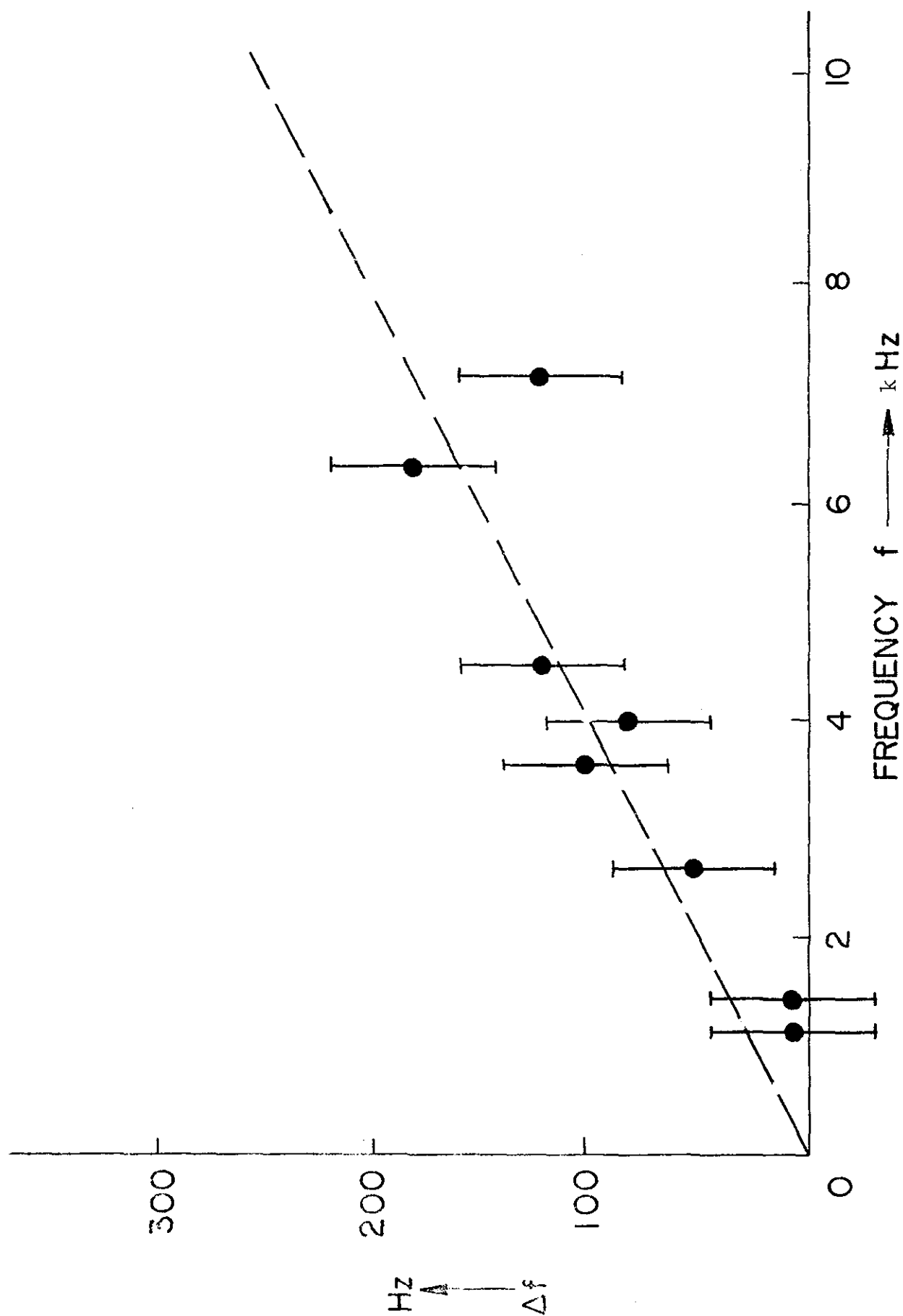


FIGURE 7.4.8. SIGNATURE DIFFERENCES AT THE RESONANT MODES FOR WHEELS 11A/C, DUE TO UNEVEN WEAR. CORRESPONDING SPECTRA ARE ILLUSTRATED IN FIG. 7.4.7

8. CONCLUSIONS AND SUGGESTIONS FOR FURTHER WORK

8.1 Conclusions

In these studies the development of a wayside system for inspection of railroad wheels in service using acoustic signature analysis was presented. The basic claim is that the improvements and modifications of Nagy's laboratory system have reached the point that the installation of a prototype system can now be contemplated. This transitional phase included hardware interfacing for wayside installation, and software development for real time operation, data acquisition and data analysis. Experimental studies and theoretical models were used to obtain more information on the effects on vibrations of wheels of geometrical variations, wear, internal stress etc. Finally a field test was performed to elucidate system problems. Tape recordings were made to permit further study of these problems, to optimize the software and to discover other wheel conditions influencing the acoustic signature. It is appropriate to review these efforts in more detail.

8.1.1 Advances in Scientific Understanding

A better understanding of wheel vibrations under various conditions and under varying forcing functions was needed for the development of the recognition logic.

A number of analyses were made using a finite element program. This is the best theoretical approach because there is no closed form solution for vibrations of elastic solids with complex geometries, such as the railroad wheels. A summary of the work is presented in Appendix F.

Parallel studies were made in the development of Stappenbeck's simple ring model for comparison and evaluation of the experimental results. It was successfully used in the evaluation of the lowest flexural modes of a 33" wheel, and later in the studies of differential wear on the tread of two wheels. Finally the effect of residual stress on wheel vibrations was demonstrated to be plausible from the theory of the effect of externally applied forces on beam vibration. In order to verify some of these theoretical predictions, several laboratory experiments were conducted. The results reconfirmed earlier indications that the important modes are those with nodal diameters.

Further experimental studies on the acoustic signatures from wheels in manufacture and under drag braking, with different residual stress, yielded a very important discovery, namely that there are measurable frequency shifts which are in agreement with theoretical evaluations. These shifts are of the order of 0-10 Hz.

8.1.2 System Improvements

The major change and improvement over the earlier laboratory system was the use of a narrow band instead of a 1/3 octave band real time analyzer. Most of the fre-

quency information of 28" to 40" railroad wheels is between 400 to 10,000 Hz. For this range a 250 channel narrow band real time analyzer has a 40 Hz per channel resolution, compared to several hundred Hz for the corresponding 1/3 octave band analyzer operating in the same frequency range. Although this is a significant improvement some experiments, such as residual stress evaluation, required even higher resolution.

A second area of improvement was in the wheel excitation. Several alternatives were evaluated and tested. The study led to the selection of a mechanical hammer, which rated superior to two other possible exciters. A redesign of the mechanical exciter with the emphasis on ruggedness produced an exciter which withstood some 27,000 impacts with minimal wear and without breaking. Despite the improvements impacts were speed dependent. Commercial all weather microphones were used and performed without problems despite high temperatures, humidity and rainstorms. A timing pulse was used in the data processing. The sound from impact excitation of a moving railroad wheel is a transient signal of short duration, and the maximum train speed restricts the sampling time to about 300 ms. Thus precise sampling becomes an important factor. A reasonable choice of a timing pulse generator seemed to be a wheel proximity detector already in use on several railroads. Field experience indicated that the actual device chosen sometimes failed to generate the required pulse, and

consideration of this must be made in the installation of a prototype. The addition of two floppy diskettes as mass memory storage devices was another improvement. Laboratory tests required a relatively small amount of memory for data storage. But in actual operation the fast collection of a large amount of data prevented true real time analysis. However, near real time operation was possible in that data processing started after the transfer of the last wheel signature. The processing time could and should be reduced in a prototype system.

8.1.3 Software and Signature Recognition Improvements

The field tests at TTC, Pueblo were made as a rehearsal for the complete test of the system at the Englewood Yard in Houston. The treatment of the data obtained during those tests led to the following principal conclusions:

1. Timing differences between the triggering pulse and impact for the two pairs of wheel sensors and exciters was found to be an important problem but could be partially corrected in the data processing.
2. Improper data transfer from the RTA to the computer can be flagged now, with appropriate changes in the assembly software.
3. Missing triggering pulses were a problem but could be accounted for in the data processing.
4. The optimum frequency range to be used in the analysis has been shown to be 0-7200 Hz.
5. The optimum DI equation has been found to be:

$$DI = C_1 SD - C_2 (NC)^2$$

where SD is the sum of the absolute values of the differences between the sound pressure levels of the two signals in the same frequency channel. NC is the number of common resonances, i.e., the number of the resonances occurring in the same frequency channels in the two signals. This simplified DI equation was obtained after the analysis of the field data, which had shown that terms such as Decay Rate (DR) or $SP_{1,2}$ (indicating the overall sound pressure level) did not improve the separation between DI values for good and defective wheels.

The criterion for the optimum DI equation was the achievement of a maximum separation between the modal DI value in a histogram of results using the sample of recordings made in the Englewood Yard and some recordings of bad wheels made in the laboratory. The improvement in this separation can be related to system reliability and false alarm rate (see Appendix G). Using such criteria, two thirds of the defective wheels could be found with one hundred percent reliability and zero false alarm rate, based on the small statistical sample presently available.

Uneven or differential wear on wheelsets was established as the major cause of high DI values. This was concluded on the following bases:

- 1) An argument on the basis of prior knowledge
- 2) A study of the data for the 10 highest DI values found in the Englewood sample using the optimum DI equation.

These instances showed a characteristic shifting of resonance peaks by amounts approximately proportional to frequency.

3) A simple theoretical treatment showing that such an effect is to be expected if there is different wear on the treads of two wheels.

4) Some measurements of wear differences among wheels in the collection at the University.

5) A comparison of the frequency shifts in the spectra of worn wheels in the laboratory, and hence a demonstration that the wear differential predicted using the theory mentioned in 3) agrees with the measurement mentioned in 4) within a factor of two.

Some method of recognition of unevenly worn wheel sets would probably yield the most significant improvement over the existing system.

8.2 Suggestions for Further Work

It is advocated that the work on Acoustic Signature Inspection should be advanced on three fronts:

a) Installation of a prototype system by a railroad.

The Union Pacific Railroad is planning to install a prototype system. Certain obvious system design improvements should be made, as detailed below.

b) Improvement of scientific knowledge. The measurement of internal stress in wheels and its effects on crack growth is probably the most important gap in knowledge at present. The effect of cyclic loading on crack growth

rates is another unknown area. It will be difficult to improve on wheel removal criteria without such knowledge.

c) System Interaction Studies, Calibrations, etc.

There is a need for a centrally located establishment where comparisons and interactions of various inspection systems could be carried out. Suggestions for development of an ASI system at such a location are also detailed below.

8.2.1 Installation of a Prototype ASI System

Planning for the installation of a prototype ASI system by the Union Pacific Railroad has already reached an advanced stage. The system will be installed in the Las Vegas, Nevada yard and the target date for commencement of operations is January 1979. The hardware will consist of a Hewlett-Packard computer system interfaced with the Spectral Dynamics RTA presently on loan to the University of Houston. A single General Radio all-weather microphone will be used. Two commercial microswitch wheel sensors have been selected. The wheel exciters will be of the same type used in the 1977 test at the Englewood Yard.

The Union Pacific plans to assemble the system at Omaha prior to installing it at Las Vegas. Implementation of the software is considered to be part of the assembly task. It will be necessary to rewrite the existing programs in FORTRAN in order to reduce the data processing time.

After installation of the system at a low speed location it is anticipated that a period of "debugging"

will be necessary. The Union Pacific intends to assign a qualified person to work full time with the system.

It is recommended that additional work to support the Union Pacific's effort could be directed toward the detection of uneven wheel wear. Successful identification of such wheels should further reduce the false alarm rate. One way to do this would be to incorporate a subroutine in the computer software to recognize resonant frequency shifts. Two possible algorithms can be envisaged: a) multiplication of the frequency values of one spectrum by a variable and use of the minimum DI value obtained, for decision making; b) elimination from consideration of wheel sets in which the DI value increases rapidly at high frequency. Obviously such a subroutine would require development time and need careful study before incorporation in the program. One problem might be that a wheel set with a cracked member could also show high differential wear. Another method to offset the high DI value of sets with high differential wear would be to include a term in the DI equation based on input from a system capable of directly measuring differential wear, such as a flange height sensor or a rim circumference indicator.

It is also suggested that some effort could be devoted to exciter design as follows:

- a) Improve the present exciter by modifying the impact delivered so that it shall be independent of train speed. A solenoid could be used to activate the impacter. Other changes, not in the exciter alone, are

needed to improve the effectiveness of the system at higher speeds.

- b) Instrument the plunger of the present hammer to permit a reading of flange depth. This reading should be used to detect uneven wear on wheels of an axle set and to indicate wear beyond condemnable limits.
- c) Instrument the hammer of the present exciter to give a reading of the impact force. This reading could be used to indicate a failure of the system or to indicate the presence of foreign material on the wheel tread. This could be used to detect wheels liable to slip through retarders.
- d) Reconfigure the mounting of the exciter to permit speedier attachment to the rail and ready adaptability to rail of different weights, between 110 lb/yd and 136 lb/yd.
- e) Design an electrical control unit to activate the hammer and provide the means to program the sequence of wheels to be struck and to deactivate the exciter entirely if so required.

Finally it is important that a data bank of tapes be compiled to permit further sensitivity studies and improvement of the DI equation. This would also permit the system reliability and false alarm rate to be monitored. Causes of high DI values should be ascertained. In order to allow such studies to be made the system should include a 2 or 4 channel analog tape recorder. Tapes should be catalogued and stored.

8.2.2 System Interaction Studies

Beyond the installation of the prototype at Las Vegas, and benefitting from experience therewith, a second system should be installed at the Transportation Test Center at Pueblo, Colorado. In order to permit systems interaction studies, operation of calibration consists, etc. the following additional developments should be undertaken:

a) Use of A/D Conversion

If the microphone signal were converted directly into digital form and stored in memory it could then be processed by a Fast Fourier Transform (FFT) program and the use of the RTA could be avoided. Hardwired FFT programs are available. If this task were successfully accomplished it appears that there would also be an improvement in system reliability. However elimination of the RTA is not recommended until it is demonstrated that the task can be accomplished without sacrifice in frequency resolution, and even then the RTA has other desirable features. The use of a line printer instead of the teletype will speed up the computer output 10 to 25 times which is another important factor in the development and use of the system.

b) Provision of Automatic Turn-on

It would be desirable to provide automatic turn-on for the system when a train approaches. This will entail the selection of a train proximity detector and turn-on

of the electronics with adequate warm-up time. Equipment costs are uncertain estimates.

c) Interfacing to a Central Processor

The minicomputer of the ASI system would need to be interfaced with the Central Processor of the Automated Wayside Facility. In addition an analog signal from the microphones should be available to the Central Processor.

8.2.3 Further Research on Residual Stress, Crack Growth and Wheel Removal Criteria

Further research is necessary in order to develop a better understanding of crack initiation and growth, the influence of internal stress, the influence of cyclic loading, etc., with a view to improving wheel removal criteria.

The Wilmerding data, together with the previous information on loading and the results of the Bessemer tests, indicate that changes in resonant frequencies occur with changes in internal stress. There is a need for additional data, and there is a need to establish a firm theoretical explanation of the effect for any complex residual stress field combined with the rotating stress field due to the external load. There also arises the question of the engineering application of the effect.

The major problem in applying the effect is that the occurrence of a resonance at a certain frequency can only be used as an indicator of internal stress if the frequency of resonance in a normally stressed wheel is known.

In principle a wayside stress measuring system could be developed by cataloguing the acoustic signatures of all the extant wheel types (about 40) under conditions of normal stress and then comparing the given wheel signature with this catalog. It would not be possible to use across the axle comparison since the likelihood is that mating wheels would have very similar conditions of internal stress. One difficulty with the wheel recognition scheme is the problem of recognizing the wheel type. This might be done by reading the wheel ID lettering or by identifying the acoustic signature. Another difficulty is that the acoustic signature is affected by wear, grease, load, etc. Thus the comparison signature of the wheel type after identification would need to be corrected according to these wheel conditions. While these difficulties appear to be almost insurmountable at present for a wayside system a program of research might be started with the aim of developing a machine shop system.

Another method that could be envisaged for shop use involves a determination of the slope of the $\Delta f - \Delta \sigma$ curve by applying a stress. If an additional load is applied to a wheel, by means of a hydraulic jack for instance, then a given resonance line will shift by different amounts in frequency, depending on its initial internal stress, and the slope of the curve at the point represented by this condition. If the curve indeed exhibits a change in slope from negative to positive for certain resonances as in

Fig. 4.3.10 then the resonance line will shift to higher values for highly stressed wheels or lower values for normally stressed wheels. The effect of frequency shift for flexural vibration with circular modal lines may be different from frequency shifts for vibration with modal diameters. If this were found to be the case the absolute stress field might be inferred again by an incremental loading.

In order to elucidate these questions the following research tasks are suggested:

a) Development of Research Instrumentation to Measure Internal Stress

In order to establish the effect of internal stress on acoustic signatures in various wheel types and under various conditions it will be necessary to select and procure or develop instrumentation to make absolute stress measurements. The ultrasonic method is favored for this purpose because it yields bulk values. It will also be necessary to secure equipment for accurate tread profile measurements.

b) Collection of Data

Data on residual stress, as measured by the ultrasonic method, together with acoustic signatures needs to be collected for a variety of wheels and for various vibrational modes. New wheels as well as wheels in service need to be evaluated. Accurate wear profiles need to be measured.

c) Establishment of $\Delta f/\sigma$ Curves

Further work needs to be done to establish the nature of the $\Delta f/\sigma$ curves. It will be necessary to secure a

frequency translator in order to accomplish this. The first order of business should be to process the remaining tape recordings from the Wilmerding tests. The apparent lack of correlation with some strain gauge readings on the rim needs to be explained. It is desirable to establish the repeatability of these curves and to correlate frequencies with absolute stress. Further dynamometer tests will be necessary although some information may be forthcoming from the data collection of task b.

d) Theoretical Prediction of Frequency Shifts

If the changes in resonant frequency are indeed due to changes in internal stress it should be possible to simulate the changes using one of the standard finite element programs. NASTRAN, for example, permits such stress distributions to be imposed. Not only would a correct prediction of natural frequency shifts enhance confidence but the study could also be of enormous value in predicting $\Delta f/\sigma$ curves because of the difficulties envisaged in collecting data.

e) Demonstration System for Residual Stress Measurement

After the tasks outlined above have been performed it should be possible to assemble a laboratory demonstration system. This should be evaluated by comparing residual stress measured by ASI with values obtained from ultrasonic tests.

f) Theoretical Prediction of Crack Growth

While the work of Carter and Caton emphasizes many important aspects of fracture in wheels, it evidently

does not treat fatigue crack growth except in an elementary manner. Even though the results reported there provide some idea of crack sizes which ought to result in a wheel being taken out of service, they do not establish any basis for estimating the number of cycles to failure for a crack of subcritical size. It is proposed that this problem could be tackled on a theoretical basis, using recent developments in fracture mechanics. There are two possible avenues of approach. One way would be to use a finite element technique, modelling the crack tip with a plastic element and having a moving network of grid points. The other way would be to use an analytical approach using path invariant integral. It is not clear at present which method would be the most satisfactory. The output of such a study would be predictions of crack growth paths and crack growth rates under various conditions of cyclic load and stress.

g) Experimental Study of Crack Growth

Some further experimental studies of crack initiation, due to braking, cyclic loading, etc. would serve to complement and confirm task f. It is possible that such a study would best be carried out on model wheels, with accelerated cycling techniques. The detailed mechanism of crack initiation needs further study.

REFERENCES

1. Nagy, K., "Feasibility Study of Flaw Detection in Railway wheels Using Acoustic Signatures," Ph.D. Thesis, University of Houston, August 1974. See also: Report No. FRA/OR & D 76-290, National Technical Information Service, Springfield, Virginia 22161.
2. Nagy, K., Dousis, D. A., Finch, R. D., "Detection of Flaws in Railway Wheels Using Acoustic Signatures," ASME paper No. 77-WA/RT-1, 1977.
3. Bray, D. E. and Finch, R. D., "Flaw Detection in Model Railway Wheels," Report No. FRA-RT-71-75, National Technical Information Service, Springfield, Virginia 22161, PB-199-956, February 1971. See also: Bray, D. E., Dalvi, N. G. and Finch, R. D., Ultrasonics II, 1973, 66-72.
4. Dousis, D., "Acoustic Signature Processing for Railroad Wheel Flat Spot Detection," M.S. Thesis, University of Houston, December 1975.
5. Bray, P. E., "Pulse Excitation of Railway Wheels," M.S. Thesis, M-2165, University Microfilms, Ann Arbor, Michigan, 48106 111 pp. 1969.
6. Leissa, A. W., "Vibration of Plates," NASA SP-160, 1969.
7. Leissa, A. W., "Vibration of Wheels," NASA SP-288, 1973.
8. Soni, S. R., Amba-Rao, C. L., "Axisymmetric Vibrations of Annular Plates of Variable Thickness," J. Sound Vibr., 38 (4), 465-473, 1975.
9. Banerjee, M. M., "On the Non-linear Vibrations of Elastic Circular Plates of Variable Thickness," J. Sound Vibr. 47 (3), 341-346, 1976.
10. Appl, F. C., Byers, J. R., "Fundamental Frequency of Simply Supported Rectangular Plates with Linearly Varying Thickness," J. Appl. Mech., 32, 163-168 (65).
11. Eastep, F. E., "Estimation of the Fundamental Frequency of Beams and Plates with Varying Thickness," AIAA, 14 (11) 1647-1649, 1976.

12. Sakata, T., "Approximate Formulas for Natural Frequencies of Rectangular Plates with Linearly Varying Thickness," J. Acoust. Soc. Am., 61 (4), 982-985, 1977.
13. Soni, S. R., Sankara-Rao, K., "Vibrations of Non-uniform Rectangular Plates: A Spline Technique Method of Solution," J. Sound Vibr., 35 (1), 35-45, 1974.
14. Mote, C. D., Szymani, R., "Circular Saw Vibration Research," The Shock Vibr. Dig., 10 (6), 15-26, 1978.
15. Harris, C. M., Crede, C. E., Shock and Vibration Handbook, McGraw-Hill Book Co., New York, 1976.
16. Beranek, L. L., Noise and Vibration Control, McGraw-Hill Book Co., New York, 1971.
17. Stappenbeck, Von H., "Das Kurvengeräusch Der Strassenbahn," Z VDI, Bd. 96, Nr. 6, 21 February 1954. (Re: Noise made by streetcar as it takes a curve)
18. Bray, D. E., "Report on the 5th International Wheelset Congress," Report No. FRA/ORD-77/65, January 1978.
19. Wetenkamp, H. R., and Kipp, R. M., "Thermal Damage in a 33-inch Railroad Car Wheel," J. Eng. Ind., 100, 363-369, August 1978.
20. Biot, M. A., "The Influence of Initial Stress on Elastic Waves," J. Appl. Phys., 11 (8) 522-530, 1940.
21. Biot, M. A., "Mechanics of Incremental Deformations," John Wiley & Sons, New York, 1965.
22. Libai, A., Rosen, A., "Transverse Vibrations of Compressed Annular Plates," J. Sound Vibr. 40 (1), 149-153, 1975.
23. Brunell, E. J., Robertson, S. R., "Vibration of an Initially Stressed Thick Plate," J. Sound Vibr. 45 (3), 405-416, 1976.
24. Nogfeh, A. H., Kamat, P. M., "Numerical-Perturbation Technique for the Transverse Vibrations of Highly Prestressed Plates," J. Acoust. Soc. Am., 61 (1), 95-100, 1977.

25. Chehil, D. S., Dua, S. S., "Buckling of Rectangular Plates with General Variation in Thickness," J. Appl. Mech., 40 (3) 745-751, 1973.
26. Dickinson, S. M., "Modified Bolotin's Method Applied to Buckling and Vibration of Stressed Plates," AIAA, 13 (12), 1672-1673, 1975.
27. Dickinson, S. M., "The Flexural Vibration of Rectangular Orthotropic Plates Subject to In-Plane Forces," J. Appl. Mech., 38, 699-700 (1971).
28. Nieh, L. T., Mote, C. D., "Vibration Stability in Thermally Stressed Rotating Disks," Exper. Mech., 15 (7) 258-264, 1975.
29. Aggarwal, R. R., Biswas, R. N., "Flexural Vibration of a Circular Plate," Acustica, 33, 238-242, (1975).
30. Carter, C. S., Caton, R. G., Fracture Resistance of Railroad Wheels, DOT, Interim Report, No. FRA-OR & D-75-12, September 1974.
31. Wandrisco, J. M., Dewey, F. J., "Service Defects in Treads of Railroad Wheels During Service," ASME Paper 60-RR-1, 1960.
32. Cullity, B. D., Elements of X-Ray Diffraction, Addison-Wesley, third edition, New York, 1967.
33. Hirooka, T., et al., "Residual Stresses in the Rim of a Railroad Solid Wheel Due to on Tread Drag Braking and Their Effect on Wheel Failure," Proc. Fourth International Wheelset Congress, Paris, 1972, p. 91.
34. King, et al., "Stress Measurement in Railroad Wheels Via the Barkhausen Effect," Final Report, Office of R & D FRA/DOT, December 1974. Contract No. DOT-TSC-713, SWRI, Prof. No. 15-3486.
35. Spectral Dynamics Corporation, Instruction Manual for SD330A Spectrascope Real Time Analyzer, San Diego, California, May 1974.
36. Association of American Railroads, Manual of Standards and Recommended Practices, AAR Issue of 1976, pp. G-174-1973/G-178-1973.
37. Car and Locomotive Cyclopedia, Centennial Edition, (1974 by Simmons-Boardmen Publishing, New York).

38. Clotfelter, W. N. and Risch, E. R., "Ultrasonic Measurement of Stress in Railroad Wheels and in Long Lengths of Welded Rails," NASA TM X-64863, July 1974.
39. Osgood, W. R., Residual Stresses in Metals and Metal Construction Reinhold Publishing Corp., New York, 1954.
40. Treuting, R. G., Residual Stress Measurements, American Society for Metals, Cleveland, Ohio, 1952.
41. Fazekas, G. A., "On Bidirectional Snapping Linkages," J. Eng. Ind., November 1976, 1363-1366,
42. Hetenyi, M., Handbook of Experimental Stress Analysis, J. Wiley, New York, 1950.
43. Smith, R. T., "Stress-Induced Anisotropy in Solids - The Acoustoelastic Effect," Ultrasonics, July-September 1963.
44. Toupin, R. A., Bernstein, B., "Sound Waves in Deformed Perfectly Elastic Materials, Acoustoelastic Effect," J. Acoust. Soc. Am., 33, 216-225, 1961.
45. Beauchamp, K. G., Signal Processing Using Analog and Digital Techniques, Halsted Press, J. Wiley, New York, 1973.
46. Box, G., and Jenkins, G., Time Series Analysis Forecasting and Control, Holden Day, San Francisco, 1976.
47. Blackman, R. B., Tukey, J. W., The Measurement of Power Spectra, Dover Publications, Inc., New York, 1958.
48. Kapur, K. C., Lamberson, L. R., Reliability in Engineering Design, J. Wiley, New York, 1977.
49. Burton, R., Vibration and Impact, Addison Wesley, Reading, Massachusetts, 1958, pp. 248-250.

50. Timoshenko, S., Young, D. H., Weaver, W., Vibration Problems in Engineering, Fourth Edition, John Wiley & Sons, 1974, pp. 453-455.
51. Carter, C. S., Caton, R. G., Guthrie, J. L., "Fracture Resistance and Fatigue Crack Growth Characteristics of Railroad Wheels and Axles," DOT, Final Report, No. FRA/ORD-77/50, November 1977.
52. Michell, J. H., Messenger of Math., Vol. 19 (1890).
53. Yanelak, J. J., Scott, C. N., "Requirements of Residual Stress Measurements Peculiar to the Railway-Freight Industry," Extended Summaries of the Technical Papers Presented at the 1978 SESA (Society of Experimental Stress Analysis) Fall Meeting, pp. 17-18.

APPENDIX A

LIST OF WHEELS ON INVENTORY
AT UNIVERSITY OF HOUSTON

<u>Axle Number</u>	<u>Wheel Size</u>	<u>Good Wheel Description</u>	<u>Bad Wheel Description</u>	<u>Manufacturer</u>
1	33"	No defect, light rusting	Thermal crack to axle	Southern
2	33"	No defect, light rusting	Overheated rim	Griffin
3	33"	No defect, heavy coat of dirt and grease on outside of plate	Large crack running circumferentially in rim fillet, heavy coat of dirt and grease on outside of plate	Southern
4	33"	No defect, light rusting	Large plate crack	ARMCO
5	36"	No defect, light rusting	Thermal crack partially extending into plate	Standard
6	36"	No defect, light rusting	Thermal cracks on outside of tread, extending into rim only	Griffin
7	33"	New wheel	New wheel	Southern
8	33"	No defect	Rim fillet crack	Griffin
9	33"	No defect	Crack on rim face	Bethlehem
10	33"	No defect	No defect	Griffin
11	33"	No defect	No defect	Southern
12	36"	12A-large flat spot (6.5 inch)	12C-large flat spot	Bethlehem
13	33"	13A-small flat spot	13C-small flat spot	Griffin
14	33"	14A-small flat spot	14C-small flat spot	Griffin
15	33"	Partial plate crack	Large plate crack	

APPENDIX B

EQUIPMENT LIST USED IN THE ENGLEWOOD YARD TESTS

1. SD330A REAL TIME ANALYZER
2. NOVA 1220 MINI-COMPUTER
3. DATA GENERAL DISKETTE SYSTEM
4. DATA GENERAL FAST PAPER TAPE READER
5. (2) BAND-PASS FILTERS
6. TRIGGERING-PULSE CIRCUIT
7. DC POWER SUPPLY FOR ITEM NO. 6
8. HP AMPLIFIER
9. GR TAPE RECORDER
10. (2) GR MICROPHONES
11. (1) OSCILLOSCOPE
12. (10) DISKETTES FOR ITEM NO. 3
13. CABLES
14. (2) MECHANICAL EXCITERS
15. SPARE PARTS FOR ITEM NO. 14
16. HAND TOOLS
17. (2) ACI WHEEL DETECTORS
18. (2) WALKY-TALKY'S

APPENDIX C
SOFTWARE FOR COMPUTER INTERFACING
AND DATA PROCESSING

APPENDIX C.1
PIN ASSIGNMENT

In general loading narrowband spectra into a digital computer can be done in two ways. First, using the FRAME-SYNC and WORD-SYNC. pulses to trigger separate computer interrupt lines. These interrupts cause the computer to abandon its current processing task and jump to an interrupt routine, and service the device which is requesting the interrupt (in this case the SD330A). The computer then returns to normal processing. Second, if it is required to load spectra only at certain defined times, the FRAME-SYNC. and WORD-SYNC. lines can be connected as data lines to the computer data register. In this case spectra would be loaded under program control by testing the individual bits in the data word which correspond to the FRAME-SYNC. and WORD-SYNC. lines. Under the present interfacing scheme the WORD-SYNC. line is connected to the External Interrupt pin and the FRAME-SYNC. to a DATA in pin (see Table C.1.1).

TABLE C.1.1 COMPUTER-ANALYZER INTERFACING

PIN ASSIGNMENT

REAL TIME ANALYZER SD330A			COMPUTER NOVA 1220	
SIGNAL NAME	PIN		PIN	SIGNAL NAME
DATA LINES (LSB) (OUTPUT)	J-17	28	22	DATA IN 15
	J-17	27	20	DATA IN 14
	J-17	26	4	DATA IN 13
	J-17	25	19	DATA IN 12
	J-17	24	5	DATA IN 11
	J-17	23	6	DATA IN 10
	J-17	22	8	DATA IN 9
	J-17	21	7	DATA IN 8
	J-17	19	9	DATA IN 7
	J-17	18	10	DATA IN 6
(MSB)				
WORD SYNC. (OUTPUT)	J-17	29	46	DIO. EXT. INT.
SWEEP FRAME SYNC. (OUTPUT)	J-17	31	11	DATA IN 4
SWEEP (OUTPUT)	J-17	16	13	DATA IN 3
GROUND	J-17	34	1	GROUND
EXT. START (INPUT)	J-18	1	21	DATA OUT 1
EXT. PEAK HOLD (INPUT)	J-18	3	24	DATA OUT 3
EXT. STOP (INPUT)	J-18	4	27	DATA OUT 4
EXT. TR. PULSE (TAPE RECORDER)		→	16	DATA IN 1
EXT. RESET (INPUT)	J-18	5	25	DATA OUT 5
EXT. SWEEP (INPUT)	J-18	6	3	DATA OUT 6
EXT. EXP. AVG.	J-18	2	23	DATA OUT 0

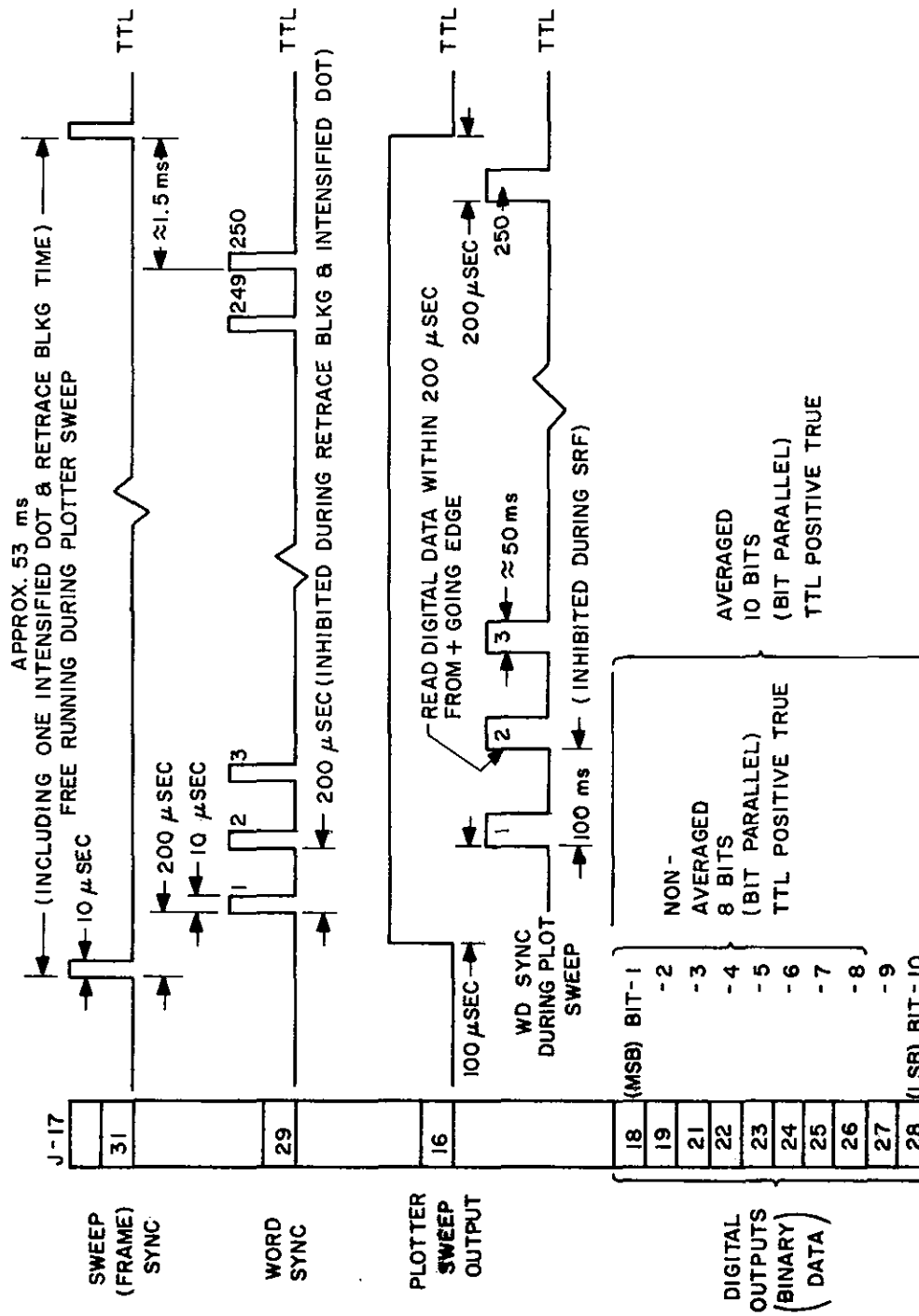


FIGURE C.1.1.2 SD 330A DIGITAL OUTPUT TIMING

APPENDIX C.2

LIST OF THE ASSEMBLER SOFTWARE USED FOR DIGITAL CONTROL OF THE
REAL TIME ANALYZER AND DATA TRANSFER TO THE COMPUTER/DISKETTE


```

0001 .MAIN
01 ; -----
02 ; TAPE A-140-XII-N
03 ; 14 SEPT. 1977
04 ;
05 ; DECK STBN.01
06 ;
07 ; -----
08 ; THIS TAPE CONTAINS THE FOLLOWING ASSEMBLY S/R
09 ; #1 START :START SAMPLING
10 ; #2 STOP :STOP AND STORE
11 ; #3 PEAK :GET PEAK SPECTRUM
12 ; #4 RESET :RESET CURSOR OR PLOTTER
13 ; #5 SWEEP :START SWEEPING
14 ; #6 CLKST :START THE CLOCK--CL.FR. 60HZ
15 ; #7 CLOCK :READ THE CLOCK
16 ; #8(10) SFRAME :SENSE THE SWEEP FRAME PULSE (53MSEC)
17 ; #9(11) SPEC :READ THE VALUE OF A CHANNEL
18 ; #10(12) RSTCL :RESET CLOCK
19 ; #11(13) EXTRG :EXTERNAL TRIGGERING
20 ; #12(14) SP250 :READ-IN SP. IN 53MSEC
21 ; USING INTERRUPT
22 ; #13(15) PNTER :RESET INPUT-OUTPUT POINTER
23 ; #14(16) OUT :READ-OUT SPECTRUM
24 ; #16(20) SPNMR :SPECTRUM NUMBER (INPUT-OUTPUT)
25 ; #17(21) EXPANV :EXPONENTIAL AVERAGING
26 ; #18(22) PLSP :PLOTTER SWEEP OUTPUT
27 ; #19(23) OPEN :OPEN DISK FOR R/W
28 ; #20(24) WRITE :WRITE ON DISK
29 ; #21(25) READ :READ FROM DISK
30 ; #22(26) CLOSE :CLOSE A R/W CALL
31 ; #23(27) CDISK :CLEAR I/O TABLES
32 ; #24(30) FLTA :CHANGE TO FLOAT AN INT. ARRAY
33 ;
34 ; -----
35
36 033000 .LOC 33000
37
38 33000 034470 SBRTB: CKINT
39 33001 000001 1
40 33002 033107 START
41 000004 .RDX 4
42 33003 100000 20000000
43
44 33004 000002 2
45 33005 033117 STOP
46 33006 140000 30000000
47
48 33007 000003 3
49 33010 033137 PEAK
50 33011 100000 20000000
51
52 33012 000004 4.
53 33013 033147 RESET
54 33014 140000 30000000
55
56 33015 000005 5.
57 33016 033157 SWEEP
3 33017 100000 20000000
)

```

0002	.MAIN	
01	33020 000006	6.
02	33021 033175	CLKST
03	33022 100000	20000000
04		
05	33023 000007	7.
06	33024 033206	CLOCK
07	33025 140000	30000000
08		
09	33026 000010	8.
10	33027 033276	SFRAME
11	33030 100000	20000000
12		
13	33031 000011	9.
14	33032 033304	SPEC
15	33033 140000	30000000
16		
17	33034 000012	10.
18	33035 033222	RSTCL
19	33036 100000	20000000
20		
21	33037 000013	11.
22	33040 033261	EXTRG
23	33041 100000	20000000
24		
25	33042 000014	12.
26	33043 033352	SP250
27	33044 170000	33000000
28		
29	33045 000015	13.
30	33046 033417	PNTER
31	33047 140000	30000000
32		
33	33050 000016	14.
34	33051 033424	OUT
35	33052 140000	30000000
36		
37	33053 000020	16.
38	33054 033437	SPNMR
39	33055 100000	20000000
40		
41	33056 000021	17.
42	33057 033127	EXPAV
43	33060 100000	20000000
44		
45	33061 000022	18.
46	33062 033267	PLSP
47	33063 140000	30000000
48		
49	33064 000023	19.
50	33065 033501	OPEN
51	33066 125260	22222300
52		
53	33067 000024	20.
54	33070 033610	WRITE
55	33071 136000	23300000
56		
57	33072 000025	21.
	3073 034015	READ
	3074 136000	23300000

0003 .MAIN

```

01
02 33075 000026      22.
03 33076 034137      CLOSE
04 33077 136000      23300000
05
06 33100 000027      23.
07 33101 034212      CDISK
08 33102 100000      20000000
09
10 33103 000030      24.
11 33104 034251      FLTA
12 33105 174000      33200000
13
14      000010      .RDX 8 ;RESTORE RADIX TO OCTAL
15
16 33106 177777      -1
17
19 33107 054544 START: STA      3,S1      ;CALL 1,<DUMMY CHARACTER>
20 33110 030535      LDA      2,MASK1
21 33111 071042      DOA      2,42
22 33112 004455      JSR      DELAY
23 33113 030506      LDA      2,ZERO
24 33114 071042      DOA      2,42
25 33115 034536      LDA      3,S1
26 33116 001401      JMP      1,3      ;RETURN
27
28 33117 054534 STOP:  STA      3,S1      ;CALL 2,<DUMMY CHAR.>
29 33120 030530      LDA      2,MASK4
30 33121 071042      DOA      2,42
31 33122 004445      JSR      DELAY
32 33123 030476      LDA      2,ZERO
33 33124 071042      DOA      2,42
34 33125 034526      LDA      3,S1
35 33126 001401      JMP      1,3      ;RETURN
36
37 33127 054524 EXPAV: STA      3,S1      ;CALL 17,<DUMMY CHAR.>
38 33130 030516      LDA      2,MASK2
39 33131 071042      DOA      2,42
40 33132 004435      JSR      DELAY
41 33133 030466      LDA      2,ZERO
42 33134 071042      DOA      2,42
43 33135 034516      LDA      3,S1
44 33136 001401      JMP      1,3      ;RETURN
45
46 33137 054514 PEAK:  STA      3,S1      ;CALL 3,<DUMMY CHAR.>
47 33140 030507      LDA      2,MASK3
48 33141 071042      DOA      2,42
49 33142 004425      JSR      DELAY
50 33143 030456      LDA      2,ZERO
51 33144 071042      DOA      2,42
52 33145 034506      LDA      3,S1
53 33146 001401      JMP      1,3      ;RETURN
54
55 33147 054504 RESET: STA      3,S1      ;CALL 4,<DUMMY CHAR.>
56 33150 030501      LDA      2,MASK5
57 33151 071042      DOA      2,42
58 33152 004415      JSR      DELAY
59 33153 030446      LDA      2,ZERO
0 33154 071042      DOA      2,42

```

```

0004 .MAIN
01 33155 034476 LDA 3,S1
02 33156 001401 JMP 1,3 ; RETURN
03
04 33157 054474 SWEEP: STA 3,S1 ; CALL 5,<DUMMY CHAR.>
05 33160 030472 LDA 2,MASK6
06 33161 071042 DOA 2,42
07 33162 004405 JSR DELAY
08 33163 030436 LDA 2,ZERO
09 33164 071042 DOA 2,42
10 33165 034466 LDA 3,S1
11 33166 001401 JMP 1,3 ; RETURN
12
13 33167 054471 DELAY: STA 3,SAVE
14 33170 020465 LDA 0,NUM
15 33171 040463 STA 0,CNT0
16 33172 014462 DSZ CNT0
17 33173 000777 JMP .-1
18 33174 002464 JMP 0 SAVE
19
20 33175 054456 CLKST: STA 3,S1 ; CALL 6,<INPUT/CLOCK FREQU.>
21 33176 031400 LDA 2,0,3 ; A. IF INPUT 0 THEN 60HZ
22 33177 021000 LDA 0,0,2 ; B. IF INPUT 1 THEN 10HZ
23 33200 025001 LDA 1,1,2 ; C. IF INPUT 2 THEN 100HZ
24 33201 006130 JSR 0.FIX ; D. IF INPUT 3 THEN 1000HZ
25 33202 044442 STA 1,INTVL ; WARNING: AVOID C OR D
26 33203 065114 DOAS 1,RTC
27 33204 034447 LDA 3,S1
28 33205 001401 JMP 1,3 ; RETURN
29
30 33206 054445 CLOCK: STA 3,S1 ; CALL 7,<OUTPUT/CLOCK READING>
31 33207 060277 INTDS
32 33210 020433 LDA 0,CLK02
33 33211 024431 LDA 1,CLK01
34 33212 006132 JSR 0.FLOT
35 33213 034440 LDA 3,S1
36 33214 031400 LDA 2,0,3
37 33215 041000 STA 0,0,2
38 33216 045001 STA 1,1,2
39 33217 060177 INTEN
40 33220 001401 JMP 1,3 ; RETURN
41
42 33221 000000 ZERO: 0
43
44 33222 054431 RSTCL: STA 3,S1 ; CALL 10,<DUMMY CHAR.>
45 33223 020776 LDA 0,ZERO ; RESET CLOCK TO ZERO
46 33224 040417 STA 0,CLK02
47 33225 040415 STA 0,CLK01
48 33226 034425 LDA 3,S1
49 33227 001401 JMP 1,3 ; RETURN
50
51 33230 000000 0
52 33231 020413 SRTC: LDA 0,INTVL
53 33232 061114 DOAS 0,RTC
54 33233 010407 ISZ CLK01
55 33234 002404 JMP 0E.RET
56 33235 010406 ISZ CLK02
57 33236 101000 MOV 0,0
58 33237 002401 JMP 0E.RET
3240 034447 E.RET: RET

```

```

0005 .MAIN
01 33241 000400 CMASK:000400
02 33242 000000 CLK01: 0
03 33243 000000 CLK02: 0
04 33244 000000 INTVL: 0
05 33245 040000 MASK1:040000
06 33246 100000 MASK2:100000
07 33247 010000 MASK3:010000
08 33250 004000 MASK4:004000
09 33251 002000 MASK5:002000
10 33252 001000 MASK6:001000
11 33253 000000 S1:0
12 33254 000000 CNT0:0
13 33255 000002 NUM:2
14 33256 000042 FTW0:42
15 33257 000000 TEL0S:0
16 33260 000000 SAVE:0
17      000130 .FIX=130
18
19
20 33261 054772 EXTRG: STA 3,S1 ;CALL 11,<DUMMY CHAR.>
21 33262 020453 LDA 0,NUM1
22 33263 064442 DIA 1,42
23 33264 107404 AND 0,1,SZR
24 33265 000776 JMP -2 ;WAIT FOR TRIG. PULSE
25 33266 001401 JMP 1,3 ;RETURN
26
27 33267 054764 PLSP: STA 3,S1 ;CALL 18,<D. CHAR.>
28 33270 020447 LDA 0,NUM3
29 33271 064442 DIA 1,42
30 33272 107404 AND 0,1,SZR
31 33273 000776 JMP -2 ;WAIT WHEN PL. OUTPUT IS HIGH
32 33274 034757 LDA 3,S1
33 33275 001401 JMP 1,3 ;RETURN
34
35 33276 054755 SFRAME: STA 3,S1 ;CALL 8,<DUMMY CHAR.>
36 33277 020441 LDA 0,NUM4
37 33300 064442 DIA 1,42
38 33301 107405 AND 0,1,SNR
39 33302 000776 JMP -2 ;WAIT FOR SWEEP FRAME P.
40 33303 001401 JMP 1,3 ;RETURN
41
42 33304 054747 SPEC: STA 3,S1 ;CALL 9,<OUTPUT/ READ VALUE
43 33305 020431 LDA 0,NUM2 ; OF EACH CHANNEL,SLOW MODE>
44 33306 064442 DIA 1,42
45 33307 107405 AND 0,1,SNR
46 33310 000776 JMP -2
47 33311 004403 JSR WAIT
48 33312 004410 JSR READ0
49 33313 001401 JMP 1,3 ;RETURN
50
51 33314 054432 WAIT: STA 3,SAV6
52 33315 020421 LDA 0,NUM2
53 33316 064442 DIA 1,42
54 33317 107404 AND 0,1,SZR
55 33320 000776 JMP -2
56 33321 002425 JMP 0 SAV6
57
-- 13322 054417 READ0: STA 3,SAV1
13323 020426 LDA 0,MASK

```

```

0006 .MAIN
01 33324 064442      DIA      1,42
02 33325 107400      AND      0,1
03 33326 102400      SUB      0,0
04 33327 006132      JSR      0,FL0T
05 33330 034413      LDA      3,SAV3
06 33331 031400      LDA      2,0,3
07 33332 041000      STA      0,0,2
08 33333 045001      STA      1,1,2
09 33334 002405      JMP      0 SAV1
10
11 33335 040000 NUM1:040000
12 33336 020000 NUM2:020000
13 33337 010000 NUM3:010000
14 33340 004000 NUM4:004000
15 33341 000000 SAV1:0
16 33342 000000 SAV2:0
17 33343 000000 SAV3:0
18 33344 000000 SAV4:0
19 33345 000000 SAV5:0
20 33346 000000 SAV6:0
21 33347 000007 CN7:7
22 33350 033603 S.PAR: .PAR
23 33351 001777 MASK:001777
24
25 33352 054514 SP250: STA      3,SAV25
26 33353 060277      INTDS
27 33354 021401      LDA      0,1,3
28 33355 040516      STA      0,LINPT
29 33356 020762 SWFR: LDA      0,NUM4
30 33357 064442      DIA      1,42
31 33360 107405      AND      0,1,SNR
32 33361 000776      JMP      .-2
33 33362 020515      LDA      0,NUM25
34 33363 040512      STA      0,CNT1
35 33364 000401 WSYNC: JMP      .+1
36 33365 060142      NIOS      42
37 33366 020752      LDA      0,NUM4
38 33367 064442      DIA      1,42
39 33370 107404      AND      0,1,SZR
40 33371 000414      JMP      EXODO
41 33372 063642      SKPDN      42
42 33373 000774      JMP      .-4
43 33374 060242      NIOC      42
44 33375 030476      LDA      2,LINPT
45 33376 020753      LDA      0,MASK
46 33377 064442      DIA      1,42
47 33400 107400      AND      0,1
48 33401 045000      STA      1,0,2
49 33402 010471      ISZ      LINPT
50 33403 014472      DSZ      CNT1
51 33404 000760      JMP      WSYNC
52 33405 000401 EXODO: JMP      .+1
53 33406 024467      LDA      1,CNT1
54 33407 102400      SUB      0,0
55 33410 006132      JSR      0,FL0T
56 33411 034455      LDA      3,SAV25
57 33412 031400      LDA      2,0,3
--- 33413 041000      STA      0,0,2
    33414 045001      STA      1,1,2

```

```

0007  .MAIN
01 33415 060177 EX1:  INTEN
02 33416 001402      JMP      2,3
03
04 33417 054445 PNTER: STA      3,SAV12
05 33420 021400      LDA      0,0,3
06 33421 040452      STA      0,LINPT
07 33422 040440      STA      0,LOUT
08 33423 001401      JMP      1,3      ; RETURN
09
10 33424 054441 OUT:   STA      3,SAV13
11 33425 030435      LDA      2, LOUT
12 33426 010434      ISZ      LOUT
13 33427 025000      LDA      1,0,2
14 33430 102400      SUB      0,0
15 33431 006132      JSR      @.FLOT
16 33432 034433      LDA      3,SAV13
17 33433 031400      LDA      2,0,3
18 33434 041000      STA      0,0,2
19 33435 045001      STA      1,1,2
20 33436 001401      JMP      1,3      ; RETURN
21
22 33437 054430 SPNMR: STA      3,SAV31
23 33440 035400      LDA      3,0,3
24 33441 021400      LDA      0,0,3
25 33442 025401      LDA      1,1,3
26 33443 006130      JSR      @.FIX
27 33444 044430      STA      1,NSP
28 33445 014427      DSZ      NSP
29 33446 000402      JMP      .+2
30 33447 000411      JMP      EX0
31 33450 020427 LSNP:  LDA      0,NUM25
32 33451 040424      STA      0,CNT1
33 33452 010421      ISZ      LINPT
34 33453 010407      ISZ      LOUT
35 33454 014421      DSZ      CNT1
36 33455 000775      JMP      .-3
37 33456 014416      DSZ      NSP
38 33457 000771      JMP      LSNP
39 33460 034407 EX0:   LDA      3,SAV31
40 33461 001401      JMP      1,3      ; RETURN
41
42 33462 000000 LOUT:  0
43 33463 000000 ZER1:  0
44 33464 000000 SAV12: 0
45 33465 000000 SAV13: 0
46 33466 000000 SAV25: 0
47 33467 000000 SAV31: 0
48 33470 000400 B7:    000400
49 33471 000001 ONE:    1
50 33472 034000 L34:    34000
51 33473 000000 LINPT:  0
52 33474 000000 NSP:     0
53 33475 000000 CNT1:   0
54 33476 000000 SAVN:    0
55 33477 000373 NUM25: 251.
57      ;*****
58      ;
59      ; DECK SKIPS.SR
60      ;

```

```
0008 .MAIN
01      102033 .DALC SLT =      ADCZ#      0,0,SNC
02      102433 .DALC SLE =      SUBZ#      0,0,SNC
03      102032 .DALC SGE =      ADCZ#      0,0,SZC
04      102432 .DALC SGT =      SUBZ#      0,0,SZC
05      ;
06      ;      -----
```


† 0009 .MAIN

```

02 ;*****
03 ;
04 ;** DECK OPEN.01      16 APRIL 1977
05 ;
06 ;** CALL (OPEN),<CHANNEL>,<UNIT>,<FIRST SECTOR>
07 ;  ,<NUMBER SECTORS>,<RECORD SIZE>,<ERROR FLAG> **
08 ;
09 33500 000006          6
10 33501 171000 OPEN:    MOV      3,2
11 33502 006406          JSR      @0.PRE
12 33503 000406          JMP      OP1
13 33504 024402          LDA      1,ECAOP ; ALREADY OPEN
14 33505 002402          JMP      @0.ERT
15 ; -----
16 33506 000151 ECAOP:    105.      ; CODE FOR ALREADY OPEN
17 33507 033770 O.ERT:    CERTN
18 33510 033720 O.PRE:    CPREP
19 ; CONVERT 4 PARAMETERS UNIT THRU
20 ; RECORD SIZE TO INTEGER
21 33511 020416 OP1:      LDA      0,C4
22 33512 040416          STA      0,CNT
23 33513 020416          LDA      0,.OPP
24 33514 040416          STA      0,.OPX
25 33515 010466 OP2:      1SZ      .PAR
26 33516 036465          LDA      3,@.PAR
27 33517 021400          LDA      0,0,3
28 33520 025401          LDA      1,1,3
29 33521 006130          JSR      @.IFIX
30 33522 046410          STA      1,@.OPX
31 33523 010407          1SZ      .OPX
32 33524 014404          DSZ      CNT
33 33525 000770          JMP      OP2
34 33526 000412          JMP      OP3
35 ; -----
36 33527 000004 C4:      4
37 33530 000000 CNT:      0
38 33531 033533 .OPP:      OUNIT
39 33532 000000 .OPX:      0
40 33533 000000 OUNIT:      0
41 33534 000000 OFSEC:      0
42 33535 000000 ONSEC:      0
43 33536 000000 ORSZ:      0
44 33537 033761 O.CT:      .CT
45 ; -----
46 ; LOOK FOR UNIT
47 33540 032777 OP3:      LDA      2,@O.CT
48 33541 020772          LDA      0,OUNIT
49 33542 034411          LDA      3,0,UT0
50 33543 025402          LDA      1,UTUN,3; TABLE NUMBER
51 33544 106475          SUBC#     0,1,SNR ; OURS?
52 33545 000410          JMP      OP4      ; YES FOUND IT
53 33546 035400          LDA      3,0,3
54 33547 174014          COM#      3,3,SZR ; CHECK FOR MORE
55 33550 000773          JMP      .-5
56 33551 024403          LDA      1,ECNSU ; * NO SUCH UNIT *
57 33552 002735          JMP      @0.ERT
58 ; -----
59 33553 035226 O.UT0:    UT330
   33554 000152 ECNSU:    106.      ; CODE FOR NO SUCH UNIT

```

```

0010 .MAIN
01      ; -----
02 33555 055002 OP4:  STA      3,CT.UT,2;REMEMBER UNIT
03      ; TREAT OTHER PARS
04 33556 020756      LDA      0,0FSEC
05 33557 024756      LDA      1,0NSEC
06 33560 107000      ADD      0,1
07 33561 034421      LDA      3,D616
08 33562 101113      MOVL#    0,0,SNC
09 33563 136433      SLE      1,3
10 33564 002415      JMP      00.EOF ;EOF ERROR
11 33565 041003      STA      0,CTSST,2
12 33566 041005      STA      0,CTSEC,2
13 33567 045004      STA      1,CTSLM,2;POSITION FILE
14 33570 102460      SUBC     0,0
15 33571 041006      STA      0,CTCWD,2
16 33572 020744      LDA      0,0RSZ
17 33573 101120      MOVZL    0,0
18 33574 024553      LDA      1,C400
19 33575 106433      SLE      0,1
20 33576 000407      JMP      OP5
21 33577 041007      STA      0,CTRSZ,2
22 33600 000567      JMP      COKR ;OK RETURN
23      ; -----
24 33601 034002 0.EOF: CEEOF
25 33602 001150 D616:  616.
26 33603 000000 .PAR:   0
27 33604 000153 ECBRS: 107.
28 33605 024777 OP5:   LDA      1,ECBRS
29 33606 000562      JMP      CERTN

```

↑ 0011 .MAIN

```

02 ;*****
03 ;
04 ;** DECK WRITE.01 **
05 ;
06 ;** CALL (WRITE),<CHANNEL>,<DATA>,<ERROR FLAG> **
07 ;
08 ;
09 33607 000003      3      ;PAR'S  CHANN.,DATA,ERF
10 33610 171000 WRITE: MOV      3,2      ;LOC. RETURN
11 33611 004507      JSR      CPREP
12 33612 000566      JMP      CENOP      ; NOT OPEN
13 33613 035010      LDA      3,CT.BH,2;IS A BUFFER ASSIGNED?
14 33614 174014      COM#     3,3,SZR
15 33615 000426      JMP      WC      ;YES
16 33616 021005      LDA      0,CTSEC,2;NO
17 33617 025004      LDA      1,CTSLM,2;CHECK FOR EOF
18 33620 106033      SLT      0,1
19 33621 000561      JMP      CEEOF
20 ;      FIND A FREE BUFFER
21 33622 034472      LDA      3,W.BH0
22 33623 021406 W1:    LDA      0,BHNU,3;THIS BUFFER IN USE?
23 33624 101014      MOV#     0,0,SZR
24 33625 000404      JMP      W3
25 33626 021405      LDA      0,BHQL,3
26 33627 101015      MOV#     0,0,SNR ;ON AN IO QUEUE?
27 33630 000405      JMP      W2      ;NO
28 33631 035400 W3:    LDA      3,BHCL,3
29 33632 174014      COM#     3,3,SZR
30 33633 000770      JMP      W1
31 33634 000550      JMP      CENBA      ;NO BUFFER
32 ;      -----
33 33635 011406 W2:    ISZ      BHNU,3
34 33636 055010      STA      3,CT.BH,2
35 33637 021002      LDA      0,CT.UT,2
36 33640 041403      STA      0,BH.UT,3
37 33641 021005      LDA      0,CTSEC,2
38 33642 041404      STA      0,BHSEC,3
39 ;      COPY DATA INTO BUFFER
40 33643 035401 WC:    LDA      3,BH.BF,3
41 33644 021006      LDA      0,CTCWD,2
42 33645 117000      ADD      0,3      ;NEXT BUFFER WORD LOC.
43 33646 025007      LDA      1,CTRSZ,2;NUMBER OF WORDS IN RECORD
44 33647 123000      ADD      1,0
45 33650 041006      STA      0,CTCWD,2
46 33651 030732      LDA      2,.PAR
47 33652 031001      LDA      2,1,2      ;LOC. OF DATA
48 33653 124400      NEG      1,1
49 33654 021000 WCL:   LDA      0,0,2
50 33655 041400      STA      0,0,3
51 33656 151400      INC      2,2      ;THE COPY LOOP
52 33657 175400      INC      3,3
53 33660 125404      INC      1,1,SZR
54 33661 000773      JMP      .-5
55 33662 030477      LDA      2,.CT
56 33663 035010      LDA      3,CT.BH,2
57 33664 011402      ISZ      BHMOD,3
58 ;      CHECK FOR BUFFER FULL
59 33665 021006      LDA      0,CTCWD,2
60 33666 025007      LDA      1,CTRSZ,2

```

```

0012 .MAIN
01 33667 123000      ADD      1,0
02 33670 024457      LDA      1,C400 ;IS THERE ROOM FOR ANOTHER RECOB
03 33671 106432      SGT      0,1
04 33672 000475      JMP      COKR   ;YES. SO JUST RETURN
05                      ;          ;NO. SO ENQUE FOR WRITING
06 33673 031010      LDA      2,CT.BH,2
07 33674 035003      LDA      3,BH.UT,2
08 33675 020420      LDA      0,W.UQH
09 33676 024420      LDA      1,W.BQL ;ENQUEUE BUFFER ON UNIT QUEUE
10 33677 163000      ADD      3,0
11 33700 147000      ADD      2,1
12 33701 006416      JSR      0W.CAL
13 33702 034321      ENQUE
14 33703 015006      DSZ      BHNU,2 ;DECREMENT USE COUNT
15 33704 000401      JMP      .+1
16 33705 030454      LDA      2,.CT
17 33706 102000      ADC      0,0 ;CLEAR THE BUFFER
18 33707 041010      STA      0,CT.BH,2; ASSIGNMENT
19 33710 102460      SUBC     0,0 ;
20 33711 041006      STA      0,CTCWD,2
21 33712 011005      ISZ      CTSEC,2
22 33713 000454      JMP      COKR   ;RETURN
23                      ;
24 33714 035270 W.BH0: BH0
25 33715 000005 W.UQH: UTQH
26 33716 000005 W.BQL: BHQL
27 33717 034403 W.CAL: CAL
28                      ;
29                      ;*****
30                      ;
31                      ;
32                      ;** DECK CPREP.01 **
33                      ;
34                      ;**CPREP -- SUPPORT FOR CHANNEL IO CALLS **
35                      ;
36                      ;  USAGE:
37                      ;      NP      ;NUMBER OF PARAMETERS
38                      ;<ENTRY>:MOV  3,2      SAVE RETURN FROM NEXT JSR
39                      ;      JSR      CPREP
40                      ;
41 33720 050663 CPREP: STA      2,.PAR
42 33721 021775      LDA      0,-3,3
43 33722 143000      ADD      2,0
44 33723 040427      STA      0,.RTEN
45 33724 054427      STA      3,CTMP
46                      ;      SET UP STACK
47 33725 020432      LDA      0,C.STK
48 33726 042426      STA      0,@C.TP
49 33727 042427      STA      0,@C.FP
50 33730 020430      LDA      0,C.STL
51 33731 042424      STA      0,@C.LP
52 33732 035000      LDA      3,0,2
53 33733 021400      LDA      0,0,3
54 33734 025401      LDA      1,1,3
55 33735 006130      JSR      0.IFIX
56                      ;      LOCATE CHANNEL TABLE
7 33736 030412      LDA      2,C.CT0
8 33737 021001      LDA      0,CTNB,2
140 106415      SUB#      0,1,SNR ;OURS?
141 000421      JMP      CP4      ;YES

```

```

0013 .MAIN
01 33742 031000 LDA 2,CTCL,2;NO
02 33743 150014 COM# 2,2,SZR;05 THERE ANOTHER
03 33744 000773 JMP --5;YES
04 33745 024404 LDA 1,ECNSC; NO SUCH CHANNEL
05 33746 000422 JMP CERTN;TO ERROR RETURN
06 ; -----
07 33747 000400 C400: 400
08 33750 035331 C.CT0: CT0
09 33751 000144 ECNSC: 100. ;CODE FOR NO SUCH CHANNEL
10 33752 000000 .RTEN: 0
11 33753 000000 CTMP: 0
12 33754 034443 C.TP: TP
13 33755 034444 C.LP: LP
14 33756 034442 C.FP: FP
15 33757 036755 C.STK: BUF+1400
16 33760 037206 C.STL: BUF+1640-LH
17 33761 000000 .CT: 0
18 ; -----
19 ; CHECK FOR OPEN
20 33762 050777 CP4: STA 2,.CT
21 33763 021002 LDA 0,CT.UT,2;THE OPEN FLAG
22 33764 100014 COM# 0,0,SZR
23 33765 010766 ISZ CTMP
24 33766 002765 JMP 0CTMP
25 ; -----
26 33767 126460 COKR: SUBC 1,1;OK RETURN
27 33770 102460 CERTN: SUBC 0,0
28 33771 006132 JSR 0.FLOT
29 33772 034760 LDA 3,.RTEN
30 33773 035777 LDA 3,-1,3;LOC OF <ERROR FLAG>
31 33774 041400 STA 0,0,3
32 33775 000401 JMP .+1; **DEG. **
33 33776 045401 STA 1,1,3
34 33777 002753 JMP 0.RTEN
35 ; -----
36 ; SPECIAL ERROR RETURNS
37 34000 024410 CENOP: LDA 1,ECNOP;NOT OPEN
38 34001 000767 JMP CERTN
39 34002 024407 CEEOF: LDA 1,ECEOF;END OF FILE
40 34003 000765 JMP CERTN
41 34004 024406 CENBA: LDA 1,ECNBA;NO BUF AVAIL.
42 34005 000763 JMP CERTN
43 34006 024405 CETMO: LDA 1,ECTMO;TIME OUT
44 34007 000761 JMP CERTN
45 ; -----
46 34010 000145 ECNOP: 101.
47 34011 000146 ECEOF: 102.
48 34012 000147 ECNBA: 103.
49 34013 000150 ECTMO: 104.
50 000130 .IFIX=130
51 000132 .FLOT=132
52 ; -----
53 ;*****
54 ;
55 ;
56 ;DECK READ.01 28 APR 77.
57 ;
58 ;** CALL (READ),<CHANNEL>,<DATA>,<ERROR FLAG> **
;
34014 000003 3 ;PAR'S -- CHANN,DATA,ERF

```

```

0014 .MAIN
01 34015 171000 READ:  MOV      3,2
02 34016 004702      JSR      CPREP
03 34017 000761      JMP      CENOP  ;*NOT OPEN*
04 34020 035010      LDA      3,CT.BH,2
05 34021 174014      COM#     3,3,SZR ;(JUST LIKE WRITE)
06 34022 000455      JMP      R5
07 34023 021005      LDA      0,CTSEC,2
08 34024 025004      LDA      1,CTSML,2
09 34025 106033      SLT      0,1
10 34026 000754      JMP      CEEOF  ;EOF ERROR
11      ;      FIND A FREE BUFFER
12 34027 034665      LDA      3,W.BH0
13 34030 021406 R1:   LDA      0,BHNU,3
14 34031 101014      MOV#     0,0,SZR
15 34032 000404      JMP      R3
16 34033 021405      LDA      0,BHQL,3
17 34034 101015      MOV#     0,0,SNR
18 34035 000405      JMP      R2
19 34036 035400 R3:   LDA      3,BHCL,3
20 34037 174014      COM#     3,3,SZR
21 34040 000770      JMP      R1
22 34041 000743      JMP      CENBA  ;*NO BUFFER AVAILABLE*
23      ;      -----
24 34042 011406 R2:   ISZ      BHNU,3
25 34043 055010      STA      3,CT.BH,2
26 34044 021002      LDA      0,CT.UT,2
27 34045 041403      STA      0,BH.UT,3
28 34046 021005      LDA      0,CTSEC,2
29 34047 041404      STA      0,BHSEC,3
30      ;      ENQUE FOR READING
31 34050 102460      SUBC     0,0
32 34051 041402      STA      0,BHMOD,3;CLEAR WRITE FLAG
33 34052 031403      LDA      2,BH.UT,3
34 34053 020642      LDA      0,W.UQH
35 34054 024642      LDA      1,W.BQL
36 34055 143000      ADD      2,0      ; ENQUE FOR READING
37 34056 167000      ADD      3,1
38 34057 006640      JSR      @W.CAL
39 34060 034321      ENQUE
40      ;      WAIT TILL READ
41 34061 030700      LDA      2,.CT
42 34062 035010      LDA      3,CT.BH,2
43 34063 030412      LDA      2,RWAIT
44 34064 126460 R4:   SUBC     1,1
45 34065 021405      LDA      0,BHQL,3
46 34066 101015      MOV#     0,0,SNR
47 34067 000407      JMP      R5A
48 34070 125404      INC      1,1,SZR
49 34071 000774      JMP      .-4
50 34072 151404      INC      2,2,SZR
51 34073 000771      JMP      R4
52 34074 000712      JMP      CETMO  ;* TIME OUT *
53      ;      -----
54 34075 177773 RWAIT: -5
55      ;      -----
56      ;      COPY DATA OUT OF BUFFER
57 34076 030663 R5A:   LDA      2,.CT
    34077 035401 R5:   LDA      3,BH.BF,3
    34100 021006      LDA      0,CTCWD,2

```

```

0015 .MAIN
01 34101 117000 ADD 0,3 ;NEXT BUFFER WORD LOC.
02 34102 025007 LDA 1,CTRSZ,2;NUMBER OF WORDS
03 34103 123000 ADD 1,0
04 34104 041006 STA 0,CTCWD,2
05 34105 032501 LDA 2,@C.PAR
06 34106 031001 LDA 2,1,2 ;LOC. DATA
07 34107 124400 NEG 1,1
08 34110 021400 RCL: LDA 0,0,3
09 34111 041000 STA 0,0,2
10 34112 175400 INC 3,3
11 34113 151400 INC 2,2
12 34114 125404 INC 1,1,SZR
13 34115 000773 JMP .-5
14 ; CHECK FOR BUFFER EMPTY
15 34116 030643 LDA 2,.CT
16 34117 021006 LDA 0,CTCWD,2
17 34120 025007 LDA 1,CTRSZ,2;INCREMENT NEXT POINTER
18 34121 123000 ADD 1,0
19 34122 024625 LDA 1,C400 ;IS BUFFER OUT?
20 34123 106432 SGT 0,1
21 34124 000643 JMP COKR ;OK RETURN
22 ; REMOVE BUFFER
23 34125 011005 ISZ CTSEC,2
24 34126 102460 SUBC 0,0
25 34127 041006 STA 0,CTCWD,2
26 34130 035010 LDA 3,CT.BH,2
27 34131 015406 DSZ BHNU,3
28 34132 000401 JMP .+1
29 34133 102000 ADC 0,0
30 34134 041010 STA 0,CT.BH,2
31 34135 000632 JMP COKR
32 ; -----
33 ;*****
34 ;
35 ;
36 ; DECK CLOSE.01
37 ;
38 ;** CALL (CLOSE),<CHANNEL>,<NEXT SECTOR>,<ERROR FLAG> **
39 ;
40 34136 000003 3
41 34137 171000 CLOSE: MOV 3,2
42 34140 006451 JSR @C.PRP
43 34141 000637 JMP CENOP ;*NOT OPEN*
44 ; RETURN THAT SECTOR NUMBER
45 34142 025005 LDA 1,CTSEC,2
46 34143 021006 LDA 0,CTCWD,2
47 34144 101004 MOV 0,0,SZR
48 34145 125400 INC 1,1
49 34146 102460 SUBC 0,0
50 34147 006132 JSR @.FLOT
51 34150 032436 LDA 2,@C.PAR
52 34151 031001 LDA 2,1,2
53 34152 041000 STA 0,0,2
54 34153 045001 STA 1,1,2
55 34154 032433 LDA 2,@C.CT
56 ; IF A BUFFER IS IN USE,CK FOR WRITE REQUIRED
57 34155 035010 LDA 3,CT.BH,2
58 34156 174015 COM# 3,3,SNR
4157 000421 JMP CL4 ;NO BUFFER
4160 021402 LDA 0,BHMOD,3;YES BUF.

```

```

0016 .MAIN
01 34161 101015      MOV#    0,0,SNR ;WRITE REQ.?
02 34162 000410      JMP      CL3      ;NO
03 34163 031403      LDA      2,BH.UT,3;YES
04 34164 020421      LDA      0,C.UQH
05 34165 024417      LDA      1,C.BQL
06 34166 143000      ADD      2,0
07 34167 167000      ADD      3,1
08 34170 006413      JSR      0C.CAL
09 34171 034321      ENQUE
10 34172 032415      CL3:      LDA      2,0C.CT
11 34173 035010      LDA      3,CT.BH,2
12 34174 015406      DSZ      BHNU,3
13 34175 000401      JMP      .+1
14 34176 102000      ADC      0,0
15 34177 041010      STA      0,CT.BH,2
16
17                  CL4:
18                  ;          CLOSE CHANNEL
18 34200 102000      ADC      0,0
19 34201 041002      STA      0,CT.UT,2
20 34202 002406      JMP      0C.OKR
21
22                  ;          -----
22 34203 034403      C.CAL:    CAL
23 34204 000005      C.BQL:    BQL
24 34205 000005      C.UQH:    UQH
25 34206 033603      C.PAR:    .PAR
26 34207 033761      C.CT:     .CT
27 34210 033767      C.OKR:    COKR
28 34211 033720      C.PRP:    CPREP
29
30                  ;          -----
31
32                  ;*****
33
34                  ; CALL <(23) CLR DISK>
35
36                  ; FOR RESETTNG ALL I/O TABLES
37
37 34212 060277      CDISK:    INTDS
38 34213 060233      NIOC      DP0
39 34214 102400      SUB      0,0
40 34215 126000      ADC      1,1
41 34216 030427      LDA      2,L.DT
42 34217 045005      STA      1,DTQH,2
43 34220 030426      LDA      2,L.UT
44 34221 041010      STA      0,UTQL,2
45 34222 045005      STA      1,UTQH,2
46 34223 031000      LDA      2,UTCL,2
47 34224 150014      COM#     2,2,SZR
48 34225 000774      JMP      .-4
49
50 34226 030421      LDA      2,L.BH
51 34227 041005      STA      0,BHQL,2
52 34230 041006      STA      0,BHNU,2
53 34231 045003      STA      1,BH.UT,2
54 34232 031000      LDA      2,BHCL,2
55 34233 150014      COM#     2,2,SZR
56 34234 000773      JMP      .-5
57
58 34235 030413      LDA      2,L.CT
59 34236 045002      STA      1,CT.UT,2
60 34237 045010      STA      1,CT.BH,2

```



```

0017 .MAIN
01 34240 031000 LDA 2,CTCL,2
02 34241 150014 COM# 2,2,SZR
03 34242 000774 JMP .-4
04
05 34243 060177 INTEN
06 34244 001401 JMP 1,3
07 ; -----
08 34245 035172 L.DT: DT33
09 34246 035226 L.UT: UT330
10 34247 035270 L.BH: BH0
11 34250 035331 L.CT: CT0
12 ; -----
† 0018 .MAIN
02 ;*****
03 ; DECK FLT.01
04 ;
05 ; CALL (NUMBER-24), <ARRAY1>,<ARRAY2>,<NO. OF DATA>
06 ;
07 34251 175400 FLTA: INC 3,3
08 34252 175400 INC 3,3
09 34253 175400 INC 3,3
10 34254 054441 STA 3,RTN1
11 34255 031777 LDA 2,-1,3
12 34256 021000 LDA 0,0,2
13 34257 025001 LDA 1,1,2
14 34260 006130 JSR 0,FX
15 34261 131000 MOV 1,2
16 34262 034433 LDA 3,RTN1
17 34263 021775 LDA 0,-3,3
18 34264 025776 LDA 1,-2,3
19 34265 004402 JSR FLX
20 34266 002427 JMP 0RTN1
21
22 34267 143000 FLX: ADD 2,0
23 34270 147000 ADD 2,1
24 34271 147000 ADD 2,1
25 34272 040421 STA 0,.A1
26 34273 044421 STA 1,.A2
27 34274 050423 STA 2,N3
28 34275 054421 STA 3,RTFX
29 34276 014415 LOOP: DSZ .A1
30 34277 026414 LDA 1,0.A1
31 34300 125113 MOVL# 1,1,SNC
32 34301 102461 SUBC 0,0,SKP
33 34302 102000 ADC 0,0
34 34303 006132 JSR 0,FL0T
35 34304 014410 DSZ .A2
36 34305 044407 STA 1,.A2
37 34306 014406 DSZ .A2
38 34307 040405 STA 0,.A2
39 34310 014407 DSZ N3
40 34311 000765 JMP LOOP
41 34312 002404 JMP 0RTFX
42
43 34313 000000 .A1: 0
44 34314 000000 .A2: 0
45 34315 000000 RTN1: 0
; 34316 000000 RTFX: 0
' 34317 000000 N3: 0

```

```

† 0019 .MAIN
02 ;*****
03 ;
04 ;DECK QUEUE.01 31 MARCH 77
05 ;
06 ;**ENQUEUE AND DEQUEUE SUBROUTINES **
07 ;
08 ;USAGE:
09 ; TO QUEUE UP AN ITEM.
10 ; JSR CAL ;WITH AC0=HEAD LOC.,AND
11 ; ENQUE ; AC1=LINK LOC.
12 ; TO DEQUEUE THE TOP ITEM
13 ; JSR CAL ;WITH AC0=HEAD LOC.
14 ; DEQUE
15 ;
16 000002 QFL = 2 ;LENGTH OF FRAME REQUIRED
17 000000 QIF = 0 ;DISPL. FOR INTERRUPT ENABLE FLAG.
18 000001 QSV = 1 ;FOR SERVER ADDRESS
19 ;
20 34320 000002 QFL ;REQUIRED FRAME SIZE (2 WORDS)
21 34321 063577 ENQUE: SKPBZ CPU ;INTERRUPT ENABLED?
22 34322 152461 SUBC 2,2,SKP ; 0 IF ON
23 34323 152001 ADC 2,2,SKP ;-1 IF OFF
24 34324 060277 INTDS
25 34325 051400 STA 2,QIF,3 ;REMEMBER ENTRY STATE
26 34326 111000 MOV 0,2 ;HEAD LOC.
27 34327 021000 LDA 0,0,2 ;TOP LINK
28 34330 100014 COM# 0,0,SZR ;IS IT THE END
29 34331 000775 JMP -3 ;NO, SO CHAIN TO NEXT
30 34332 043773 STA 0,0,AC1,3;YES. SET NEW ITEM'S LINK -1
31 34333 045000 STA 1,0,2 ;LINK NEW ITEM INTO CHAIN
32 34334 021772 LDA 0,AC0,3 ;HEAD LOC.
33 34335 112414 SUB# 0,2,SZR ;WAS IT THE FIRST ENTRY?
34 34336 000437 JMP QRT ;NO, SO RETURN
35 ; NOTE: AC2=HEAD AND AC1=LINK
36 34337 021001 QE2: LDA 0,1,2 ;YES. CALL SERVER BUT FIRST
37 34340 041401 STA 0,QSV,3 ; MOVE SERVER ADDRESS
38 34341 141000 MOV 2,0 ;AC0=HEAD AND AC1=LINK
39 34342 006436 JSR 0Q,CAL ;CALL SERVER
40 34343 000001 QSV
41 34344 101013 MOV# 0,0,SNC ;WAS THERE AN ERROR?
42 34345 000430 JMP QRT ;NO, SO RETURN
43 34346 000407 JMP QD2 ;YES, SO DEQUE
44 ; -----
45 ; DEQUEUE. AC0=HEAD
46 34347 000002 QFL
47 34350 063577 DEQUE: SKPBZ CPU
48 34351 152461 SUBC 2,2,SKP
49 34352 152001 ADC 2,2,SKP
50 34353 060277 INTDS
51 34354 051400 STA 2,QIF,3
52 34355 031772 QD2: LDA 2,AC0,3;AC2=HEAD LOC
53 34356 035000 LDA 3,0,2 ;AC3=TOP LINK
54 34357 025400 LDA 1,0,3 ;SECOND LINK
55 34360 045000 STA 1,0,2 ;MOVE IT TO TOP
56 34361 102460 SUBC 0,0 ;SET REMOVED LINK WORD TO 0.
57 34362 041400 STA 0,0,3
58 34363 034457 LDA 3,FP ;RECOVER FRAME POINTER
1364 124014 COM# 1,1,SZR ;IS THE NEW TOP EMPTY?
1365 000752 JMP QE2 ;NO AC2=HEAD AC1=LINK

```

```

0020 .MAIN
01 34366 021002 LDA 0,2,2 ;IDLER S/R LOC.
02 34367 100015 COM# 0,0,SNR ;IS THERE ONE?
03 34370 000405 JMP QRT
04 34371 041401 STA 0,QSV,3
05 34372 141000 MOV 2,0 ;LOC. HEAD
06 34373 006405 JSR @Q.CAL
07 34374 000001 QSV
08 34375 011400 QRT: ISZ QIF,3 ;TEST INTERRUPT ENABLE
09 34376 060177 INTEN
10 34377 006402 JSR @Q.RET ;RETURN
11 ; -----
12 34400 034403 Q.CAL: CAL
13 34401 034447 Q.RET: RET
14 34402 034442 Q.FP: FP
15 ; -----
17 ;*****
18 ;
19 ;DECK STACK.01 08 APR 77.
20 ;
21 ;** CALL,RETURN,AND STACK MECHANISM **
22 ;
23 ; A CALL SAVES THE CALLER'S REGISTERS AND ALLOCATES
24 ; A FRAME ON THE STACK FOR USE BY THE SUBROUTINE.
25 ; A RETURN RELEASES THE FRAME AND RETURNS
26 ; TO THE CALLER. A FRAME POINTER,FP,POINTS TO THE
27 ; BASE OF THE CURRENT FRAME, A TOP POINTER,TP,POINTS
28 ; TO THE NEXT AVAILABLE WORD IN THE FRAME, AND A
29 ; LIMIT POINTER,LP,IS THE HIGHEST VALUE ALLOWED FOR
30 ; FP AND SP. LP SHOULD BE 7 LESS THAN THE END OF THE
31 ; STACK. THE SBED (S/R ENTRY DESIGNATOR)
32 ; BELOW MAY BE EITHER THE ADDRESS OF THE
33 ; FIRST INSTRUCTION OF A S/R OR (IF BITS
34 ; 0 THRU 7 ARE 0) A DISPLACEMENT IN THE
35 ; CALLER'S FRAME WHICH CONTAINS THE ADDRESS OF
36 ; THE S/R. THE ENTRY INSTRUCTION OF EACH S/R MUST
37 ; BE PRECEDED BY THE NUMBER OF WORDS REQUIRED
38 ; IN THE STACK FRAME.
39 ;
40 ;
41 ;
42 ;
43 ; USAGE:
44 ; JSR CAL ;TO CALL A S/R
45 ; <SBED>
46 ; <RETURN>
47 ;
48 ; JSR RET :TO RETURN TO CALLER
49 ; DESIGNED BY J F HERBSTER, 23-27 MAR 77
50 ;
51 000007 LH = 7 ;LENGTH OF FRAME HEADER
52 177771 RTN = -LH ;DISPLACEMENT FOR RETURN ADDRESS
53 177772 AC0 = RTN+1
54 177773 AC1 = RTN+2
55 177774 AC2 = RTN+3
56 177775 OFP = RTN+4 ;FOR OLD FRAME POINTER
57 177776 SBE = RTN+5 ;FOR S/R ENTRY
58 177777 FSZ = RTN+6 ;FOR FRAME SIZE (FSZ=-1)
; BEGINNING OF CALL
34403 175400 CAL: INC 3,3 ;PREPARE RETURN ADDRESS

```

```

0021 .MAIN
01 34404 056437 STA 3,0TP ;AND SAVE
02 34405 034436 LDA 3,TP ;TOP OF STACK
03 34406 051403 STA 2,AC2+LH,3
04 34407 045402 STA 1,AC1+LH,3
05 34410 041401 STA 0,AC0+LH,3
06 34411 030434 LDA 2,.LH ;LENGTH OF HEADER
07 34412 157000 ADD 2,3 ;NEW FRAME POINTER
08 34413 024427 LDA 1,FP ;OLD FRAME POINTER
09 34414 045775 STA 1,0FP,3 ;SAVE IT
10 34415 054425 STA 3,FP
11 34416 031771 LDA 2,RTN,3 ;ADDRESS OF SBED PLUS 1.
12 34417 031377 LDA 2,-1,2 ;THE SBE DESIGNATOR
13 34420 020426 LDA 0,SBEDM ;MASK WITH BITS 0-7
14 34421 113414 AND# 0,2,SZR ;IS SBED THE ENTRY ADDRESS?
15 34422 000403 JMP .+3 ;YES
16 34423 133000 ADD 1,2 ;NO. ITS A DISPL. ON OFP
17 34424 031000 LDA 2,0,2 ;SO GET ADDRESS FROM OLD FRAME
18 34425 051776 STA 2,SBE,3 ;SAVE IN HEADER
19 34426 031377 LDA 2,-1,2 ;REQUIRED FRAME SIZE
20 34427 051777 STA 2,FSZ,3 ;SAVE
21 34430 173000 ADD 3,2 ;NEW TOP OF STACK
22 34431 020413 LDA 0,LP ;LIMIT FOR TP AND FP
23 34432 112432 SUBZ# 0,2,SZC ;IS LP.GT.TP?
24 34433 004431 JSR PANIC ;NO
25 34434 050407 STA 2,TP ;SET NEW POINTER
26 34435 021772 LDA 0,AC0,3
27 34436 025773 LDA 1,AC1,3 ;LOAD UP AND ENTER S/R
28 34437 031774 LDA 2,AC2,3
29 34440 003776 JMP 0SBE,3
30 ; -----
31 34441 000000 RTMP: 0
32 34442 000000 FP: 0
33 34443 000000 TP: 0
34 34444 000000 LP: 0
35 34445 000007 .LH: LH
36 34446 177400 SBEDM: 177400
37 ; -----
38 ;
39 ; THE BEGINNING OF THE RETURN
40 34447 030773 RET: LDA 2,FP
41 34450 021371 LDA 0,RTN,2
42 34451 040770 STA 0,RTMP
43 34452 020773 LDA 0,.LH ;PREPARE OLD TOP POINTER
44 34453 112460 SUBC 0,2
45 34454 050767 STA 2,TP ;SET TP
46 34455 035004 LDA 3,0FP+LH,2;RESTORE OLD FRAME POINT.
47 34456 054764 STA 3,FP
48 34457 021001 LDA 0,AC0+LH,2
49 34460 025002 LDA 1,AC1+LH,2;RESTORE REGISTERS AND
50 34461 031003 LDA 2,AC2+LH,2; RETURN TO CALLER
51 34462 000401 JMP .+1 ;****DEBUG POINT****
52 34463 002756 JMP 0RTMP
53 ; -----
54 34464 063077 PANIC: HALT
5 34465 000777 JMP .-1
6 ; -----

```

```

† 0022 .MAIN
02 ; *****
03 ;
04 ; DECK ISTEAL.01          APRIL 1977
05 ;
06 ; ** INTERRUPT STEALER, SAVE, AND RESTORE **
07 ;
08 ; THE FOLLOWING IS AN INTERRUPT PREPROCESSER
09 ; WHICH WILL PICK OUT OUR OWN INTERRUPTS
10 ; AND PASS THE OTHERS TO THE REGULAR
11 ; PROCESSER.
12 ;
13 ;
14 ; TO ADD DEVICE CODES SEE THE EXAMPLE BELOW
15 ;
16 ; -----
17 34466 000530 I.REG: 530
18 34467 035172 I.DT:  DT33
19 ; -----
20 34470 040466 CKINT: STA 0,SV+0
21 34471 044466 STA 1,SV+1
22 34472 050466 STA 2,SV+2
23 34473 000401 CK2:  JMP .+1
24 34474 061477 INTA 0
25 34475 030772 LDA 2,I.DT
26 34476 025001 LDA 1,DTDC,2
27 34477 106475 SUBC# 0,1,SNR
28 34500 000412 JMP ISAVE
29 34501 031000 LDA 2,DTCL,2
30 34502 150014 COM# 2,2,SZR
31 34503 000773 JMP .-5
32 34504 020452 LDA 0,SV+0
33 34505 024452 LDA 1,SV+1
34 34506 030452 LDA 2,SV+2
35 34507 002757 JMP @I.REG
36 ; -----
37 34510 035172 I.D33: DT33
38 34511 000400 CMSK:400
39 ; -----
40 ; COMMON SAVE STATE PROCESSER
41 34512 054447 ISAVE: STA 3,SV+3
42 34513 102560 SUBCL 0,0
43 34514 040446 STA 0,SV+4
44 34515 020725 LDA 0,FP
45 34516 040445 STA 0,SV+5
46 34517 020724 LDA 0,TP
47 34520 040444 STA 0,SV+6
48 34521 020723 LDA 0,LP
49 34522 040443 STA 0,SV+7
50 34523 020716 LDA 0,RTMP
51 34524 040442 STA 0,SV+10
52 34525 034445 LDA 3,IFP ; SET UP STACK FOR INTERRUPT
53 34526 054714 STA 3,FP ; PROCESSING
54 34527 054714 STA 3,TP
55 34530 020443 LDA 0,ILP
56 34531 040713 STA 0,LP
57 34532 021003 LDA 0,DT.IS,2
58 34533 010710 ISZ TP ; PUT OUR SERVER'S ADDRESS
34534 041400 STA 0,0,3 ; ON THE STACK AND CALL IT
34535 004646 JSR CAL

```

```

0023 .MAIN
01 34536 000000      0
02 34537 020427 DI SM: LDA      0,SV+10
03 34540 040701      STA      0,RTMP
04 34541 020424      LDA      0,SV+7 ; RESTORE STACK
05 34542 040702      STA      0,LP
06 34543 020421      LDA      0,SV+6
07 34544 040677      STA      0,TP
08 34545 020416      LDA      0,SV+5
09 34546 040674      STA      0,FP
10 34547 020413      LDA      0,SV+4
11 34550 101200      MOVR     0,0 ; RESTORE REGISTERS
12 34551 034410      LDA      3,SV+3
13 34552 030406      LDA      2,SV+2
14 34553 024404      LDA      1,SV+1
15 34554 020402      LDA      0,SV+0
16 34555 002711      JMP      0I.REG ; AND RETURN
17 ; -----
18 34556 000000 SV:    0
19 34557 000000      0
20 34560 000000      0
21 34561 000000      0
22 34562 000000      0
23 34563 000000      0
24 34564 000000      0
25 34565 000000      0
26 34566 000000      0
27 34567 000000      0
28 34570 000000      0
29 34571 000000      0
30 34572 037215 IFP:   BUF+1640
31 34573 037346 ILP:   BUF+2000-LH
32 ; -----

```

† 0024 .MAIN

```

02 ;*****
03 ;
04 ;** DECK SEEK.01 **
05 ;
06 ;** SEEK AND RECALL INITIATION **
07 ;
08 34574 000001 1
09 34575 030444 ISEEK: LDA 2,S.UQH ;NEG. OF Q HEAD DISPL. IN UT
10 34576 113000 ADD 0,2 ;LOC. UT
11 34577 034443 LDA 3,S.BQL ;NEG OF Q LINK DISPL. IN BH.
12 34600 137000 ADD 1,3
13 34601 055011 STA 3,UT.BH,2
14 34602 020447 LDA 0,NTRY ;NUMBER OF TRIES ALLOWED
15 34603 041016 STA 0,UTTTG,2 ;TRIES TO GO
16 34604 025404 LDA 1,BHSEC,3
17 34605 020443 LDA 0,D7
18 34606 123400 AND 1,0
19 34607 125220 MOVZ R 1,1
20 34610 125220 MOVZ R 1,1
21 34611 125220 MOVZ R 1,1
22 34612 045013 STA 1,UTRCY,2;REQUESTED CYLINDER
23 34613 035015 LDA 3,UTNCY,2;NUMBER OF CYL. ON DISK
24 34614 136033 ADCZ# 1,3,SNC ;SKIP IF RCY LESS THAN NCY
25 34615 000437 JMP SERC ;**NO. OF CYL. TOO LARGE**
26 34616 103120 ADDZL 0,0
27 34617 103120 ADDZL 0,0
28 34620 035003 LDA 3,UTUNI,2
29 34621 163000 ADD 3,0
30 34622 041012 STA 0,UTSSC,2
31 34623 006415 JSR 0S.USL ;SELECT UNIT
32 34624 000426 JMP SERT ;TIME OUT ERROR RETURN
33 34625 000402 JMP RSEEK
34 ; -----
35 34626 000001 1
36 34627 021013 RSEEK: LDA 0,UTRCY,2
37 34630 024414 LDA 1,SKCMD
38 34631 123000 ADD 1,0
39 34632 025014 LDA 1,UTCCY,2
40 34633 124015 COM# 1,1,SNR
41 34634 020411 LDA 0,RCCMD
42 34635 061333 DOAP 0,DP0 ;START THE SEEK AND RECAL.
43 34636 101020 MOVZ 0,0
44 34637 006404 JSR 0S.RET
45 ; -----
46 34640 035142 S.USL: USEL
47 34641 177773 S.UQH: -UTQH
48 34642 177773 S.BQL: -BHQL
49 34643 034447 S.RET: RET
50 34644 001000 SKCMD: 1000
51 34645 001400 RCCMD: 1400
52 34646 000001 ERCY: 1
53 34647 000002 ERT0: 2
54 34650 000007 D7: 7
55 34651 000012 NTRY: 10.
56 ; -----
57 34652 024775 SERT: LDA 1,ERT0 ;TIME OUT ERROR
58 34653 000402 JMP .+2
34654 024772 SERC: LDA 1,ERCY ;CYL. NO. ERROR
34655 035011 LDA 3,UT.BH,2

```

```

0025 .MAIN
01 34656 041410 STA 0,BHEC0,3;RETURN ERROR DATA
02 34657 045411 STA 1,BHEC1,3
03 34660 101040 MOVO 0,0 ;SET ERROR FLAG
04 34661 002762 JMP 0S.RET ;RETURN
05 ;
07 ;*****
08 ;
09 ; DECK DMA.01
10 ;
11 ; ** READ AND WRITE QUEUE SERVER **
12 ;
13 ;
14 34662 000000 0 ;FRAME SIZE
15 34663 030433 IDMA: LDA 2,I.DQH ;NEG. OF Q HEAD DISPL. IN DT.
16 34664 113000 ADD 0,2 ;LOC. DT.
17 34665 034432 LDA 3,I.UQL ;NEG. OF Q LINK DISPL. IN UT.
18 34666 137000 ADD 1,3 ;LOC. UT.
19 34667 055011 STA 3,DT.UT,2;REMEMBER WHICH UNIT IN DT
20 34670 021412 LDA 0,UTSSC,3
21 34671 041014 STA 0,DTSSC,2
22 34672 021413 LDA 0,UTRCY,3;REQUESTED CYLINDER
23 34673 035411 LDA 3,UT.BH,3;BUFFER HEAD
24 34674 055012 STA 3,DT.BH,2
25 34675 025401 LDA 1,BH.BF,3;BUFFER ADDRESS
26 34676 045013 STA 1,DT.BF,2
27 34677 035402 LDA 3,BHMOD,3
28 34700 055016 STA 3,DTMOD,2
29 34701 126460 SUBC 1,1
30 34702 175014 MOV# 3,3,SZR
31 34703 125700 INCS 1,1
32 34704 123000 ADD 1,0
33 34705 041015 STA 0,DTCCW,2
34 34706 061033 ID2: DOA 0,DP0 ;SET COMMAND AND CYLINDER
35 34707 021013 LDA 0,DT.BF,2
36 34710 062133 DOBS 0,DP0
37 34711 101020 ID3: MOVZ 0,0
38 34712 002406 JMP 0I.RET
39 ;
40 ;
41 ; ENTRY FOR DMA RW RETRIES AC2=LOC DT
42 34713 000000 0
43 34714 021015 RDMA: LDA 0,DTCCW,2
44 34715 000771 JMP ID2
45 ;
46 34716 177773 I.DQH: -DTQH
47 34717 177770 I.UQL: -UTQL
48 34720 034447 I.RET: RET ;LOC RETURN ROUTINE
49 ;
50 ;
51 ; THIS S/R IS CALLED WHEN A RW QUEUE BECOMES EMPTY
52 ; AC0 = LOC. OF DT
53 34721 000000 0
54 34722 111000 SDMA: MOV 0,2
55 34723 021377 LDA 0,DTDNF-DTQH,2
56 34724 061233 DOAC 0,DP0
57 34725 000764 JMP ID3 ;RETURN
58 ;
-- ;*****
;

```



```

01      ; DECK DPIS.01          APRIL 1977
02      ;
03      ;** DISK INTERRUPT SERVER **
04      ;
05      ; THIS ROUTINES RECEIVES CONTROL ON DISK
06      ; INTERRUPTS WITH AC2=LOC. OF THE DEVICE
07      ; TABLE. SEE THE FLOW CHART FOR AN OVERALL
08      ; PICTURE OF ITS ACTIONS. THE EXIT MUST BE
09      ; TO LOC. DISM
10      ;
11      ;
12      ; DESIGNED DY JFH 1 APRIL 77
13      ;
14      0000000 SHOLD = 0
15 34726 000001      1
16 34727 060433 D33SV: DIA      0,DP0      ;GET STATUS DONE FLAG
17 34730 025004      LDA      1,DTDNF,2
18      1
19 34731 123415      AND#      1,0,SNR ;IS A READ OR WRITE DONE?
20 34732 000465      JMP      D3CKS      ;NO
21 34733 021014      LDA      0,DTSSC,2;YES. SO RESELECT AND GET STATE
22 34734 006535      JSR      0D.US
23 34735 000411      JMP      D3REC      ;SELECT FAILURE
24 34736 101213      MOVR#     0,0,SNR ;SEL. OK. CHECK RW STATUS
25 34737 000440      JMP      DOK        ;OK
26 34740 024532      LDA      1,DFEM ;NOT OK. CHECK RW STATUS
27 34741 123414      AND#      1,0,SZR
28 34742 000404      JMP      D3REC      ;ITS FATAL
29 34743 035011      LDA      3,DT.UT,2
30 34744 015416      DSZ      UTTTG,3
31 34745 000406      JMP      D3CSE
32 34746 035411 D3REC: LDA      3,UT.BH,3
33 34747 024524      LDA      1,DEC5 ;RETURN ERROR CODES
34 34750 041410      STA      0,BHEC0,3
35 34751 045411      STA      1,BHEC1,3
36 34752 000434      JMP      D3DQ      ;DEQUE RW.
37      ;
38 34753 024521 D3CSE: LDA      1,DSEF
39 34754 123414      AND#      1,0,SZR ;IS IT A SEEK ERROR
40 34755 000406      JMP      D3RSK
41 34756 006526      JSR      0D.CAL
42 34757 034714      RDMA
43 34760 101012      MOV#      0,0,SZC
44 34761 000425      JMP      D3DQ      ;YES,SO GIVE UP
45 34762 000435      JMP      D3CKS      ;NO ERROR
46      ;
47 34763 020512 D3RSK: LDA      0,D.DQH
48 34764 143000      ADD      2,0
49 34765 006517      JSR      0D.CAL
50 34766 034350      DEQUE
51 34767 031011      LDA      2,DT.UT,2
52 34770 102000      ADC      0,0 ;THEN INDICATE UNKNOWN CYLINDER
53 34771 041014      STA      0,UTCCY,2;AND START A RECALL
54 34772 006512      JSR      0D.CAL
55 34773 034627      RSEEK
56 34774 101012      MOV#      0,0,SZC
57 34775 000416      JMP      D3DQS
34776 000421      JMP      D3CKS
34777 021016 DOK:   LDA      0,DTMOD,2

```

```

0027 .MAIN
01 35000 101015      MOV#    0,0,SNR
02 35001 000405      JMP      .+5
03 35002 035012      LDA      3,DT,BH,2
04 35003 025402      LDA      1,BHMOD,3 ; THE BHMOD COUNTER GETS DECRE-
05 35004 106400      SUB      0,1      ; MENTED BY ITS VALUE BEFORE THE
06 35005 045402      STA      1,BHMOD,3 ; WRITE STARTED. NO CHG ON REAS
07 35006 020467 D3DQ: LDA      0,D,DQH
08 35007 143000      ADD      2,0
09 35010 006474      JSR      @D,CAL ; DEQUE THE READ-WRITE OP.
10 35011 034350      DEQUE
11 35012 031011      LDA      2,DT,UT,2
12 35013 020465 D3DQS: LDA      0,D,UQH
13 35014 143000      ADD      2,0
14 35015 006467      JSR      @D,CAL ; DEQUE THE UNIT
15 35016 034350      DEQUE
16                ; PROCESS SEEK AND RECAL DONES BELOW
17 D3CKS:
18 35017 060433      DIA      0,DP0 ; FETCH STATUS DONE FLAGS.
19 35020 024456      LDA      1,D3DM
20 35021 123405      AND      1,0,SNR ; SAVE ONLY UNIT FLAGS.
21 35022 006463      JSR      @D,RET
22 35023 031010      LDA      2,DTUCH,2
23 35024 000411      JMP      D3CKF
24                ; -----
25 35025 021400 D3LFM: LDA      0,SHOLD,3; CHECK FOR MORE WORK
26 35026 101015      MOV#    0,0,SNR
27 35027 002456      JMP      @D,RET
28 35030 031000 D3TNX: LDA      2,UTCL,2; NEXT UNIT TABLE
29 35031 150014      COM#    2,2,SZR ; IS THERE MORE?
30 35032 000403      JMP      .+3
31 35033 061033      DOA      0,DP0 ; CLEAR THE GHOSTS
32 35034 002451      JMP      @D,RET
33 35035 025004 D3CKF: LDA      1,UTDNF,2
34 35036 123415      AND#    1,0,SNR
35 35037 000771      JMP      D3TNX
36 35040 102400      SUB      1,0
37 35041 041400      STA      0,SHOLD,3
38 35042 065033      DOA      1,DP0
39 35043 021005      LDA      0,UTQH,2
40 35044 100015      COM#    0,0,SNR
41 35045 000760      JMP      D3LFM
42 35046 021012      LDA      0,UTSSC,2
43 35047 006422      JSR      @D,US ; SELECT AND GET STATUS
44 35050 000457      JMP      D3TOX
45 35051 024452      LDA      1,D3SER ; SEEK ERROR MASK
46 35052 123414      AND#    1,0,SZR
47 35053 000442      JMP      D3CFE
48 35054 021014      LDA      0,UTCCY,2; WAS IT A RECAL.
49 35055 100015      COM#    0,0,SNR ;
50 35056 000430      JMP      D3FRC ; YES
51 35057 021013      LDA      0,UTRCY,2; MOVE REQUESTED CYLINDER
52 35060 041014      STA      0,UTCCY,2; TO CURRENT CYLINDER
53 35061 020414      LDA      0,D,DQH
54 35062 024415      LDA      1,D3,UL ; ENQUEUE A READ OR WR.
55 35063 035001      LDA      3,UT,DT,2
56 35064 147000      ADD      2,1
57 35065 163000      ADD      3,0
-- 0066 006416      JSR      @D,CAL
0067 034321      ENQUE

```

```

0028 .MAIN
01 35070 000735 JMP D3LFM
02 ; -----
03 35071 035142 D.US: USEL
04 35072 000200 DFEM: 200 ; FATAL RW ERRORS
05 35073 000015 DEC5: 15 ; ERROR CODE
06 35074 000040 DSEF: 40 ; SEEK ERROR
07 35075 000005 D.DQH: DTQH
08 35076 074000 D3DM: 074000
09 35077 000010 D3.UL: UTQL
10 35100 000005 D.UQH: UTQH
11 35101 000022 D3TOE: 22
12 35102 000023 D3STE: 23
13 35103 000005 D3.UH: UTQH
14 35104 034403 D.CAL: CAL
15 35105 034447 D.RET: RET
16 ; -----
17 35106 102460 D3FRC: SUBC 0,0 ; A RECAL IS COMPLETE.
18 35107 041014 STA 0,UTCCY,2; SET CURRENT CYLINDER TO 0
19 35110 006774 JSR 0D.CAL
20 35111 034627 RSEEK ; SEEK REQUESTED CYLINDER
21 35112 101012 MOV# 0,0,SZC ; ERROR?
22 35113 000422 JMP D3SDQ ; YES
23 35114 000711 JMP D3LFM
24 ; -----
25 35115 024407 D3CFE: LDA 1,D3SFT ; ERROR, BUT WAS IT FATAL
26 35116 123414 AND# 1,0,SZR
27 35117 000412 JMP D3STX ; YES
28 35120 015016 DSZ UTTTG,2 ; NO. HAVE WE TRIED ENOUGH?
29 35121 000404 JMP D3IRC ; NO
30 35122 000407 JMP D3STX ; YES
31 ; -----
32 35123 000240 D3SER: 240 ; SEEK ERROR FLAGS
33 35124 000200 D3SFT: 200 ; SEEK FATAL ERROR FLAGS
34 ; -----
35 35125 102000 D3IRC: ADC 0,0 ; CHANGE TO RECALL REQUEST
36 35126 000761 JMP D3FRC+1 ; AND RESTART SEEK
37 ; -----
38 35127 024752 D3TOX: LDA 1,D3TOE ; TIME OUT ERROR CODE
39 35130 000402 JMP .+2
40 35131 024751 D3STX: LDA 1,D3STE ; STATUS ERROR CODE
41 35132 035011 LDA 3,UT.BH,2
42 35133 041410 STA 0,BHEC0,3; RETURN ERRORS
43 35134 045411 STA 1,BHEC1,3
44 35135 020746 D3SDQ: LDA 0,D3.UH ; DEQUE DISK UNIT
45 35136 143000 ADD 2,0
46 35137 006745 JSR 0D.CAL
47 35140 034350 DEQUE
48 35141 000664 JMP D3LFM ; LOOK FOR MORE WORK
49 ; -----
51 ; *****
52 ;
53 ; DECK UNSEL.01
54 ;
55 ; ** UNIT SELECT **
56 ;
57 35142 054426 USEL: STA 3,RLOC ; NOR REENTRANT
58 35143 115000 MOV 0,3 ; SELECT AND SECTOR COMMAND
59 35144 024423 LDA 1,USTT
60 35145 125405 US1: INC 1,1,SNR

```

```

0029 .MAIN
01 35146 000416      JMP      USER
02 35147 060433      DIA      0,DP0      ; READ STATUS
03 35150 101300      MOVVS     0,0
04 35151 103133      ADDZL#    0,0,SNC
05 35152 000773      JMP      US1
06                      ;
07 35153 077033      D0C      3,DP0      ; OUTPUT SELECT COMMAND
08                      ;
09 35154 024413      LDA      1,USTT
10 35155 125405 US2:   INC      1,1,SNR
11 35156 000406      JMP      USER
12 35157 060433      DIA      0,DP0
13 35160 101300      MOVVS     0,0
14 35161 103133      ADDZL#    0,0,SNC
15 35162 000773      JMP      US2
16 35163 010405      ISZ      RLOC
17 35164 101300 USER:  MOVVS     0,0
18 35165 036404      LDA      3,@U.FP
19 35166 002402      JMP      @RLOC
20                      ;      -----
21 35167 177266 USTT:  -330.
22 35170 000000 RLOC:  0
23 35171 034442 U.FP:  FP
24                      ;      -----
26                      ; *****
27                      ;   DECK   DDTBL.0
28                      ;
29                      ; ** DISKETTE DEVICE TABLE **
30                      ;   DISPLACEMENT DEFINITIONS:
31      000000 DTCL  = 0      ; DEVICE TBL LINK
32      000001 DTDC  = DTCL+1 ; DEVICE CODE
33      000002 DTMSK = DTDC+1 ; RESERVED
34      000003 DT.IS = DTMSK+1 ; ADDRESS OF INTERRUPT SERVER
35      000004 DTDNF = DT.IS+1 ; DMA DONE FLAG POSITION(100000)
36      000005 DTQH  = DTDNF+1 ; DMA QUEUE HEAD(INIT. TO -1)
37                      ; DTQH+1      ADDRESS OF QUEUE SERVER
38                      ; DTQH+2 ; ADDRESS OF QUEUE IDLER (OR -1, IF NONE)
39      000010 DTUCH = DTQH+3
40      000011 DT.UT = DTUCH+1 ; LOC. OF UT BEING SERVED
41      000012 DT.BH = DT.UT+1 ; LOC. OF BH BEING SERVED
42      000013 DT.BF = DT.BH+1 ; LOC. OF BUFFER BEING READ OR WRITTEN
43      000014 DTSSC = DT.BF+1 ; SELECT AND SECTOR COMMAND
44      000015 DTCCW = DTSSC+1 ; CYLINDER AND COMMAND WORD
45      000016 DTMOD = DTCCW+1 ; COPY OF BHMOD, JUST BEFORE READ OR WRITE
46                      ;      -----
47 35172 035212 DT33:  DT14
48 35173 000033      33
49 35174 000000      0
50 35175 034727      D33SV      ; DT.IS
51 35176 100000      100000    ; DTDNF
52 35177 177777      -1        ; DTQH
53 35200 034663      IDMA      ; SERVER
54 35201 034722      SDMA      ; IDLER
55 35202 035226      UT330     ; DTUCH
56 35203 000000      0         ; DT.UT
57 35204 000000      0         ; DT.BH
58 35205 000000      0         ; DT.BF
      206 000000      0         ; DTSSC
      207 000000      0         ; DTCCW

```

```

0030 .MAIN
01 35210 000000      0      ;DTMOD
02 35211 000000      0      ;SPARE
03      ;      -----
04 35212 035216 DT14:  DT42
05 35213 000014      14
06 35214 000000      0
07 35215 033231      SRTC
08
09 35216 177777 DT42:  -1
10 35217 000042      42
11 35220 000000      0
12 35221 035223      SV42
13
14 35222 000000      0
15 35223 060242 SV42:  NIOC      42
16 35224 002401      JMP      @D.RT
17
18 35225 034447 D.RT:  RET
19      000033 DP0 = 33
21      ;*****
22      ;
23      ;   DECK DUTBL.01
24      ;
25      ;** DISK UNIT TABLES **
26      ;
27      ; DISPLACEMENT DEFINITIONS:
28      000000 UTCL = 0      ;LINK TO OTHER DT'S(DON'T CHANGE)
29      000001 UT.DT = UTCL+1 ;MOTHER DEVICE TABLE
30      000002 UTUN = UT.DT+1 ;UNIT NUMBER
31      000003 UTUN1 = UTUN+1 ;UNIT NUMBER FOR SELECT & SECTOR
32      000004 UTDNF =UTUN1+1 ;POSITION OF DONE FLAG
33      000005 UTQH = UTDNF+1 ;UNIT'S QUEUE HEAD(FOR BHQL'S)
34      ;UTQH+1      ;QUEUE SERVER
35      ;UTQH+2      ;QUEUE IDLER (PROBABLY -1.)
36      000010 UTQL = UTQH+3 ;LINK FOR DMA. QUEUE
37      000011 UT.BH = UTQL+1 ;BUFFER HEADER BEING SERVED
38      000012 UTSSC = UT.BH+1 ;SELECT AND SECTOR COMMAND
39      000013 UTRCY = UTSSC+1 ;REQUIRED CYLINDER
40      000014 UTCCY = UTRCY+1 ;CURRENT CYLINDER (OR -1 IF UNKNOWN)
41      000015 UTNCY = UTCCY+1 ;NUMBER OF CYLINDERS ON DISK
42      000016 UTTTG = UTNCY+1 ;TRIES TO GO BEFORE GIVING UP
43      000017 UTTMP = UTTTG+1 ;TEMPORARY
44      ; UNIT 0 TABLE
45 35226 035247 UT330:  UT331 ;UTCL
46 35227 035172      DT33      ;UT.DT
47 35230 000000      0      ;UTUN
48 35231 000017      000017 ;UTUN1
49 35232 040000      040000 ;UTDNF
50 35233 177777      -1      ;UTQH
51 35234 034575      ISEEK      ;SERVER
52 35235 177777      -1      ;IDLER
53 35236 000000      0      ;UTQL
54 35237 000000      0      ;UT.BH
55 35240 000000      0      ;UTSSC
56 35241 000000      0      ;UTRCY
57 35242 177777      -1      ;UTCCY
58 35243 000115      77.      ;UTNCY
      35244 000000      0      ;UTTTG
      35245 000000      0      ;UTTMP

```

```

0031 .MAIN
01 35246 000000      0      ; SPARE
02      ; -----
03      ;
04      ; UNIT 1 TABLE
05 35247 177777 UT331: -1      ; UTCL
06 35250 035172      DT33      ; UT.DT
07 35251 000001      1      ; UTUN
08 35252 040017      040017    ; UTUN1
09 35253 020000      020000    ; UTENF
10 35254 177777      -1      ; UTQH
11 35255 034575      1 SEEK    ; SERVER
12 35256 177777      -1      ; IDLER
13 35257 000000      0      ; UTQL
14 35260 000000      0      ; UT.BH
15 35261 000000      0      ; UTSSC
16 35262 000000      0      ; UTRCY
17 35263 177777      -1      ; UTCCY
18 35264 000115      77.      ; UTNCY
19 35265 000000      0      ; UTTTG
20 35266 000000      0      ; UTTMP
21 35267 000000      0      ; SPARE
22      ; -----
24      ; *****
25      ;
26      ; DECK BHTBL.01
27      ;
28      ; ** BUFFER HEADER TABLES **
29      ;
30      ; DISPLACEMENT DEFINITIONS
31      000000 BHCL = 0      ; LINK TO OTHER BH'S (SHOULD BE ZERO)
32      000001 BH.BF = BHCL+1 ; LOC. BUFFER
33      000002 BHMOD = BH.BF+1 ; INCREMENTED EACH TIME BUFFER IS MODIFIED
34      000003 BH.UT = BHMOD+1 ; UNIT TABLE (OR -1)
35      000004 BHSEC = BH.UT+1 ; SECTOR CORRESPONDING TO BUFFER (OR -1)
36      000005 BHQL = BHSEC+1 ; UNIT QUEUE LINK
37      000006 BHNU = BHQL+1 ; NUMBER OF USERS
38      000007 BHLRU = BHNU+1 ; LEAST RECENTLY USED COUNTER
39      000010 BHEC0 = BHLRU+1 ; FOR RETURNED ERROR CODES
40      000011 BHEC1 = BHEC0+1 ;
41      ; -----
42      ;
43 35270 035303 BH0: BH1      ; BHCL
44 35271 035355      BUF      ; BH.BF
45 35272 000000      0      ; BHMOD
46 35273 177777      -1      ; BH.UT
47 35274 000000      0      ; BHSEC
48 35275 000000      0      ; BHQL
49 35276 000000      0      ; BHNU
50 35277 000000      0      ; BHLRU
51 35300 000000      0      ; BHEC0
52 35301 000000      0      ; BHEC1
53 35302 000000      0      ; SPARE
54      ; -----
55 35303 035316 BH1: BH2
56 35304 035755      BUF+400
57 35305 000000      0
58 35306 177777      -1
59 35307 000000      0
60 35310 000000      0

```

```

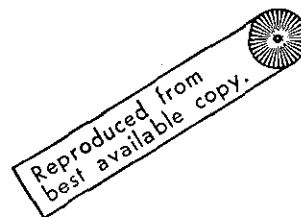
0032 .MAIN
01 35311 000000 0
02 35312 000000 0
03 35313 000000 0
04 35314 000000 0
05 35315 000000 0
06 ; -----
07 35316 177777 BH2: -1
08 35317 036355 BUF+1000
09 35320 000000 0
10 35321 177777 -1
11 35322 000000 0
12 35323 000000 0
13 35324 000000 0
14 35325 000000 0
15 35326 000000 0
16 35327 000000 0
17 35330 000000 0
18 ; -----
20 ;*****
21 ;
22 ; DECK CHTBL.01
23 ;
24 ;** CHANNEL TABLES **
25 ;
26 ; DISPLACEMENT DEFINITIONS
27 000000 CTCL = 0 ; CHANNEL TABLES LINK
28 000001 CTNB = 1 ; CHANNEL NO.
29 000002 CT.UT = CTNB+1 ; LOC. UNIT TABLE (OR -1)
30 000003 CTSST = CT.UT+1 ; START SECTOR
31 000004 CTS LM = CTSST+1 ; LIMIT SECTOR
32 000005 CTSEC = CTS LM+1 ; CURRENT SECTOR
33 000006 CTCWD = CTSEC+1 ; CURRENT WORD
34 000007 CTRS Z = CTCWD+1 ; RECORD SIZE(IN 16-BIT WORDS)
35 000010 CT.BH = CTRS Z+1 ; CURRENT BUFFER LOC.
36 000010 CTSPT = CT.BH ; SPARE
37 ; -----
38 ;
39 35331 035343 CT0: CT1 ; CTCL
40 35332 000001 1 ; CTNB
41 35333 177777 -1 ; CT.UT
42 35334 000000 0 ; CTSST
43 35335 000000 0 ; CTS LM
44 35336 000000 0 ; CTSEC
45 35337 000000 0 ; CTCWD
46 35340 000000 0 ; CTRS Z
47 35341 177777 -1 ; CT.BH
48 35342 000000 0 ; CTS PR
49 ; -----
50 ;
51 35343 177777 CT1: -1 ; CTCL
52 35344 000002 2 ; CTNB
53 35345 177777 -1 ; CT.UT
54 35346 000000 0 ; CTSST
55 35347 000000 0 ; CTS LM
56 35350 000000 0 ; CTSEC
57 35351 000000 0 ; CTCWD
58 35352 000000 0 ; CTRS Z
59 35353 177777 -1 ; CT.BH
60 35354 000000 0 ; CTS PR

```

```
0033  .MAIN
01      ;      -----
† 0034  .MAIN
02      002000 BUF:  .BLK 2000
03      000010      .LOC 10
04 00010 033000 LOC10: SBRTB
05      .END
```


APPENDIX C.3

LIST OF THE BASIC SOFTWARE USED IN THE ENGLEWOOD YARD FIELD TESTS



```

50 PRINT "-----"
52 PRINT "      T-562-VIII"
53 PRINT "      EXP. AVG."
54 PRINT "      SPECTRA PROCESSING ROUTINES"
55 PRINT "      ENGLEWOOD YARD TESTS-JUNE 77"
56 PRINT "      +ASSEMBLY A-140-IX"
58 PRINT "      12 JULY 1977"
60 PRINT "-----"
65 REM      **REF:T-560-A140-IX**
66 REM      **REF:T-560-II**
67 REM      **REF:T-562-I,VII**
75 LET K5= 0
90 DEF FNE(X)=8.68589* LOG (X)-8.6
95 CALL 23,D3
100 LET N=250
102 LET N8=N/2
104 DIM Q[2]
105 DIM A[N],C[N]
110 DIM B[N],M[N],S[N],Y[N],W[15]
114 READ L2,L5,L6,L7,L8
116 DATA 8, 4400, 25, 50, 12
120 READ T2,T3,T4,T7
122 DATA 30, 30, 800, 10
124 READ N1,N2,N3,N4,N5,N6
126 DATA 250, 24, 2, 40, 8, 0
128 READ P1,P2,P3,P4,P5,P6
130 DATA 61, 85, 110, 8, .2, 8
132 READ U,U1,U2,U3,U8,U9
134 DATA 1, 0,-1, 150, 500, 280
136 LET N9=N2/2

```

```

140 PRINT
145 PRINT "NUMBER OF CHANNELS;";N1
150 PRINT "NUMBER OF SPECTRA ;";N2
160 PRINT "FREQUENCY FACTOR DBAND HZ;";N4
165 PRINT "DISCRIMINATION LEVEL;";N5
170 PRINT "D.INDEX DECISION LEVEL;";P2
180 PRINT "DATE-TIME";
185 INPUT T1
190 PRINT
195 PRINT "TAPE#";
200 INPUT T0
205 PRINT
215 REM -----
220 GOSUB 800
222 PRINT "CAR I.D.";
223 INPUT P8
224 PRINT
225 GOSUB 1100
228 PRINT
230 GOTO 220
249 REM -----
250 REM ** START CLOCK **
255 CALL 6,B6
780 REM -----
790 REM ** READ IN EXP. AVG. **
800 CALL 2,B2
802 LET U2=-1
806 FOR I=1 TO N9
808 LET U2=U2+2
810 FOR I1= 0 TO 1
811 CALL 22,U,J6,E
820 CALL 19,U,I1,U2,U3,126,E
822 IF E= 0 GOTO 840
824 STOP
840 CALL 17,D7
865 IF I>T4 GOTO 880
870 CALL 11,D1
890 REM ** DELAY LOOP **
892 FOR J9=1 TO 2
895 FOR J3=1 TO 222
900 NEXT J3
910 IF J9=2 GOTO 925
920 CALL 12,AI 01
921 GOTO 926
925 CALL 12,BI 01
926 NEXT J9
928 CALL 20,U,AI 01,E
929 CALL 20,U,BI 01,E
930 IF E> 0 GOTO 990
935 NEXT I1
950 NEXT I
975 RETURN

```

```

990  STOP
1099  REM          -----SUB 1100-----
1100  REM          -----*** READ-OUT FROM MEMORY ***-----
1110  LET I5=-1
1115  LET I5=I5+2
1120  FOR J1= 0 TO 1
1122    FOR I9= 0 TO 1
1125      CALL 22,U,J6,E
1130      CALL 19,U,J1,(I5+I9),1,126,E
1135      IF E= 0 GOTO 1145
1140      STOP
1145      LET A[ 0]= 0
1150      CALL 21,U,A[ 0],E
1155      CALL 13,A[ 0]
1160      FOR J= 0 TO N1
1165        CALL 14,P7
1170        IF P7>4 GOTO 1180
1175        LET P7=4
1180        LET B[J]= FNE(P7)
1185      NEXT J
1190      IF I9=1 GOTO 1200
1192      FOR I=1 TO N
1194        LET M[I]=B[I]
1196      NEXT I
1200    NEXT I9
1205    LET K1=1
1210    LET K2= 0
1215    FOR L1=1 TO N
1220      IF M[L1]<P4 GOTO 1260
1225      LET K1=K1+1
1230      LET K4=M[L1]-B[L1]
1240      IF K4<L2 GOTO 1260
1250      LET K2=K2+1
1260    NEXT L1
1270    PRINT "J1,K1,K2 ";J1;K1;K2
1280    LET Q[J1]=K2/K1
1290    IF J1=1 GOTO 1400
1300    GOSUB 7500
1400    GOSUB 8000
1410    IF J1=1 GOTO 1430
1420    GOSUB 8500
1430  NEXT J1
1450  GOSUB 1500
1460  IF I5=(N2-1) GOTO 1480
1470  GOTO 1115
1480  RETURN

```

```

1499 REM          -----SUB 1500-----
1500 REM          S/R TO COMPUTE SP. DIFFERENCE
1520 LET R0= 0
1530 LET R1= 0
1540 LET R2= 0
1545 LET Z3= 0
1550 LET Z4= 0
1555 LET Z5= 0
1560 LET Z6= 0
1760 FOR J=1 TO (N-1)
1770   LET Z1=S[J]
1780   LET Z2=B[J]
1790   IF Z1>P4 GOTO 1810
1800   LET Z1= 0
1810   IF Z2>P4 GOTO 1830
1820   LET Z2= 0
1830   IF Y[J+1]=1 GOTO 1850
1840   GOTO 1880
1850   LET R3= 0
1860   IF Y[J+1]=C[J+1] GOTO 1880
1870   GOTO 1900
1880   LET R3=R3+1
1890   IF R3<3 GOTO 1920
1900   LET D= ABS (Z1-Z2)
1910   LET R0=R0+D
1920   LET R1=R1+Z1
1930   LET R2=R2+Z2
1931   LET C[J]= 0
1932   IF J>N8 GOTO 1940
1934   LET Z3=R1
1936   LET Z4=R2
1940 NEXT J
1942 LET Z5=R1-Z3
1944 LET Z6=R2-Z4
1946 LET R0= INT (R0- ABS ((R1-R2)/P6))
1949 PRINT R0;
1950 LET R0= INT (R0/L3)
1951 PRINT R0;
1952 LET R0= INT (R0+L5*(1/R1+1/R2))
1953 PRINT R0;
1954 LET R0= INT (R0+L6*(Q[ 0]+Q[ 1]))
1955 PRINT R0
1956 LET R0= INT (R0+L7* ABS (Q[ 0]-Q[ 1]))
1960 LET R1= INT (R1/10)
1970 LET R2= INT (R2/10)
1980 GOTO 2100
1990 PRINT

```

```

2000  FOR I= 0 TO N1
2002    IF I>5 GOTO 2020
2010    PRINT I,B[I],S[I]
2020  NEXT I
2022  GOTO 2100
2060  FOR J=1 TO N
2070    LET M[J]=J*N4
2075    LET C[J]= INT (S[J]-B[J])
2080    PRINT M[J],B[J],S[J],C[J];
2085    PRINT
2090  NEXT J
2095  STOP
2100  LET K5=K5+1
2110  IF P9>1 GOTO 2200
2120  LET P9=2
2130  PRINT
2140  PRINT "I-----";
2150  PRINT "-----I"
2160  PRINT "I TEST I  SP1  I  SP2  I";
2170  PRINT "D.INDEX I          REMARKS          I"
2180  PRINT "I-----I-----I-----I";
2190  PRINT "-----I-----I-----I"
2200  PRINT "I"; TAB (2);K5; TAB (7);"I";R1;
2210  PRINT TAB (15);"I";R2; TAB (23);"I";R0;
2220  PRINT TAB (32);"I";
2400  IF R1<P1 GOTO 2430
2410  IF R2<P1 GOTO 2450
2420  GOTO 2470
2430  PRINT " INSUFFICIENT DATA WHEEL #1  I"
2440  RETURN
2450  PRINT " INSUFFICIENT DATA WHEEL #2  I"
2460  RETURN
2470  IF ABS (R1-R2)<P3 GOTO 2500
2480  PRINT "SIGNIFF. ENERGY DIFF."; TAB (63);"I"
2490  RETURN
2500  IF R0<P2 GOTO 2630
2505  IF (R1+R2)>U3 GOTO 2660
2510  IF R1>U9 GOTO 2660
2515  IF R2>U9 GOTO 2660
2520  REM  **CHECK FOR GREASY OR DEFECTIVE WHEELS**
2555  GOTO 2565
2560  PRINT Z3,Z4,Z5,Z6
2565  LET R5=Z5/Z3
2570  LET R6=Z6/Z4
2575  IF R5<P5 GOTO 2590
2580  IF R6<P5 GOTO 2590
2585  GOTO 2600

```

```

2590 PRINT "    GREASY WHEELS"; TAB (63); "I"
2595 RETURN
2600 PRINT "    HIGH VALUE";
2610 PRINT TAB (63); "I"
2620 RETURN
2630 PRINT "    GOOD WHEELS";
2640 PRINT TAB (63); "I"
2650 RETURN
2660 PRINT "    OVERLOAD"; TAB (63); "I"
2670 RETURN
6999 REM      -----SUB 7000-----
7000 FOR J1=1 TO N6
7010     CALL 11,D1
7020     FOR J2=1 TO 333
7025     NEXT J2
7030 NEXT J1
7040 RETURN
7499 REM      -----SUB 7500-----
7500 FOR I=1 TO N
7520     LET S[I]=B[I]
7540 NEXT I
7550 RETURN
7600 FOR I=1 TO N
7620     LET M[I]=B[I]
7640 NEXT I
7660 RETURN
7939 REM      -----SUB 8000-----
7990 REM      ** LINE SPECTRA S/R **
8000 FOR I=2 TO (N-2)
8010     IF B[I]<N5 GOTO 8100
8020     IF B[I]>B[I-1] GOTO 8040
8030     GOTO 8090
8040     IF B[I+1]<B[I] GOTO 8130
8050     IF B[I+1]>B[I] GOTO 8090
8080     IF B[I+2]<B[I+1] GOTO 8120
8090     IF C[I]=1 GOTO 8140
8100     LET C[I]= 0
8110     GOTO 8140
8120     LET C[I+1]=1
8130     LET C[I]=1
8140 NEXT I
8150 RETURN
8499 REM      -----SUB 8500-----
8500 FOR I=1 TO N
8520     LET Y[I]=C[I]
8540 NEXT I
8550 RETURN

```

APPENDIX D

RESONANCES OF THE WHEELS TESTED AT THE GRIFFIN
WHEEL PLANT IN BESSEMER, ALABAMA

(A spectrum translator was used to obtain the recorded resonant frequencies)

TABLE D.1 Resonances of CJ33 Type Wheels with
Different Internal Stresses

WHEEL TYPE/I.D.	CJ33 11092	CJ33 97803	CJ33 30695	CJ33 31029
INTERNAL STRESS	Normal Stress	Normal Stress	High Stress	High Stress
TAPE NO. (EVENT)	152(110)	149(82)	152(101)	149(92)
RESONANCES	440.4	434.4	444.4	432.8
	1142.4	1135.2	1136.0	1129.6
	2030.8	2021.2	2019.6	2014.0
	3020.8	3011.6	3008.8	3003.2
	4061.8	4052.8	4044.8	4036.0

TABLE D.2 Resonances of CJ36 Type Wheels with
Different Internal Stresses

WHEEL TYPE/I.D.	CJ36-32769	CJ36-32784	CJ36-23089	CJ36-27910	CJ36-26425	CJ36-26171
INTERNAL STRESS	Normal Stress	Normal Stress	Normal Stress	High Stress	High Stress	High Stress
TAPE NO. (EVENT)	154 (128)	145 (42)	148 (65)	148 (56)	141 (1)	144 (24)
RESONANCES	390.4	390.8	392.4	386.8	395.2	395.6
	1040.0	1041.2	1043.2	1038.0	1038.0	--
	1865.2	1867.2	1868.4	1866.0	1862.0	1863.6
	2350.0	--	--	2350.0	2341.6	2343.2
	Weak Resonance	Weak Resonance	Weak Resonance	Weak Resonance		
	2468.8	2465.6	2470.0	2478.8	2483.2	2493.6
	2794.8	2798.8	2795.6	2795.2	2788.0	2785.6
					2789.6	2787.2
	2935.6	2941.2	2943.6 W.R. 2966.4	2973.2 W.R. 2975.6	2994.0	2995.6 2998.4
	3780.0	3787.2	3787.6	3790.0	3780.4	3784.0 3785.6
	4821.2	4820.0	4818.0	4826.4	4808.6	4809.6
	5856.8	5864.8	5864.8 5875.6	5873.6	5860.0	5861.2

APPENDIX E

DYNAMICS OF A HAMMER EXCITER

Fig. A.E.1 shows a rigid hammer to be used as an exciter, in a generalized form. The hammer is pivoted at point M and impacts at point N. The dynamics of the hammer are governed by the rotational form of Newton's 2nd Law:

$$\tau = I\ddot{\theta} \quad (\text{E.1})$$

where τ is the applied torque, I the moment of inertia of the hammer about M and $\ddot{\theta}$ is the angular acceleration. Let F_i be the component of a driving force in a transverse (i.e. nonradial) direction. Then

$$\sum F_i l_i - mgk \cos \theta = I\ddot{\theta} \quad (\text{E.2})$$

where l_i is the moment arm of the driving force F_i , k is the distance from M to the center of mass of the hammer and m is its mass.

In the exciter used in the tests there were two driving forces: due to the coiled spring and due to impact at the roller (see Fig. 4.1.1). Both of these forces are time varying, and in the case of the spring force the moment arm is also time varying. Consequently, a full solution of eqn. (E.2) is complicated and has yet to be achieved. However, some insight into the problem can be achieved by solving some simple versions of eqn. (E.2).

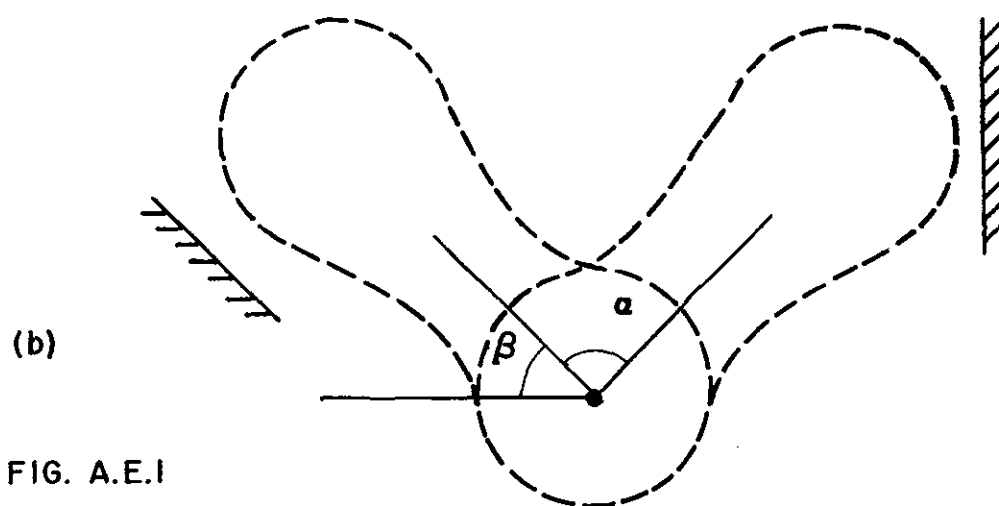
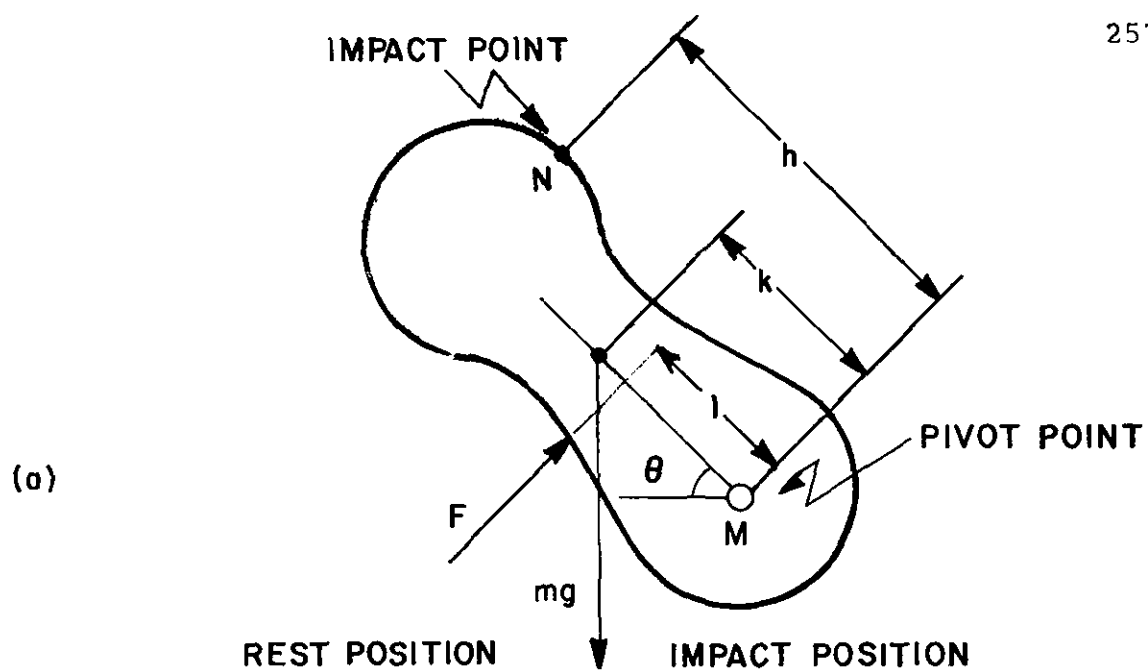


FIG. A.E.1

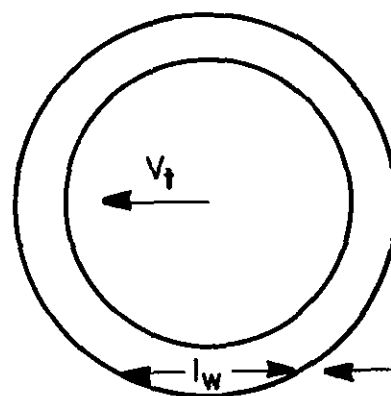


FIG. A.E.2

Consider a single constant driving force F and suppose that this force were much greater than the weight mg , then

$$\dot{\theta} = \frac{Fl}{I} t \quad (\text{E.3})$$

assuming the hammer started from rest and where t is time.

Similarly,

$$\theta = \frac{Fl}{I} \frac{t^2}{2} + \beta \quad (\text{E.4})$$

Thus the time taken to contact the wheel will be given by:

$$t_c = \left(\frac{2\alpha I}{lF} \right)^{\frac{1}{2}} \quad (\text{E.5})$$

and the velocity on impact will be:

$$\begin{aligned} v_c &= h\dot{\theta}_c = h \frac{Fl}{I} t_c \\ &= h \left(\frac{2\alpha lF}{I} \right)^{\frac{1}{2}}. \end{aligned} \quad (\text{E.6})$$

If the hammer hits the wheel, it must do so within a time l_w/v_t where l_w is a chord on the wheel at the height of impact and v_t is the train speed (see Fig. A.E.2).

$$\begin{aligned} \text{Thus} \quad t_c &< \frac{l_w}{v_t} \\ \text{or} \quad \frac{2\alpha I}{lF} &< \frac{l_w^2}{v_t^2} \end{aligned} \quad (\text{E.7})$$

$$\text{Hence} \quad F > \frac{2\alpha I v_t^2}{l \cdot l_w^2} \quad (\text{E.8})$$

Now in the case of a hammer consisting of a heavy ball on a light shaft,

$$I = mh^2 \quad (E.9)$$

and from (6) and (8)

$$F > \frac{2\alpha mh^2 v^2}{l l_w^2} t$$

$$\text{and} \quad v_c = \left(\frac{2\alpha l F}{m} \right)^{\frac{1}{2}} \quad (E.10)$$

Thus at 20 mph ≈ 10 m/sec, with $l_w \approx 10^{-1}$ m; $l = 10^{-2}$ m; $m = 0.5$ kg; $h = 10^{-1}$ m and $\alpha = \pi/2$ radians,

$$F > 15 \times 10^3 \text{ n} = 3,000 \text{ lb}$$

$$\text{and} \quad v_c = 30 \text{ m/sec}$$

This crude calculation shows that at relatively high train speeds, since the hammer does indeed impact the wheel, that the driving force must be very large. It is inconceivable that these forces are generated by compression of the coil spring and can only be brought about by an impulsive force at impact. On the other hand, at a low speed, e.g. 2 mph ≈ 1 m/sec

$$F \approx 30 \text{ lb}$$

$$\text{and} \quad v_c = 3 \text{ m/sec}$$

At this end of the speed range the spring force is probably effective.

APPENDIX F

FINITE ELEMENT ANALYSIS

F.1 Finite Element Analysis of a Railway Wheel

The finite element method of structural analysis was used for the mode-frequency analysis of railway wheel vibrations. The method embodies the concept of representing the distributed continuum of a physical structure by a model consisting of a finite number of idealized elements that are inter-connected at a finite number of points. The analysis is performed utilizing the ANSYS computer program developed by Swanson Analysis Systems, Inc.

The ANSYS program employs the matrix displacement method of finite element analysis. The stiffness matrix $[K]$ must be generated from a description of the geometrical and physical properties of the structure. To solve the resulting system of simultaneous linear equations, ANSYS uses the wavefront solution method. The "wavefront" is equal to the number of equations active at any point in the solution procedure. Each equation is associated with a particular degree of freedom in the structure. An active equation is one which has been identified and previously used in the solution and is required again at a further point. Equations are activated by the element to which they are connected as the solution progresses from element to element.

F.2 Mode Frequency Analysis

The equation of motion for a structural system is

$$[M]\{\ddot{u}\} + [c]\{\dot{u}\} + [K]\{u\} = \{F(t)\}$$

where

$[M]$ = Structure Mass Matrix

$[c]$ = Structure Damping Matrix

$[K]$ = Structure Stiffness Matrix

$\{u\}$ = Vector of Nodal Displacements

$\{F(t)\}$ = Force at Each Node as a Function of Time.

For an undamped structure with no force applied,

$$[M]\{\ddot{u}\} + [K]\{u\} = 0$$

If $\{u\} = \{u_n\} \cos \omega_n t$,

there are n values of ω^2 and n eigenvectors which satisfy the equation above.

The ANSYS program forms the matrices $[M]$ and $[K]$ by forming the matrices $[M_e]$ and $[K_e]$ for each element. The eigenvalue problem is solved by a technique called "Matrix Condensation" (Guyan Reduction). In this process a set of n "master" degrees of freedom which characterize the natural frequencies of interest in the system are specified, and the eigenvalue problem is solved for the n degrees of freedom.

In the force spectrum option of the ANSYS program, the input consists of a force distribution on the structure nodes and a table of force amplitude multipliers vs. frequency. The structural response to force loading is obtained by superimposing the response of individual

vibrational modes and weighting by their "modal participation factors". The output contains the eigenvalue solution, the corresponding participation factors, mode coefficients and equivalent masses, the eigenvector solution, the expanded mode shapes and the element stress solution.

Natural frequencies and mode shapes are obtained from

$$([k] - \omega_i^2 [m]) \{\psi\}_i = 0$$

where

$[k]$ = the stiffness matrix of the structure

$[m]$ = the mass matrix of the structure

ω_i = the circular natural frequency of mode i

$\{\psi\}_i$ = the mode shape vector of mode

$\{\psi\}_i$ is normalized such that

$$\{\psi\}_i^T [m] \{\psi\}_i = 1,$$

The equivalent mass for the i th mode

$$m_{ei} = 1 / \{\psi\}_i^T \{\psi\}_i$$

The participation factor is defined as

$$\gamma_i = \{\psi\}_i^T [m] \{F\}$$

where $\{F\}$ is the force vector.

The mode coefficient is defined as

$$(m.c.)_i = \frac{\gamma_i}{\omega_i} F_i$$

Assumptions

(i) The wheel is rigidly fixed at the hub ($U_X = U_Y = U_Z = 0$) and constrained in radial and circumferential directions at a point on the tread just above the

wheel flange where it is in contact with the railway track, ($UX = UY = 0$).

(ii) The wheel is made of homogeneous material with Young's Modulus $E = 30 \times 10^6$ psi, and Poisson's ratio $\nu = 0.3$ and density $\rho = 7.3 \times 10^{-4} \frac{\text{lb} \cdot \text{sec}^2}{\text{in}^4}$.

In the previous contract the ANSYS finite element analysis program has been used to determine the natural frequencies and mode shapes for a 33 in. wheel with i) no cracks and ii) a large plate crack. This study was extended further as follows:

1. The finite element model showing the 33 in. wheel geometry was improved by increasing the number of elements from 192 to 240.
2. The boundary conditions were changed slightly. In addition to fixing all the node points on the hub, an additional node on the tread of the wheel just above the flange was fixed in radial and circumferential directions. This is the point where the wheel is in contact with the railway track.
3. The wavefront size is dependent upon the order in which elements are input. In the case of a railway wheel model there are two possible ways in which the elements can be input to determine the size of the wavefront - radial and circumferential. Both ways were scanned to find out which one gives the smaller wavefront. It was found that the wavefront is smaller if the elements are input in a radial arrangement.

4. A modification of the ANSYS model for the plate portion of the 33 in. wheel was made to determine if a significant cost reduction could be achieved in the execution of this program when the plate geometry was simplified. The simplification involved modeling the plate portion of the wheel by 3-D plate elements having 6 degrees-of-freedom per node instead of the 3-D solid elements having 3 degrees-of-freedom per node. It was hoped that this type of element simplification would allow more computer runs for the same cost. However, this attempt was unsuccessful in achieving a reduction in computer costs. The increase in the degrees-of-freedom for the four nodes for each plate element from 3 to 6 (to allow for plate element rotation) caused the number of simultaneous equations associated with the computer generated wavefront to exceed that of the previous element description.

Various cracks were simulated in the ANSYS model of the wheel by providing double and disconnected nodes in the crack area. The following cracks were simulated:

1. One small radial crack, provided by detaching one boundary on one of the rim elements (Fig. F.2.1).
2. One small radial crack through the rim, but not extending into the plate (Fig. F.2.2).
3. One large radial crack extending from the rim through to the axle (Fig. F.2.3).
4. One large plate crack (open on both sides and extending slightly in the radial direction at both ends (Fig. F.2.4).

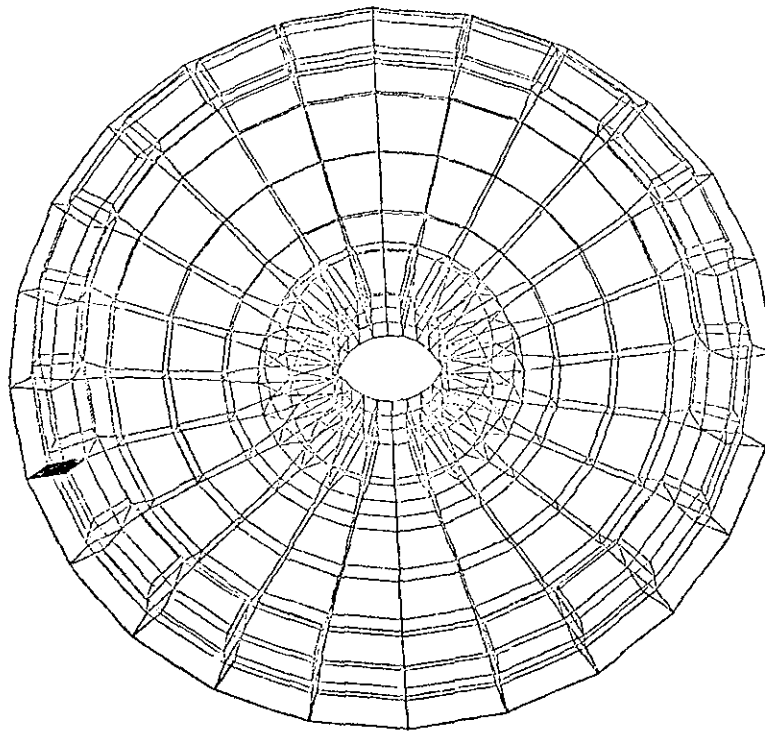


FIG. F.2.1 VIEW OF A 33 INCH WHEEL WITH ONE SMALL RADIAL FLANGE CRACK - ANSYS GEOMETRY

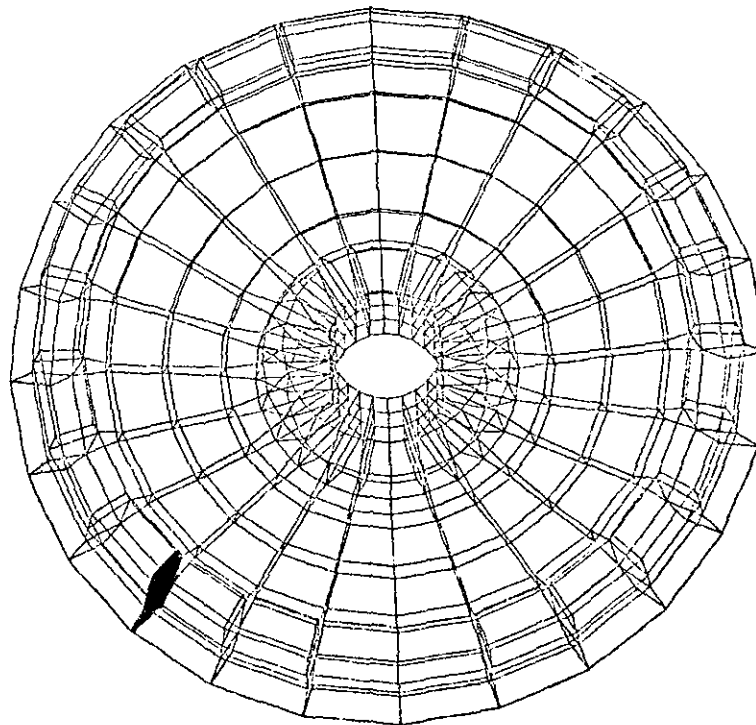


FIG. F.2.2 VIEW OF A 33 INCH WHEEL WITH ONE COMPLETE RADIAL FLANGE AND TREAD CRACK - ANSYS GEOMETRY

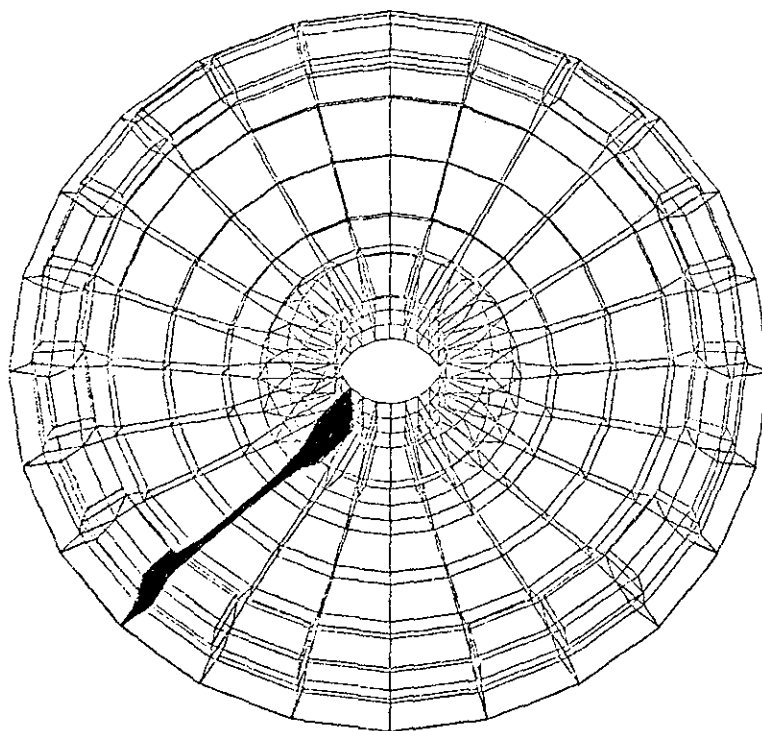


FIG. F.2.3 VIEW OF A 33 INCH WHEEL WITH ONE COMPLETE RADIAL CRACK - ANSYS GEOMETRY

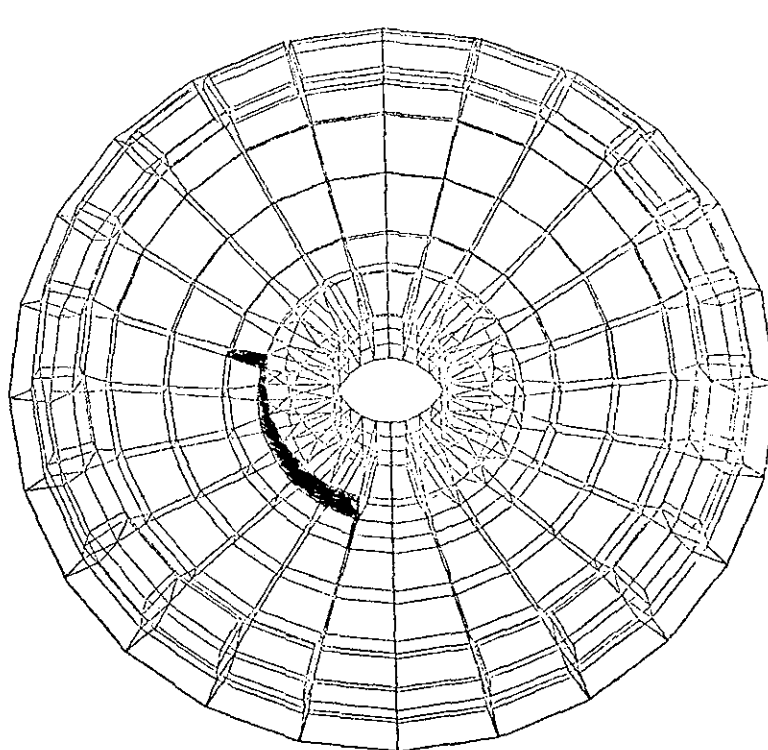


FIG. F.2.4 VIEW OF A 33 INCH WHEEL WITH ONE LARGE PLATE CRACK - ANSYS GEOMETRY

The following forcing functions were investigated to determine the vibration response of a wheel with or without simulated cracks.

- (i) a square pulse: to simulate a single impact
- (ii) repetitive square pulses: to simulate repetitive impact
- (iii) a sawtooth: to simulate slip-stick action such as with a retarder or brake shoe.

Excitation of Cracked Wheels

Several studies were made to determine the effect on the spectrum of cracks of various sizes and in various locations. In addition there was some interest in determining the effect of varying the direction and point of contact on the wheel of the forcing function and the position of this point relative to the crack. These studies are summarized in Table F.2.1.

Figure F.2.5 shows the calculated line spectra for the good wheel and for wheels with different cracks.

In general, the introduction of a crack results in removal of degeneracy of modes and the introduction of new resonances. Both of these effects cause the appearance of additional lines in the spectrum. Even one small crack in the flange causes significant differences in the spectrum, especially in the range 2000 to 4000 Hz.

Figures F.2.6 and F.2.8 show Mode Coefficient (related to the amplitude) vs. Frequency plots for good wheel and

TABLE F.2.1 SUMMARY OF ANALYSIS

Study No.	Wheel Description	Type of Excitation	Direction and Location of Excitation
1	33 in. wheel - no cracks	Square pulse	Axial on load line and 30 degree from load line
2	"	Square pulse with extended duration	"
3	"	Two successive square pulses	"
4	33 in. wheel - one small radial flange crack	Square pulse	Axial on load line and 30, 60, 90, 120, 150 and 180 degree from load line
5	"	Square pulse	Radial on load line and 30, 60, 90, 120, 150 and 180 degree from load line
6	33 in. wheel - one large plate crack	Square pulse	Radial on load line
7	33 in. wheel - one complete radial crack	-	-
8	33 in. wheel - one radial rim crack	-	-

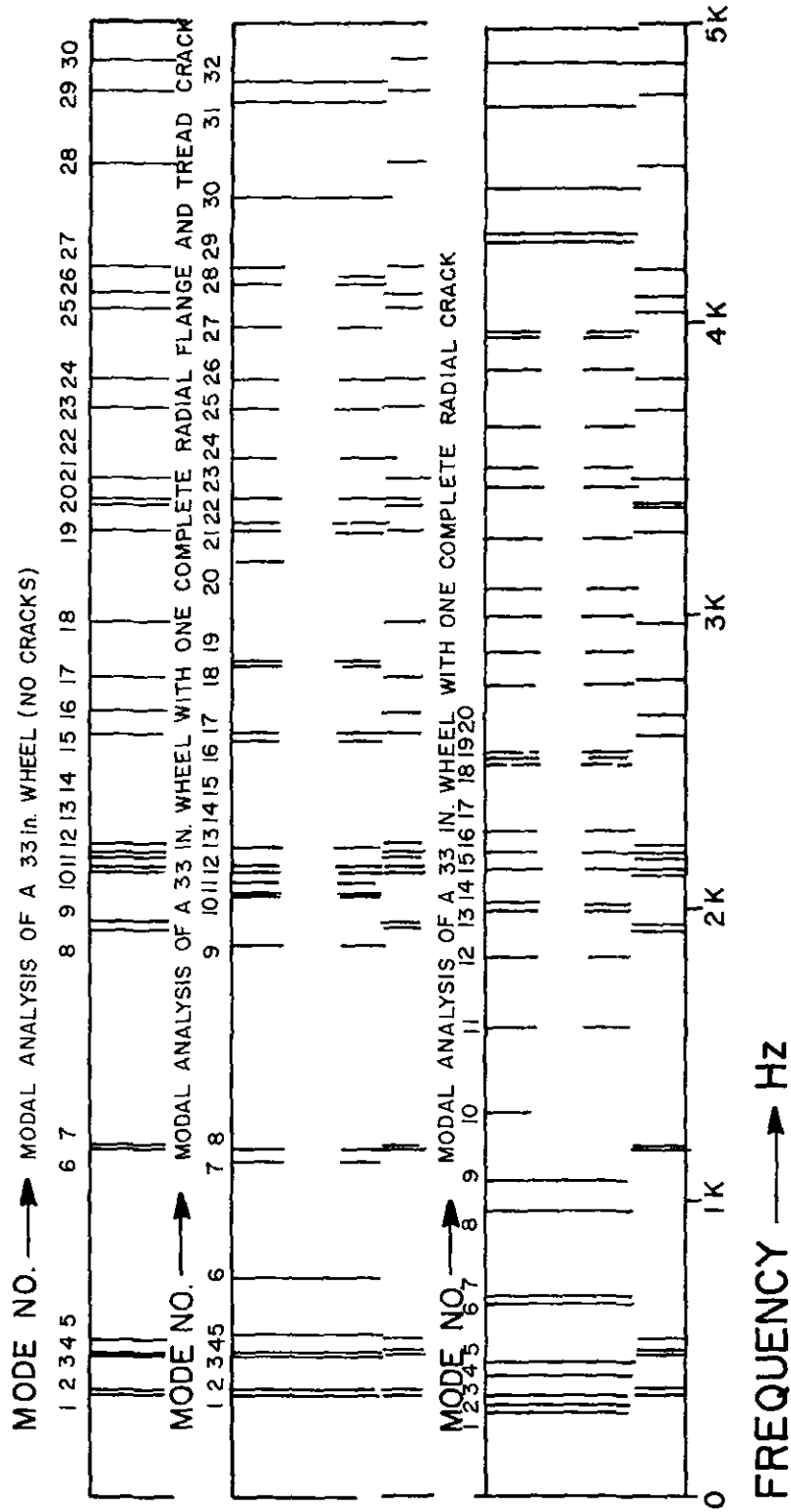


FIG.F.2.5 COMPARISON OF NATURAL MODES FOR 33 in. WHEELS

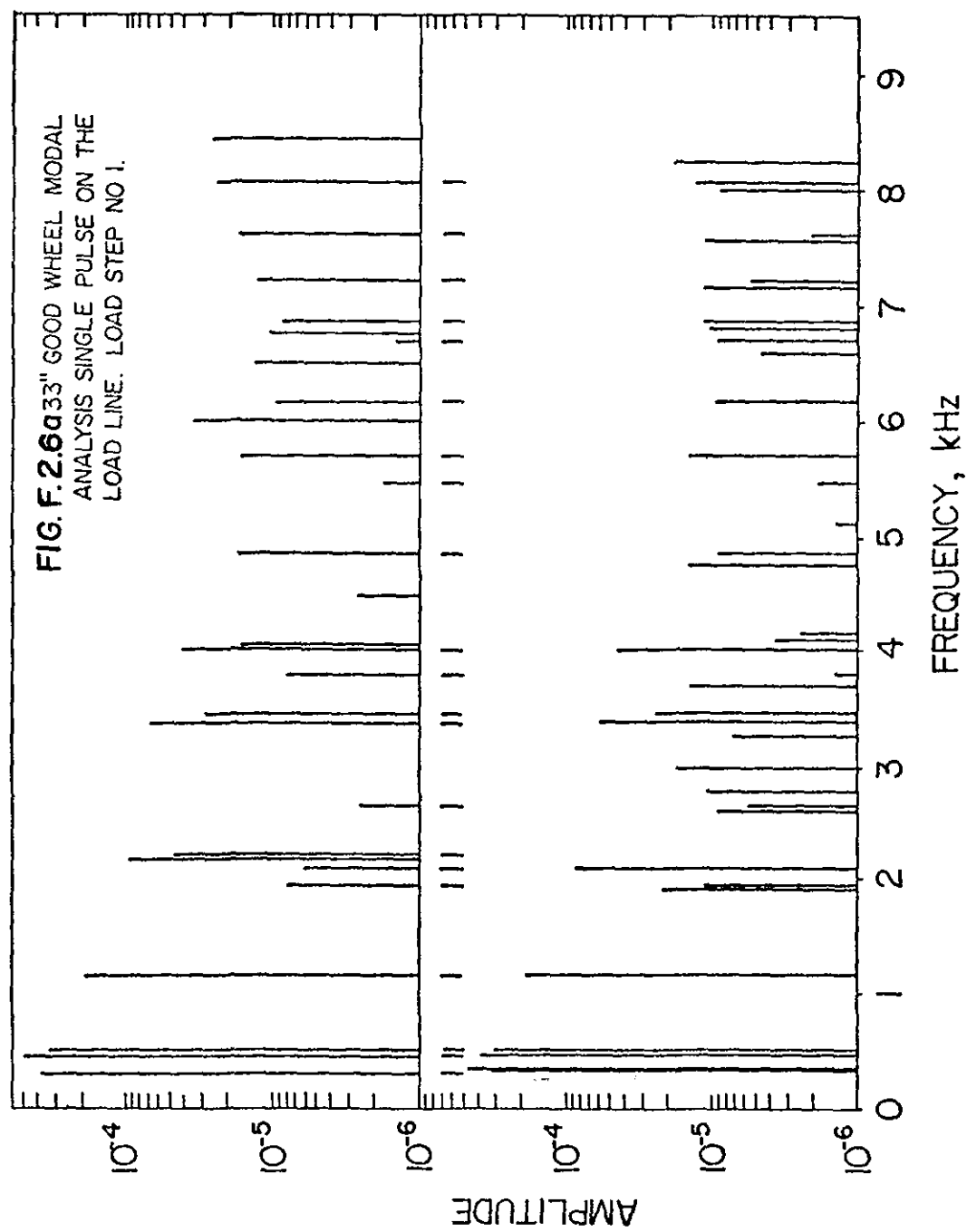


FIGURE F.2.6b 33" GOOD WHEEL MODAL ANALYSIS SINGLE PULSE 30°
FROM LOAD LINE LOAD STEP NO. 2

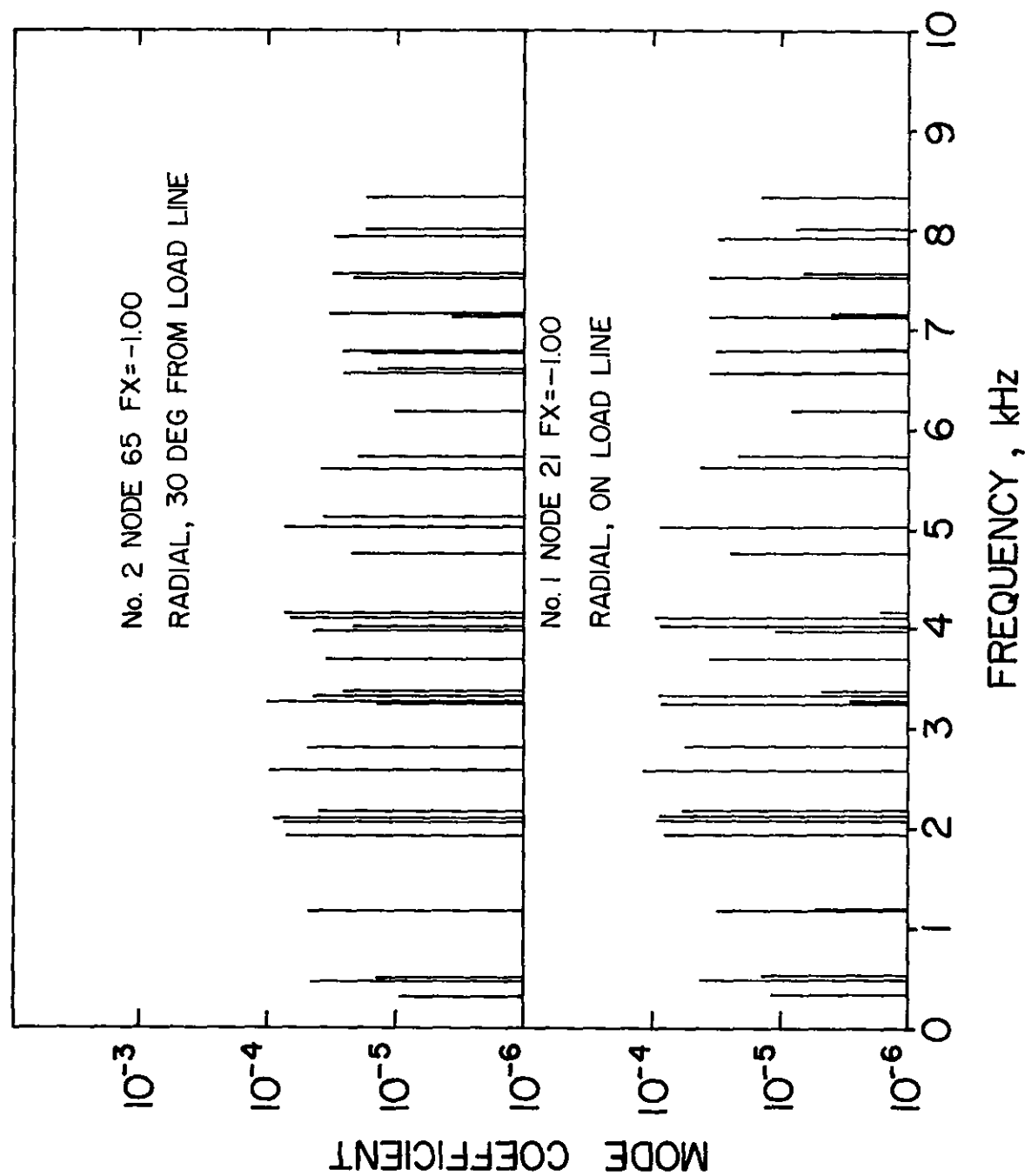


FIGURE F.2.7 MODAL ANALYSIS OF A 33in WHEEL WITH ONE SMALL RADIAL FLANGE CRACK-A SINGLE PULSE APPLIED

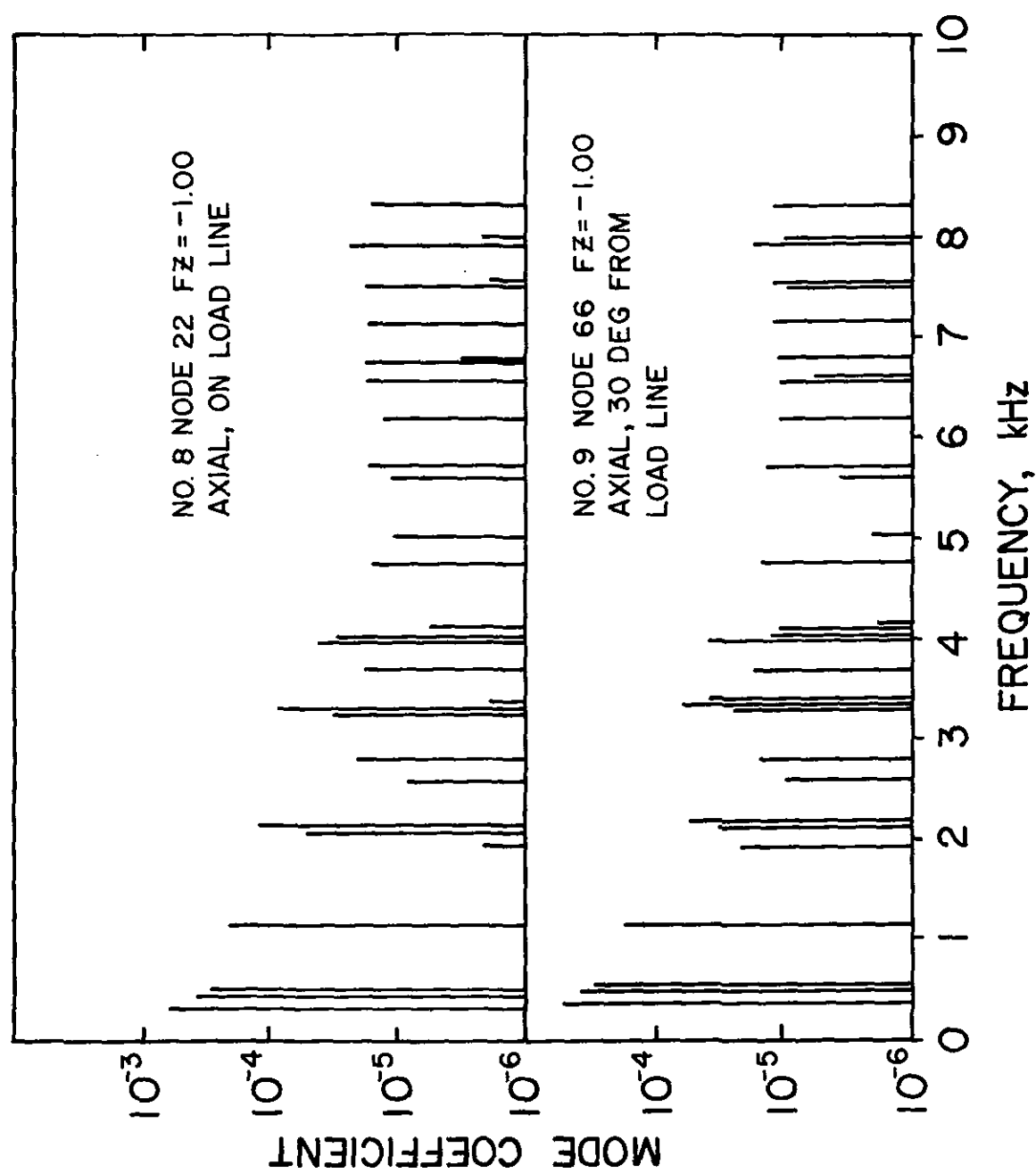


FIGURE F.2.8 MODAL ANALYSIS OF A 33in. WHEEL WITH ONE SMALL RADIAL FLANGE CRACK - A SINGLE PULSE APPLIED.

wheels with different cracks excited by a square pulse. For good wheel excitation, it is seen that different modes are excited depending upon location of the point of excitation relative to the load line. Also the modal amplitude varies somewhat. A study of the effect of different impact points was made for the wheel with the smallest possible rim crack.

Axial and radial excitation on the flange by a square pulse was carried out separately at various angular distances (15 degrees apart) from the load line. The purpose was to determine if the small crack so simulated is evident in spectral changes, and secondly, to determine if the small crack may be discovered regardless of the point of wheel excitation. The results show that the number of resonances excited between 300 and 10000 Hz in the faulty wheel varied between 27 and 40 depending upon the nodal location on which the impulse was applied, and on whether this impulse was applied axially or radially. However, the amplitude of the major resonances was not greatly affected and it was concluded that there was no great advantage to be gained by impacting the wheel off the load line.

APPENDIX G

RELATIONSHIP AMONG OPERATING PARAMETERS

In assessing progress towards the goal of helping the Railroads find defective wheels it is necessary to have some "yardsticks" or "figures of merit" by which to measure the performance of the acoustic signature system in comparison with current practice and other systems and to measure the cost/benefit ratio of developing and operating such systems. Such measures are not easy to come by partly because some of the information that it is necessary to have (e.g., the percentage of defective wheels in service) is not available in a precise form.

It is possible to define two figures of merit which could be used to assess progress. First, reliability is defined as:

$$R = \frac{\text{Number of correct decisions}}{\text{Total number of decisions}}$$

where a decision is a good/bad wheel choice as made by the system. The false alarm rate is defined as:

$$F = \frac{\text{Number of unconfirmed indications}}{\text{Total number of bad wheel indications}}$$

Let the number of axles passing the inspection point in a given period be N_A . Suppose that N_D of these axles carry a defective wheel and that the fraction of these identifiable by acoustic signature inspection is g . Then the number of bad wheels correctly found will be

$$N_B = gN_D.$$

Let:

$$N_D = fN_A,$$

so that f is the fraction of axles with defective wheels.

Now if the total number of indications made during this period is N_i the false alarm rate will be:

$$F = \frac{N_i - N_B}{N_i},$$

so that,

$$N_i = \frac{N_B}{1-F} = \frac{gfN_A}{1-F}.$$

The number of incorrect indications will be $(N_i - N_B)$

and so the number of correct decisions will be $(N_A + N_B - N_i)$.

Thus the system reliability for this period will be given by:

$$R = \frac{N_A + N_B - N_i}{N_A} = 1 - \frac{Fgf}{1-F}.$$

Rearranging

$$F = \frac{1-R}{1+gf-R} = 1 - \frac{gf}{1+gf-R}$$

This formula states the problem in a nutshell. F , the false alarm rate, is an operating parameter. The question is how many wrong indications would be accepted by the railroads for every bad wheel detected. Suppose an acceptable value is $F = 1/2$. To accomplish such a low value we would need a reliability of the order $(1 - gf)$. Now g is a measure of our scientific knowledge i.e., our ability to recognize defective wheels. Using the optimum ID equation, it can be seen from Fig. 7.3.4 that if a decision level of 64 is selected then g is unity, but if a

decision level of 69 is selected then g is two thirds. Let us assume $g = 1$. The real problem is with f , the fraction of axles with defective wheels, which is a very small number. Despite the lack of precise information on the exact figure, estimating from the number of wheel failures reported to the AAR and the total size of the U.S. fleet of cars indicates that there is one defective wheel in every 10,000

$$\text{i.e., } f = 10^{-4}$$

and the reliability has to be about $(1-10^{-4})$ i.e., $(1-0.001) = 0.9999$ or 99.99%. Putting it another way, the system has to work so well that only 1 incorrect decision is made in 10^4 .

On the other hand, consider the following case

$$F = 0.9 \text{ (one bad wheel indication in } 10 \text{ is substantiated)}$$

$$f = 10^{-4}$$

then $R \approx 1 - 9gr \approx 1 - 10^{-3} = 99.9\%$, representing one incorrect decision in 10^3 . As can be seen from the statistics in Fig. 7.3.4 there were 3 incorrect decisions in 371 or about 1 in 123. Thus to find all the defective wheels would require a reduction of the incorrect decisions by a factor of 8. This would not appear to be beyond the bounds of possibility for a prototype system. On the other hand, with a decision level of 69, based on the same sample, two thirds of the defective wheels would be found with 100% reliability and zero false alarm rate.

APPENDIX H

REPORT OF NEW TECHNOLOGY

In the earlier report (FRA/OR&D 76-290 or DOT-TSC-FRA-76-6), three items were listed as possibly patentable. In the present work, a number of improvements are described and these are now listed under the same three headings:

- 1) The system for Acoustic Signature Inspection of Railroad Wheels is described again on page 6-9 and 109-110 with some new ideas to bypass some problem areas.
- 2) The mechanical impacter, as actuated by the wheel itself, is described with improvements on pages 93, 13-14, and 90-94. Additional ideas for excitation methods are given on pages 94-99.
- 3) The improved computer programs for analysis of acoustic signatures are described on pages 107-122 and printed in full in Appendix C on pages 211-252.

